**RESEARCH ARTICLE**

# Importance of Transition Cow Management in Kerala

K Lalu[1]* N P Sakkariya[2], M. T Dipu[2] and S K George[2]

[1]Head, Department of Dairy Husbandry, College of Dairy Science and Technology, Thiruvananthapuram KVASU, Kerala, India.
[2]Department of Dairy Husbandry, College of Dairy Science and Technology, Thiruvananthapuram KVASU, Kerala, India.

*Address for Correspondence
**K Lalu**
Head, Department of Dairy Husbandry,
College of Dairy Science and Technology,
Thiruvananthapuram KVASU, Kerala, India.
Email:lalu@kvasu.ac.in

**ABSTRACT**

Transition cow management has been one of the most significant advances in dairy nutrition and production world-wide over the past 20 years, providing a major opportunity to improve cow health, milk production and reproductive performance. Cows that fail to transition successfully into lactation are vulnerable to a host number of disease problems which occur just after the calving. Dry matter intake (DMI) starts to decrease a few weeks before parturition with the lowest level occurring at calving. During the dry period, energy and protein requirements are lower, as there are no needs by the udder for milk production. But after calving cows require around two times more energy for milk production than maintenance with a progress in the lactation period. There is evidence clearly confirming that the transition period represents a brief but critically important period of time in a cow's life where careful manipulation of diet can impact substantially on subsequent health and productivity.

**Key words**: Transition, Lactation,Management.

## INTRODUCTION

The transition period is very important in the productive cycle of the cow since it is a challenging time and need scientific management. The transition period is defined as the four weeks before and after calving, and is characterised by greatly increased risk of disease (Stevenson and Lean 1998).This period is dominated by a series of adaptations to the demands of lactation, a type process termed 'homeorhetic' (Bauman and Currie 1980). Homeorhetic processes are the long -term adaptations to a change in state, such as from being non-lactating to lactating, and involve an orchestrated series of changes in metabolism that allow an animal to adapt to the challenges

16401
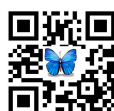
**Lalu *et al.***

of the altered state. Diseases that result from disordered homeorhetic change reflect disorders in homeostasis. The common diseases associated with the transition period in cow are as follows

a. acidosis
b. hypocalcaemia and downer cows;
c. hypomagnesaemia;
d. ketosis and fatty liver;
e. udder oedema;
f. abomasal displacement;
g. RFM/metritis; and
h. Poor fertility and poor production.

## All Metabolism are Interrelated

All Metabolic processes are intricately linked. This concept reflects a need for effective homeostatic control of metabolism. A failure of one metabolic process will inevitably impact on the efficiency others. As research progresses, intricate homeostatic links between metabolic processes once thought to be distant and unrelated are continually uncovered. As a result of the increased understanding of homeostatic processes, the concept of transition feeding has evolved from one focused on only control of one disease to an integrated nutritional approach that optimises:

• Rumen function;
• Calcium and bone metabolism;
• Energy metabolism;
• Protein metabolism; and
• Immune function.

While addressing any one of these areas in isolation will be of some benefit, developing integrated nutritional strategies based on an understanding of the homoeostatic and homeorhetic processes involved in the transition from a non-lactating to lactating animal will have substantial benefits.

## Intervention in transition

There are specific interventions of transition cow management. Cows should be managed so as to:
• reduce ruminal disruption;
• minimise macro mineral deficiencies (conditioned or otherwise);
• minimise lipid mobilisation disorders; and
• Avoid immune suppression.
   To achieve these objectives following managemental practices need to be followed.

## Providing Sufficient Dry Period to Lactating cows

Animals should be given a sufficient time to rest and regenerate mammary tissue, which can be attained by providing a dry period of 45 to 60 days duration (Rastani *et al.*, 2005). The method of complete cessation of milking is a common practice in the low producing cows (<6 kg). In case of high yielders, incomplete milking or alternate day milking for 1-2 weeks followed by complete cessation is an effective method to dry off the animals.
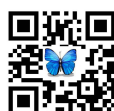
### Implementing a proper dry cow therapy

Dry cow therapy is the treatment of cows at the end of lactation with a long acting antibiotic preparation with or without a teat sealant. This is to treat for any intra-mammary infections contracted during lactation and provides protection against new infections during the dry period. Recently, dry cow therapy is being practiced via two different techniques i.e. use of intra mammary and systemic administration of antibiotics prior to calving. Systemic administration of antibiotics at drying off or some weeks before parturition looks to be nominal accompanying treatment for intra-mammary therapy, which may be advisable for practice (Ahmad *et al.*, 2015).

### Optimum Feeding Management

A decrease in DMI occurs due to the rapid growth of the fetus taking up abdominal space and displacing rumen volume. This decrease ranges from 2% of body weight in the first weeks of the dry period to 1.4% of body weight in the 7-10 days period before calving. This 30% decrease in DMI appears to occur very rapidly in the transition period (Bertics *et al.*, 1992). During the 3 weeks post calving, DMI increases at the rate of 1.5 to 2.5 kg per week, which is more rapid in multiparous cows than primiparous cows. The optimum DMI during prepartum and postpartum should be 1.7% and 2-3% of body weight, respectively. Optimum nutrient and dry matter intake can be supplied by augmenting nutrient density of feed. Therefore, peripartum diet of animal should contain high concentrate and high quality low roughage. Sudden shift to high concentrate diet predisposes the animal to ruminal impaction and metabolic acidosis. The practice of gradual increase in peripartum diet quantity and quality will acclimatize the ruminal microflora to high concentrate ration without disturbing ruminal ecology. Some experts have suggested that when prepartum nutrient restriction is followed by increased postpartum nutrient intake, the negative effect of prepartum nutrient restriction may be overcome partially. However, the effectiveness of elevated postpartum nutrient intake may depend on the severity of prepartum nutrient restriction (Lalman *et al.*, 1997).

### Proper Housing management

For better feeding and care, the animals in dry period should be separated from lactating animals, at least 60 days before expected date of calving. This practice will protect the pregnant animals from injuries due to infighting and hence abortion, torsion, dystocia and other complications. Preferably 10 to 15 days before parturition, the animal must be transferred to loose housing type shed. Shifting the animals to confined housing on the day of calving instead of earlier, and use of restraint measures at milking increases the somatic cell count, indicates the incidence of mastitis (Svensson et al., 2006). The shed may consist of centrally placed manger with curbs of 0.6 meter length and width per animal under a roof in paddock. The manger should be surrounded by a 2.2 meter wide paved platform with drains. The roofed portion should be 5.6 meter wide and may be gabled.

## CONCLUSION

The transition period constitutes a turning point in the productive cycle of the cow since it imposes a number of abrupt changes on the cow which are in 'physiological transit' from one lactation to the subsequent lactations and hence it requires proper management for successful dairy farming. All the concepts of sound nutrition that are important in the pre-calving transition period are equally important in the post-calving transition period. Continued ruminal adaptation to high concentrate diets is critical to control the risk of ruminal acidosis, careful attention to mineral metabolism, as well as energy and protein metabolism, is essential for a successful lactation. Again, the concepts of homeostatic and homeorhetic changes are crucial. Failure to adequately support one area of metabolism will inevitably impact negatively on other metabolic processes. Careful attention to minimise the depth and length of negative energy and protein balance are equally as important as the provision of adequate calcium, magnesium and phosphorus. Apart from the nutritional aspects, housing is also very important for effective management of

transition cows especially to reduce the incidence of the probable complications arising out of metabolic disturbances.
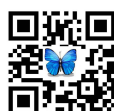
# REFERENCES

1. Ahmad T, Nadeem A, Saleem MI, Nadeem M, Saqib M 2015. Control of Mastitis through Dry Cow Therapy: A Review. Sch Adv Anim Vet Res; 2 Suppl 3:128-135.

2. Al Jassim RAM, Rowe JB1 999;. Better understanding of acidosis and its control. Rec adv Anim Nutr Austr 12:91-

3. Bauman, D.E. and W.B. Currie 1980, Partitioning of nutrients during pregnancy and lactation: A review of mechanism involving homeostasis and homeorhesis. J. Dairy Sci. 63:1514-1529.

4. Bertics SJ, Grummer RR, Cardorniga-Valino C, Stoddard EE 1992. Effect of prepartum dry matter intake on liver triglyceride concentration and early lactation. J. Dairy Sci; 75:1914.

5. Dawson KA. 1995 The use of yeast strain 8417 in manipulating ruminant high concentrate diets. In proc. 56th Minnesota Nutrition Conference & Alltech, Inc. Technical Symposium, Minn. Ext. Serv., St. Paul, MN;. p. 25-36.

6. Dufva GS, Bartley EE, Dayton AD, Riddell DO 1983. Effect of niacin supplementation on milk production and ketosis of dairy cattle. J Dairy Sci; 66:2329-36.

7. Hamada T, Ishii T, Taguchi S. 1982 Blood changes of spontaneously ketotic cows before and four hours after administration of glucose, xylitol, 1,2-propanediol, or magnesium propionate. J Dairy Sci; 65:1509.–1513.

8. Lalman DL, Keisler DH, Williams JE, Scholljegerdes EJ, Mallet DM 1997. Influence of postpartum weight and body condition change on duration of anestrus by undernourished suckled beef heifers. J. Anim. Sci.; 75:2003-2008.

9. Mann S, Abuelo A, Nydam DV, Leal Yepes FA, Overton TR, Wakshlag JJ 2016;. Insulin signaling and skeletal muscle atrophy and autophagy in transition dairy cows either overfed energy or fed a controlled energy diet prepartum. J Comp Physiol B 186(4):513-525.

10. Nagaraja TG, Taylor MB, Harmon DL, Boyer JE 1987. Invitro lactic acid inhibition and alterations in volatile fatty acid production by antimicrobial feed additives. J Anim Sci; 65:1064-1076.

11. Svensson C, Nyman AK, Persson Waller K, Emanuelson U. 2006.Effect of housing, management and health of dairy heifers on first-lactation udder health in southwest Sweden. J Dairy Sci; 89 Supl 6:1990 – 1999.

12. Stevenson, M.A. and I.J. Lean (1998) Culling in eight New South Wales dairy herds: Part 1 Descriptive epidemiology. Aust Vet. J. 76:482-488.

13. Rastani RR, Grummer SJ 2005. Reducing Dry Period Length to Simplify Feeding Transition Cows: Milk Production,Energy Balance, and Metabolic Profiles. J Dairy Sci; 88:1004–1014.

14. Razzaghi H, Aliarabi MM, Tabatabaei AA, Saki R, Valizadeh, Zamani P 2012;. Effect of Dietary Cation-Anion Difference during Prepartum and Postpartum Periods on Performance, Blood and Urine Minerals Status of Holstein Dairy Cow. Asian-Australas J Anim Sci 25(4):486–495.

15. Thilsing-Hansen T, Jorgensen RJ, Ostergaard S 2002. Milk Fever Control Principles: A Review. Acta Veterinaria Scandinavica; 43 Suppl 1:1 -19

**Table 1. Strategies to prevent diseases during transition period**

| SI No | Disease | Details | Preventive strategies |
|---|---|---|---|
| 1 | **Acidosis** | Milking cows are very vulnerable to lactic acidosis and sub-acute ruminal acidosis SARA) resulting from suppressed appetite and rapid introduction of grains/concentrate | Provide the ration containing more than 32% NDF, with greater than 80% being from long forage and avoid sudden dietary shifts. Use nutralizing agents such as sodium carbonate, potassium carbonate, magnesium oxide, sodium hydroxide and calcium hydroxide @ 2 to 4% Ionophore rumen modifiers like Monensin, lasalocid, narasin and salinomycin Yeast culture (Dawson, 1995); Virginiamycin (Al Jassim and Rowe, 1999); and Tylosin (Nagaraja *et al.*, 1987). |
| 2 | **Milk Fever/grass tetany** | Mainly refers to calcium, magnesium and phosphorus. Milk fever and grass tetany (hypomagnesaemia) can result from a conditioned deficiency where excess potassium reduces the capacity of the cow to maintain stable blood concentrations of calcium and magnesium | Supplementation of calcium gel- 3 doses each 300 gms. Feeding negative Dietary Cation Anion Diets (DCAD) in late gestation period and high DCAD in early lactation (Razzaghi *et al.*, al., 2012), Maintain proper Ca and P (2:1) ration in the diet and Prepartum administration of  itamin-D (Thilsing-Hansen *et al.*, 2002). |
| 3 | **Fatty liver and ketosis** | Diseases that are largely influenced by a failure to provide sufficient or effective energy sources around calving. | Starvation of the pregnant animal should be avoided. Supplementation of Niacin @ 3 to 12 gm/day reduces the NEFA mobilization from adipose tissues (Dufva *et al.*, 1983). Intravenous administration of glucose may decrease blood ketones (Hamada *et al.*, 1982). Oral drenching of propylene glycol  & Monensin hydrochloride @2.5 mg/day; and salts of  propionic acid may be effective in lowering the blood ketones. |
| 4 | **Displacement of abomasum** | Over feeding and stress during parturition | Over feeding of cows should be avoided during dry period (Mann *et al.*, 2016). Diet should constitute about 50% forage and fed long and/or coarsely chopped good quality forage during the dry period and early lactation. Minimize stress due to other periparturient diseases like milk fever and ketosis. |

**RESEARCH ARTICLE**

# Geometric Investgation of Satillte Pushbroom Image Ray for Spot Satillte Image of Musol City and Suranded Aera

Israa Hussein[1]* and  Nawal K.Ghazal[2]

[1]Department of Physics, Collage of Science, University of Baghdad, Baghdad, Iraq.
[2]Department of Remote Sensing ,Collage of Science, University of Baghdad, Baghdad, Iraq.

*Address for Correspondence
**Israa Hussein**
Department of Physics,
Collage of Science,
University of Baghdad,
Baghdad, Iraq.
E-Mail:Asraahm81@gmail.com

**ABSTRACT**

This paper includes geometric correction to 1A,1B levels for spot satellite image to Musol city with around aera as study region by using 2Dpolynomial method in ERDAS 2014 program .Aset of ground control points GCPs on the satellite scene are to locate these points. The accuracy assessment of this model achived by calculating of the root mean square error (RMSE) ,X residual, Y residual , that show There are many points have low RMSE in both levels (1A,1B) used as check  points  notes that X RMSE and RMSE total  in  1B level is lower than 1A level, while Y RMSE in 1A level  is lower than its for 1B level.

**Key words** : geometric correction ,polynomial, ground control point,RMSE.

## INTRODUCTION

The spot satellite with 10m pixel size and stereo viewing competence offers atool for mappers with greater potential than other civilian remote sensing satellite ,it is accuracies of the order of 0.5 to 1 pixels are obtainable from scanned remote sensing  imagery. It was anticipated that positional accuracies of the order 5 to 10 m RMSE might be achieved in mapping from panchromatic spot imagery ,this well within  1:50000 mapping specifications [Priebbenow, 1986]. While topographic feature for the map scale of 1:100000 can mostly and the the feature for the map with scale of 1:50000 can patially be  extracted  from spot satellite images [Gugan  et al.,1988;Ahokas et al., 1990; Jacobsen ,1990,1992]. The geometric correction prosses required 2D image maps from the uncorrected satellite images .The method could be selected considered like 2D transformation polynomial distorting or such as 3D transformation with

**Israa Hussein and  Nawal K.Ghazal**

cpllinearity equations of imagery  and rotional functions ,in figure(1) show diagram for geometric correction process[ Hossenini  et al., 2005].

The computer graphics viewed the art and science of creating synthetic images by programming the geometry  and appearance of the contents of the images then displaying the result s by display devices which support graphical output [Cunningham,2001].  When the object is imaged ,the geometric model is used to calculate position and the visibility of the pixel,while the color of the pixel is determined by the approriate part of the grain map [ Mikhail et al.,2001]. Geometric correction conversion transform s the imagery  aquired by the sensors  to much certain cartografic  projection free of distortions and each pixel is dispersed  with specfic coordiate.[ Estec , 1999]. The suitability of geometric correction of these models for selected  imagery .An accuracy analysis is achieved  ,with emphasis being laid on the number and location of ground control points [Santhosh,Thirun avukkarasu , 2014].

## MATERIALS AND METHODS

### Study area and data set

Study aera concederd in north of iraq ,this region is cvered by spot2 PANwith GRS index 277J 132 K ,it contains Mosul city with its enclosed regions,at(latitude 37 Nlongitude168 E).

### Data used

The used data can be divided  in to three types :Spot scene  with two levels (1A,1B) as showing in figures (1) and (2)

1.  Mosul city map with scale 100000 as showing in figure (3).
2.  Ground control points taken by using GPS diveice  as showing in table (1)

### The geometric correction

Polynomial models needed for the transformation between image and object coordinates .alinear trans formation  is the first order polynomail transformation , which can change the location ,rotation ,scale and skew , the first polynomial is used to project raw image to an object for data covering smalland large area .The polynomial equation can calculate new output ground control point location[ ERDAS (a), 1999;Santhosh,Thirun avukkarasu , 2014]

$X = [\sum_{i=0}^{t}] [\sum_{j=0}^{i}] a_k . X^{i-j}Y^j$          (1)

$Y = = [\sum_{i=0}^{t}] [\sum_{j=0}^{i}] b_k . X^{i-j} Y^j$          (2)
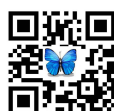
Where t:is the order of the polynomial

$a_k$ ,$b_k$ :are coefficients the subscript k is determined from equation :

$k = \frac{i.i+j}{2} + i$          (3)

for 1st order polynomail (k=1),then equation becomes

$X = a_0 + a_1 x + a_2 y$

$Y = b_0 + b_1 x + b_2 y$ (4)

16407

**Israa Hussein and  Nawal K.Ghazal**

Given a coordinate (x,y) in the model parameter.SPOT scenes will be used with two preprocessing levels (1A,1B) fits toMosul city and its surronded regions by using ground control points GCPs taken by GPS device for geometric correction by using ERDAS 2014 program

## RESULTS

SPOT images with assciated data concerned the scene acquisition process which saved in spatial format named CAPformat (spot imag,1998)to applicate any process on these images ,they to be reformatted from CAPformat in to imagine format (ERDASimagine,2014) as showon as in figures (1) and (2).A set of GCPs  positioningchoosing  to applied geometric  correction  process and these points might be positioned on the source (1A,1B) images and their reference points.The Reference GCPs are 23 points  have taken by GPS device (in meter units)  distributed on study area with positions named  which illustrated in table (1). Their points matched with Mosul map scale 100000as shown in figure (3).

The  geometric correction technique is implemented by polynomial model after selection the  UTM projection, spheroid WGS84,Datum WGS84 and 23 GCPs points  distribution on study region  .Figure (5)shows the location of GCPs which appear as green color on the image of the SPOT(1A) for the city of Mosul,while the check points producing the red color.The GCPs which appear as light blue color on the image of the SPOT(1B) for the city ofMosul,while the check points producing as the red color that illustrated in figure (8). Figures (4and7) that containthe(A,B,C,D,E,F,…..) below are illustrated the location of each point for 1A and1Bimages,while thetables (2and6)represent the input  GCPs and their references  for 1Aimage and 1Bimage.The tables (3,4and 5) are calculating the X residual ,Y residual ,check points  RMSE and for 1A  images  respectively .The  results that obtained from 1Brepresenting  the tables (7,8 and 9) which illustrated the X residual ,Y residual, RMSE for check points and total RMSE. After the geometric correction can be obtained the two images which illustrated in figures (6and9)which have the RMSE 0.9 and 1.5 respectively .Then comparing  X-RMSE,YRMSE and total RMSE for 1Aand1B images as shown in table (10).

## DISCUSSION

After applied polynomial model for geometric correction and calculating RMSE show There are many points have low RMSE in both levels (1A,1B) used as check  points notes that X RMSE and RMSE total  in  1B level is lower than 1A level, while Y RMSE in 1A level is lower than its for 1B level.

## REFERENCES

1. Ahokas E.,JaakkolaP., 1990, Interpretability of Spot Data for General Mapping ,European Organization for Experimental Photogrammetric Reseach ,Special Publication, no.24.
2. Cunningham S.,2001,Notes for a Computer Graphics Programming Course ,Computer Science Department ,California State university ,www.cs.csustan .edu/~rsc/cs366f00/frontstuff.pdf
3. ERDAS (a),Erdas Field Guide,1999,5th edition ,ERDAS,Inc., Atlanta,Georgia.
4. Estec ,Exploitation of Chris Datda From The Ppoba Mission For Science and Application ,ESA Scientic Copaign Unit ,Estec 1999 ,Noordwijk,The Netherlands
5. Gugan D.J.and Dowman I.J.,1988, Accuracy and Completeness of Topographic Mapping From Spot Imagery , Photogrammetric Record 12 (72) October ,pp.787-796.
6. Hosseini M.,Amini J., Comparison Between 2Dand3D Transformation for Geometric Correction of Ikonos  Images , http://www.ipi.uni-hannover.de/html /publikationen/2005/ workshop/100-hosseini.pdf.
7. Jacobson K.,1990, Cartographic Potential of Space Image ,International Archives of Photogrammetry and Remote Sensing,28,part 2pp.127-134.

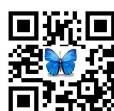**Israa Hussein and  Nawal K.Ghazal**

8.  Jacobson K.,1992, Advantages and Disadvantages of Different Space Images for Mapping ,International Archives of Photogrammetry and Remote Sensing 29,B2pp.162-168.
**9.**  Mikhail E.M., Bethel,J.S.and McGlone,J.C.,2001,Introduction to Modren Photogrammetry ,John Wiley & Sons,inc,479 pwith aCD
10. Priebbenow R., 1986,Cartographic Applications of Spot imagery ,Image utilization ,assessment,results ,images satellite spot ,lacamargue ,France ,and pp.1189-1194.
11. Santhosh,Thirun avukkarasu ,Geometric Correction in High Ressolution Satellite Imagery Using Mathematical Metods : Acase Study in Kiliyar Sub Basin , Global Journal of Computer Science and Technology :Fgraphics &Vision, Volume 14 Issue 1 Version 1.0 year 2014 ,USA

**Table.1.The  GCPs points from GPS and their positions for Mosul city**

| ID | position | Point x (meter) | Point y(meter) |
|----|----------|-----------------|----------------|
| 1 | Al athar | 334282.35 | 4025683.82 |
| 2 | Near al musol airport | 332473.58 | 4020195.89 |
| 3 | Al resala | 329017.89 | 4022826.74 |
| 4 | The forests | 332131.07 | 4026587.83 |
| 5 | Al faisalea | 333755.82 | 4024385.51 |
| 6 | Al muthana | 336574.61 | 4026017.9 |
| 7 | Right side | 332712.35 | 4023004.75 |
| 8 | Al nabi yunis | 334672.7 | 4024208.39 |
| 9 | Public hospital | 330302.37 | 4025307.13 |
| 10 | Bab singar | 330887.45 | 4023634.21 |
| 11 | Adwasa- fourth bridge | 333266.59 | 4022093.17 |
| 12 | Azahuor- hamlet al garar | 336826.98 | 4026489.8 |
| 13 | Asuas cycle | 331478.61 | 4021557.19 |
| 14 | Al yarmouk cycle | 328795.89 | 4023706.03 |
| 15 | Bagdad cycle | 330773 | 4020111.36 |
| 16 | Beauty mss | 336680.47 | 4026911.72 |
| 17 | Near fifth bridge | 332622.14 | 4025444.97 |
| 18 | Near fourth bridge | 335051.36 | 4022877.37 |
| 19 | University tunnel | 333315.72 | 4026939.26 |
| 20 | Al bo seif village | 334696 | 4015826 |
| 21 | Al ruman tal | 328404 | 4020342 |
| 22 | Al kuba village | 334705 | 4030127 |
| 23 | Orta kharab village | 341495 | 4032070 |

**Table 2. Show GCPs points and their reference  for 1Aimage**

| Point ID | Input x | Input y | X ref | Y ref |
|----------|---------|---------|-------|-------|
| GCP #2 | 3311.204 | -3560.673 | 332473.580 | 4020195.890 |
| GCP #3 | 2643.363 | -3387.323 | 329017.890 | 4022826.740 |
| GCP #4 | 2745.039 | -2988.951 | 332131.070 | 4026587.830 |
| GCP #5 | 3138.410 | -3158.968 | 333755.820 | 4024385.510 |
| GCP #6 | 3376.766 | -2957.282 | 336574.610 | 4026017.900 |
| GCP #8 | 3274.534 | -3155.634 | 334672.700 | 4024208.390 |
| GCP #9 | 2609.471 | -3138.410 | 330302.370 | 4025307.130 |

**Israa Hussein and  Nawal K.Ghazal**

| | | | |
|---|---|---|---|
| GCP #11 | 3261.755 | -3373.988 | 333266.590 | 4022093.170 |
| GCP #12 | 3371.210 | -2909.499 | 336826.980 | 4026489.800 |
| GCP #14 | 2544.465 | -3311.760 | 328795.890 | 4023706.030 |
| GCP #16 | 3317.872 | -2873.940 | 336680.470 | 4026911.720 |
| GCP #17 | 2903.943 | -3082.294 | 332622.140 | 4025444.970 |
| GCP #18 | 3428.993 | -3270.089 | 335051.360 | 4022877.370 |
| GCP #19 | 2873.940 | -2933.946 | 333315.720 | 4026939.260 |
| GCP #20 | 3958.488 | -3915.706 | 334696.000 | 4015826.000 |
| GCP #21 | 2766.152 | -3623.456 | 328404.000 | 4020342.000 |
| GCP #22 | 2795.600 | -2620.027 | 334705.000 | 4030127.000 |
| GCP #23 | 3530.114 | -2317.221 | 341495.000 | 4032070.000 |

**Table .3.GCP points with X residual, Y residual and RMSE for 1A image using polynomial model**

| Point ID | X residual | Y residual | RMSE |
|---|---|---|---|
| GCP #2 | 0.145 | -0.342 | 0.372 |
| GCP #3 | 0.323 | 0.165 | 0.363 |
| GCP #4 | 1.349 | 0.566 | 1.463 |
| GCP #5 | 0.427 | 1.391 | 1.455 |
| GCP #6 | -0.697 | 0.156 | 0.714 |
| GCP #8 | -0.926 | -0.885 | 1.281 |
| GCP #9 | 1.047 | -0.100 | 1.052 |
| GCP #11 | -0.653 | -0.368 | 0.750 |
| GCP #12 | -0.402 | -0.172 | 0.437 |
| GCP #14 | -1.453 | 0.112 | 1.458 |
| GCP #16 | -0.620 | -0.244 | 0.666 |
| GCP #17 | -0.116 | -0.458 | 0.473 |
| GCP #18 | 2.604 | 0.063 | 2.605 |
| GCP #19 | -0.629 | -0.507 | 0.808 |
| GCP #20 | 0.104 | 0.298 | 0.316 |
| GCP #21 | -0.914 | -0.234 | 0.944 |
| GCP #22 | 0.756 | 0.252 | 0.797 |
| GCP #23 | -0.484 | 0.110 | 0.496 |

**Table 4. Checkpointswith RMSE**

| point | region | Input x | Input y | X ref | Y ref | X res | Y res | RMSE |
|---|---|---|---|---|---|---|---|---|
| GCP #1 | Al athar | 3102.296 | -3030.066 | 334282.350 | 4025683.820 | 0.041 | -0.081 | 0.090 |
| GCP #7 | Right side | 3113.963 | -3302.315 | 332712.350 | 4023004.750 | 0.223 | 0.196 | 0.297 |
| GCP #10 | Bab singar | 2823.380 | -3278.979 | 330887.450 | 4023634.210 | 0.039 | -0.160 | 0.164 |
| GCP #13 | Asuas cycle | 3070.070 | -3456.218 | 331478.610 | 4021557.190 | -0.078 | -0.042 | 0.089 |
| GCP #15 | Bagdad cycle | 3095.073 | -3600.676 | 330773.000 | 4020111.360 | -0.086 | 0.283 | 0.296 |

**Israa Hussein and  Nawal K.Ghazal**

**Table  5. X RMSE,YRMSE and RMSE TOTAL  used GCPs of polynomial model for 1A image**

| X RMSE | 0.8486 |
|---|---|
| Y RMSE | 0.4321 |
| RMSE TOTAL | 0.9523 |

**Table 6.GCP points with X residual, Y residual and RMSE for 1B image using polynomial model**

| Point ID | Input x | Input y | X ref | Y ref |
|---|---|---|---|---|
| GCP #1 | 3302.000 | -3036.000 | 334282.350 | 4025683.820 |
| GCP #3 | 2817.000 | -3391.000 | 329017.890 | 4022826.740 |
| GCP #4 | 2940.000 | -2991.000 | 332131.070 | 4026587.830 |
| GCP #6 | 3584.000 | -2962.000 | 336574.610 | 4026017.900 |
| GCP #7 | 3301.000 | -3308.000 | 332712.350 | 4023004.750 |
| GCP #8 | 3471.000 | -3162.000 | 334672.700 | 4024208.390 |
| GCP #9 | 2794.000 | -3142.000 | 330302.370 | 4025307.130 |
| GCP #10 | 3005.000 | -3284.000 | 330887.450 | 4023634.210 |
| GCP #11 | 3449.000 | -3382.000 | 333266.590 | 4022093.170 |
| GCP #12 | 3582.000 | -2916.000 | 336826.980 | 4026489.800 |
| GCP #13 | 3249.000 | -3464.000 | 331478.610 | 4021557.190 |
| GCP #15 | 3268.000 | -3607.000 | 330773.000 | 4020111.360 |
| GCP #16 | 3529.000 | -2880.000 | 336680.470 | 4026911.720 |
| GCP #17 | 3097.000 | -3086.000 | 332622.140 | 4025444.970 |
| GCP #18 | 3627.000 | -3277.000 | 335051.360 | 4022877.370 |
| GCP #19 | 3073.000 | -2938.000 | 333315.720 | 4026939.260 |
| GCP #21 | 2931.000 | -3630.000 | 328404.000 | 4020342.000 |
| GCP #22 | 3009.000 | -2621.000 | 334705.000 | 4030127.000 |

**Table 7 .GCP points with X residual, Y residual and RMSE for 1B image using polynomial model**

| Point ID | X residual | Y residual | RMSE |
|---|---|---|---|
| GCP #1 | -0.066 | 1.002 | 1.004 |
| GCP #3 | 0.073 | -0.412 | 0.418 |
| GCP #4 | 0.312 | -0.392 | 0.502 |
| GCP #6 | 0.867 | -0.940 | 1.279 |
| GCP #7 | 0.525 | -0.203 | 0.563 |
| GCP #8 | 0.047 | -0.717 | 0.719 |
| GCP #9 | 0.636 | 0.468 | 0.790 |
| GCP #10 | 0.610 | 0.235 | 0.654 |
| GCP #11 | -0.747 | 0.560 | 0.934 |
| GCP #12 | -0.323 | 0.745 | 0.812 |
| GCP #13 | 0.297 | 1.195 | 1.231 |
| GCP #14 | -0.276 | -0.104 | 0.295 |
| GCP #15 | 0.194 | -0.680 | 0.707 |
| GCP #16 | -0.390 | 0.636 | 0.746 |
| GCP #17 | -0.231 | -0.903 | 0.933 |
| GCP #18 | 0.185 | -0.455 | 0.492 |
| GCP #19 | -0.576 | 0.180 | 0.603 |
| GCP #21 | -0.662 | 0.463 | 0.808 |
| GCP #22 | -0.697 | -0.419 | 0.813 |

**Table 8. Check points with RMSE**

| point | region | Input x | Input y | X ref | Y ref | X res | Y res | RMSE |
|-------|--------|---------|---------|-------|-------|-------|-------|------|
| GCP #2 | Near al mosull airport | 3491.000 | -3569.000 | 332473.580 | 4020195.890 | -0.015 | -0.142 | 0.142 |
| GCP #5 | Al faisalea | 3333.000 | -3163.000 | 333755.820 | 4024385.510 | 0.352 | -0.151 | 0.383 |
| GCP #14 | Al yarmouk cycle | 2718.000 | -3315.000 | 328795.890 | 4023706.030 | -0.276 | -0.104 | 0.295 |
| GCP #20 | Al bo seif village | 4136.000 | -3928.000 | 334696.000 | 4015826.000 | -0.264 | -0.095 | 0.280 |
| GCP #23 | Orta kharab village | 3771.000 | -2321.000 | 341495.000 | 4032070.000 | 0.148 | 0.129 | 0.196 |

**Table  9. X RMSE,YRMSE and RMSE TOTAL used GCPs of polynomial model for 1B image**

| X RMSE | 0.4763 |
|--------|--------|
| Y RMSE | 0.6493 |
| RMSE TOTAL | 0.8053 |

**Table 10. Show GCPs error, X RMSE, Y RMSE and RMSE TOTAL**

| GCPs error | 1A level | 1B level |
|------------|----------|----------|
| X RMSE | 0.8486 | 0.4763 |
| Y RMSE | 0.4321 | 0.6493 |
| RMSE TOTAL | 0.9523 | 0.8053 |
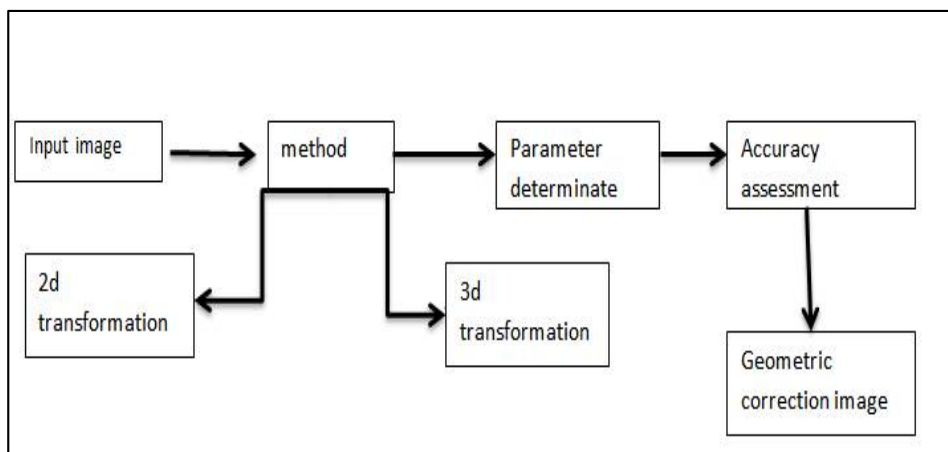


**Figure 1. diagram for geometric correction process [ Hossenini  et al., 2005]**

**Israa Hussein and  Nawal K.Ghazal**
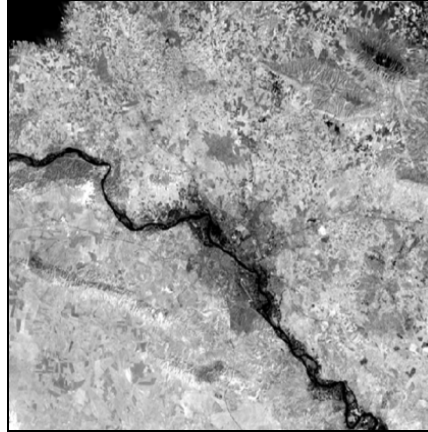


**Figure 2.Showing the study area of 1A image of SPOT satellite**



**Figure 3. Showing the study area of 1B image of SPOT satellite**



**Figure 4. Mosul map scale 100.**

16413
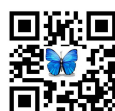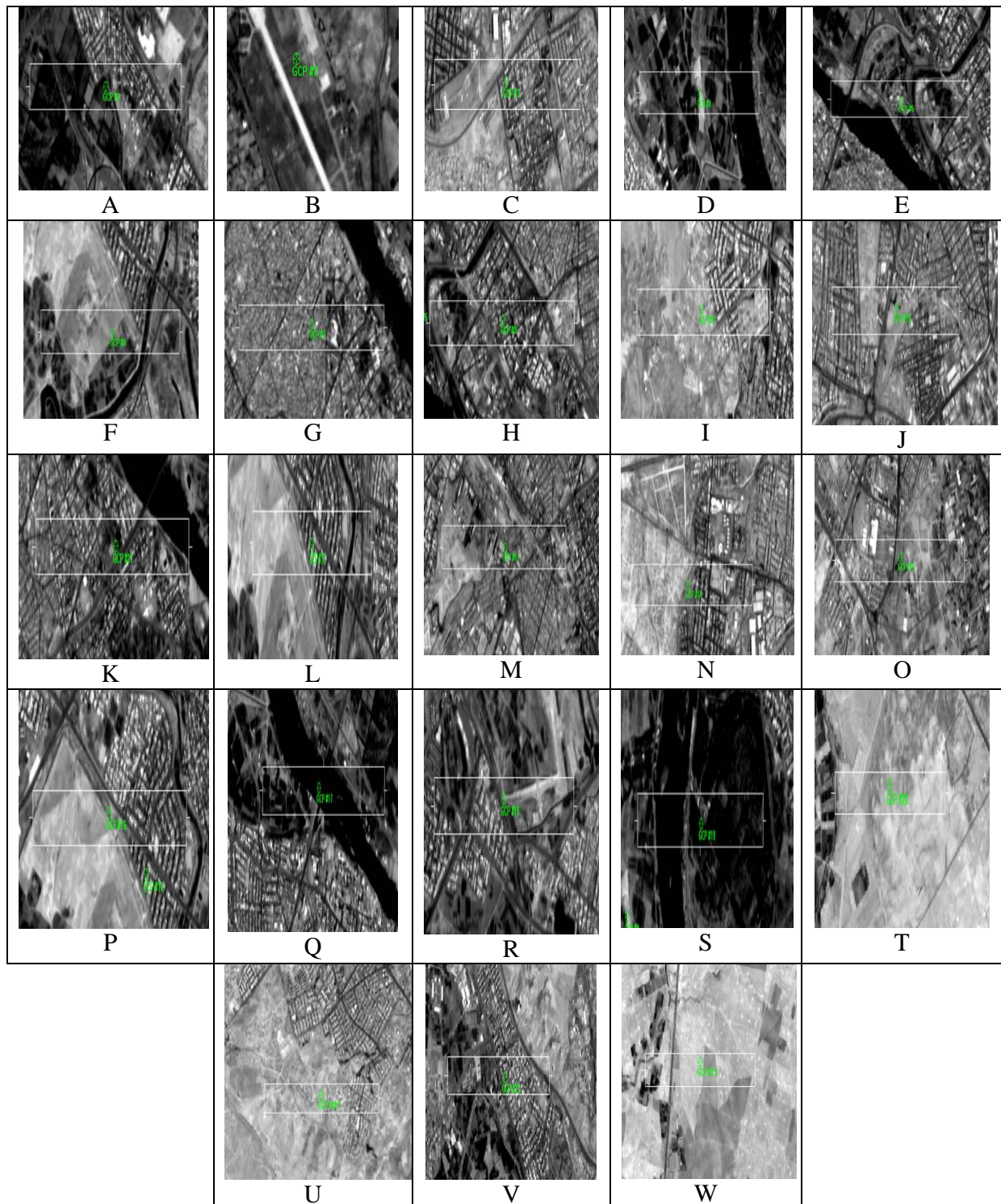
**Figure 5.Show the location of each GCPs (A,B,C,D,E,F….)**

**Israa Hussein and  Nawal K.Ghazal**
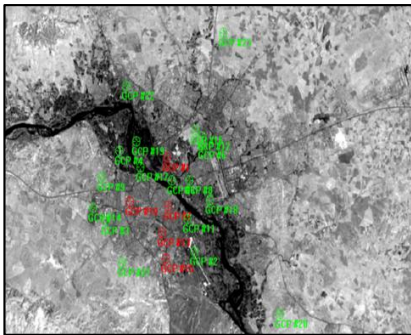


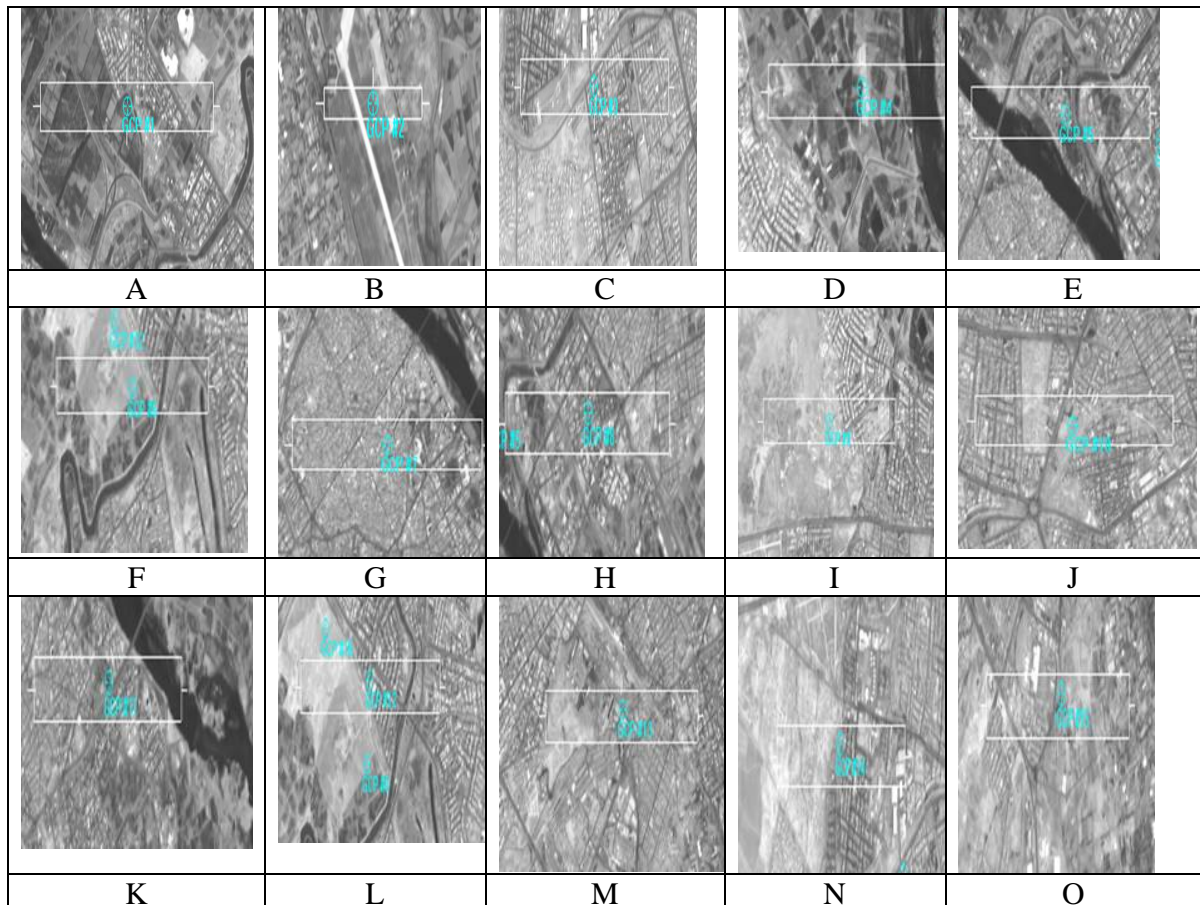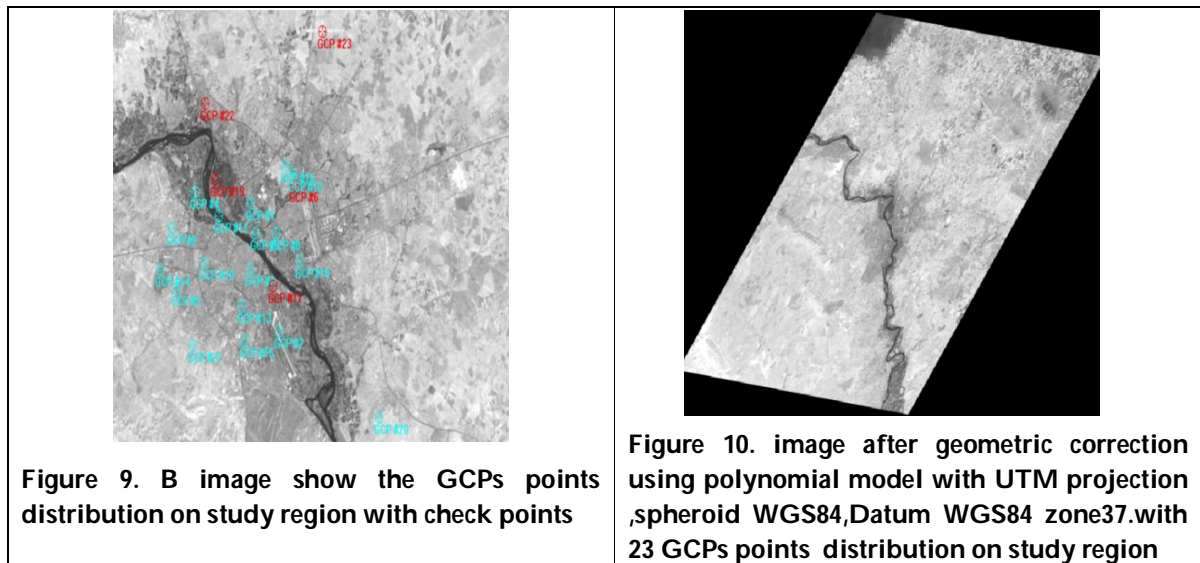**Figure 6.A image show the GCPs points distribution on study region with check points**
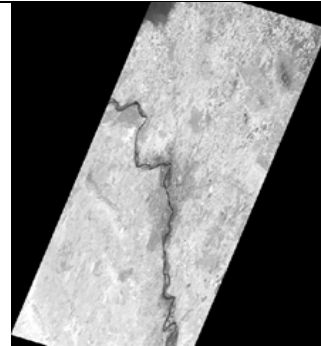


**Figure 7.A image after geometric correction using polynomial model with UTM projection ,spheroid WGS84,Datum WGS84 zone37.with 23 GCPs points  distribution on study region**



| | | | | |
|---|---|---|---|---|
| A | B | C | D | E |
| F | G | H | I | J |
| K | L | M | N | O |

**Israa Hussein and  Nawal K.Ghazal**



| P | Q | R | S | T |



| U | V | W |
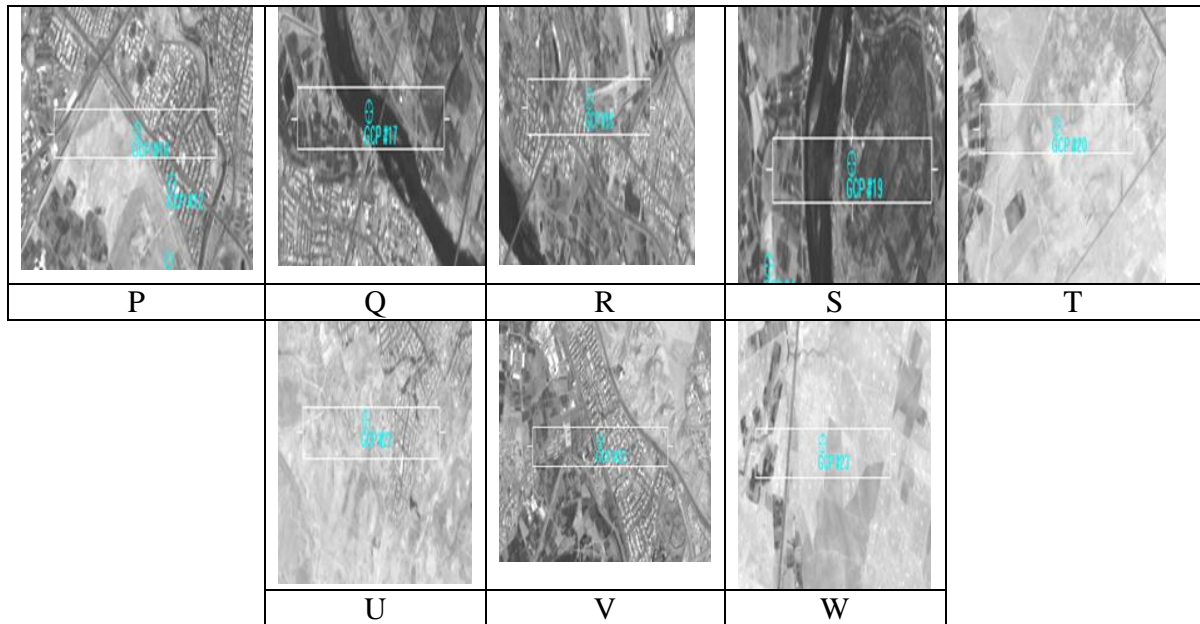
**Figure  8.producing the GCPs points with their location for each points** .



**Figure 9. B image show the GCPs points distribution on study region with check points**



**Figure 10. image after geometric correction using polynomial model with UTM projection ,spheroid WGS84,Datum WGS84 zone37.with 23 GCPs points  distribution on study region**

**RESEARCH ARTICLE**

# Radiological Assessment of Hazard Index for Clay Sample in Iraq

Akram M. Ali and Iman E. Turki*

Department of Physics, College of Sciences, University of Anbar, Iraq.

*Address for Correspondence
**Iman E. Turki**
Department of Physics,
College of Sciences,
University of Anbar, Iraq.
E-Mail: hommam2002@yahoo.com

## ABSTRACT

The concentration of the radiation dose was calculated in several types of Iraqi clays obtained from quarries at AL-Rutba region, west of Anbar province, Iraq, using sodium Iodide Thallium [NaI (TI)] detector. The clay samples are main raw material including in the industry of ceramics, bricks, cement etc... The average specific activity value of $^{238}U$, $^{232}Th$ and $^{40}K$ and radium equivalent activity ($Ra_{eq}$) were calculated The indoor and outdoor of gamma dose rate have been computed and compared with worldwide limit. So in safety range we found all results in the healthy range.

**Keywords:** Radioactivity, Radiation Hazard, Clay, Iraq.

## INTRODUCTION

The rock-forming minerals has its characteristic background radioactivity due to disintegration of potassium, uranium and thorium that refer to all rocks have a natural radioactivity. It is important to know the radioactivity and investigate the up normal levels, where higher levels indicated there is addition of these elements to rocks by a geological process while the lower indicted a removal of these elements by for example weathering leaching process. The main problem is to find the anomalous level that will be effect the human. Natural uranium (half-life 4.49 x $10^9$ y) are transformed by a series of a Mona lies that emit alpha, beta particles and gamma ray until they reach the stable lead element (Skvar, Skvar and Golovchenko, 2003). The report of the United Nations on natural radiation sources confirms the importance of knowing the level of natural radiation activity in the environment in order to assess the exposure of human radiation (UNSCEAR, 1982). The samples from the quarries and enterer in many industries contain quantities of radiation activity inside them, and these radiations has several risk including tuberculosis and lunch cancer and other disease by swallowing or inhaling a mounts of free silica during mixing mud for example. Many searchers measurement the naturel radioactivity in the most of the world such as for clay samples in Tiruvannamalaidistrict, Tamilnadu, India by using NaI(TI) detector. The results had shown that the activity concentration of these radio nuclides is compared with word average values (Raghu et al.,2016). Concentrations of

16417

**Akram M. Ali and Iman E. Turki**

$^{238}U$, $^{232}Th$ and $^{40}K$ in virgin soil and agricultural in Najaf city south western part of Iraq by using NaI (TI) detector given values lower than the worldwide average (Hussain ,et al., 2017). Determined the natural radioactivity in clays was used as raw materials (bricks, ceramic, cement, etc.) in Albanian all results were safety and within worldwide average (Anastas, 2000). As clays is the main material in different products as building materials, it was exhibit radiation levels of uranium, thorium and potassium and the known these levels are very important to have the main radiological hazards to workers in the quarries. The work give a good understanding of the radionuclide distribution in the quarries compare the results with the global average value of the united nations ( Report,1988).

## MATERIALS AND METHODS

Samples collected from the main quarries at different dimensions, for the purpose of study the a mount of radiation activity issued, from the AL-Rutba region west of Anbar province- Iraq.. Samples have different type and color with total of (9) sample collected from (7) quarries, Fig.1.After samples taken in polythene bags and dried the wet samples at room temperature and sampling configuration to grind in porcelain mill well to convert it into a powder with grain size 4mm (4000 microns) and began to put a quantity of each type of samples (500 grams) separately inside the [NaI(TI)] detector four a full hour to reach secular equilibrium. Using the count spectra for each sample, the activity determine in Bq/kg.

## RESULTS AND DISCUSSION

### Specific activity

It is radiation efficiency during the mass unit of radioactive material for the calculated for each of the $^{238}U$, $^{232}Th$ and $^{40}K$ radionuclides by using relation (Yousuf and Abullah, 2015).

$$A \ (Bq/kg) = \frac{N}{\varepsilon(E_\gamma) \cdot I_\gamma(E_\gamma) \cdot M \cdot t}$$ ………………………..1

Where $N$: count of gamma rays, $\varepsilon (E_\gamma)$: The efficiency of gamma rays detector, $I_\gamma (E_\gamma)$: The relative intensity of each energy of the irradiated source, M: Mass the form in unity *(Kg)*, $t$: The time of count *(3600min)*.

Table 1 shown the mean results of the specific activity for all samples. The highest activity value of ($^{238}U$) is (29.540*Bq/kg*), while the lowest (15.730*Bq/kg)*, with an average value of (23.449±3.9*Bq/kg*). These results in all samples were less than the recommended value (35*Bq/kg*) given by (UNSCEAR, 2000), Fig. 2. For ($^{232}Th$), maximum value is (31.290*Bq/kg*), while the minimum is (15.430*Bq/kg*), with an average value of (26.346±2.5*Bq/kg*) and these values were less than the recommended value (30*Bq/kg*) given by (UNSCEAR, 1993) except (R.R.I) was more than recommended. The variation in these values in uranium and thorium reflect the thorium accompanies uranium in the magmatic series (Moura et al., 2011). Thorium activity concentration is higher than uranium one due to difficultly of thorium migration from the minerals crystals lattice because of its greater ionic radius, besides the uranium have a great dispersions and nobility that causing fall back from the crystals.

The present results of specific activity of ($^{40}K$) have shown that values of specific activity for ($^{40}K)$ in all samples were less than the recommended value of (400*Bq/kg*) given by (UNSCEAR, 2000) as it is shown in the Fig. 2. The clay content a main minerals that consider as main sources of potassium either released from the surface of clay particle or absorbed inside layer crystal lattices as it is has large size that cause fixed potassium ion . So this content may appear as high values as our samples in calculation.

**Akram M. Ali and Iman E. Turki**

### Radium equivalent activity (Ra$_{eq}$)

To represent the activity concentrations of $^{238}U$ ($^{226}Ra$), $^{232}Th$ and $^{40}K$ by a single quantity, which takes into account the radiation hazards associated with them, a common radiological index has been introduced. The index is called radium equivalent activity ($Ra_{eq}$) which is used to ensure the uniformity in the distribution of natural radionuclides $^{238}U$ ($^{226}Ra$), $^{232}Th$ and $^{40}K$ and it is given by the following relation (*Vosniakos*, Zavalaris and Papaligas, 2003)

Ra$_{eq}$ *(Bq/kg)* = A$_U$ + 1.43A$_{Th}$ + 0.077A$_K$...................................................2

Where, A$_U$ , A$_{Th}$ and A$_K$ are the specific activities concentrations of $^{238}U$, $^{232}Th$ and $^{40}K$ in *(Bq/kg)* units. The highest value (88.439 *Bq/kg*) and the lowest value (48.850*Bq/kg*), with mean value (78.482±8.01 *Bq/kg*), as it shown in Table 2, are presents that radium equivalent activity in all samples were less more than the recommended safe limit of (370 *Bq/kg*) (OECD, 1979), as its show in Fig. 3, and this refer to no significant radiological hazard for all samples.

### Annual effective dose equivalent

The estimated annual effective dose equivalent received by a person was obtained by using a conversion factor of (0.7*Sv/Gy*), which was used to convert the absorbed rate in air to human effective dose equivalent with an outdoor occupancy of (20%) and (80%) for indoors and by using the following relations (UNSCEAR, 1993) :

(AED) $_{in}$ *(mSv/y)* =D$_\gamma$ *(nGy/h)* × $10^{-6}$×8760 h/y × 0.80 × (0.7 Sv/Gy)............................3

(AED)$_{out}$ *(mSv/y)*=D$_\gamma$ *(nGy/h)* × $10^{-6}$ × 8760h/y × 0.20 ×(0.7 Sv/Gy).

The total effective dose, *A$_{tot}$= A$_{in}$ + A$_{out}$*, are ranged from 0.139 to 0.249 and still less than (1) that given by (UNSCEAR, 2000), Fig. 4. All results are shown in Table 2. This indicate that the doses come from ionize radiation that may came from radiation of uranium and thorium are less than the recommended dose level for exposure of the worker in the quarries.

### Absorbed gamma dose rate (D$_\gamma$)

Outdoor air absorbed gamma dose rate ($D_\gamma$) in (*nGy/h*) due to terrestrial gamma rays at (1 m) above the ground surface which can be computed from specific activities using the following relation with main coefficients:

D$_\gamma$ *(nGy/h)* = 0.462A$_U$ + 0.604A$_{Th}$ + 0.0417A$_K$........................................................4

The value that estimated for absorbed dose rate (*D$_\gamma$)* was found in range 40.650 to 22.574 *nGy/h* with average value of 36.147±3.6 *nGy/h*, as it is shown in Table 2. The present results shows that were less than the recommended value of 55 *nGy/h* for the absorbed gamma dose rate given by (UNSCEAR, 2000), Fig. 5.

### Activity concentration index (I$_\gamma$)

This index used to estimate the gamma radiation that combined with concentration of specified natural radionuclide which calculated by (Mohammed and Jazzar,2013):

$$I_\gamma = \frac{A_U}{150} + \frac{A_{Th}}{100} + \frac{A_K}{1500} \qquad \le 1...........................................5$$

16419

The highest value of activity concentration index was found in (R.W.K) sample which was equal to (0.319), while the lowest value of activity concentration index was found in (R.R.C) sample which was equal to (0.177), with an average value of (0.285±0.028) as it is shown in Table 2. All samples has less than the recommended value of (1) for the activity concentration index given by (UNSCEAR, 2000), Fig. 6.

**External and internal index (H)**

The internal hazard index ($H_{in}$) gives the internal exposure to radon that lead to cancer and short-lived progeny of radon. The internal hazard is given by the relation (Jose et al. , 2005):

$$H_{in} = \frac{A_U}{185Bq/kg} + \frac{A_{YH}}{259Bq/kg} + \frac{A_K}{4810Bq/kg} \leq 1 \quad \text{..............6}$$

To give the external gamma radiation jet from clay sample one must evaluate the external hazard index that given by relation (Beretka & Matthew, 1985):

$$H_{ex} = \frac{A_U}{370Bq/kg} + \frac{A_{TH}}{258Bq/kg} + \frac{A_K}{4810Bq/kg} \leq 1 \quad \text{...............7}$$

The internal and external hazard values must be less than unity in order to keep the radiation hazard to be pettiness. The calculated values of two indexes are shown in Table 1and Fig.7. Radioactivity may cause harm to the population if the calculated value is higher the unity, so the results show values bellow limit for two indexes.

## CONCLUSIONS

Form the observation a fall the results obtained and comparing them with the global limit it was found that the specific effectiveness values $^{238}U$ and $^{40}K$ were within the permissible limits ($35Bq/kg$) to$^{238}U$ and ($400Bq/kg$) $^{40}K$ [8], as for $^{232}$Th where there was a value for a specimen higher than the limit which is ($30Bq/kg$) UNSCEAR (2000), this is due to the geological nature of the studied area. This study also showed that all other results of the absorbed dose, the annual effective dose and the radium efficacy of the equivalent of the studied samples were all of which are within the internationally permitted limits are not dangerous to living organisms, andthe internal and external Hazard present in most of the studied are relativity lower that the average of world wide, as it acceptable dose limits of the UNSCEAR (2000), it can therefore be inferred from the results obtained that the people living in AL-Rutba area generally receive acceptable dose.

## REFERENCES

1.  Anastas Dodona, (2000). Estimation of the natural radioactivity of the Albanian clays. *Journal of the Balkan Geophysical society.* vol. 3, No.2, pp. 7-12,
2.  Hayder H. Hussain ,et al. (2017). Natural radioactivity levels of agricultural and virgin claysoil samples at AL-Najaf Governorate", *American Journal of research.* No.8-9(8-9), (2017).
3.  Jose A, Jorge J, Cle0macio M, Sueldo V and Romilton D. S. (2005). Analysis of the K-40levels in soil using gamma spectrometry. *Brazilian archives of biology and technology,* 48, 221-228.
4.  *Mohammed K. and Jazzar M.M. (2012). Natural Radioactivity Levels and Estimation of Radiation Exposure in Environmental Soil Samples from Tulkarem Province-Palestine. Open Journal of Soil Science. **2**,No.1,12-16.*

**5.** Skvar R. I, Skvar J and Golovchenko A. N. (2003).Nuclear tracks: present and future perspectives. Radiation measurements, 36(1-6): 83-88.

6. UNSCEAR. (1982). Ionizing radiation sources and Biological effects. Report to the General Assembly. United Nation. New York: United Nation Scientific Committee on Effects of Atomic Radiation..

7. UNSCEAR. (1988). Sources, Effects and risks of Ionizing Radiation. Report to the General Assembly, with Annexes. , New York: United Nation Scientific Committee on Effects of Atomic Radiation.

8. UNSCEAR. (1993). Sources and Effects of Atomic Radiation. Report to General Assembly. New York: United Nation Scientific Committee on Effects of Atomic Radiation.

9. UNSCEAR. (2000). Report to the General Assembly. Annex B: Exposures from Natural Radiation Sources. New York: United Nation Scientific Committee on Effects of Atomic Radiation.

10. Y. Raghu, R. Ravisnkar, A. Chandrasekaran, P. Vijaygopal and B. Venkatraman. (2016). Assessment of natural radioactivity in clay samples of Tiruvannamalaidist,Tamilnadu, India and their associated radiation Hazard. INT. J. Chem. Sci.: 14(S1), 235-240. ISSN0972-768X.

11. Yousuf R.M. and Abullah M. K.O. (2015). Measurement of natural radioactivity in soil collected from the eastern of Sulaimanyi governorate in Kurdistan-region, Iraq. ARPN Journal of Science and Technology, 3, No.7,749-757.

12. Vosniakos F, Zavalaris K and Papaligas T. (2003). Indoor concentration of natural radioactivity and the impact to human health. Journal of Environ. Protect. Ecol., 4, No.3, 733-737.

**Table 1. Activity concentration of Radionuclide and Hazard Indexes (Internal, External)**

| Code samples | Samples name | Activity concentration(Bq/kg) | | | Hazard indices(Bq/kg) | |
|---|---|---|---|---|---|---|
| | | U-238 | K-40 | Th-232 | $H_{in}$ | $H_{ex}$ |
| R.R.C | Rutba Red Clay | 15.730 | 143.570 | 15.430 | 0.174 | 0.132 |
| R.Z.S | RutbaZfl al-selka | 17.080 | 243.820 | 27.820 | 0.250 | 0.204 |
| R.W.K | Rutba White Kaolin | 29.540 | 231.550 | 28.720 | 0.319 | 0.239 |
| R.R.I | Rutba Red Iron | 23.420 | 233.250 | 31.290 | 0.296 | 0.233 |
| R.F | RutbaFeldspare | 27.320 | 173.760 | 27.530 | 0.290 | 0.216 |
| R.A.C | RutbaAmij Clay | 23.680 | 288.910 | 26.820 | 0.292 | 0.228 |
| R.W.C.C | Rutba White Clay colored | 25.230 | 183.910 | 29.210 | 0.287 | 0.219 |
| R.W.C.W | Rutba White Clay Woolen | 18.760 | 202.430 | 28.050 | 0.252 | 0.201 |
| R.R.C.C | Rutba Red Clay Colored | 27.370 | 263.210 | 26.810 | 0.306 | 0.232 |
| Ave | _ | 23.449± 3.9 | 225.439 ± 37.6 | 26.346 ± 2.5 | 0.275± 0.032 | 0.212 ± 0.022 |
| SD | σ | 11.82 | 4.5 | 46.17 | 0.043 | 0.032 |

**Table 2. Main hazard indices that calculated for clay samples.**

| Code samples | Samples name | Ra$_{eq}$ (Bq/kg) | D$_\gamma$ (nGy/h) | Effective dose (mSv/y) | | | I$\gamma$ (Bq/kg) |
|---|---|---|---|---|---|---|---|
| | | | | AED$_{in}$ | AED$_{out}$ | AED$_{tota}$ | |
| R.R.C | Rutba Red Clay | 48.850 | 22.574 | 0.111 | 0.028 | 0.139 | 0.177 |
| R.Z.F | RutbaZfl al-selka | 75.637 | 34.862 | 0.171 | 0.043 | 0.214 | 0.277 |
| R.W.K | Rutba White Kaolin | 88.439 | 40.650 | 0.199 | 0.050 | 0.249 | 0.319 |
| R.R.I | Rutba Red Iron | 86.125 | 39.446 | 0.194 | 0.048 | 0.242 | 0.312 |
| R.F | RutbaFeldspar | 80.067 | 36.496 | 0.179 | 0.045 | 0.224 | 0.287 |
| R.A.C | RutbaAmij Clay | 84.279 | 39.187 | 0.192 | 0.048 | 0.237 | 0.309 |
| R.W.C.C | Rutba White Clay colored | 81.161 | 36.968 | 0.181 | 0.045 | 0.226 | 0.291 |
| R.W.C.W | Rutba White Clay Woolen | 74.459 | 34.051 | 0.167 | 0.042 | 0.209 | 0.270 |
| R.R.C.C | Rutba Red Clay Colored | 85.975 | 39.814 | 0.195 | 0.049 | 0.244 | 0.303 |
| Ave | - | 78.482 ± 8.01 | 36.147 ± 3.6 | 0.177 ± 0.018 | 0.044 ± 0.005 | 0.220 ±0.0115 | 0.285 ± 0.028 |
| SD | Standard deviation | 12.037 | 5.53 | 0.027 | 0.006 | | 0.043 |
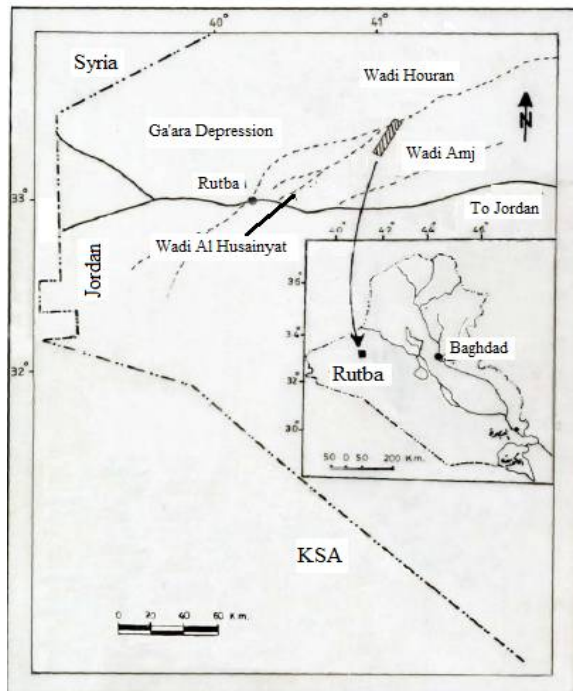


**Fig.1. Represented the region of clay samples, west of Iraq.**

**Akram M. Ali and Iman E. Turki**
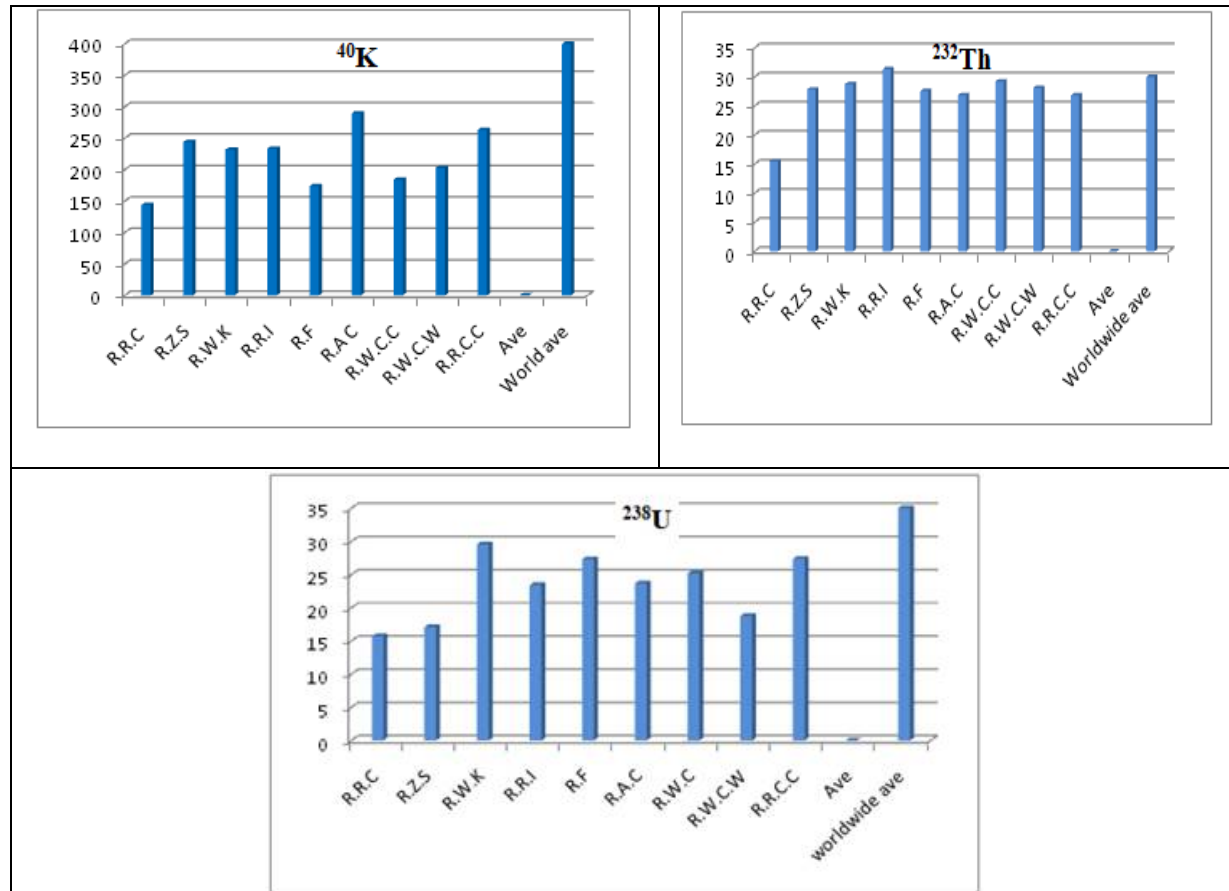
**Fig .2.$^{238}U$, $^{232}Th$ and $^{40}K$ concentration in samples.**
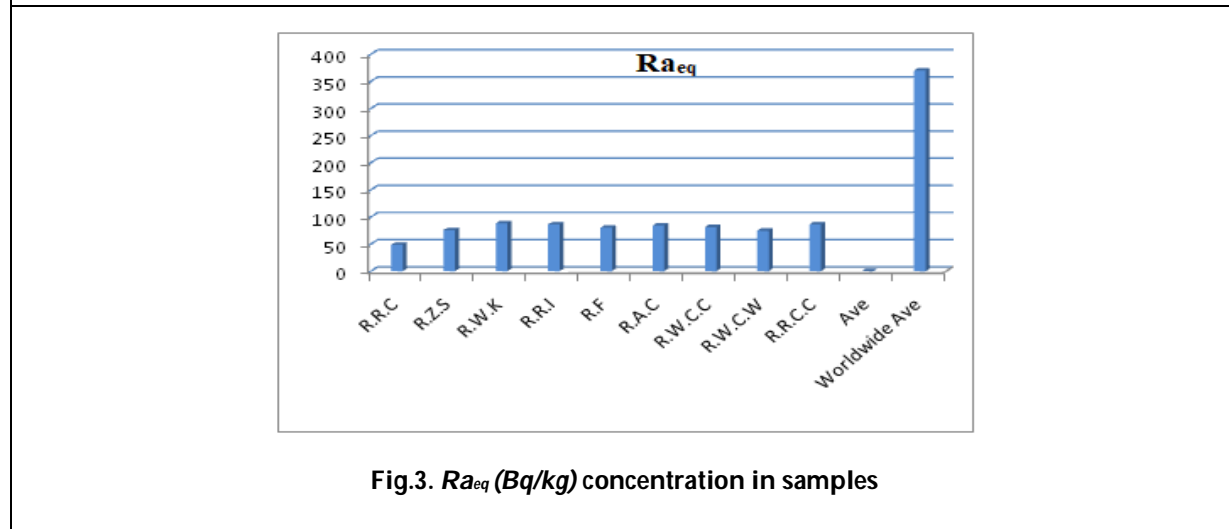


**Fig.3. $Ra_{eq}$ (Bq/kg) concentration in samples**

**Akram M. Ali and Iman E. Turki**
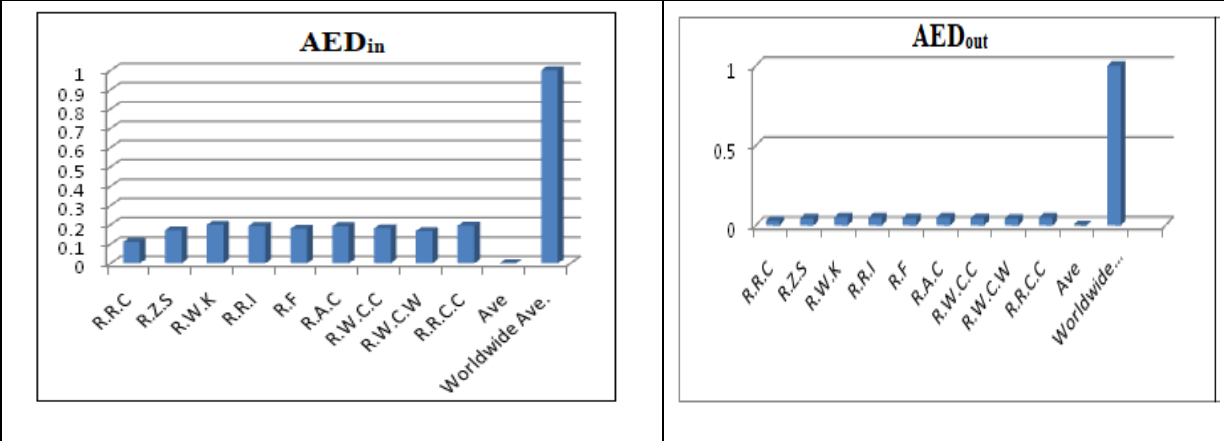


**Fig.4.Indoor and outdoor Annual Effective Dose Equivalent.**
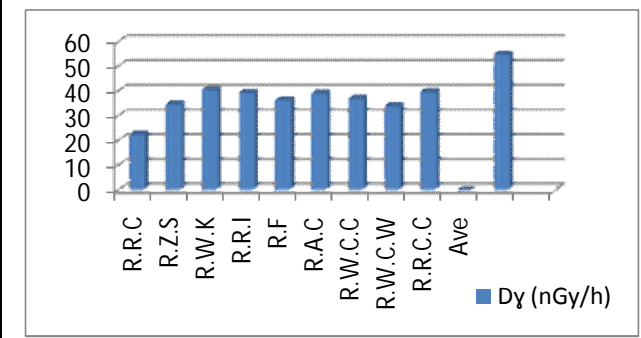


**Fig. 5. Absorbed dose rate ($D_\gamma$).**
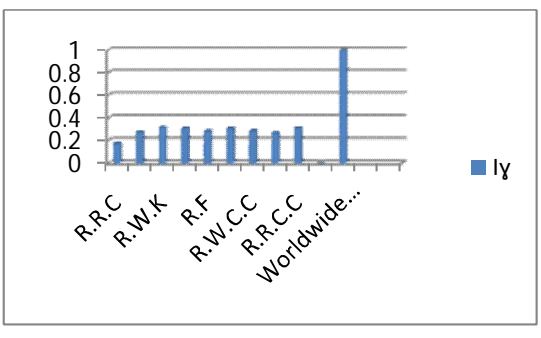


**Fig.6. Activity concentration Index ($I_\gamma$).**
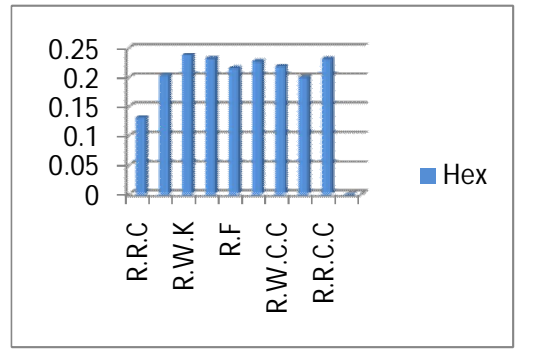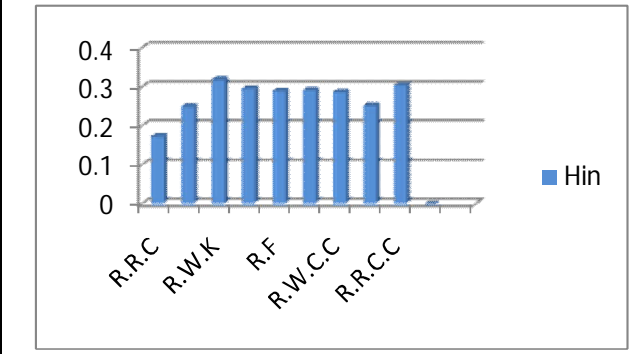


**Fig. 7. Internal and External Hazard Index.**

**RESEARCH ARTICLE**

# Socio-Economic Impacts of Afghan Refugees on the Indigenous Population of Balochistan

Muhammad Yaseen[1]* and Kaneez Fatima[2]

[1]PhD Student, Department of Sociology, University of Karachi, Karachi, Pakistan.
[2]Assistant Professor Department of Sociology, University of Karachi, Karachi, Pakistan.

*Address for Correspondence
**Muhammad Yaseen**
PhD Student,
Department of Sociology,
University of Karachi,
Karachi, Pakistan.
Email: yaseendashti.soc@gmail.com

**ABSTRACT**

The present research examines the socio economic impact of Afghan refugees on the indigenous population of Balochistan. The protracted refugees generated drastic changes in the socio-economic, environmental, political and cultural aspects on the host communities. The factors included in the study were; health, education, economic, shelter, social disorder, insecurity, unemployment, spread of arms, cheap labouring.Universe of the study was Balochistan. Calculated sample of the study was 770. Stratified proportionate sampling was used for the distribution and allocation of the response unit. The techniques for the data collectionwas a structured questionnaire for the local population. SPSS was used to analyse the data. Chi square test and phi values were used to examine the relationship among the bivariate tables and their significance of the relationships. It is found that protracted refugees leave out drastic impacts on the local population socially and economically. As their health, education, economic activities, water and sheltering are extensively affected by the refugees as well as the refugees insecure the local people in their own residential areas.

**Keywords:** Refugees, social impacts, economic impacts, social disorder, insecurity.

## INTRODUCTION

Refugees, one of the key factor in the distribution and composition of the population growth in a country and leave out drastic changes in the social, economic, environmental, political and cultural aspects of the host communities. However, the effects on the mentioned aspects are seemingly insufficiently documented in the local, national and international levels as well, mainly in the third world countries because the data required for the assessment of

impacts has never been collected or published sufficiently, mainly the negative impacts of protracted refugees. Though the protracted refugees in poor developing countries are considered burdens and are the key actors bringing out social changes in the country.According to the 1951 Convention Relating to the Status of Refugees ("Refugee Convention"), a refugee is a person "who owing to a well-founded fear of being persecuted for reasons of race, religion, nationality, membership of a particular social group, or political opinion, is outside the country of their nationality, and is unable to or, owing to such fear, is unwilling to avail him/herself of the protection of that country". (UN, 2009).

Worldwide, 68.5 million people were displaced forcefully owing to oppression, conflict, war or generalized violence by the end of 2017.Hence, the record of the forcibly displaced population still remained at a high record in 2017 as well. In spite of this, forcefully displaced population were 68.5 million and the refugee population was 25.4 million.From this 25.4 million refugees, 19.9 million refugees are under the mandate of UNHCR and the remaining 5.4 million Palestine refugees come under the mandate of URWA. Internally Displace people are 40.0million and asylum seekers are 3.1 million. (UNHCR, 2018).According to UNCHR official webpage, 1,395,592 Afghan refugees are registered in Pakistan till August 2018. Among them 801,221 lives in KPK, 319,242 lives in Balochistan, 161,042 lives in Panjab, 63,104 in Sindh, 33,340 in Islamabad, 13,735 in FATA, 3,903 in Azad Jammu and Kashmir and 5 in Gilgit Baltistan. (UNHCR, 2018 August).

Indeed, the arrival of refugees create socio-political divisions, weaken the territorial sovereignty, threaten the local balance of power in host communities, and so on. These factors result in human rights violation, institutional breakdown and put strains on the local and national economy such as an increase in prices, insufficient provision of social services, overuse of existing infrastructure, fierce competition for jobs in the labour markets of host communities have a detrimental effect on wages and employment opportunities. Crowding of labour markets and schools also reduces the opportunity, causing crime, increasing the likelihood of offenses in host communities. Besides this, the security and military issues have disabled the government to provide basic services resulting in an insufficient and ultimate increase in inequality and leading to the deterioration of social cohesion. Other factors include; formation of armed groups, economic incentives for dissidence, unprotected borders subject to smuggling of weapons and the spread of transnational networks, and an overstrained security institution that cannot cope with the challenges brought upon by the flow of displaced persons (UN, 2015).

Afghans, who sought refuge in Pakistan after the Soviet invasion of Afghanistan are still living in Pakistan. Among the Afghans 70% are uneducated and even they do not show interest in their children's education. They work for lower wages than Pakistanis. These labours are hired in business, transport and construction sector. Beside this, Afghans who live in Pakistan do not pay taxes. Afghan trades have earned billions and not paying a penny in taxes. They have put the heavy burden on the local businessmen and as well as the revenue department. In addition, the political instability, energy crises, high rate of unemployment and tense relationships between the Pakistan and Afghanistan were the causes. Afghan refugees are considered to be extra pressure on the society and economy of Pakistan.Furthermore, the Afghans are not only involved in mafias, like drugs and arms trafficking into Pakistan but also a large number of Afghans are involved in the culturally unacceptable issues like paedophilia and human trafficking through the coastal belt of Balochistan(Khan, 2016).

Balochistan hosts the second biggest refugees' population in the country and facing different issues due to the refugees. Refugees influx kept the province of Balochistan in a transitional stage of demographic change and as well as left out the diverse impact on the local people of Balochistan. Because the refugees affected the indigenous population socially, economically, culturally, environmentally. Moreover, the influx of refugees increased child labour, crime ratio, environmental pollution in the Balochistan. They also widely disrupted the social system of the province with the spreads of arms and drugs. Besides these all, the refugees also increased the levels of insecurity, alienation, and tensions among the indigenous people of Balochistan. Furthermore, the bulk of Afghan refugees affected the livelihoods of local people and increased the demands of the rentals and facilities, hiked the foodstuffs

**Muhammad Yaseen and Kaneez Fatima**

prices in the local markets. The refugees provided cheap labour as compared to the local labours which had affected the lives of local people. Indeed, the Afghan is considered to be a burden for the indigenous population of Balochistan. And the socio-economic reports of the districts and the experiences of the indigenous people can be studied to examine the pre and post situations of the regions.

**Literature Review**

Watol & Assefa (2018) found that refugees affect the host population on the social and economic level. Socially the host community got knowledge and skill but promoted crime and theft. Economically the host community benefitted by selling the local products and buying goods and services but food prices hiked suddenly.Baloch, Amdadullah. et al. (2017) found that The economic growth of Pakistan was largely affected by the Afghan refugee. This bulk arrival of the refugee affect is short run and long run both and also lower real economic activity of the country. Finally, hosting refugees can never be a positive point to the economy of Pakistan.Borthakur; Anchita (2017) found that Refugees had brought a great alteration in the demography. This has led to the appearance of episodic ethnic and sectarian violence within Pakistan. The worsening situation of the security, with an increasing number of armed groups upraising arms against the state of Pakistan. And the country is also concerned with the growth of criminal activities and the increasing number of drug addicts.

From the initial phase of Afghan refugees in the country, drug trafficking became more common. And Afghans are also involved in militant and terrorist activities in Pakistan.Taha, S.M., &Aamir, A. (2012) explored that The socio-economic impacts largely lie in the city of Peshawar by the Afghan refugees. The researchers found further that there was a tough competition between the local inhabitants and refugees on the ground realities. As family values, the pattern of social interaction, gender, and demography had profoundly affected by the influx of refugees.World Development Report (2011) explored that Economic, social, environmental, political and security impacts are experienced by the nations who hosts refugees for a long term. The economic impacts of refugee presence on neighbouring countries have been both negative (e.g. uncompensated open consumption and weight on the financial framework) and positive (e.g. invigorated neighbourhood economies by expanding the span of nearby markets and lessening ware costs).

The social effects of displaced people likewise setting explicit incorporate disparities among outcasts and non-exiles and the subsequent social pressures, which can be diminished by improvement ventures focusing on the two evacuees and the host networks.The development of renegade social networks and spreading of violence, spreading of arms in an extensive scale, warriors, and belief systems strong to war and arrangement of common strains are the negative political and security effects of the evacuees in a nation. The existence of substantial inundations of displaced people has additionally been related with ecological effects ashore, water, normal assets, and ghetto development. Rahman, U (2010) explored that refugees created security dilemma and strain for the host country. Close to this they are associated with arms and drug dealing for the assets and have solid coordination with Islamic fanatics' groups in Bangladesh. However, these refugees had created various economic, social and security problems for the host country. The illegal businesses were common and cheap labouring as well which resulted in lashes and conflict between the hosts and refugees.

Additionally, anti-social activities were on the ascent among the unregistered Rohingya evacuee community. The social indecencies in the Rohingya people: business sexual misuse, counterfeit relational unions, the phony proposition of work, and the predominance of explicitly transmitted contaminations (STI) undermine the neighbourhood public activity and harm the steadiness of the Bangladesh-Myanmar fringe area. Justin Pini (2008) found that African refugees in host country are the active facilitator of increasing insecurity and violence. And they also cause political violence across the region.Boamah-Gyau, K. (2008) found that Liberian refugees had positive impacts on the economics, infrastructural development, health and education of Buduburam community. And the increase of population resulted in physical infrastructure development of local people. tremendous negative impacts

on sanitation and environmental issues, land acquisition and usage, security and traditional values and norms.Moughari, Z. K. (2007) explored that Afghan Refugees had effected the Iran labour force because refugees work with low wage, work harder and also do dirty jobs. But this did not affect the rate of high unemployment in Iran because the demand for labour is high and the rate of unemployment is slow.Bhatti, Saad. (1987) explored that the presence of the Afghan refugees led towards a conflict between the refugees and local population among theland, employment, animal grazing-pasture, and water supply. Moreover, the Afghan refugees' presence is also a nonstop menace to Pakistan's internal security and political stability.

### Objectives

The main objective of the study was:
To explore the social impact of the refugees on the local population
To explore the economic impact of the refugees on the local population

## METHODS AND PROCEDURE

The present research was quantitative and explanatory in nature.The universe of the study was Balochistan and the target population of the study was the local population of the Balochistan. Researcher selected five districts of Balochistan i.e. Quetta, Pishin, Loralahi, Killah Abdullah and Chaghi for the universe.  Researcher got the total population of these districts from the website of Pakistan Burue of Statistics. The calculated sample size of the research was 770. And researcher used stratified proportionate technique of sampling for the distribution and allocation for the respondents. Then, the researcher used a structured interview schedule for the collection of data. After the data collection, the data were analysed by using SPSS and statistically test of chi square test of independent and phi value were used for the examination of bivariate relationships.

## RESULTS OF THE FINDINGS

Table No.1 shows thatthere was relationship between number of refugees and unemployment among the locals. As the calculated value of chi square at 18 df on the level of significance 0.05 was 19.838 which was greater than the table value of chi square which was 18.307. So, the null hypothesis was rejected and $H_1$was accepted. It means that there was relationship between number of refugees and unemployment among the locals. The p-value 0.031 shows strong significance between the number of refugees and unemployment among the locals. Thus, the observation of the researcher in the field verified the result of test that the refugees in the private sectors were employed in a large scale including the self-employed businesses like transport, shops, markets and labour force as well. This had reduced the opportunities for the local residents and thus creating high unemployment rates among the locals.

Table No.2 shows that there is relationship between the number of refugees and effect on the daily wages of local labours. As the calculated value of chi square at df 2 on the level of significance 0.05 was 12.821 which was greater than the table value of chi square 5.991. Therefore, null hypothesis was rejected and alternate hypothesis was accepted meaning relationship between the presence of the refugees and effects on the daily wage of the locals exists. The p-value 0.002 shows significant relationship between the presence of the refugees and the effect on the daily wage of locals. Thus, the researcher had observed during his study that the refugees were involved in most of the labour force. Most of the labour force in the construction sector, catering, agriculture and markets was comprised of refugees which had severely affected the daily wages of the local labour force. These refugees worked far cheaper and had more skills as compared to the locals, thus, capturing the labour market.

Table No. 3 shows that there is no relationship between the number of refugees and access to shelter. As the calculated value of chi square at 4 df on the level of significance 0.05 was 7.738 which was lesser than the table value

**Muhammad Yaseen and Kaneez Fatima**

of chi square which was 9.488. So, the null hypothesis was accepted and H₁was rejected. It means that there was no relationship between number of refugees and access to shelter of local people. The p-value 0.102 shows insignificance relationship between the number of refugees and access to shelter of local people. Thus, the observation of the researcher in the field verified the result of test that the refugees did not create any sheltering or housing problem for the local people. As most of refugees are residing either in camps or in huts within the city at a road side.

Table No.4 shows that there was relationship between the number of refugees and access to educational services. As the calculated value of chi square at 4 df on the level of significance 0.05 was 31.424 which was greater than the table value of chi square which was 9.488. So, the null hypothesis was rejected and H₁was accepted. It means that there was relationship between number of refugees and access to educational services of local people. The p-value 0.0001 shows strong significance relationship between the number of refugees and access to educational services of local people. Thus, the observation of the researcher in the field verified the result of test that the refugees' children are also admitted in the same schools of the local communities. This had created overcrowded on the schools because these schools had already limited facilities.

Table No.5 shows that there was relationship between number of refugees and access to healthcare services of local people. As the calculated value of chi square at 4 df on the level of significance 0.05 was 16.439 which was greater than the table value of chi square which was 9.488. So, the null hypothesis was rejected and H₁was accepted. It means that there was relationship between number of refugees and access to healthcare services of local people. The p-value 0.002 shows strong significance relationship between the number of refugees and access to healthcare services of local people. Thus, the observation of the researcher in the field verified the result of test that the refugees are also admitted in the same hospitals of the local communities. This had created overcrowded on the healthcare services because these healthcare services had already limited facilities.

Table No.6 shows that there was relationship between the number of afghan refugees and level of social disorder in the local community. As the results of the hypothesis indicated that the calculated value of chi square was9.638 which was greater than the table value of chi-square which was 9.488. Hence, the null hypothesis was rejectedwhilealternate hypothesiswas accepted meaningthat the relationship between the number of afghan refugees and level of social disorder in the local community exists. The p-value of 0.047 showed that there was significant association between the number of Afghan refugees and level of social disorder in the local community. Thus, the researchers concluded that most of the local communities were suffering from the social disorders in the society although it was approved by the results. This highlighted that these societies had lost their all traditional social values which existed prior to the arrival of refugees and had adopted the cultural norms and values of the refugees.

## CONCLUSIONS AND DISCUSSION

Thus, the researcher concluded that the refugees had effected the lives of local people in various aspects of as social, economic, and cultural. The data had been collected primarily and had been analysed through the SPSS program and the following conclusion had been drawn from the analyses of the data.

**Economic Impacts**

The research data revealed that the influx of mass refugee created economic impacts on the host population. The data shows that approximately 58.0% of the respondents had insufficient opportunities to make a living due to the refugees while 18.0% of the respondents had sufficient opportunities to make a living due to the refugees. This finding is supported by Doris Carrion (2015) that the local population of Jordon felt a fear over the competition for the resources and opportunities because of the existence of thousands of refugees in the heat of cities rather than in camps. It is obvious that refugees effect the livelihood of the local people. Furthermore, the research data indicates

that approximately 65.0% of the respondents agreed that unemployment is causing tension in their community which is supported by the findings of the Calderón-Mejía, V., Cantú-Bazaldúa, F. &Chaitani, Y. (2015) & Rubenstein, (2016) that mass influx of the refugee generate a severe competition in employment opportunities in the host market. Beside, this the research data revealed that approximately 75.0% of the respondents told that labour forcewas very cheap in their community due to refugees and 25. % of the respondents told that labour forcewas not cheap in their community due to refugees.The availability of cheap labour forcewas affecting the daily wages of local labours. Moreover, the refugees labour worked cheaper than the locals in construction work, catering work, housekeeping work, and other similar works. This finding was supported in the work of Moghari, (2007) that Afghanis worked with low pay in manual jobs even though they were hard jobs. They could also work more efficiently than Iranians and the cost of the production decreased with Afghan workers.

Furthermore, the research data explored that approximately75.0% of the respondents viewed that refugees are burden on the national income and economy of the country.Lozi (2013) explored this indicator in his study and also found the same results that the refugees had effected the economy of Jordan. Thus, it is clear from the research data that refugees affected the livelihood, employment opportunities, local labour wage, and burden on the economy of the society.

## Social Impacts

The research data revealed that the arrival of refugees had created burden on the resources of the local communities, like health, education, water, shelter etc. This finding was also reflectedin the work of Yigzaw (2013) who found that depletion and reduction of the local resources like firewood, buildings materials and health, education and security issues were the effects of refugee influx in the local community. The data in the research indicated that the approximately 28.0% of the respondents told that they felt unsafe in their homes while 18.0 % of the respondents of the opinion that they felt unsafe at the markets and stores, 16.0 % of the respondents told that they felt unsafe in the streets, mosques, schools and workplaces due to the refugees.Hence majority of the respondents were of the view that the presence of the Afghan refugees had increased the crime rate in the community and most of crimes which were taking place in those communities were; killing, theft, snatching, abduction and smuggling.

Hence, research data also revealed that most of the respondents told that arm supplying was common in the communities where the Afghan refugees were inhabiting. Approximately 67.0% of the respondents told that refugees used the local politics or such sources in order to get nationality and national identity card and told that refugee camps were safe place for the terrorists. Approximately 51.0% of the respondents told that the level of crime and safety and social disorder was high in the community. The finding is supported by the Hilali, A.Z (2002) that the Afghan refugees posed an alarming threat to Pakistan security. Internally, the refugees created political, economic, social and cultural problems for Pakistan. And also introduced the Kalashnikov and drugs culture. They also strengthened the sectarianism and Islamic fundamentalism in the country. Further, the Afghan war and refugees had shattered the Pakistan international image, spreading a narrow and violent face of Islam internationally throughout the globe. Thus, the refugees had affected the existing infrastructure of the society like health, education, water, shelter services of the local community and also multiplied the crime rate in the local communities.

## Recommendations of The Study

All the variable selected for the research work were significant to prove the socioeconomic impacts of the refugees on the local population of the selected districts of Balochistan. From the study, the researcher had drawn some of the recommendation which are:

- In order to address the issue of refugees, policies of national government and international organizations must be inclusive to take the potential impacts of the refugees on the local community and their population must be taken seriously.
- The international organizations and national government should initiate the policy of burden sharing. The burden sharing policy should be for the local and refugees both.
- The state should clarify the laws regarding the status of the refugees and those laws should be implemented properly throughout the country.
- The refugees need to be kept in the premises of the refugee camps only, where all the facilities should be available within the vicinity of the camps.
- The protracted refugees should be provided the same standard of the education as in other parts of the country.
- Separate facilities like health, education, water, and infrastructure should be provided to the refugees within their camps.
- The skills of the labour force of the refugees should be used privately by the government only for the purpose of boosting the local economy of the areas.
- The vocational trainings of the refugees should be arranged in order to make them independent from the state.
- They should be repatriated according to the international laws of the refugee.

## REFERENCES

1. UN. (2009). *Trends and Impacts in conflict Settings: The socio economic impact of conflict Driven Displacement in the ESCWA region.* New York: United Nation.
2. UNHCR. (2018). *Global Trends: Forced Displacement in 2017.* Geneva, Switzerland: the UN Refugee Agency.
3. UN. (2016). *Refugees: the numbers.* Retrieved from http://www.un.org/en/globalissues/briefingpapers/refugees/
4. Khan, F. S. (2016, February 1). Afghan Refugees: It is high time they were sent back? *Pakistan Today.* Retrieved from https://www.pakistantoday.com.pk/author/falaksherkhan/
5. Watol , B. S., & Assefa, D. T. (2018). The Socio-Economic Impact of Refugees on the Neighboring Countries: The Case of Sherkole Refugee Camp, Western Ethiopia. *Global Journal of Human-Social Science: E Economics, 18*(4), 36-48.
6. Baloch, A., Shah, S. Z., Noor, Z. M., & Lacheheb, M. (2017). The Economic Effect of Refugee Crises on Neighbouring Host Countries: Empirical Evidence from Pakistan. *International Migration, 55*(6), 90-106.
7. Borthakur, A. (2017). Afghan Refugees: The Impact On Pakistan. *Asian Affairs, 48*(3), 488–509. doi:10.1080/03068374.2017.1362871
8. Taha, S. M., & Aamir, A. (2012). History Culture and Cross-Border Migration: Impact of Afghan Refugees on Socio-Economic Environment of Peshawar. *International Journal of Independent Research and Studies, 1*(4), 174-185.
9. REPORT, W. D. (2011). *The Impacts of Refugees on Neighboring Countries: A Development Challenge.* The World Bank.
10. Rahman, U. (2010). The Rohingya Refugee: A Security Dilemma for Bangladesh. *Journal of Immigrant & Refugee Studies, 8*(2), 233–239.
11. Pini, J. (2008). Political Violence and the African Refugee Experience. *International Affairs Review.* Retrieved from http://www.iar-gwu.org/node/19
12. Boamah-Gyau, K. (2008). *The Socio-cultural and economic impact of Refugees on the host Indigenous Communities in West Africa: A case study of Liberian Refugees at Buduburam Community in Ghana.* Thesis, University of Tromso, Indigenous Studies, Norway.
13. Moughari, Z. K. (2007). The Effects of Afghan Immigrants on the Iranian Labour Market. *Iranian Economic Review, 13*(20), 55-84.
14. Bhatty, S. (1987). *Impact of the Afghan refugees on Pakistan.* International Studies. FIU Electronic Theses And Dissertations. doi:10.25148/etd.FI14051147 (http://dx.doi.org/10.25148/etd.FI14051147)
15. Carrion, D. (2015). *Syrian Refugees in Jordan Confronting Difficult Truths.* London: The Royal Institute of International Affairs,.

**Muhammad Yaseen and Kaneez Fatima**

16. Calderón-Mejía, V., Cantú-Bazaldúa, F., & Chaitani, Y. (2015). *The Socioeconomic Impact Of Forced Migration On Host Communities: Challenges And Opportunities For The Arab Region.* New York: Economic And Social Commission For Western Asia (ESCWA) UN.
17. Rubenstein, E. S. (2016). *The Impact Of Refugees On The Size And Security Of The U.S. Population.* Negative Population Growth, Inc.
18. Lozi, B. M. (2013). The Effect of Refugees on Host Country Economy Evidence from Jordan. *Interdisciplinary Journal Of Contemporary Research In Business, 5*(3), 114-126.
19. Yigzaw, S. M. (2013). *The Socio-Economic Relations And Impacts Of The Eritrean Refugees On Local Population The Case Of Assayitaworeda, Afar Regional State, Ethiopia.* Research Report, Addis Ababa University, Center For African Studies.
20. Hilali, A. Z. (2002). The costs and benefits of the Afghan War for Pakistan. *Contemporary South Asia, 11*(3), 291-310.

**Table. 1 Contingency Table Showing the Relationship between Number of Afghan Refugees and Unemployment**

| Opinion about Quantity of Refugees | Unemployment Among Locals | | | | | | Total |
|---|---|---|---|---|---|---|---|
| | Strongly Agree | Agree | Neutral | Disagree | Strongly Disagree | I do not know | |
| High Number of Refugees | 87 (80.6) | 133 (131.3) | 31 (32.1) | 23 (25.3) | 26 (27.9) | 25 (27.9) | 325 |
| Normal Number of Refugees | 74 (78.1) | 132 (127.2) | 28 (31.1) | 23 (24.5) | 36 (27.0) | 22 (27.0) | 315 |
| Low number of Refugees | 30 (32.2) | 46 (52.5) | 17 (12.8) | 14 (10.1) | 4 (11.1) | 19 (11.1) | 130 |
| Total | 191 | 311 | 76 | 60 | 66 | 66 | 770 |

**Table 2.Contingency Table Showing the Relationship between Number of Afghan Refugees and Wage Affect of Local Labours**

| Opinion about Quantity of Refugees | Wage of Local labour effected by Refugees. | | Total |
|---|---|---|---|
| | Yes | No | |
| High Number of Refugees | 231 (242.7) | 94 (82.3) | 325 |
| Normal Number of Refugees | 256 (235.2) | 59 (79.8) | 315 |
| Low number of Refugees | 88 (97.1) | 42 (32.9) | 130 |
| Total | 575 | 195 | 770 |

**Table 3. Contingency Table Showing the Relationship between Number of Afghan Refugees and Access to Shelter**

| Opinion about Quantity of Refugees | Access to shelter | | | Total |
|---|---|---|---|---|
| | High | Moderate | Low | |
| High Number of Refugees | 154 (153.6) | 149 (146.0) | 22 (25.3) | 325 |
| Normal Number of Refugees | 160 (148.9) | 127 (141.5) | 28 (24.5) | 315 |
| Low number of Refugees | 50 (61.5) | 70 (58.4) | 10 (10.1) | 130 |
| Total | 364 | 346 | 60 | 770 |

**Muhammad Yaseen and Kaneez Fatima**

**Table 4. Contingency Table Showing the Relationship between Number of Afghan Refugees and Access to Educational Services**

| Opinion about Quantity of Refugees | Access to education | | | Total |
|---|---|---|---|---|
| | **High** | **Moderate** | **Low** | |
| High Number of Refugees | 204  (194.2) | 102 (111.4) | 19 (19.4) | 325 |
| Normal Number of Refugees | 206  (188.2) | 91 108.0 | 18 (18.8) | 315 |
| Low number of Refugees | 50  (77.7) | 71  (44.6) | 9 (7.8) | 130 |
| Total | 460 | 264 | 46 | 770 |

**Table No.5 Contingency Table Showing the Relationship between Number of Afghan Refugees and Access to Health Services**

| Opinion about quantity of refugees | Access to health | | | Total |
|---|---|---|---|---|
| | **High** | **Moderate** | **Low** | |
| High Number of Refugees | 203  (187.8) | 112 (120.3) | 10 (16.9) | 325 |
| Normal Number of Refugees | 184 (182.0) | 109 (116.6) | 22  (16.4) | 315 |
| Low number of Refugees | 58  (75.1) | 64  (48.1) | 8 (6.8) | 130 |
| Total | 445 | 285 | 40 | 770 |

**Table.6. Contingency Table Showing the Relationship between Number of Afghan Refugees and Social Disorder**

| Opinion about quantity of refugees | Social Disorder | | | Total |
|---|---|---|---|---|
| | **High** | **Moderate** | **Low** | |
| High Number of Refugees | 209 (198.8) | 95 (102.1) | 21 (24.1) | 325 |
| Normal Number of Refugees | 198 (192.7) | 94 (99.0) | 23  (23.3) | 315 |
| Low number of Refugees | 64 (79.5) | 53 (40.9) | 13 (9.6) | 130 |
| Total | 471 | 242 | 57 | 770 |

**RESEARCH ARTICLE**

# Preparation and Study of Some Optical Properties for [PVA:PVP] Polymer Blends Films

Ali A. Sallal*, Sabah A. Salman and Ammar A. Habeeb

Department of Physics, College of Science, University of Diyala, Diyala, Iraq.

*Address for Correspondence
**Ali A. Sallal**
Department of Physics,
College of Science,
University of Diyala,
Diyala, Iraq.

**ABSTRACT**

In this study  pure (PVA) polymer film and films  of [PVA:PVP] polymer blends at weight  ratios (([100:0], [90:10], [80:20], [70:30], [60:40], [50:50], [40:60], [30:70], [20:80], [10:90], wt%) preparation using  the casting method. The optical properties of [PVA:PVP] polymer blends films  have been studied. The transmission and absorption spectra have been recorded in the wavelength range  (190-1100) nm, the effect of the weight  ratio of the [PVA:PVP] polymer blend film on the optical parameters (transmittance, absorption coefficient) have been studied,  the practical results have shown that the transmittance of [PVA:PVP] polymer blends films decreases with the increase of the weight ratio  for  (PVP) polymer , while the absorption coefficient  increases with increasing the weight ratio of the (PVP) polymer. The results also revealed that electronic transitions are indirect, and that the energy gap increases then decreases with increasing the weight ratio of the (PVP) polymer, while Urbach's energy decreases with the increase of the weight ratio for (PVP) polymer.

**Keywords:** Polyviny Alcohol (PVA), Polyviny Pyrrolidone (PVP), Optical Properties, Energy Gap ($E_g$), Urbach Energ ($E_u$), Films, Polymer blend.

## INTRODUCTION

The subject of polymer blends has been one of the primary areas in polymer science and technology over the past several decades. As new areas of interest develop in polymer science, polymer blends technology often becomes an important segment [1]. Polymer blends offer versatile industrial applications through property enhancement and economic benefits. The blending of two or more  polymers of similar or dissimilar natures has been practiced for many years [2]. Polymer blends are defined as any combination of two or more polymers resulting from common processing step [3]. These blends are used to improve some thermal, physical and mainly mechanical properties of

16434

polymer [4]. The use of polymer blends and alloys has grown so fast compared with other polymeric materials system mainly because of their low cost and their acceptable performance [5]. Polymer blends and alloys have received a great interest due to their essential specifications which are demanded in many applications. These specifications are formulated by contribution of the properties of each component that forms the blend [6]. In general, blends are made by mixing of homo polymers or copolymers which have different chemical structures. The blends may be named as binary, ternary, quaternary depending on the number of polymeric components, which comprise them [7].

## EXPERIMENTAL PART

In the preparation of polymer blends films we are used Polyvinyl alcohol (PVA), which is product by Central House (P) Ltd of India with molecular weight of (13000-23000) g / mol, and Polyviny Pyrrolidone (PVP) K-30, is product by India's (HIMEDIA) company with molecular weight (40,000 g / mol). A pure  (PVA) polymer film and [PVA:PVP] polymer  blends films was prepared using the casting method by using special molds made of glass. The pure (PVA) polymer film  was prepared by adding a certain weight of (PVA)  polymer to distilled water using a magnetic sterrier for (1/2h) at (80 °C) to obtain a homogeneous solution, and then pour the solution in a special glass mold placed on a mild surface until the solvent evaporates to obtain the pure (PVA) polymer film. In order to prepare the [PVA:PVP] polymer blends films, certain weight ratios of (PVA) polymer  were mixed with certain weight ratios of (PVP) polymer  and the distilled water was added using the magnetic stirrer for (1/2h) at (80 °C) to obtain a homogeneous solutions, the solutions are then poured into special glass molds placed on a mild surface and left until the solvent evaporates to obtain the [PVA:PVP] Polymer blends films. The thickness measurement are mode by using digital micrometer, the thickness of the [PVA:PVP] polymer blends films is (40±0.05) μm. The absorbance and transmittance measurements were carried out using a Shimadzu UV/VIS-160A double beam spectrophotometer in the wavelength range (190-1100) nm.

## RESULTS AND DISCUSSION

### Transmission Spectrum

Figure (1) shows the transmission spectrum as a function of the wavelength of the pure (PVA) polymer film and [PVA:PVP] polymer blends films with different weight ratios, the figure shows that the transmittance increases by increasing the wavelength and for all polymer blends films, and then the transmittance appears almost constant at the long wavelengths and for all polymer blends films, and when adding (PVP) polymer to pure (PVA) polymer with different weight ratios we show a decrease in transmittance due to the form of a layer of covalent bonds between chains of (PVA) polymer and (PVP) polymer  which reduces the transmittance of incident light especially at short wavelengths, also the reason for the decrease of transmittance when mixing of (PVA) polymer  and (PVP) polymer with different weight ratios, so that the electrons in the outer orbits of added (PVP) polymer can absorb the electromagnetic energy of the incident light and then the electrons move to higher energy levels, this process is not accompanied by the emission of radiation because the electrons that move to the upper levels have occupied vacant positions of the energy bands, so that a part of the incident light is absorbed by the material and can not penetrate it. The pure (PVA) polymer film has the highest transmittance due to the absence of free electrons (Any sense that the electrons associated with atoms by covalent bands), and this occurs because break the electronic connection and direction of the electron towards the valence band needs a photon with high energy [8].

### Absorption Coefficient

Figure (2) shows the absorption coefficient as a function of the wavelength of pure (PVA) polymer and [PVA:PVP] polymer blends films with different weight ratios, we note from the figure that the absorption coefficient is small at

**Ali A. Sallal *et al.***

low energies, this means that the possibility for electronic transition is low because the energy of the incident photon is not enough to move the electron from the valence band to the conduction band ($h\upsilon<Eg$), at high energies the absorption coefficient is great, which means that there is great possibility for electronic transition, consequently the incident photon energy is sufficient to move the electron from the valence band to the conduction band, meaning that the incident photon energy is larger than the energy gap [8]. The absorption coefficient helps to know the nature of electronic transition, and found that the absorption coefficient of pure (PVA) polymer film and [PVA:PVP] polymer blends films with different weight ratios is less than ($10^{-4}$ cm$^{-1}$) which means that the electronic transition is indirect, we also note from the figure an increase in the absorption coefficient when mixing of (PVA) polymer and (PVP) polymer with different weight ratios [8].

**Energy Gap of the Allowed Indirect Transition**

Figure (3) shows the relationship between $(\alpha h\upsilon)^{1/2}$ and photon energy ($h\upsilon$) of pure (PVA) polymer film and [PVA:PVP] polymer blends films with different weight ratios, and it is the best straight line to pass most points after the absorption edge and then extend a tangent line to cut the photon energy-axis (x-axis) at point $(\alpha h\upsilon)^{1/2} = 0$, which represents the value of the energy gap for the allowed indirect transition. Table (1) shows the energy gap values of all polymer blends films. We note from the table that the value of energy gap of a pure (PVA) polymer film is (4.31 eV), but when mixing of (PVA) polymer and (PVP) polymer with different weight ratios, the energy gap value starts to increase slightly by increasing the weight ratio of (PVP) polymer to reach a higher value at weight ratio (40% wt%) of (PVP) polymer, but after this weight ratio, the value of the energy gap starts to decrease slightly by increasing the weight ratio of (PVP) polymer. This is due to the interaction between the (OH-groups) of the (PVA) polymer and the (CH-Groups) of the (PVP) polymer and this can affect on the degree of mixing of the mixture [9].

Figure (4) shows the relationship between ($\ln\alpha$) and photon energy ($h\upsilon$) of pure (PVA) polymer film and [PVA:PVP] polymer blends films with different weight ratios, the Urbach energy represents the widh of the allowed localized states within the energy gap and is calculated by taking the inverted value of the linear line slope of the exponential region, We note that the value of Urbach energy for the polymer blend is reduced by the increase of the weight ratio of (PVP) polymer, this indicates that the (PVP) polymer has a greater structural disturbance compared with the [PVA:PVP] polymer blend [9]. The change in the value of Urbach energy to all polymers blends (a decrease in the value of Urbach energy with the increase in the weight ratio of (PVP) polymer) can be understood by looking at the concept of kinetics as proposed by (Mott and Davis) which reveals that blend greatly affects the Urbach energy. The blend process introduces additional defect levels in the polymer material. It was found that the density of the localized levels corresponded to the concentration of these defects and therefore with the weight ratio of the (PVP) polymer. Increase the weight ratio of the (PVP) polymer may cause overlapping localized levels of different color centers and stretch in the kinetics gap, and that this interference may give evidence of the great change in the Urbach energy when the weight ratio of polymer (PVP) is incrased in the polymer material (PVA) [10]

The main conclusions of this study were:

❖ The absorption coefficient of [PVA:PVP] polymer blends films increased with increase the weight ratio of the (PVP) polymer, while the transmittance of [PVA:PVP] polymer blends films decreased with increasing the weight ratio of (PVP) polymer.
❖ The absorption coefficient of [PVA:PVP] polymer blends films with different weight ratios is less than ($10^4$ cm$^{-1}$) which means that the electronic transition is indirect.
❖ The value of the energy gap for the allowed indirect transition of [PVA:PVP] polymer blends films increases and decreases by increasing the weight ratio of the (PVP) polymer, and all these values of the energy gap are greater than the value of the energy gap of a pure (PVA) polymer film, while Urbach energy decreased by increasing the weight ratio of the (PVP) polymer.

16436

**Ali A. Sallal** *et al.*

## REFERENCES

1. M. L. Robeson, "Polymer Blends Handbook", KIwer Academic Publishers, Netherlands, (2003).
2. J. R. Fried, "Polymer Science and Technology", Prentice Hall, Inc, Upper Saddle Rivers, Newjerscy, (2003).
3. R. D. Paul and S. Newman, "Polymer Blends", Academic press, Inc., New York, (1978).
4. J. Kovar, I. Fortelny and M. Bohdanecky, "International Polymer Science and Technology", Vol. 9, No. 11, (1982).
5. B. G. Kenneth and M. Senior, "Engineering Materials, Properties and selection", 5th Edition, Prentice-Hill, Inc., New Jersey, (1996).
6. K. Chiba, "International Polymer Science and Technology", Vol. 16, No. 3, (1989).
7. J. W. Work, K. Horie, M. Hess and F. R. Stepoto, "Polymer Blends Definitions", International Vnion of Pure and Applied Chemistry, Vol. 76, No. 11, pp. 1985-2007, (2004).
8. Z. A. Al-Ramadhan, J. A. Salman and H. A. Hmud, "Optical and Morphological Propreties of (PVA-PVP-Ag) Nanocomposites", International Journal of Science and Research (IJSR), Vol.5, pp. 1828-1836, (2014).
9. R. M. Ahmed, "Optical Properties and Structure of Cobalt Chloride Doped PVA and Its Blend with PVP", World Scientific, Vol.28, pp. (13Pages), (2014).
10. A. El-Khodary, "Evolution of the Optical, Magnetic Morphological Properties of PVA Films with $CuSO_4$", Physica B 405, pp. 3401-3408, (2010).

**Table 1. Energy gap values of the allowed indirect transition for [PVA: PVP] polymer blends films with the weight ratio of the blend.**

| Blending Ratio of [PVA:PVP] (wt%) | $E_g$ (eV) |
|---|---|
| [100:0] | 4.31 |
| [90:10] | 5.23 |
| [80:20] | 5.24 |
| [70:30] | 5.25 |
| [60:40] | 5.26 |
| [50:50] | 5.12 |
| [40:60] | 5.04 |
| [30:70] | 5.02 |
| [20:80] | 5.01 |
| [10:90] | 5.00 |

**Table 2. Urbach energy values for [PVA:PVP] polymer blends films with the weight ratio of the blend.**

| Blending Ratio of [PVA:PVP] (wt%) | $E_u$ (meV) |
|---|---|
| **[100:0]** | 659.6 |
| **[90:10]** | 128.7 |
| **[80:20]** | 125.7 |
| **[70:30]** | 120.03 |
| **[60:40]** | 112.56 |
| **[50:50]** | 112.22 |
| **[40:60]** | 109.11 |
| **[30:70]** | 106.28 |
| **[20:80]** | 104.34 |
| **[10:90]** | 102.3 |

**Ali A. Sallal** *et al.*
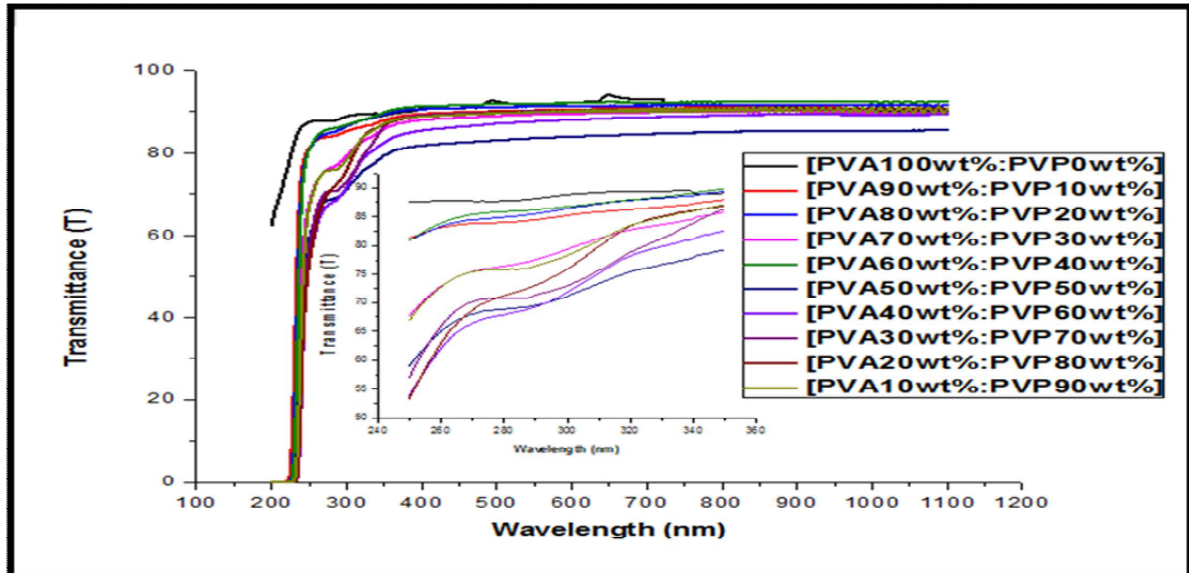


**Figure 1. Transmission Spectrum as a function of the wavelength for [PVA:PVP] polymer blends films with different weight ratios.**
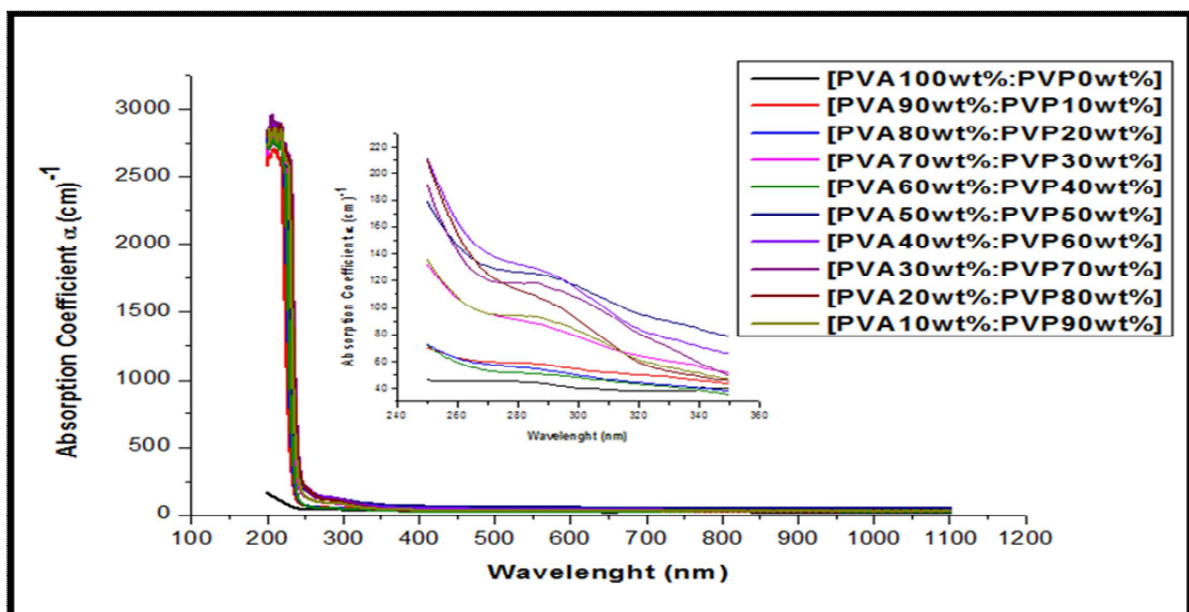


**Figure 2. Absorption coefficient as a function of the wavelength for [PVA:PVP] polymer blends films with different weight ratios.**
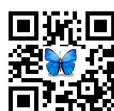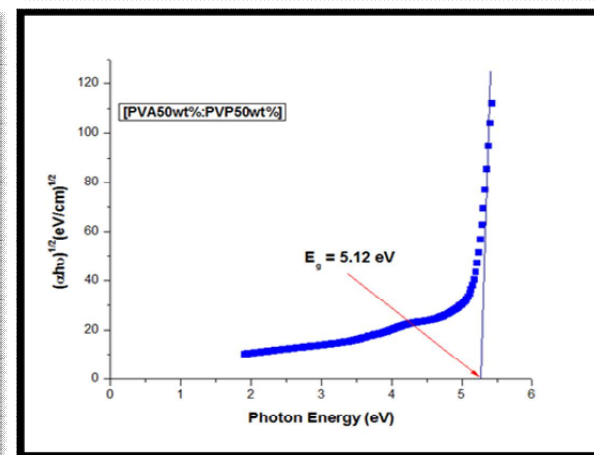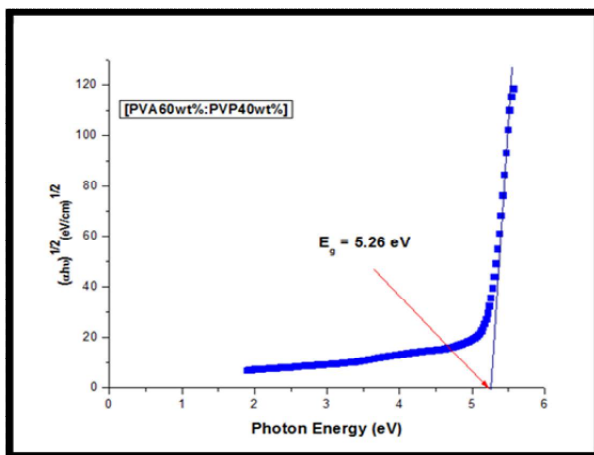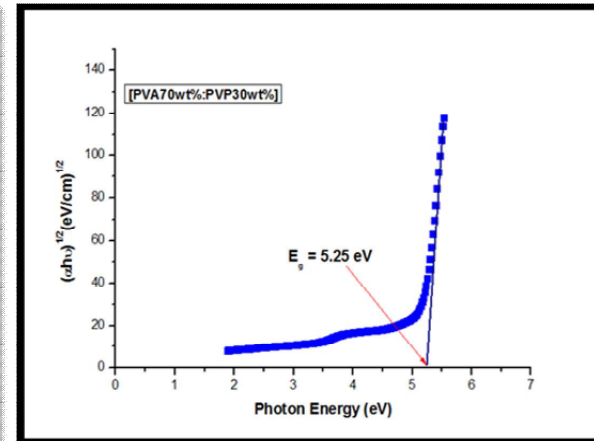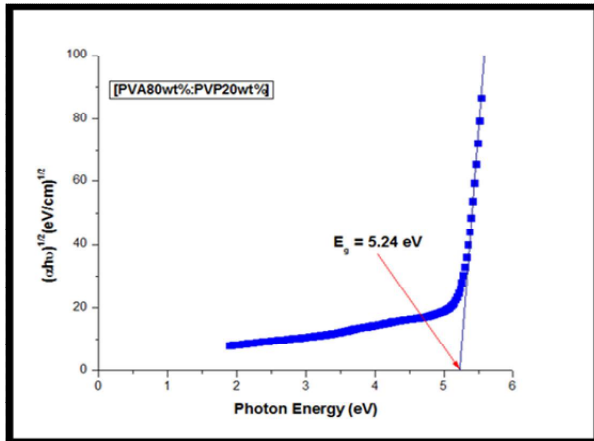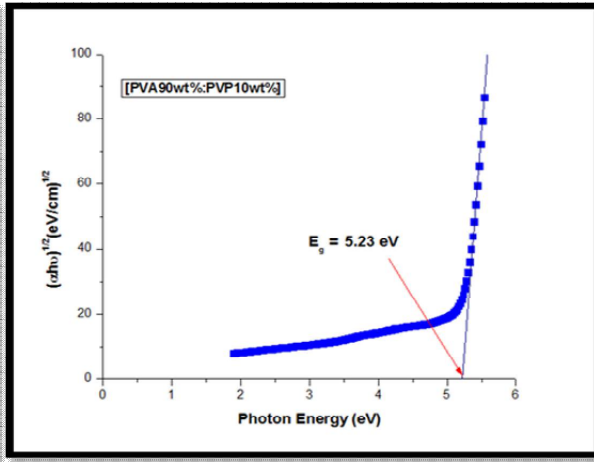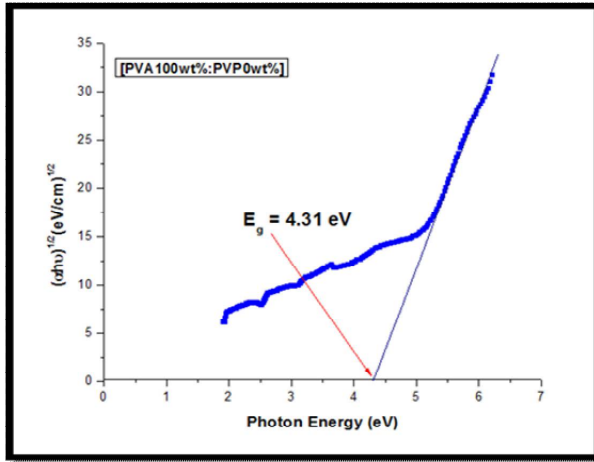
**Ali A. Sallal** *et al.*
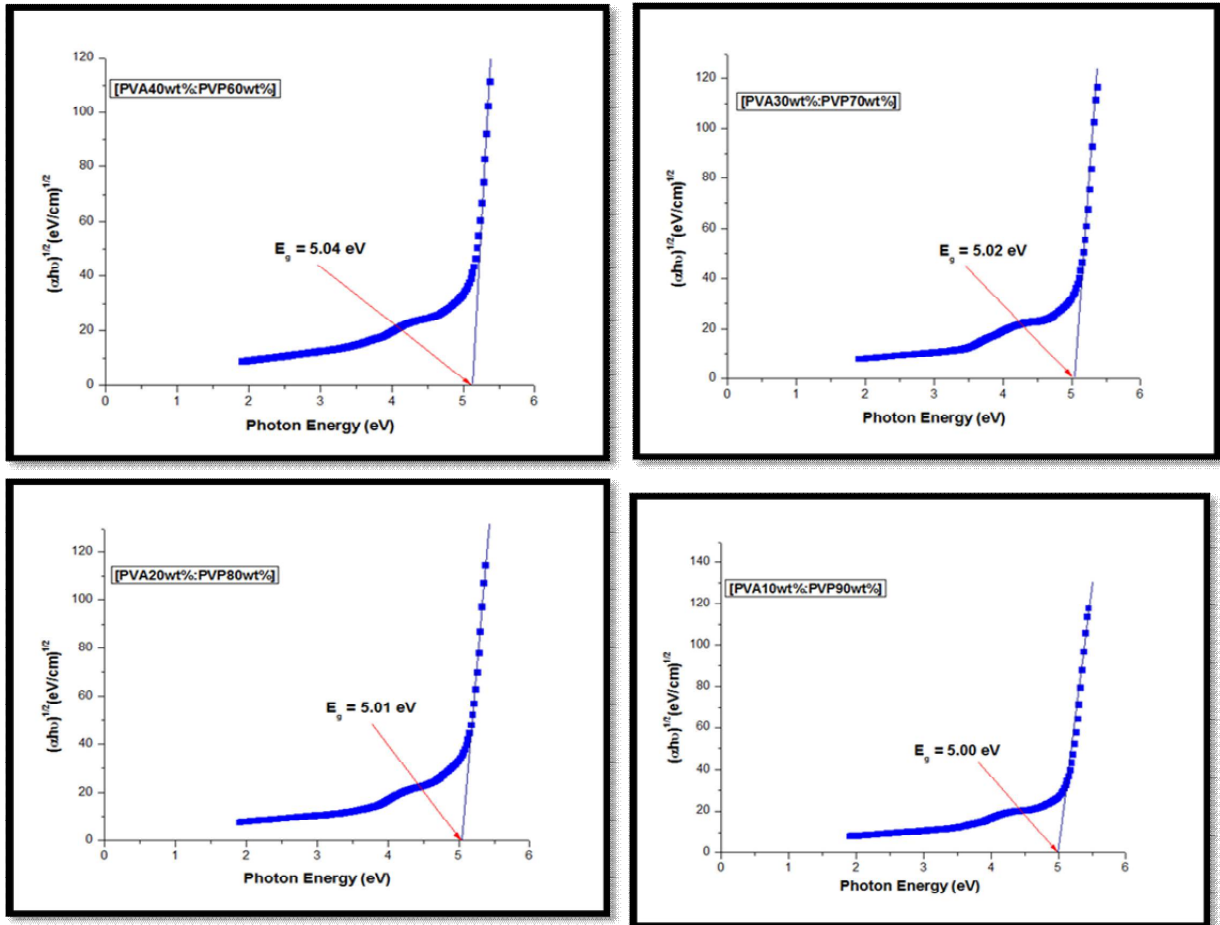


**Figure 3. Energy gap of the allowed indirect transition for [PVA:PVP] polymer blends films with different weight ratios**

**Ali A. Sallal** *et al.*
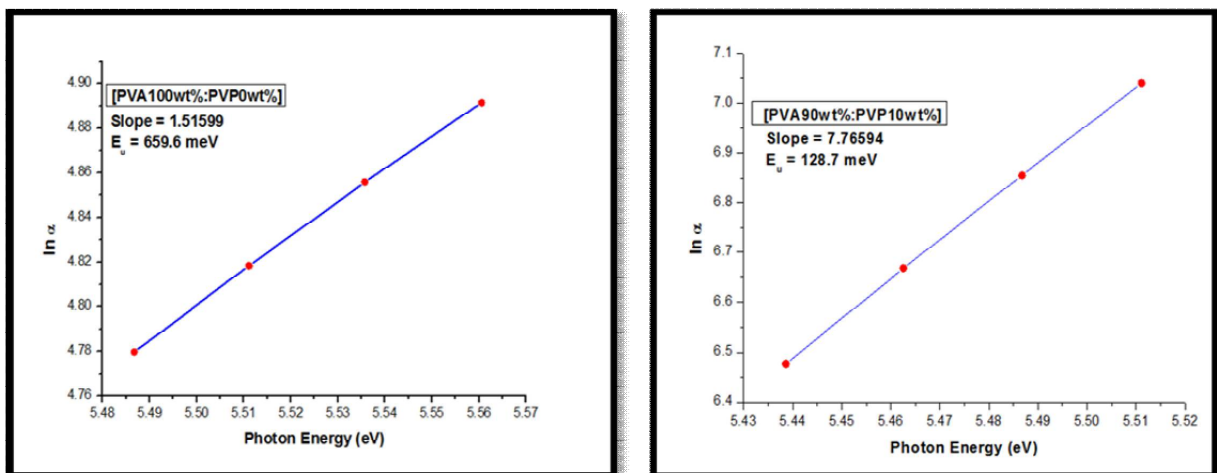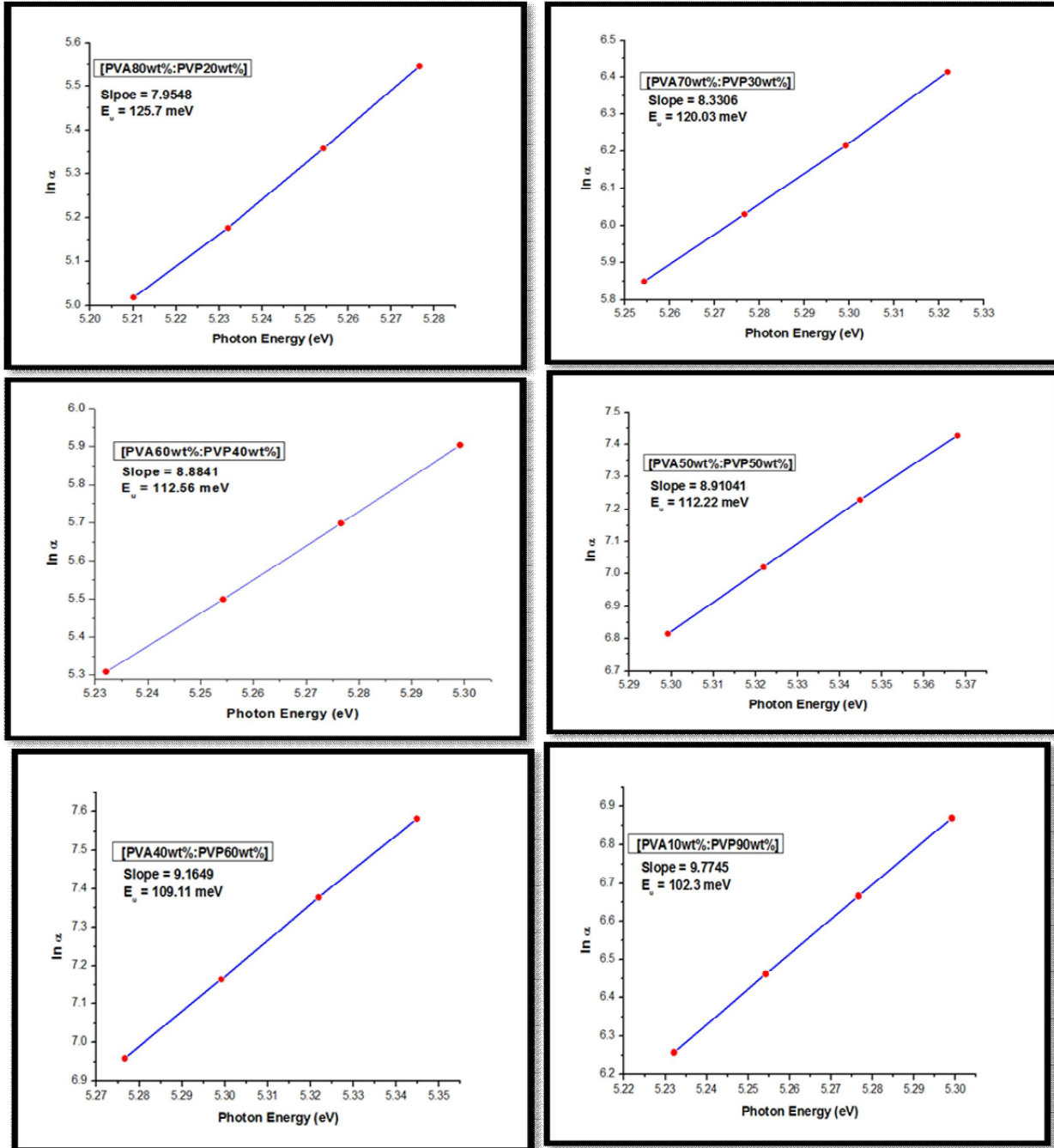


**Figure 4.Urbach energy for [PVA:PVP] polymer blends films with different weight ratios**

**RESEARCH ARTICLE**

# Assessment of Sediment Transportin Hilla - Diwaniya Project

Zainab Ali Omran*, Zahra Abd Saleh, and Nariman Yahya Othman

Department of Civil Engineering, Faculty of Engineering, University of Babylon, Babil, Iraq.

*Address for Correspondence
**Zainab Ali Omran**
Department of Civil Engineering,
Faculty of Engineering,
University of Babylon,
Babil, Iraq.
Email: zainabalialtaee@yahoo.com

**ABSTRACT**

The sediment transport concentration in Hilla –Diwaniya riverwas studied in this paper at Al-Hilla city in Iraq. HEC-RAS version (5.0.0) program was used for calculatingthe volume of sediment load in the studied portion of the river. Four cross-sections along the riverreach(at0+000, 1+000, 2+000 and, 3+000)for 100 m long for each station were selected, Yang method was usedfor transport function and Ruby method is used for calculating the fall velocity, with the Thomas (Ex5) as a sorting method. The result showed that there is not big difference between the selected four station recording to sediment transport concentration, velocity of flow, effective depth and effective width, and this project (Hilla –Diwaniya river) is not useful for irrigation.

**Keywords:** Sediment concentration, HEC-RAS, sorting method, fall velocity.

## INTRODUCTION

In rivers, Sediment transport has been widelyconsidered, resulting in numeroussimulations that are being used to date for load forecast. Overland flow, stream-channel erosion, bank cutting and small erosion channels made in unconsolidated soil were the main sources of sediment in natural rivers [1]. Rivers and channels are considered to be vitalincomes for supply of water, irrigation, and other public uses. The bed deformation increases because of the solid material erosion of the beds and banks of canal, which will decrease the water depth in some seats and the capacity of the water way for navigation or hydraulic purposes were decreases. [2] In this paper, (HEC-RAS)(5.0.0) program was used for modeling the sediment concentration for Hilla – Diwaniya river project.

16442

**Zainab Ali Omran** *et al.*

**Study area description**

Hilla – Diwaniya river is selected, in Al-Hilla city in Iraq, located to the right of shatt al Hilla and extends from the city of Hilla at 40 km to the Shatt al Diwaniya at 94 km from the Shatt al Hilla, it's a project of irrigation which contains regular irrigation and drainage networks and an area of 282000 dunums,0+000, 1+000, 2+000, and 3+000 stationswere specified along the river which were selected. **[3]**

# METHODOLOGY

## Determination of Input Parameters

The input parameters which were used in the program:
(n): Manning coefficient (Constant depends on channel types and description),
(Q) Discharge of water (maximum and minimum values in (m³/s)).
Channel friction slope
Velocity of the channel (m/s)
Each parameter values were measured directly or calculated from equations or was already scored in the program.

## Surveying

This stage contained the collection of all available information for supporting the simulation,it isnecessary step to calculation the difference in cross sections along the specific longitudinal part of the river, this step had completed by using of famous satellite websites like Google earth and by using information of the river from Iraqi Meteorological Office of Water Source, Babylon governorate **[3]**. For the simulation of the sediment transport in the river, data for each cross section in research's area must be available, this data related to the shape of the cross section and elevation of it's water surface as shown in Figure (1). The data used for this paper werecollected from four sections in Al-Hilla-Diwaniyariver dispersed along the study area. Discharge, velocity, cross-sectional area, and observed suspended sediment load were collected from the field measurements. Minimum and maximum dischargeequal to 4.5and 7.2 m³/sec respectively.The flow velocities ranges from (0.94 to 2.55) m/s. Table (1) summarized results about one cross section.For simulation, it is necessary to provide information about the river discharge and bed's soil gradation. Table2and Fig.2were showed type of soil and grading in the bottom of the river.

## Simulation by HEC-RAS Model

For this paper, sediment concentration was established using HEC-RAS [5.0.0].Figure (3) showing the HEC-RAS program main window. Formaking sediment simulation two necessary file sorts are necessary:

## Geometric File

Fordeveloping HEC-RAS model, it is necessary to generate a HEC-RAS geometric file. Which includesriver system representation; records of cross section; reach length, function losses, contraction and expansion losses; and stream intersection information.  These data were entered to theprogram through the menu of cross section, geometrical data as shown in Figure (4). **[4,5].** Reach length is the distance measured between any two cross sections. The cross section is termed by entering the stations and their elevations (x-y) records from left to the right.

**Zainab Ali Omran *et al.***

### Sediment Data

Sediment data involves of the essentialrecords that related to the sediment simulation: Transport function: using,Yang (1973) method, the formula of this method shown in Equation below **[6]**.

$$\log C_t = 5.435 - 0.286 \log\left(\omega\, D_{50}/\upsilon\right) - 0.457 \log\left(u_*/\omega\right) + \left\{1.799 - 0.409 \log\left(\omega\, D_{50}/\upsilon\right) - 0.314 \log\left(u_*/\omega\right)\right\} \log\left(V\, S/\omega - V_{cr}\, S/\omega\right)$$

The value $V_{cr}/\omega$ is given by:

$$\frac{V_{cr}}{\omega} = \frac{2.5}{\log\dfrac{u_* D}{\nu} - 0.06} + 0.66, \quad 0 < \frac{u_* D}{\nu} < 70$$

$$\frac{V_{cr}}{\omega} = 2.05, \qquad\qquad 70 < \frac{u_* D}{\nu}$$

Where:

$C_t$ : total average sediment concentration

D, $D_{50}$ : sediment diameter

S: water surface slope

$U_*$: shear velocity

$V_{cr}$ : critical velocity

$\upsilon$: kinematic viscosity

$\omega$ :fall velocity of sediment

### Bed sorting method

In most of the river systems, the full bed gradation is covered by a layer of coarse material called an armor layer. This layer can be formed by static armoring or the differential transport of the finer materials. Exner 5: A three layer active bed model  (see Figure 5) that contains the ability of forming a course surface layer that will limit erosion of deeper material thereby simulating bed armoring.**[7,8]**

### Fall velocity method

Currently four methods for computing fall velocity in HEC-RAS, Ruby, Toffaleti, Van Rijn and Report 12. The employed method is Ruby, these recordsare entered to the model through the menu of sediment data (seeFigure (6))

## RESULTS AND DISCUSSION

In this paper, after completed inserting sediment data in the suitable places and clicked on "Run" button in the Sediment Analysis, the program completed simulating the sediment transport data and showed the result in View/ Sediment Output. The results of simulation appeared that:

- Velocity of the river changes according to the cross section and can be noticed that the velocity drops when the river pass inside center of Al-hilla city because of sediment concentration for all stations. (see Fig. 7)
- The concentration of sediment decreases in the part of river when pass the center of Al-hilla city, this could make the problem of contamination very huge and needed heavy cost for treatment and effect negatively on human life and activates. See Figure (8).
- Effective depth increases along the river (with channel station) for all stations as shown in Fig. (9).

## CONCLUSION

The result showed that there is not big difference between the selected four station recording to sediment transport concentration, velocity of flow, effective depth and effective width, that means this project is not usefulfor irrigation with respect to the values of discharge, flow velocity and sediment volume, and showed that the change in river's bed differed according to the river sections and sediment material type and the concentration of sediment

## REFERENCES

[1]Sechu Laurent Gasper, (2015), "Sediment transport in Säveån and its implications for erosion and bank stability", Master Thesis Division of Water Resources Engineering Department of Building & Environmental Technology Lund University Box 118 221 00 Lund, Sweden, Water Resources Engineering TVVR-15/5013 ISSN 1101-9824 ,www.tvrl.lth.se

[2] Al-kassarHana'a Mahmood Amer,( 2015), "Estimation of Sediment Quantity Upstream of Al-Yaa'o Regulator" Journal of Babylon University/Engineering Sciences/ No.(3)/ Vol.(23): 2015

[3] Iraqi Meteorological Office of Water Source, Babylon governorate.

[4] Zainab Ali Omran, Nariman Yahya Othman and Zahra Abd Saleh,(2018)," STEADY FLOW ANALYSIS FOR SHATTAL- HILLA USING HEC-RAS PROGRAM" (IJCIET)Volume 9, Issue 6, June 2018, pp. 524–533.

[5]Kadhim Naief Kadhim "Evaluation of the Maximum Rainfall Magnitude in Mid-Mesopotamian Plain by Using Frequency Factors Method" (IJCIET), Volume 9, Issue 6, (Jun 2018)

[6]M. MONOWAR HOSSAIN & M. LUTFOR RAHMAN(1998), "Sediment transport functions and their evaluation using data from large alluvial rivers of Bangladesh",Modelling Soil Erosion, Sediment Transport and Closely Related Hydrological Processes (Proceedings of a symposium held at Vienna, July 1998). IAHS Publ. no. 249.

[7] GHARESIFARD, M., et. al., "Determining the Suitable Sediment extraction Locations of Existing Sand and Gravel Mines on Boshar River in Iran using HEC-RAS Modeling" Civil Engineering Expert/Asmari Consultant Engineers, ICSE6-134 Paris-August, 27-31.

[8] Kadhim Naief Kadhim (Estimating of Consumptive Use of Water in Babylon Governorate-Iraq by Using Different Methods). (IJCIET), Volume 9, Issue 2, (Feb 2018)

**Zainab Ali Omran** *et al.*

**Table 1: Summarized of surveying results (Data of Al-Hilla-diwaniya, 0+000 station)**

| River Sta | Profile | Area Channel (m2) | Min Ch El (m) | W.S. Elev (m) | Crit W.S. (m) | E.G. Elev (m) | E.G. Slope (m/m) | Vel Chnl (m/s) | Flow Area (m2) | Top Width (m) | Froude # Chl | Area (m2) | Area Channel (m2) | Center Station (m) | Flow Area (m2) | Hydr Radius (m) |
|---|---|---|---|---|---|---|---|---|---|---|---|---|---|---|---|---|
| 100 | Q1 | 4.45 | 0.00 | 1.34 | | 1.38 | 0.001709 | 0.94 | 4.45 | 5.45 | 0.33 | 4.45 | 4.45 | 3.60 | 4.45 | 0.71 |
| 100 | Q2 | 6.53 | 0.00 | 1.69 | | 1.75 | 0.001949 | 1.15 | 6.53 | 6.55 | 0.37 | 6.53 | 6.53 | 3.60 | 6.53 | 0.87 |
| 90.000* | Q1 | 4.34 | 0.00 | 1.32 | | 1.37 | 0.001826 | 0.97 | 4.34 | 5.38 | 0.34 | 4.34 | 4.34 | 3.60 | 4.34 | 0.71 |
| 90.000* | Q2 | 6.38 | 0.00 | 1.66 | | 1.73 | 0.002076 | 1.18 | 6.38 | 6.48 | 0.38 | 6.38 | 6.38 | 3.60 | 6.38 | 0.86 |
| 80.000* | Q1 | 4.22 | 0.00 | 1.30 | | 1.35 | 0.001964 | 0.99 | 4.22 | 5.31 | 0.36 | 4.22 | 4.22 | 3.60 | 4.22 | 0.70 |
| 80.000* | Q2 | 6.22 | 0.00 | 1.64 | | 1.71 | 0.002224 | 1.21 | 6.22 | 6.40 | 0.39 | 6.22 | 6.22 | 3.60 | 6.22 | 0.85 |
| 70.000* | Q1 | 4.10 | 0.00 | 1.27 | | 1.33 | 0.002128 | 1.03 | 4.10 | 5.24 | 0.37 | 4.10 | 4.10 | 3.60 | 4.10 | 0.69 |
| 70.000* | Q2 | 6.04 | 0.00 | 1.61 | | 1.69 | 0.002401 | 1.24 | 6.04 | 6.31 | 0.40 | 6.04 | 6.04 | 3.60 | 6.04 | 0.83 |
| 60.000* | Q1 | 3.96 | 0.00 | 1.25 | | 1.30 | 0.002330 | 1.06 | 3.96 | 5.06 | 0.39 | 3.96 | 3.96 | 3.60 | 3.96 | 0.67 |
| 60.000* | Q2 | 5.85 | 0.00 | 1.58 | | 1.66 | 0.002614 | 1.28 | 5.85 | 6.21 | 0.42 | 5.85 | 5.85 | 3.60 | 5.85 | 0.82 |
| 50.000* | Q1 | 3.81 | 0.00 | 1.22 | | 1.28 | 0.002584 | 1.10 | 3.81 | 5.06 | 0.41 | 3.81 | 3.81 | 3.60 | 3.81 | 0.66 |
| 50.000* | Q2 | 5.64 | 0.00 | 1.54 | | 1.63 | 0.002884 | 1.33 | 5.64 | 6.10 | 0.44 | 5.64 | 5.64 | 3.60 | 5.64 | 0.81 |
| 40.000* | Q1 | 3.64 | 0.00 | 1.18 | | 1.25 | 0.002916 | 1.15 | 3.64 | 4.96 | 0.43 | 3.64 | 3.64 | 3.60 | 3.64 | 0.65 |
| 40.000* | Q2 | 5.41 | 0.00 | 1.51 | | 1.60 | 0.003232 | 1.39 | 5.41 | 5.98 | 0.47 | 5.41 | 5.41 | 3.60 | 5.41 | 0.79 |
| 30.000* | Q1 | 3.45 | 0.00 | 1.14 | | 1.22 | 0.003376 | 1.22 | 3.45 | 4.83 | 0.46 | 3.45 | 3.45 | 3.60 | 3.45 | 0.63 |
| 30.000* | Q2 | 5.14 | 0.00 | 1.46 | | 1.57 | 0.003709 | 1.46 | 5.14 | 5.83 | 0.50 | 5.14 | 5.14 | 3.60 | 5.14 | 0.77 |
| 20.000* | Q1 | 3.22 | 0.00 | 1.09 | | 1.18 | 0.004075 | 1.31 | 3.22 | 4.68 | 0.50 | 3.22 | 3.22 | 3.60 | 3.22 | 0.61 |
| 20.000* | Q2 | 4.81 | 0.00 | 1.40 | | 1.53 | 0.004418 | 1.56 | 4.81 | 5.66 | 0.54 | 4.81 | 4.81 | 3.60 | 4.81 | 0.74 |
| 10.000* | Q1 | 2.91 | 0.00 | 1.03 | 0.77 | 1.13 | 0.005355 | 1.45 | 2.91 | 4.46 | 0.57 | 2.91 | 2.91 | 3.60 | 2.91 | 0.58 |
| 10.000* | Q2 | 4.38 | 0.00 | 1.33 | 1.03 | 1.47 | 0.005685 | 1.71 | 4.38 | 5.41 | 0.61 | 4.38 | 4.38 | 3.60 | 4.38 | 0.71 |
| 0 | Q1 | 1.86 | 0.00 | 0.77 | 0.77 | 1.03 | 0.017814 | 2.26 | 1.86 | 3.64 | 1.01 | 1.86 | 1.86 | 3.60 | 1.86 | 0.46 |
| 0 | Q2 | 2.94 | 0.00 | 1.03 | 1.03 | 1.37 | 0.016550 | 2.55 | 2.94 | 4.48 | 1.01 | 2.94 | 2.94 | 3.60 | 2.94 | 0.58 |

**Table 2: Soil type and grading in the bottom of the river from field.**

| Soil class | Particle Size (mm) | % Pass |
|---|---|---|
| Fine Silt | 0.008 - 0.016 | 5 |
| Medium Silt | 0.016 - 0.032 | 10 |
| Coarse Silt | 0.032 - 0.0625 | 19 |
| V. Fine Sand | 0.0625 - 0.125 | 30 |
| Fine Sand | 0.125 - 0.25 | 40 |
| Medium Sand | 0.25 - 0.5 | 55 |
| Coarse Sand | 0.5 - 1 | 82 |
| V. Coarse Sand | 1 - 2 | 90 |
| V. Fine Gravel | 2 - 4 | 100 |
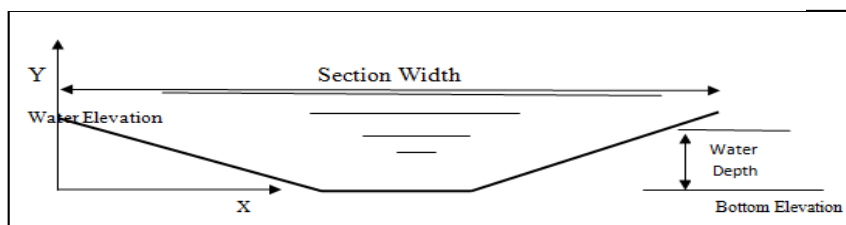


**Fig 1.  Cross section of Al-Hilla- Diwaniya river**

16446

**Zainab Ali Omran** *et al.*
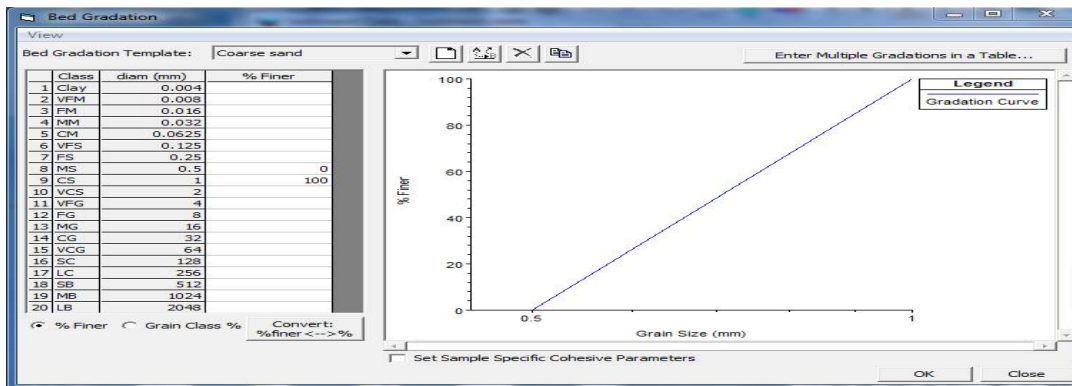


**Fig. 2. Bed Gradation**
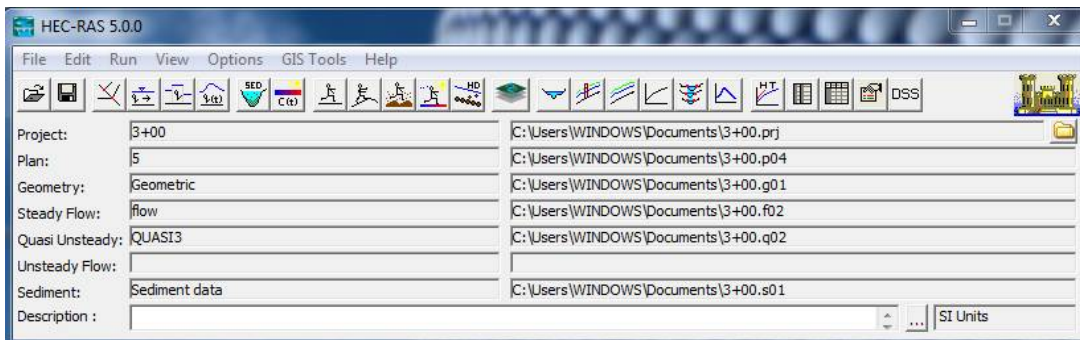


**Fig. 3. Main menu of HEC-RAS software.**

Zainab Ali Omran *et al.*
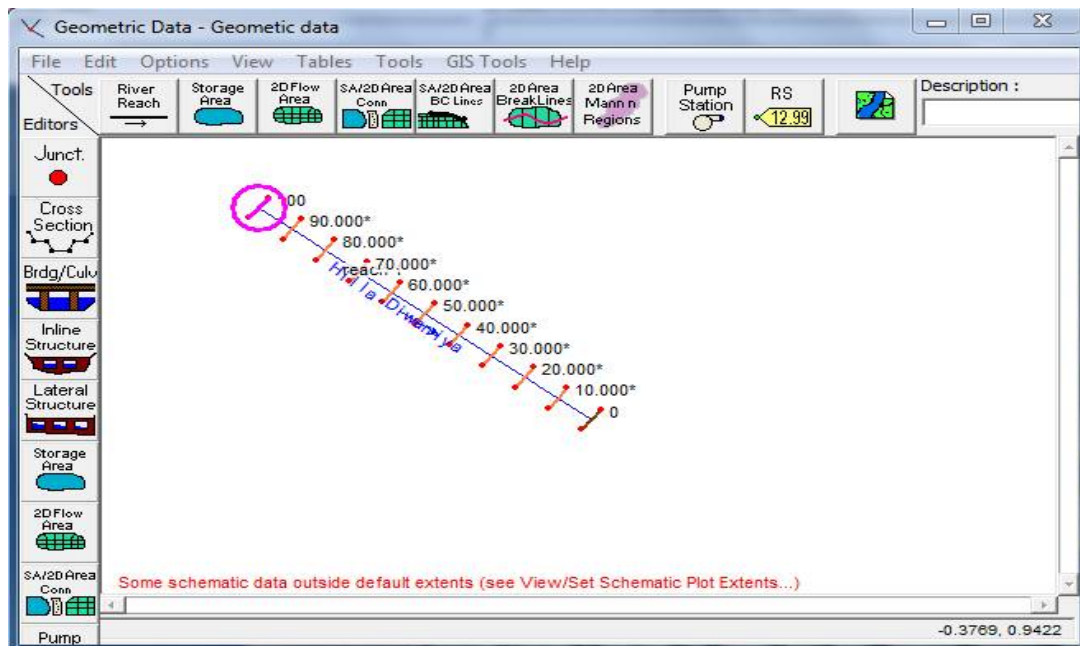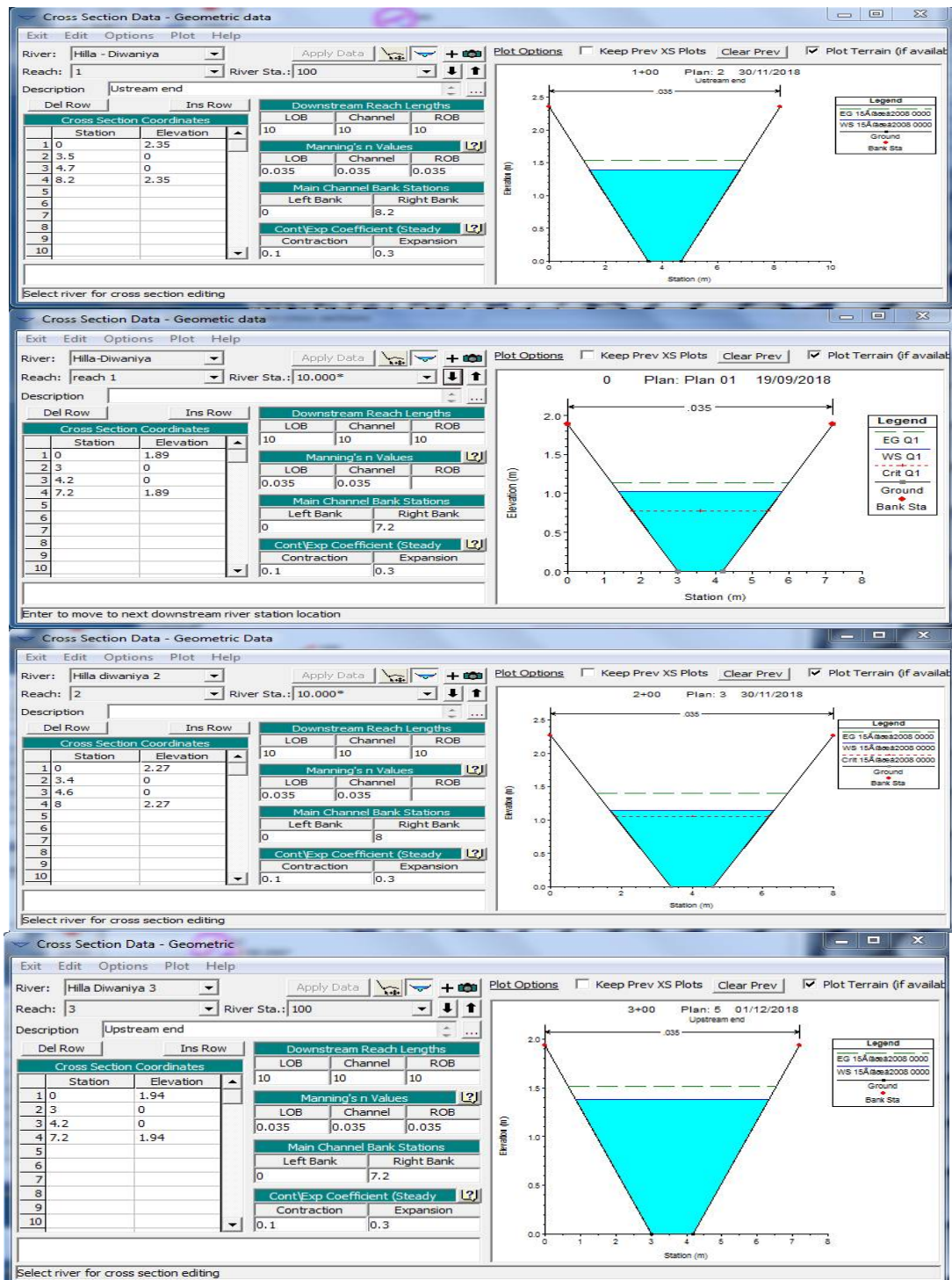
**Fig .4. Menu of cross section data for Al-hilla Diwaniya River for different stations**

**Zainab Ali Omran** *et al.*
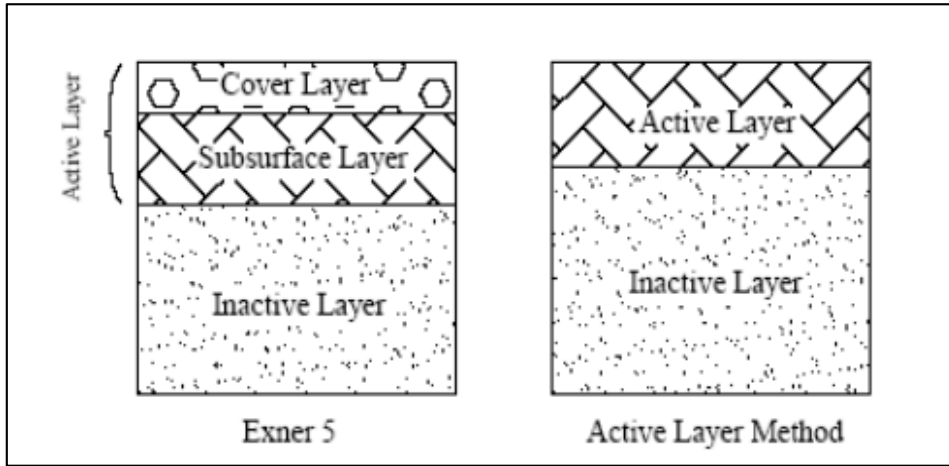


**Fig .5. Diagram of the mixing layers, sorting methods**
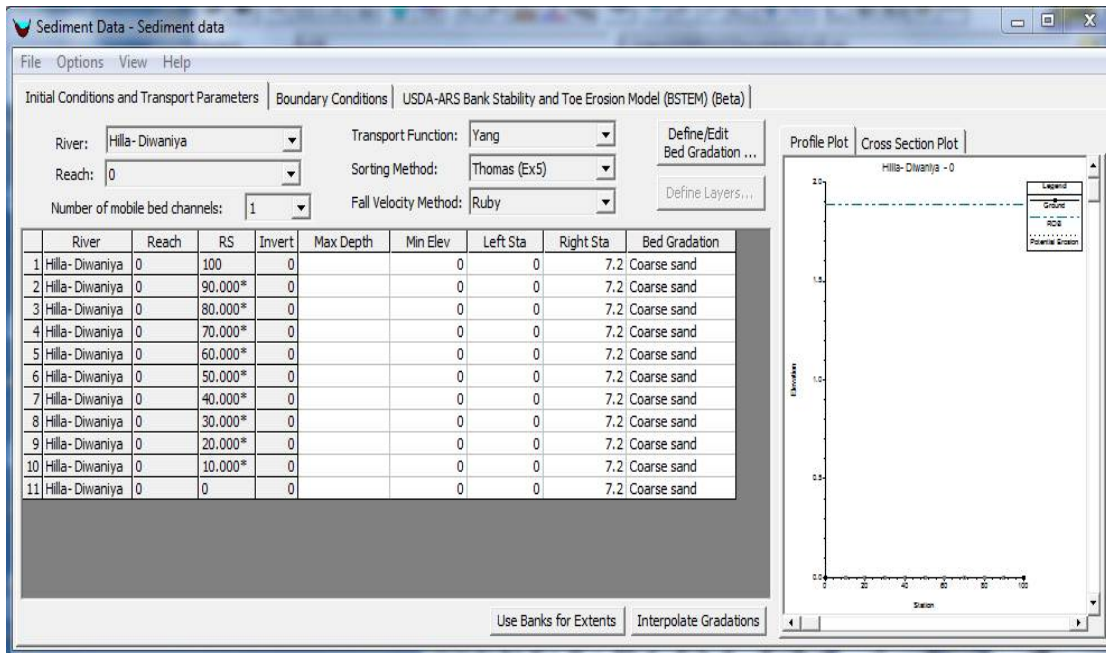


**Fig.6. Sediment records in HEC-RAS**

16449

**Zainab Ali Omran** *et al.*
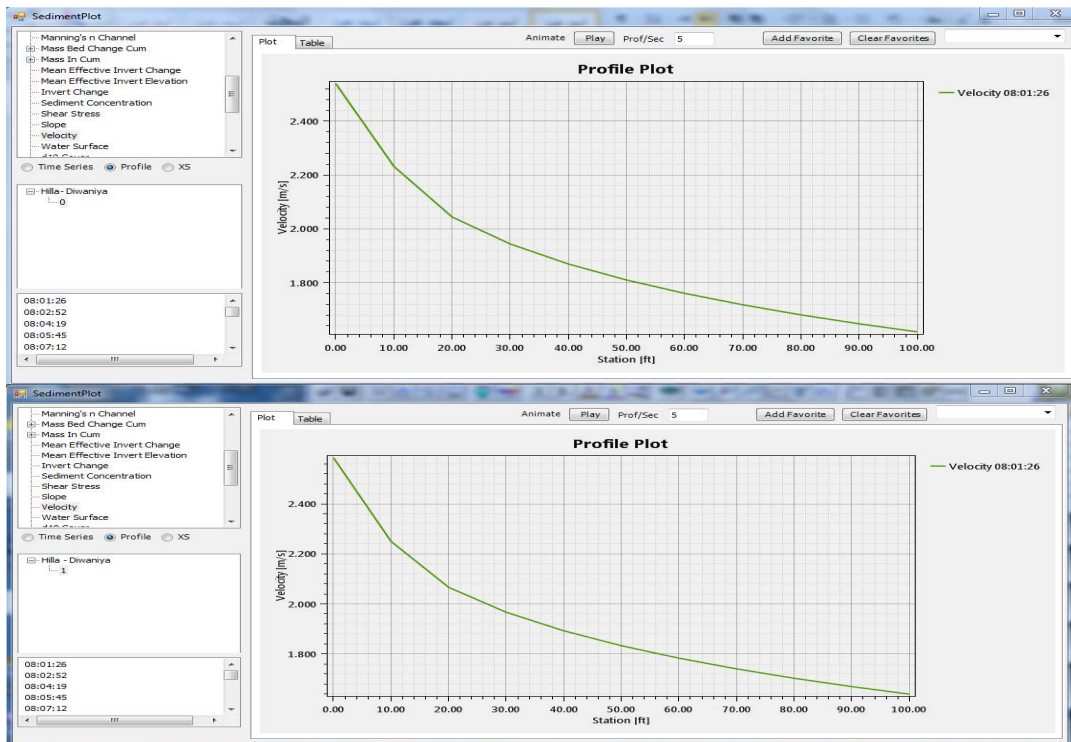


**Fig.7. The relationship between velocity and its station for two stations.**
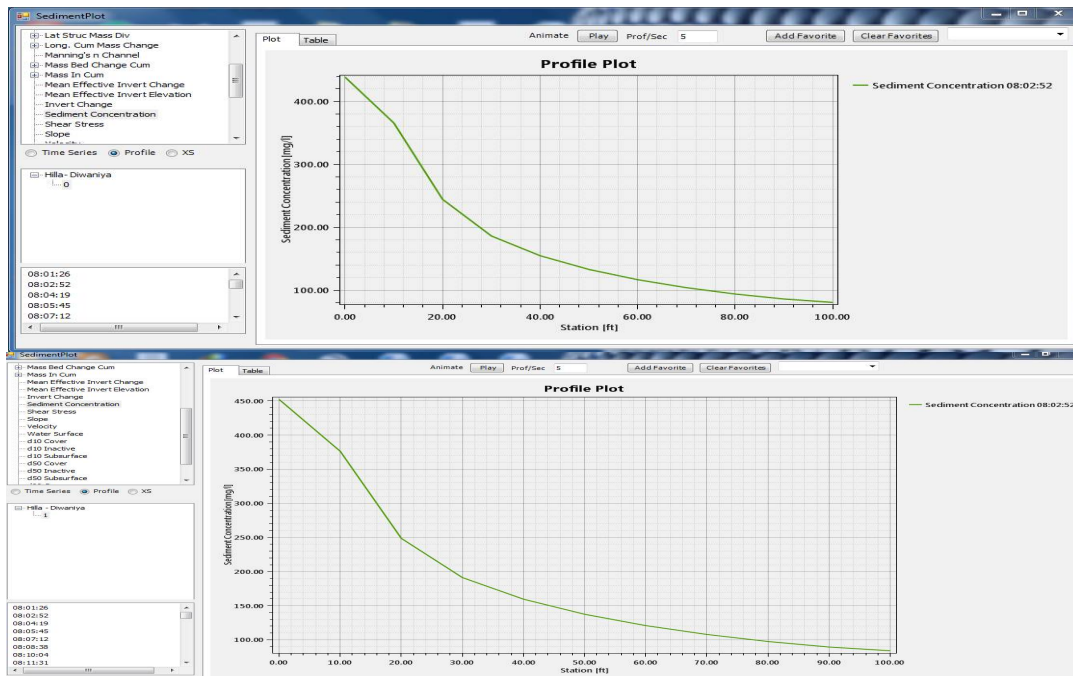


**Fig .8. The relationship between sediment concentration and its station for two stations**
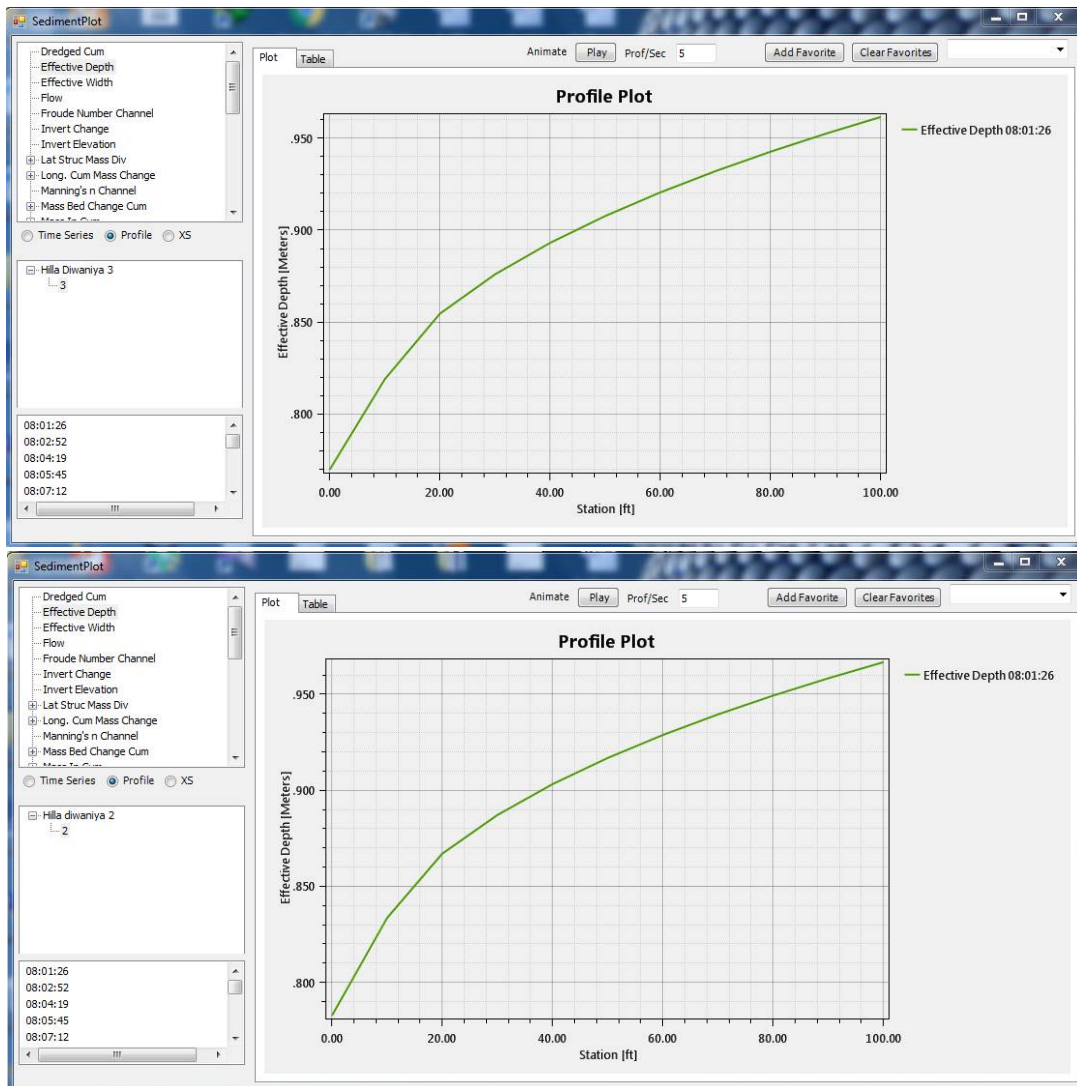
**Fig.9.The relationship between effective depth and its station for two stations.**

**RESEARCH ARTICLE**

# Enhancement Characteristics Clay Soil by using Demolition Waste

Abeer Abduljabbar Al-saeedi[1] * and Ahmed. T. Al-Janabi[2]

[1]Faculty of Materials Engineering, University of Babylon,Babil, Iraq.
[2]Faculty of Engineering, University of Babylon, Babil, Iraq.

*Address for Correspondence
**Abeer Abduljabbar Al-saeedi**
Faculty of Materials Engineering,
University of Babylon,
Babil, Iraq.
Email:abeerabduljabbar75@gmail.com

**ABSTRACT**

Demolition waste is a collection of redundant materials that does not benefit the uses it collects from the building. It consists of several layers of building materials, which are the result of demolition, removal, construction and restoration in residential and commercial areas. The problem is when these materials accumulate any building materials that have remained after the end of each item of the building and are excessively useless and useless at the site, which affects the place, environment, money, and other influences that affect the work. In order to solve this problem, efforts must be made by all parties, whether implementing companies, municipalities, or specialized associations in the environment or individuals, to reduce the pollution of the places on which the building is built and to contribute personally to solving this problem, we should encourage industrial companies in the field of recycling waste. This paper presents the study of the Enhancement characteristics clay soil by using Demolition waste. The samples were taken from a newly constructed building site from a Hilla city / Iraq and mixed with waste ceramic dust. Increases in the percentage of dust from 0 to 50% due to decreased in properties of soil.

**Keywords:** WCD, L.L, P.L, PI, U.C.S, OMC, MDD.

## INTRODUCTION

It is known that the cheapest materials in construction are soil, and so most of the research and civil engineer focused on Enhancement characteristics of this soil, and one of the first methods used to Enhanced the soil is the removal and replacement of old soil with new soil and since this method is more negative than the positives in terms of length In the period required for the completion of the project, which is more than 6 months, as well as the need for loading and unloading equipment and the space needed to complete the work[1]. Therefore, our focus was on finding solutions and alternative ways to Enhancement the soil. The usual ways to Enhancement the soil with additions,

16452

**Abeer Abduljabbar Al-saeedi and Ahmed. T. Al-Janabi**

However, in this research, a new type of additive was used, which is the waste resulting from the demolitions waste of buildings, including the waste ceramic dust residues, which are considered the cheapest types of additives, in the first instance, and the environment can be cleared from the waste accumulated in the empty squares, Of environmental pollution capacity [2]. The clay Soil is a soil that has the ability to expand and Swelling in the event of submerged water and the groundwater in this type of soils cause us a lot of problems, some of which leads to the collapse of soil and others cause distortions to occur within the soil due to lack of resistance and these factors all to lead to the failure of soil If it is under the influence of the burdens imposed on it. However, it is not repeated in the construction of civil engineering, but what concerns us is the distortion in the soil, including clay Soil.

# EXPERIMENTAL PART

### Clay Soil

Clay Soil is one of the basic components of bentonite, which can be obtained from volcanic weathering. Because of its expansion properties, Clay Soil has its original size when contact with water occurs. have been used as drilling ditches because of the Keep holes open and therefore can be used in the walls of dams and areas with high groundwater. The characteristics are given as the Table 1 .

### Waste Ceramic Dust Additives

The ceramic dust is one of the most important materials resulting from the demolition of buildings and to reduce of the amount of debris resulting from the demolition can take advantage of the first materials used in the construction of these buildings to improve the properties of clay soil [3] . The characteristics are given as the table 2**.**

### Testing procedure

The ceramic was taken from places to be demolished and then crushed in the soil laboratories dedicated for this purpose and then grind them by the Los Angeles device to obtain the dust that we would like to use in our various experiments after mixing it with  clay soils of 0-50%, an increase of 5% of the total of 11 samples of soils mentioned Previouslythat have the ability to absorb water and improve their properties later.

- Atterberg Limits.
- Standard Proctor compaction tests (S.P.T).
- Unconfined Compressive Strength (UCS).

### Analysis of Test Results

Various laboratory experiments were performed and the results were obtained below.

### Atterberg Limits

For a fine grain soil (silt and clay), the general properties change with water through figure 1.

**a) Liquid Limit Test: (L.L, WL)**
It is the water content at which the soil starts to behave like a liquid.

**Abeer Abduljabbar Al-saeedi and Ahmed. T. Al-Janabi**

**b) Plastic Limit Test; (P.L, WP)**

It is the water content at which the soil starts to behave as a plastic without cracks.

**c) Plasticity Index (P.I):**

It is the rang in a water content and We can get it from the following relationship

$$P.I = L.L - P.L$$

**Standard proctor test SPT**

The test was performed on the WCD with samples of a clay soil. We see that MDD value Inversely proportional the water content, and we can show this in Charts 2 - 3. Chart-2 shows the Maximum Dry Density (MDD) variation with a percentage of WCD. From the chart, it is clear that the percentage of WCD Proportional with the MDD of soil goes on increasing [4]. The MDD increases from 1.49 g/cc to1.96 g/cc when WCD is increased from 0 to 50%. The reason for such behavior is Due to the replacement of low-Specific gravity soil particles (2.68) with higher ones (2.82) of ceramic dust particles. Also, the void spaces in the soil are filled by dust particles [5]. So that the void ratio also decreases.

$$\gamma_d = \frac{G}{1+e}\gamma_w$$

From the above equation we note that the relationship is Proportional between the specific gravity (G) and thedry density, and Inversely proportional a void ratio (e). Chart-3 shows the relation between Optimum Moisture Content with WCD%. OMC is the optimum content for water in which the dry density becomes higher at the level. Clay soil has a large tendency to attract water molecules toward it [6]. For this reason, the optimum moisture content in this soil is 20.6% higher in unstable conditions. When the WCD increases from 0 to 50%. Note that the value of OMC drops from 20.6% to 15.8% [7] [8].The main reason for the low moisture content is due to the low gravity of water molecules in the soil. This is due to the substitution between the soil particles and the dust of the waste ceramic dust [9].

**Unconfined compression strength (UCS):**

Uncompressed compressive force (UCS) is the prevailing experience To study and analyze a stable soil by knowing its resistance. It is the main recommended test Where specific amounts of WCD are taken from (0% -50%) which will be added for the purpose of Enhancement characteristics soil properties[10,11]. This has been seen in the Chart 4. Chart-4 shows the variation of Unconfined compression strength with WCD%. The Unconfined compression strength test was increased in all added percentage.

## CONCLUSION

Many of those interested in cleaning the environment seek to protect them from waste, whether industrial, construction or agricultural. We are civil engineers, so we must preserve our environment from the Demolition waste. We tried to reduce the waste of demolition because of the large quantities of them. Through the addition of certain proportions from WCD, we obtained the: 1-Decrease the liquid limit with the increase in the proportion of WCD and this a good feature. 2-Increase the Unconfined compression strength for all added percentage and change the failure type from shear failure to bearing failure that may be a result from the high strain occurs after adding WCD.3-The characteristics of clay soil have been enhancement and the environment cleared from demolition waste.

## REFERENCES

1. http://article.sapub.org/10.5923.j.re.20170704.03.html
2. C. Neeladharan. V. Vinitha (2017). Stabilisation of Soil by using Tiles waste with Sodium Hydroxide as Binder, International Journal of Innovative Research in Science, Engineering and Technology .ISSN (P): 2347-6710; ISSN (E): 2319-8753, Vol. 6, Issue 4, pp. 1-7.
3. Md. Safiuddinand Mohd Zamin Jumaat. (2010). Utilization of solid wastes in construction materials.International Journal of the Physical Sciences.ISSN 1992 – 1950;Vol. 5(13), pp. 1952-1963.
4. Md Ali Ashraf, S. M. Shazeebur Rahman (2018). Determination of Optimum Cement Content forStabilization of Soft Soil and Durability Analysis of Soil Stabilized with Cement, American Journal of Civil Engineering.ISSN (P): 2330-8729; ISSN (E): 2330-8737, Vol. 6, Issue 1, pp. 39-43.
5. M.Pathania, D.K.Soni, 2017. COMBINED EFFECT OF QUARRY DUST & CERAMIC DUST ON STABILISATION OF CLAY. International Journal of advance research in science and engineeringISSN (P): 2319-8346; ISSN (E): 2319-8354, Vol. 6, Issue 1, pp. 297-302..
6. I.R.Martinez,M.D.Toe and J.Zornberg (2016) Swelling Potential Behavior of Expansive SoilsTreated with Hydrated Lime." XVIII BrazilianConference on Soil Mechanics and GeotechnicalEngineering, COBRAMSEG 2016, 19-22 October, BeloHorizonte, Brazil.
7. M.A.AI-Bared. I.S.H.Harahap and A.Marto (2018)"SUSTAINABLE STRENGTH IMPROVEMENT OF SOFT CLAY STABILIZED WITH TWO SIZES OF RECYCLED ADDITIVE, "International Journal of GEOMATE, ISSN (P): 2186-2982ISSN(E):2186-2990. Vol.15, Issue 51, pp.39-46.
8. Parimal jam , Nisheet Tiwari (2016) "Effect of Lime and Rice Husk Ash on Engineering Properties of Black Cotton Soil international journal of innovative technology and research Volume No.4, Issue No.3, April – May 2016, 2924 – 2926.
9. Zainab A. Hussan and Ahmed. T. Al-Janabi " Studying Some Mechanical properties of soft soils Treated by CaCo3-Nano material, International Journal of Civil Engineering and Technology (IJCIET), Volume 9, Issue 11, 2018.
10. Ahmed. T. Al-Janabi and Abeer A. Al-saeedi "Evaluation the Swelling Soil Stabilized by Waste Corn Ash (WCA)" Journal of Engineering and Applied Sciences, Vol:14 (No.15-16) 2019.
11. Kadhim Naief Kadhim and Ghufran A. (The Geotechnical Maps For Gypsum By Using Gis For Najaf City (Najaf - Iraq) (IJCIET), Volume 7, Issue 44, July-August 2016, pp. 329–338.

**Table 1. The Physical characteristics of soil used**

| | |
|---|---|
| 1. Grain Size Distribution | (a) Gravel  = 0<br>(b) sand size%  =2<br>(c) silt size %  =25<br>(d) clay size %  =73 |
| 2. Specific gravity | = 2.68 |
| 3. Atterberg's limits | (a) liquid limit %  = 75<br>(b) plastic limit %  = 35<br>(c) plasticity index %  = 40 |
| 4. Standard Proctor Test (SPT)<br>Opt. Moisture content%<br>Max. Dry Densitygm/cc | (a) OMC  = 20.6<br>(b) MDD  = 1.49 |
| 5. Unconfined C.S KN/m² | =55 |
| 6. Color | Greyish black |
| 7. Unified classification system | CH |

**Abeer Abduljabbar Al-saeedi and Ahmed. T. Al-Janabi**

**Table 2. The Physical characteristics of Waste Ceramic Dust used**

| 1. Grain Size Distribution | (a) Gravel = 0<br>(b) sand size =46<br>(c) silt size =32<br>(d) clay size =22 | |
|---|---|---|
| 2. Specific gravity | = 2.82 | |
| 3. Standard Proctor Test<br>Opt. Moisture content%<br>Max. Dry Density gm/cc | (a) OMC = 17<br>(b) MDD = 2.1 | |
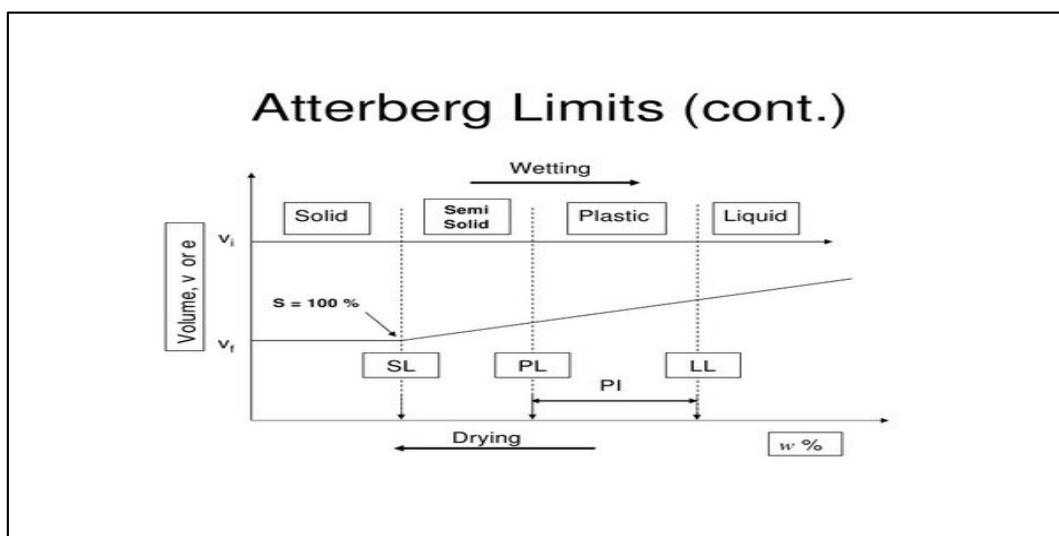


**Figure 1. Atterberg Limits.**
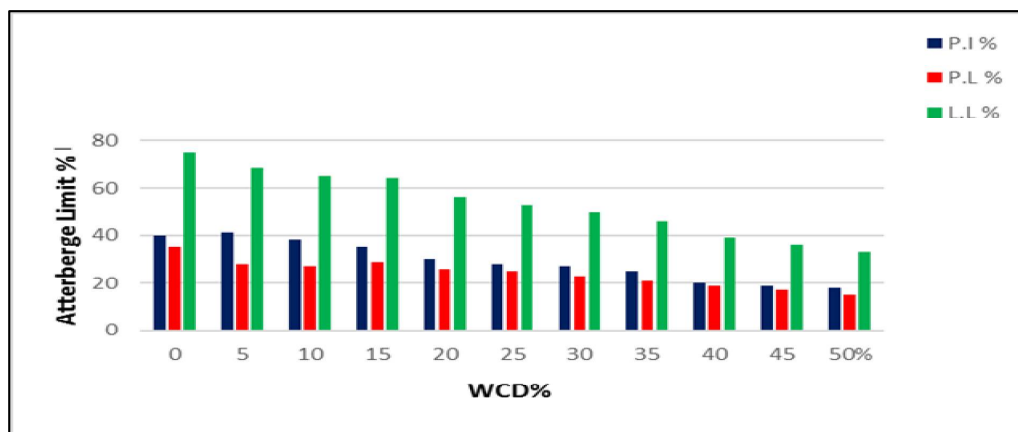


**Chart -1: The relation between Atterberg Limits with the percentage of Ceramic dust**

**Abeer Abduljabbar Al-saeedi and Ahmed. T. Al-Janabi**
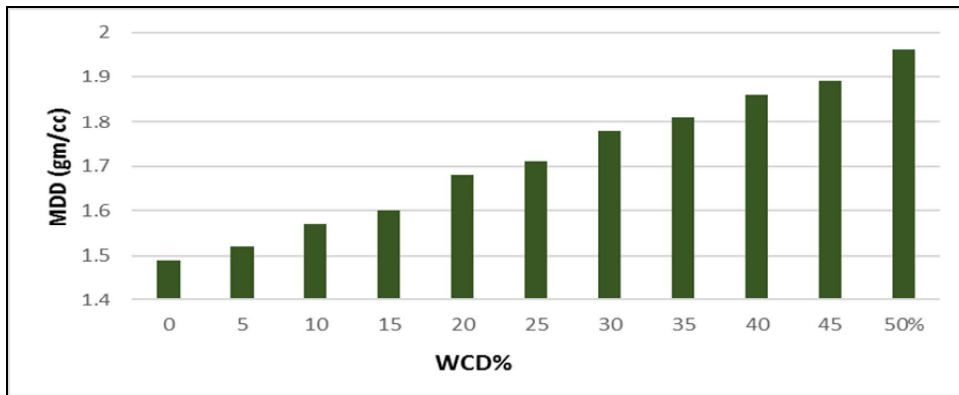


**Chart -2: The relation between MDD and WCD%**
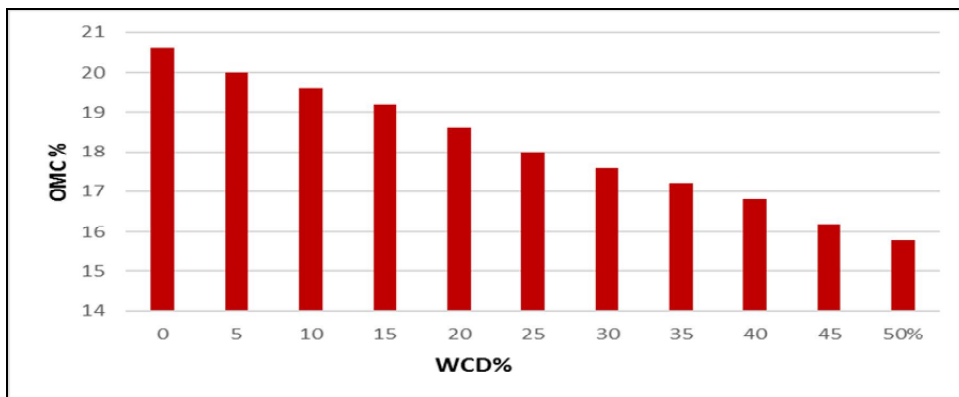


**Chart -3: The relation between OMC and WCD%**
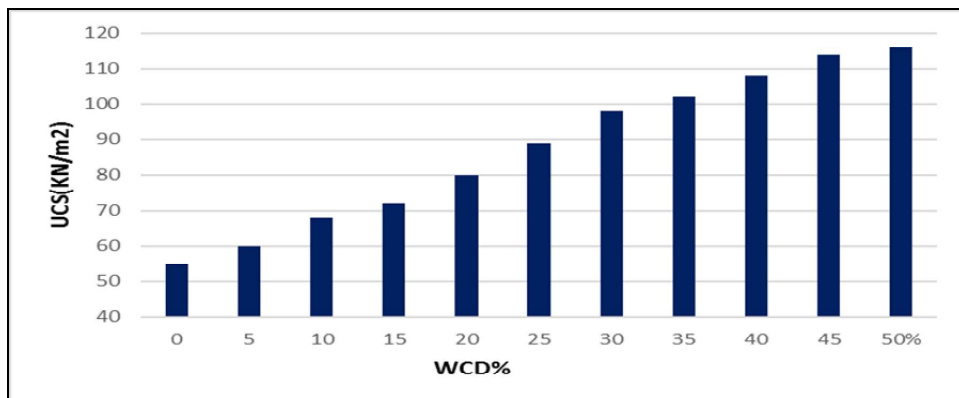


**Chart -4: The relation between Unconfined compression and WCD%**

**RESEARCH ARTICLE**

# Histomorphology and Histochemical Study of Esophagus and Stomach in Grey Mongoose (*Herpestes edwardsii*) In Iraq

Hussein Bashar Mahmood[1] and Khalid.K.Kadhim[2*]

[1]Department of Anatomy and Histology, College of Veterinary Medicine, University of Karbala, Iraq.
[2]Department of Anatomy and Histology, College of Veterinary Medicine, University of Baghdad, Iraq.

**ABSTRACT**

Histomorphology of the esophagus and stomach of wild adult grey Iraqi mongoose were studied. Fourteen samples were collected from orchards near the Tigris River. Target organs topography, shape, and their blood supplywere described. Histological sections were stained with routine H&E stain, Masson's trichrome stain for collagen fibers and Verhoffe's stain for elastic fibers, combined PAS + Alcian blue for mucin type detection. Anatomically, the esophagus was narrow muscular folded tube, (13) cm length extends dorsally to trachea at larynx level than turn gradually to left side. It was situated to the right of thoracic aorta at tracheal bifurcation. One cm length of abdominal part penetrates the diaphragm through the esophageal hiatus. The stomach of was simple, J shape. The stomach had middle constriction divided the stomach into two compartments. Inner stomach surface showed eight longitudinal folds in different length. Left gastric branch of celiac artery supplied both visceral and parietal surface ofstomach thatcontinued to ventral margin of the esophageal-gastric junction to form right artery.Histologically, themucosa of upper esophagus was stratified squamous epithelia.The keratinization was decreased gradually toward the stomach. The muscularis mucosa was thin scattered interrupted smooth muscles bundles. Esophageal mucous glands were restricted only in esophageal stomach junction. Tunica muscularis was skeletal, mixed and smooth muscle fibers in cranial, middle and caudal region respectively. The stomach lined bysimple columnar epithelia without goblet cells. The gastric pits in cardiac region were deep and bounded by the thick band of stratum compact. The fundic and pyloric gastric pits were shorter than cardiac pits.The gastric glands had a large numbers of pyramidal parietal cells, chief cells, G cells and large unknown clear cells. These were simple tubular glands more coiled towards pylorus,secretion with neutral mucin was located superficially and that with both neutral and acid mucin were located deeply.

**Hussein Bashar Mahmood and Khalid.K.Kadhim**

## INTRODUCTION

Mongooses (Herpestidae) are small, wide spread carnivores occupying various habitats from Africa to Southeast Asia [1]. The genus Herpestes contains 10 species and is considered the oldest genus within the order Carnivora [2]. The Indian gray mongoose or common grey mongoose (Herpestes edwardsii) is a species of mongoose mainly found in southern Asia mainly India, Pakistan, Nepal, Sri Lanka and some other parts of Asia. This omnivorous scavenger preys on rodents, snakes, birds' eggs and hatchlings, lizards and variety of invertebrates [3]. Generally, esophagus divided into cervical, thoracic and abdominal parts. Desorption of its course was mentioned in different types of animals [4]. The esophagus in canine and feline begins cranially at the cranial esophageal sphincter and continues to the esophageal hiatus at the diaphragm. Anatomy of stomach was studied in different typs of animals.The simple stomach had glandular region only in cat[5]. The stomach of domestic ruminants classified in to compound (multilocular), the rumen, reticulum and omasum (non-glandular region) while, abomasum, was comparable to the glandular stomach of the other simple stomached domestic mammals.

Compound stomach andcharacterized by the presence of a diverticulum surmounting the fundus in pig. Horse stomach is simple and divided into two regions; glandular and non-glandular[6]. Similar finding is reported inhamster and rodent's stomach [7] respectively. Arterial blood supply of cat stomach is contributions from five major sources [8]. Theoesophagus is lining by a stratified squamous epithelium,may be keratinized depending on animal's diet [9]. [10]who stated that themuscularis mucosa is, however, absent cranially whileesophageal mucous glands are present and the tunica muscularis is smooth or skeletal muscle, depending on the species. The tunica muscularis is different, its skeletal muscle fibers gradually transfers to smooth muscle fibers caudally in dog.While itsrepresented by two layers of muscle fibers, inner layer ispredominant striated muscle in Rock rats [11]. The fore-stomach of rat is lined by stratified squamous epitheliumor only the non-glandular forestomach [12]. Gastric glands are located in sub mucosa of fore stomach and lamina propria of posterior part of the stomach in Caspian pony [13]. In rat, the cardiac glands are branched simple tubular [14]. In canines, the pyloric glands occupied the thickness of mucous membrane [15]. The pyloric glands are simple branched coiled tubular glands and relatively shorter compared to other gastric glands [16]. There is paucity of information regarded the Histomorphology of the digestive organs of Iraqi grey mongoose. So this research was designed to provide basic knowledge about esophagus and stomach in this wild animal.

## MATERIALS & METHODS

Fourteen healthy grey mongooses of both sexes were used in this study. The average body weight was (350 ±23.3) gm. The average body length was (54±5.7) cm,The relative length of the esophagus and stomach to the body length was (18%,6%)cm respectively (Fig,1). The animals were caught from orchards near Tigris Rivers. The animals euthanized by intra muscular administration of diazepam (1mg/1kg) combined with ketamine HCL (30Mg, 1Kg)[17]. Longitudinal incision at ventral aspect of neck, chest and abdomen was done to viewed esophagus and stomach. The morphological parameters of the target organs included shape, length, weight and relation with other organs. Length were recorded in centimeter (cm) using a calibrated scale. The weight was recorded in gram (gm) using the sensitive electronic balance. The samples were fixed in 10% neutral buffered formalin, sections (5µm.) thickness of three regions of esophagus (cranial, middle and caudal) and from stomach (cardiac, fundic and pyloric regions) were taken. Sections were stained with routine H&E, Masson's trichrome stain for collagen fibers and Verhoffe's stain for elastic fibers, combined PAS + Alcian blue (PH 2.5) for Neutral and acid mucin[18]. The thickness of the tunica mucosa, submucosa and muscularis were recorded. The collected data were represented by mean ± standard deviation. Analysis was done using SPSS version 20 at (P<0.05).

**Hussein Bashar Mahmood and Khalid.K.Kadhim**

## RESULTS

### Esophagus

Anatomically, the esophagus was narrow amusculo-membranous folded tube, which extends from the pharynx to the stomach. It'sdivided into cervical, thoracic and abdominal parts. In cervical region, the esophagus bounded ventrally by the trachea, dorsally by the cervical vertebrae, and laterally by the common carotid artery. It's curved into left side at the thyroid gland region at second ring of trachea, but it returned to left side at thoracic inlet. In thoracic region the esophagus become dorsally to tracheal bifurcation (Fig 2) and crossed dorsally through mediastinum then extended in right side of descending aorta (Fig,3). Abdominal part of esophagus was very short about (1) cm, penetrating the diaphragm through the esophageal hiatus, then become wide and thick. The esophagus connects with stomach by esophageal opening. The cross section of esophagus appeared folded. The mean length of the fresh esophagus was (13±0.8) cm. The relative length of the organ to the body length was 18% cm.

The stomach was a hollow, muscular, large dilatation organ located caudal to the diaphragm, which intervenes between the esophagus and small intestine, in hypochondrial region. Cranially, occupied space between lobes of liver, caudally, bounded with jejunum and cecum, dorsally contact with spleen and part of left kidney, ventrally was bounded partially with caudrate lobe of liver. In right side bounded with caudal duodenal flexure while bounded by part of costal arch in left side. The stomach was simple( J) shaped, had light narrowing that divided stomach into two sac. Stomach had two opening cardiac and pyloric, two surface parietal and visceral, two curvatures lesser and greater and two extremity. The lesser curvature was very short connected by omentum that extend to small intestine, while the greater curvature very broad and contact with spleen which slightly extend dorsally (Fig, 4). Internally, the stomach can divided into three main sites, including the cardiac region (around the superior opening of the stomach) connected with the esophagus; it was thicker and rougher than other regions (Fig, 5). The fundus (the body) greater portion of the stomach and the pyloric region (connect with duodenum).In pyloric region, there were pyloric antrum as a depression connected with stomach body and the pyloric canal which continues to the duodenum. The internal surface characterized by present numerous of longitudinal folds, these folds appeared high and greater in size in fundic region and decrease gradually toward cardiac and pyloric region. However, there was no clear line of demarcation between these regions (Fig, 6).

### Blood supply

The main artery that supplies stomach was the celiac artery.  It had three branches; (first) the common hepatic artery that supplies the liver. (Second) left gastric branch for stomach, this branch gives many of short vessels distribution in both visceral and parietal surface of stomach. (third) the left gastric artery divided into two divisions; cranial and caudal part, the cranial part of left gastric artery was supplied left surface while the caudal part was continued to the lesser curvature near the esophageal-gastric junction to supply right side (Fig,7). Histologically,the sections of esophagus showed some differences among cranial, middle and caudal part. However, all those regions were consisted of four basically layers; mucosa, submucosa, muscularis and adventitia (Fig, 8). The mucosa in the cranial region was keratinized stratified squamous epithelium; the epithelium was composed of (8-12) cell layers (Fig.9). While it was about (6-8) cell layers in middle region which had less keratinized layers (Fig.10). However, at the caudal region, the epithelium was composed of (4-6) cell layers but there was no keratinization of the outer layer (Fig. 11). The lamina propria represented by connective tissue fibers and scattered by lymphatic tissue. In the caudal region of esophagus, the collagen bundles extended to the stomach formed the (stratum compact), this layer of collagen was appeared as stripe extend a long of caudal region of esophagus and continued to  stomach wall.At the esophageal stomach junction, there were simple tubular serous and mucous esophageal glands, these glands located in lamina propria and few number extended into submucosa, these glands were located at the site of  epithelial changed from squamous to the columnar epithelia (Fig,12,13). The muscularis mucosa was thin and consisting of

**Hussein Bashar Mahmood and Khalid.K.Kadhim**

scattered interrupted smooth muscles bundles but become thick in middle region of esophagus. The submucosamade up of loose connective tissue rich by collagen fibers intermingled by few of elastic fibers. No glandswere observed in esophagus. Thickness of submucosa in cranial, middle and caudal region of esophagus was (144, 131, 104) µm respectively. The tunica muscularis, was distributed as inner circular and outer longitudinal laminae, it was striated muscle fibers in cervical region (200) µm in thickness, mixed in middle region with (170) µm thickness and smooth fibers in caudal region with (315) µm thickness. Adventitia, this tunica contains loose connective tissue, elastic fibers and blood vessels (Table,2), (Fig,14,15,16).

The stomach wall represented by four basic layers; mucosa, submucosa, muscularis and serosa. The stomach was simple glandular, had three glandular regions, cardiac, fundic and pyloric region. Each region had some characteristics feature differsthan the other region (Fig,17).Gastric mucosa was lined by typically simple columnar epithelia without goblet cells (Fig, 18). The thickness of mucosa was (565, 722, 700 µm) in cardiac, fundic and pyloric region respectively.In cardiac region, the gastric pits were extended deeply; however, it was shorter in fundic and pyloric regions. The depth of gastric pits in cardiac, fundic and pyloric regions was (504, 148, 198) µm respectively. The mucosa of stomach contain high and low folds, the mean of thickness about (565, 722, 700) µm in three region respectively (Table,3) (Fig,19,20,21). The mucosa of all parts of stomach was supported by thick stripe of collagen fibers (stratum compactum) and two to three layers of thick smooth muscle fibers of muscularis mucosa extend between these networks of collagen fiber (Fig 22). In general, the gastric glands in cardiac region were simple short coiled glands, lined by columnar cells had elongated nuclei were located in base of glands.

There were numerous of parietal cell distributed randomly among epithelium. In addition to high numbers of chief cells can be seen (Fig,23). The fundic region featured by thick lamina propria, simple tubular glands, the cells of these glandsarranged as longitudinal cords, the amount of connective tissue between the glands were reduced because the glands were tightly packed. There was large number of parietal cells in fundic region that distinguished from other cells as chief and clear cells by their bright acidophilic staining andlarge spherical or ovoid shaped with round nuclei. The chief cells were dark pyramidal or cuboidal shape basally positioned, there were number of clear cells which appear spindle or elongated in shape were located in base of laminea propria (Fig, 24, 25). In pyloric region, the lamina propria was consisted of two types of simple coiled gastric glands, there are a numbers of G cells can be distinguished in pyloric region located in base of pyloric glands which appear asfried egg-like, bright color had rounded nucleus centrally positioned (Fig,26,27). Submucosa was loose connective tissue, rich by collagen, elasticfibersand blood vessels (Fig,28,29). No glands were seen in this lamina, thickness of Submucosa in three region was (151, 150, 101)µm respectively. Serosa was lined by simple squamous and consisted of network of collagen and elastic fibers (Table,3). Histochemical observation reveled to positive reaction of the gastric bits and mucous neck cells to PAS stain which appeared magenta in color (Fig,30). The superficial gastric glands appear magenta color due to the presence of neutral secretions while the deep glands that located in base of mucosa appearance mixed purple blue and red color due to the secrete acid and neutral (Fig,31).

## DISCUSSION

There is scarcity of morphological details of the digestive system the grey mongoose in Iraq. The esophagus in grey mongoose appeared as a narrow amusculo-membranous folded tube.The walls of the esophagus in feline are protected from damage by hard food by presence of longitudinal folds, this allows for expansion as the food travels down to the stomach[19].In current study, the cervical region of the esophagus passed dorsally to the trachea at second ring of trachea but before entering the thoracic cavity turn to left side of trachea. However, it was noticed that the esophagus is deviated slightly to the left around the cervical region in rat, cat and dog[20]. But seemed followed similar course that of other animals [21]. The stomach in grey mongoose was (J) in shaped, this is similar to rabbit stomach [22]in rabbits. While its (C) shaped in dog, cat and in pigs [6]. Externally, Mongoose stomach hadnarrowing in its middle part, this constrictionmay be consider as a kind of adaptation for this animal to resist shortage in

seasonal food. However, this is unlike any stomach in all species of animals.[23]whostated that the great differences between carnivores and herbivores are seen in these organs.This result were different as well as for that reported in laboratory animals such as rat, guinea pig and hamster, by presence of a limiting ridge between glandular and non-glandular regions [7]. The stomach of grey mongoose was simple type (glandular) or monogastric.Therefore, it seemed like carnivores stomach [24,25]. While it is classified as a compound (glandular and nonglandular chambers)or multilocular in ruminants [7].[26]who stated that the stomach of pig and horse where these have compound monogastric stomachwhile, the rat and hamster stomach have simple stomach but have separated non glandular chamber. In the current study, the internal surface of grey mongoose stomach had longitudinal folds,thesefolds extended in all regions of the stomach.Higher foldswerefound in fundic region. These folds may be occurred when stomach is empty, in addition, the presence of these folds may be allowed to more distention of stomach after consumed large amount of food in short time as a gluttonous predator animal.However, the stomach of tayra has longitudinal cord to grind up and digest food because the carnivores and especially wild animal need compact organs for digestion[27]. Whereas, the stomach of other animals like hamster and rabbits have no folds at all [7,26].

Histologically,mongoose esophagus had basically four layers as in all other animals; the keratinization of epithelia was appeared clearly a long esophagus regions. However,the degree of keratinization was reduced gradually towards stomach. The keratinization of esophageal mucosa of gray mongoose was more in its cranial part may be for natural of mongoose's diet, as the rats, mice, snack and rabbits, may be due to consumed hard types of food. However, the degree of keratinisation of the oesophagus depends on the animal's diet [9].The presentstudy revealed that the muscularis mucosa was thin, scattered interrupted smoothmuscles bundles.However, in dog and rock rat, its restrict as smooth muscle fibers in caudal region of esophagus only [28,29].Whereas there is no muscularis mucosain Giant African rat [9,29].

In this study, the epithelial layer of the caudal part of esophagus had rested on the stripe of collagen fibers (stratum compactum).This structure firstly registered by [30] who find the stratum compactum present in sub-glandular mucosa of stomach in carnivores only.Another report mentioned that the stomach mucosa of canineis lackingto stratum compactum [31].In mongoose, The tunica muscularis of thecranial region of esophagus had striated skeletal fibers and changed to mixed (skeletal and smooth) fibers in middle region then become smooth fibers in the last part near cardiac region.These results were similarto dog esophagus[9].The mongoose is a wild animal and in need for fast swallowed of food. This is described by [32]who stated the rate of passage of swallowed food is faster in the striated than in the smooth muscles.In current study, the esophageal glands were restricted onlyat esophagus-stomach junction.The gray mongoose is considered carnivoresand its food not need lubrication to facilitate their passage.Some carnivores species lack or had less numbers of esophageal glands due to food regurgitation reflex don't accrue[33].Conversely, these esophageal glands are importantin herbivorous animal to facilitate rough food passage [34].

The stomach in gray mongoose was lined by simple glandular mucosa for its three regions cardiac, fundic and pyloric.Similar observation was reported in in ferret and dog[35].However, in herbivorous animals, in addition to a glandular region, there is a non-glandular region lined with stratified squamous epithelium [36]. The stomach mucosa of grey mongoose was thrown into folds giving it a rumen like appearance. These observations are seen in rat stomach[37]. The cardiac region of grey mongoose characterized by presence of simple columnar epithelia withoutgoblet cells and the gastric pits were extended deeply and occupied on the thick lamina propria which is in correspondence with that in dog[38]. Nevertheless, there are a distinct keratinized stratified squamous epithelium of fore stomach of in rats, mouse, hamster and gerbil [39]. In this study,numerous of clear cells, irregular or spindle greater cellswere located closely with chief cells in glandular area,these cells were negative for H&E and combined AB+PAS. These cells may be havingcertain function in mongoose stomach secretion. Similar to these cells were mentioned in guinea pig stomach, as irregular cells contact with chief cells more than parietal cells which secrete the histamine during too much concentration of acidity [40]. The cardiac glands of mongoose stomach were short simple

16462

coiled glands. Which wassimilar to that mentioned in monkeys and most of domesticanimals[41] and in Caspian pony [42,43]. The mucosa of fundic region of grey mongoose stomach resting on thick layer of lamina muscularis and stripe of collagen fibers (stratum compactum), this was similar tocanine stomachs[30].Thisdense fibrous membrane may bestrength stomach wall and give protection from perforations in carnivores[44].The fundic glands of mongoosestomach were simple tubular gland with large numbers of parietal cells;this result indicates that mongoose stomach had high efficiencyto digest hard food.[45] who stated the described that the carnivores and omnivores would be expected to have higher stomach acidities than herbivores. In this study, the epithelial cells of pyloric region showed high simple cylindrical cells, arranged regularly and compactly with basal nucleus. These cells in this region had highly mucous secretion as reported in rat, horse and dog[37,46,47].The cardiac pits in in stomach were deeper than in other regions of the stomach in domestic animals while, the pyloric pits were shorter[48]. In the present study, the lamina propria of pyloric regionhad short and long simple coiled gastric gland that represented by two zones dark and light respectively. Similar observation is reported in pyloric region of dog stomach [16]. However, it'slong coiled tubular glands in stomach of domestic animals [49] histochemical reaction of thestomach mucosa in gray mongooseafter AB+PAS stainshowedthat epithelial cells and mucous neck cells of gastric pits had neutral muco-polysaccharides.While the other parts of the gastric glands showed moderate neutral mucin reaction due to acidic secretion of parietal cells. The presence of neutral muco-polysaccharidesis important to protect the stomach wall against acid digestion[50].In cat, the gastric glands showed moderate to strong reaction to PAS-AB stain(38). In conclusion, the histomorphological observations of the esophagus and stomach in gray mongoose showing too much similarity to carnivorous species in which its belong.

# REFERENCES

1.  Thulin, C.G., Simberloff, D., Barun, A., Pascal, M., & Islam, M.A. (2006). Genetic divergence in the small Indian mongoose (Herpestes auropunctatus), a widely distributed invasive species. Molecular Ecology. 15: 3947–3956.
2.  Nowak, E., Kuchinka, J., Szczurkowski, A. and Kuder, T. (2015).Extrahepatic Biliary Tract in Chinchilla(Chinchilla laniger, Molina). Anat. Histol. Embryol., 44: 236–240.
3.  Choudhury, A., Wozencraft, C., Muddapa, D., Yonzon, P., Jennings, A. and Geraldine, V. (2011).Herpestesedwardsii. In: IUCN.IUCN Red List of Threatened Species.Version.1.
4.  Gendron, K., McDonough, S. P., Flanders, J. A., Tse, M., &Scrivani, P. V. (2018). The pathogenesis of paraesophageal empyema in dogs and constancy of radiographic and computed tomography signs are linked to involvement of the mediastinal serous cavity. Veterinary Radiology & Ultrasound, 59(2), 169-179.
5.  Bremner, C. G., Shorter, R. G., & Ellis, F. H. (1970).Anatomy of feline esophagus with special reference to its muscular wall and phrenoesophageal membrane. Journal of Surgical Research, 10(7), 327-331.
6.  Konig H E and Liebich(2007).Veterinary Anatomy of Domestic Mammals. 3rdEdn. Schattauer GmbH, HolderIinstrapp: 324-343.
7.  Ghoshal N G and Bal H S (1989): Comparative morphology of the stomach of some laboratory mammals. Laboratory Animals 23: 21-29.
8.  Soybel, D.I.( 2005).Anatomy and physiology of the stomach.SurgClin North Am,. 85(5): p.
9.  Alsafy, M.A.M., S.A.A. El-Gendy (2012) Gastroesophageal junction of Anatolian shepherd dog: a study by topographic anatomy, scanning electron and light microscopy. Vet Res Commun 36:63-69.
10. Mann, C. V. and Shorter, R. G (1964). Structure of the canine oesophagus and its sphincters. *J. surg. Res.,* 4: 160–163.
11. Alexey E, Gashkova,V, Alexander P. , Saveljev& Alexei .V. (2015). Histologic features of the gastrointestinal tractof Laonastesaenigmamus (Rodentia: Diatomyidae). Russian Research Institute of Game Management and FurFarming, 79 Preobrazhenskaya St., Kirov, 610000, Russia — 2 Zoological Institute of the Russian Academy ofSciences, UniversitetskayaEmb. 1, Saint Petersburg, 199034, Russia — Corresponding author: Alexey Scopin;scopin (at)bk.ru. 65 (1): 151–163 4.5.

12. Berg, B. N. (1942): Pathological changes in nutritional gastritis in rat. The American Journal of Pathology 18 (1): 49-61.

13. Obadiah B, Abdu P A and Shekaro A (2011).Histomorpholgy of the gastrointestinal tract of domesticated Grasscutter(Thyronomysswinderianus) in Northern Nigeria. Journal of research in biology 6: 429-434.

14. Ojo, Gideon B, Caxton-Martins, Ezekiel, A, Odukoyo and Samson O A (2010). Morphometric effects of colonitida extract on the stomach of adult male wistar rats. Electronic Journal of Biomedicine 2: 18-24.

15. Jackson B M, Reeder D D, Searcy J R, Watson L C, Hirose F M and Thompson J C (1972).Correlation of the surface pH, Histology and gastrin concentration of gastric mucosa. The American Journal of Surgery 176 (6): 727-731.

16. Eurell J A. and Frappier B L (2006).Dellman‟s Textbook of Veterinary Histology. 6thEdition Blackwell Publishing Ames,Iowa50014, USA. 248-251.

17. Thurmon, J.C., Tranquilli, W.J., Benson, G.J. (1996): Lumb& Jones Veterinary Anesthesia. 3rd ed. Lea & Fibiger, London.

18. Bancroft, J.D., and Stevens, A. (2012). Theory and Practice of Histological Techniques.7th Edition. Churchill Livingstone. Pp: 127-129.

19. Samadi, F., Levine, M. S., Rubesin, S. E., Katzka, D. A., &Laufer, I. (2010). Feline esophagus and gastroesophageal reflux. *American Journal of Roentgenology*, *194*(4), 972-976.

20. Rudolf H, Strombery MW (1976). The Digestive System, In: Anatomy of laboratory 43-51.

21. Berghes, C., Tanase, P., Parvu, M., Dinu, C., &Cuca, D. (2011). Contributions to the study of the esophagus and stomach morphology in guinea pig. *Scientific Papers Animal Science and Biotechnologies*, *44*(2), 150-154.

22. Johnson-Delaney, C. A. (2006).Anatomy and physiology of the rabbit and rodent gastrointestinal system.In *Proc. Assoc. Avian Vet* (pp. 9-17).

23. Milton R. and Mills, M, (2017). The Comparative Anatomy of Eating.Statement from: *http://www.goveg.com/naturalhumandiet.asp*.

24. Mills, M. R. (1996). The comparative anatomy of eating. *VegSource Interactive Inc, 26.*

25. Larson, M. M., & Biller, D. S. (2009). Ultrasound of the gastrointestinal tract. *Veterinary Clinics of North America: Small Animal Practice*, *39*(4), 747-759.

26. Brewer, N. R., & Cruise, L. J. (1994). The Guinea pig heart--some comparative aspects. *Contemporary topics in laboratory animal science*, *33*(6), 64.

27. Lima, A. L. D. S. N., Gonçalves, T. C., Branco, É. R., Rodrigues, R. A. R., Giese, E. G., do Carmo, D. C., ...& de Lima, A. R.(2018). Morphology of the Stomach of Tayra (Eirabarbara). *Acta Scientiae Veterinariae*, *46*(1), 6.

28. Singhal, S. S., Ahmad, H., Sharma, R., Gupta, S., Haque, A. K., &Awasthi, Y. C. (1991). Purification and characterization of human muscle glutathione S-transferases: evidence that glutathione S-transferase ζ corresponds to a locus distinct from GST1, GST2, and GST3. *Archives of biochemistry and biophysics*, *285*(1), 64-73.

29. Ali MN, Byanet O, Salami SO, Imam J, Maidawa S, et al. (2008) Gross anatomical aspect of gastrointestinal tract of the wild African giant rat (Cricetomysgambianus). Journal of Scientific Research and Essay 3: 518.

30. Zahariev, P., Sapundzhiev, E., Pupaki, D., Rashev, P., Palov, A., &Todorov, T. (2010). Morphological characteristics of the canine and feline stomach mucosa. *Anatomia, histologia, embryologia*, *39*(6), 563-568.

31. Frappier BL (1998).Digestive system.IN.DellmannHD,EurelIJ,editors. Textbook of veterinary Histology (V).Baltomore, Maryland, USA: Williams &Wilkins:P. 80_164.

32. Talley, N. J., DeVault, K. R., & Fleischer, D. E. (2011). *Practical Gastroenterology and Hepatology: Esophagus and Stomach*. John Wiley & Sons.

33. Rus, V., Ruxanda, F., Ratu, C., Gal, A. F., &Miclaus, V. (2016). The presence and significance of the esophageal glands in the abdominal esophagus in dog. *Annals of the Romanian Society for Cell.*

34. AtteyatSelim*, Hazaa E and Goda W (2017). Comparative Histological Studies of the Esophagus Wall of Oryctolaguscuniculus Rabbit Adult, Young and Lactating Using Light Microscope.Zoology Department, Faculty of ScienceTanta University, Tanta, Egypt.Volume 8.Issue 2. 1000456

35. Poddar, S., &Murgatroyd, L. (1976). Morphological and histological study of the gastro-intestinal tract of the ferret. *Cells Tissues Organs*, *96*(3), 321-334.
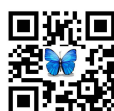
36. Frandson, R. D., & Spurgeon, T. L. (1992). Physiology of Male Reproduction. *Anatomy and Physiology of Farm Animals (5th edition)(Philadelphia: Lea and Febiger) pp*, 417-418.
37. SatyaSAI Chandana, G. A. D. U. L. A. (2011). HistologicalandHistochemicalkstudy on the stomach ofalbino rat (Rattusnorvegicus) (Doctoral dissertation, SRI VENKATESWARA VETERINARY UNIVERSITY TIRUPATI–517 502.(AP) INDIA).
38. Shibata, T., Imai, M., Moriguchi, k. and Takada, Y. (1990). Do the cardiac glands Excist, The Cat. Okajimas FoliaAnatomica. 67 (1):31-36.
39. Bal H S, Ghoshal N G and Magilton J H (2007). Histomorphology of torus pyloricus of domestic pig.Anatomia, Histologia, Embryologia, 1(4): 289-298.
40. Kamoshida, S., Saito, E., Fukuda, S., Kato, K., Iwasaki, A., & Arakawa, Y. (1999). Anatomical location of enterochromaffin-like (ECL) cells, parietal cells, and chief cells in the stomach demonstrated by immunocytochemistry and electron microscopy. *Journal of gastroenterology*, *34*(3), 315-320.Haryana Agricultural University.pp 29-32
41. Leus, K., Macdonald, A. A., Goodall, G., Veitch, D., Mitchell, S., &Bauwens, L. (2004). Light and scanning electron microscopy of the cardiac gland region of the stomach of the Babirusa (Babyrousababyrussa–Suidae, Mammalia). *Comptesrendusbiologies*, *327*(8), 735-743.
42. ADIB, MORADI M., and MT SHEYBANI (2006). "Histological study of stomach in Caspian pony.": 249-254.
43. Krystev, H., &Vitanov, S. (1993). Textbook of Cytology and Histology. *Sofia: Zemizdat Scientific Publishers*, 251-255.
44. Fayed M.H, Elnasharty M. Shoaib M. (2010). Localisation of sugar residues in the stomach of three soecies of monkeys(*Tupaiidaeglis,Nycticebuscocang*and *Callithrixjacchus*) by lectinhistochemistry. International Journal of Morphology. 28(1):111-120.
45. Beasley, D. E., Koltz, A. M., Lambert, J. E., Fierer, N., & Dunn, R. R. (2015). The evolution of stomach acidity and its relevance to the human microbiome. *PloS one*, *10*(7), e0134116.*Biology*, *20*(2),
46. Trang P H, Ooi P T, Zuki ABZ and Noordin M (2012).Comparative gastric morphometry of Muong indigenous and Vietnamese wild pigs, The Scientific World Journal,Volume: 1-9.
47. Nitovski A, Radovic B, Greak D, Milanovic V, Potic M, Milenkovic M and Greak M (2015).Flourescent microscopy of gastric mucosal tissue of cattle and pigs. International Journal of Agriculture Innovations and Research, 4(1):2319-1473.
48. Banks, W. J. (1993). *Applied veterinary histology.* Mosby-Year Book, Inc.
49. Samuelson, D. A. (2007). *Textbook of veterinary histology*(No. V200 SAMt).
50. Al-Saffar, F. J., &Eyhab, R. M. (2016). Histomorphological and histochemical study of stomach of domestic pigeon (Columba liviadomestica). *The Iraqi Journal of Veterinary Medicine*, *40*(1), 89-96.

**Table 1.Measurements of lengths and weight for target organs**

| Title | Mean &SD absolutely | | Relatively |
|---|---|---|---|
| Length animal | 53± 5.09 | cm | ----------- |
| Weight of animal | 351±12.7 | gm | ---------- |
| Length of Esophagus | 13± 0.8 | cm | 18% |
| Length of Stomach | 4± 0.5 | cm | 6% |

**Table ( 2 ) Mean thickness of mucosa, sub mucosa, muscularis and adventitia in cranial, middle and caudal regions of esophagus of the grey mongoose.**

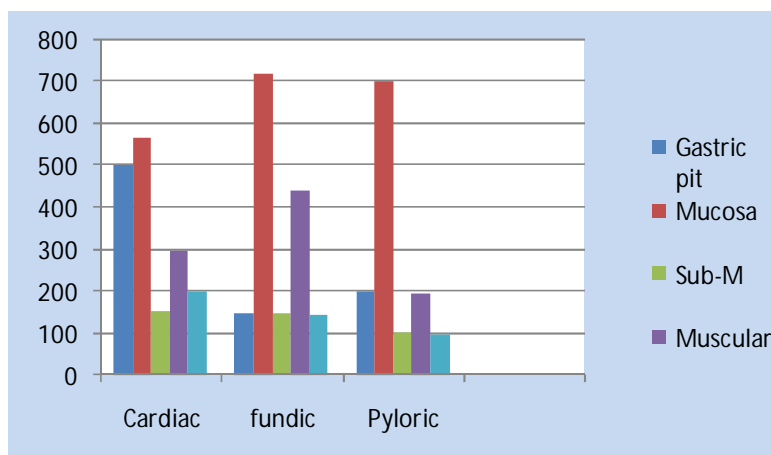| Organ | Mucosa | submucosa | Tunica muscularis |
|---|---|---|---|
| Esophagus\cranial | 102 ±12.5 | 144 ±18.1 | 200±31.09 |
| Esophagus\Middle | 70±18.2 | 131±17.7 | 170±28.8 |
| Esophagus\caudal | 80±15.2 | 104±13.9 | 315 ±26.3 |

**Hussein Bashar Mahmood and Khalid.K.Kadhim**

**Table .3. Mean thickness of gastric pit, mucosa, sub mucosa, muscularis and serosa of cardiac, fundic and pyloric regions of stomach of the grey mongoose.**

| Organ | Gastric pit | mucosa | submucosa | Tunica muscularis | Tunica serosa |
|---|---|---|---|---|---|
| Cardiac region | 504 ±39.09 | 565 ±38.6 | 151 ±21.1 | 300±20 | 201 ±13.4 |
| Fundic region | 148 ±13.4 | 722 ±24.2 | 150±16.3 | 440±21.6 | 145 ±17.1 |
| Pyloric region | 198 ±13.4 | 700±31.6 | 101 ±13.4 | 195 ±13.4 | 98 ±13.4 |
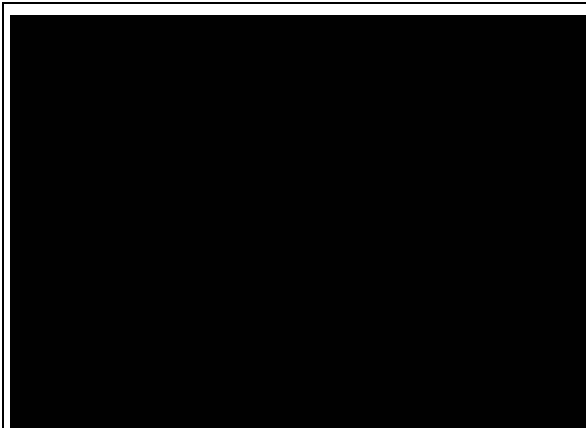


**Fig.1. Show the ratio the length of stomach andesophagus to the length of animal (cm). The numbers represent the mean ± standard divisions**
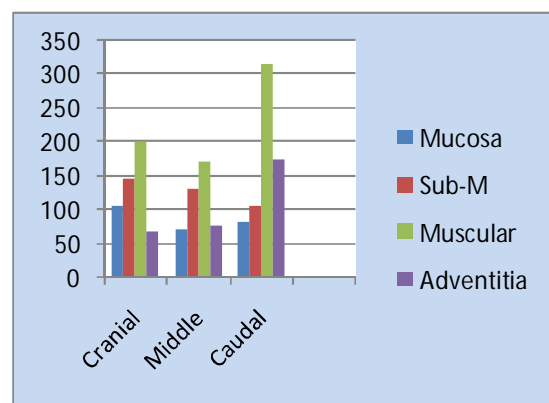


**Chart .1. Chart representing the mean thickness of mucosa, sub mucosa, muscularis and adventitia of cranial, middle and caudal region of esophagus of the gray mongoose**



**Chart.2. Chart representing the mean thickness of gastric pit, mucosa, sub mucosa, muscularis and serosa of cardiac, fundic and pyloric regions of stomach of the gray mongoose**

**Hussein Bashar Mahmood and Khalid.K.Kadhim**



**Fig. 2. Esophagus of gray mongoose (E) showing the esophagus passes between common carotid artery (A) and left side to trachea (T).**
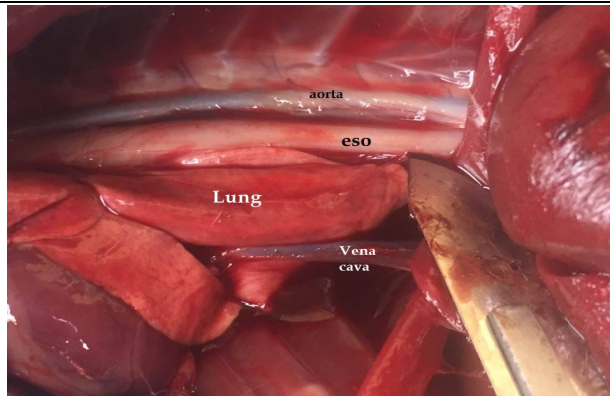


**Fig. 3. Esophagus course thought thoracic cavity passes in right side of thoracic aorta.**
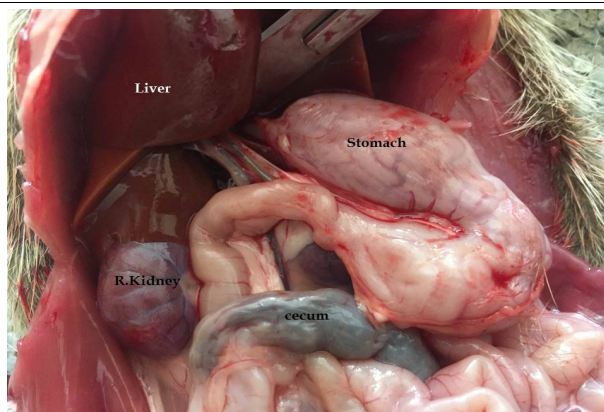


**Fig.4.Stomach of grey mongoose (J) shape, bounded by liver cranially, right kidney and cranial flexure in right side and small intestine and cecum caudally.**

**Hussein Bashar Mahmood and Khalid.K.Kadhim**



**Fig.5.Internal surface of stomach explained junction area between esophagus and stomach**
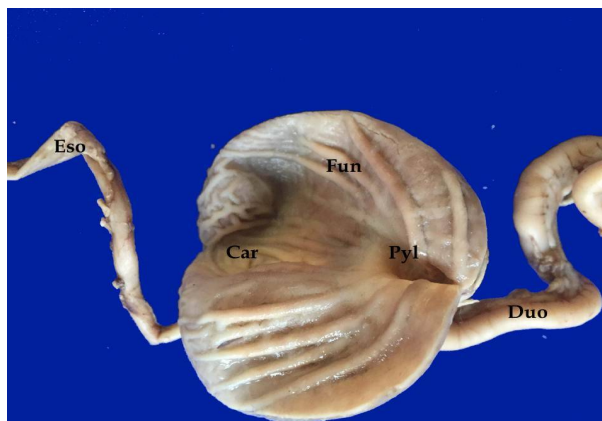


**Fig .6. Internal surface of stomach showing cardiac, Fundic, pyloric antrum and pyloric canal.**
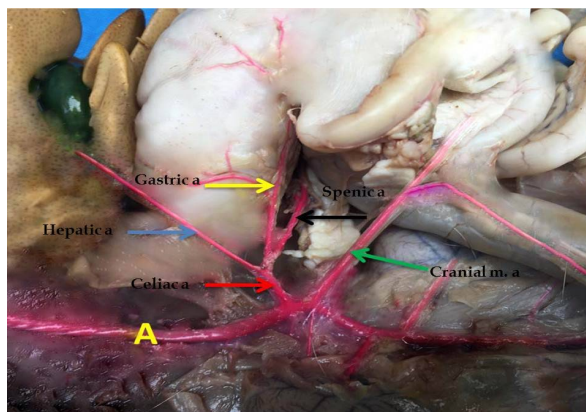


**Fig .7.Blood supply of digestive stomach by celiac artery which divided in three branches**

16468

**Hussein Bashar Mahmood and Khalid.K.Kadhim**
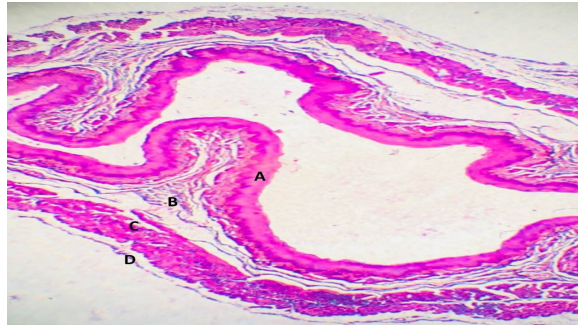
**Fig.8. Esophagus (cervical region)of grey mongoose showing A- mucosa,B-submucosa,C-tunica muscularis and D-tunica adventitia. H&E stain.40X**
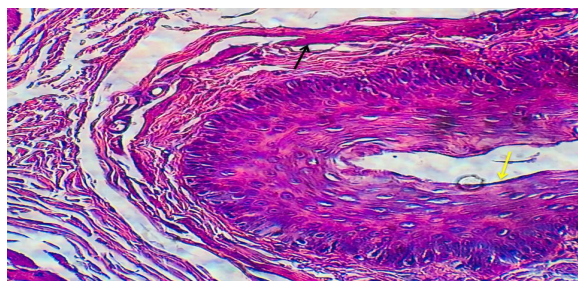


**Fig.9. Cranial part of esophagus lined by stratified squamous keratinized (yellow arrow), muscularis mucosa had interrupted muscles bundles (black arrow).H&E stain.400X**
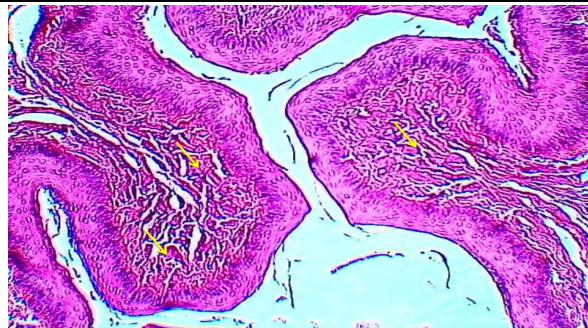


**Fig.10. Tunica mucosa of middle part of esophagus explained interrupted bundle of smooth muscle (yellow arrows). H&E stain.100X**
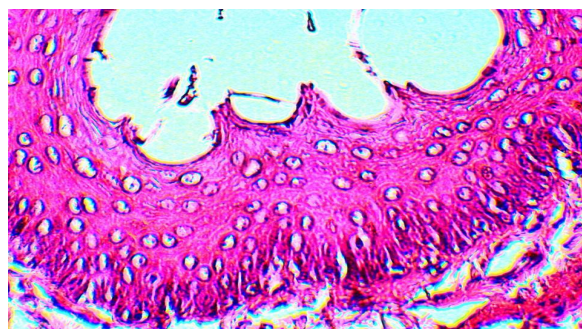


**Fig.11. Caudal part of esophagus lined by stratified squamous very-delicate of keratine.H&E stain.400X**

16469
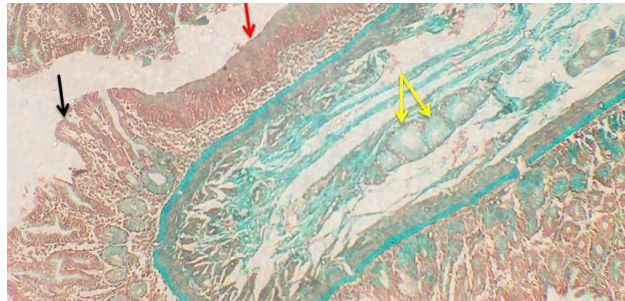
**Fig.12. Gastro-esophageal junction showing transition of epithelia from stratified squamous (red arrow) to simple columnar (black arrow), esophageal glands in submucosa (yellow arrows).Masson's trichrome.40X.**
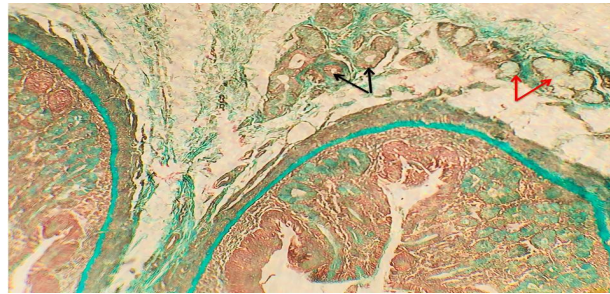


**Fig.13. Gastro-esophageal junction showing the serous glands (black arrow), mucous glands red arrows) in submucosa. Masson's trichrome.100X**
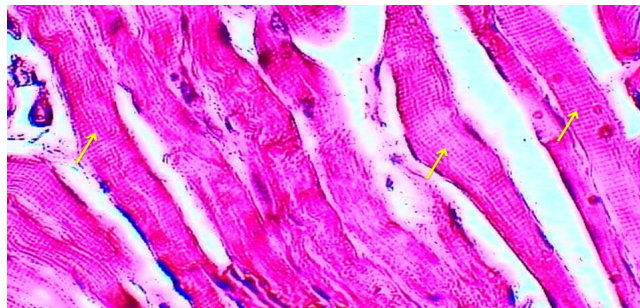


**Fig.14. Tunica muscularis in cranial part of esophagus showing striated muscle (yellow arrows). H&E stain. 400X**
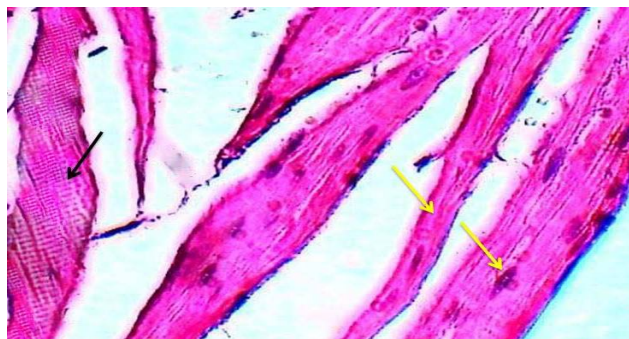


**Fig.15. Esophagus (mid region) showing: Tunica muscularis had mixture of striated muscles (black arrows) and smooth muscles (yellow arrows). H&E stain.400X**
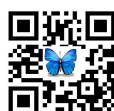
**Fig.16. Esophagus(caudal region) Tunica muscularis in caudal part of esophagus had smooth muscles fibers (yellow arrows). H&E stain. 400X**
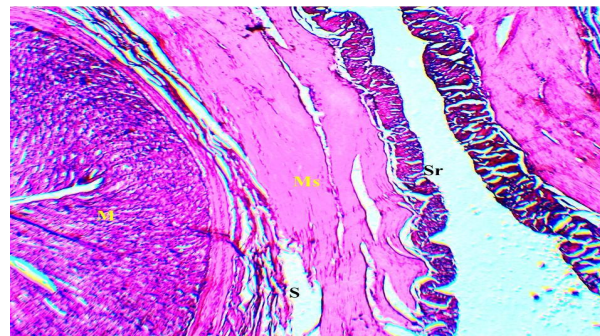


**Fig.17. Stomach (cardiac region)of gray mongoose explained four basic layers, M- tunica mucosa, S submucosa, Mr-tunica muscularis and Sr-Serosa.H&E stain.40X**
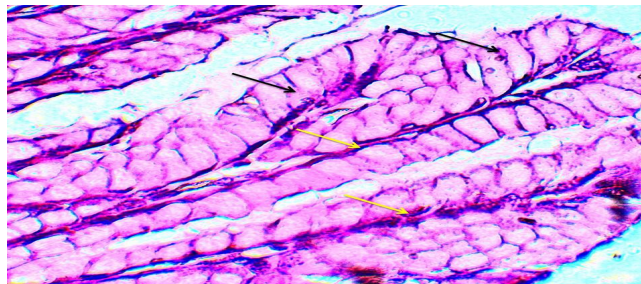


**Fig.18. Stomach (cardiac region)of grey mongoose showing, simple columnar epithelia without goblet cell (black arrows) contains elongated nuclei (yellow arrows) H&E stain.400**
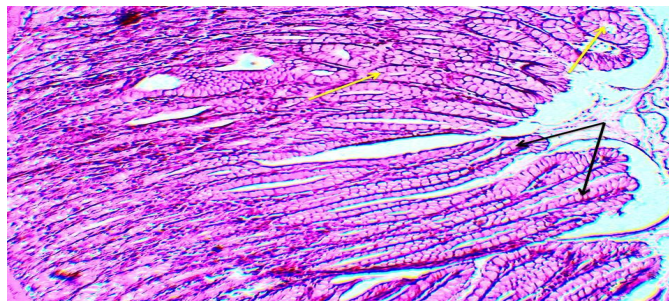


**Fig,19. Cardiac region of stomach showing gastric pits (black arrows) and simple gastric glands (yellow arrows).H&E stain.100X**

**Hussein Bashar Mahmood and Khalid.K.Kadhim**
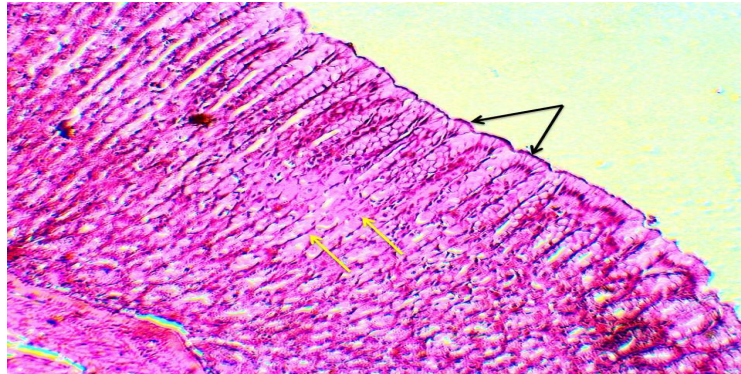
**Fig.20.Fundic region of stomach explained gastric pits oval in shape (black arrows) and the simple tubular gastric glands in lamina propria appeared as a cords (yellow arrows). H&E stain. 100X.**
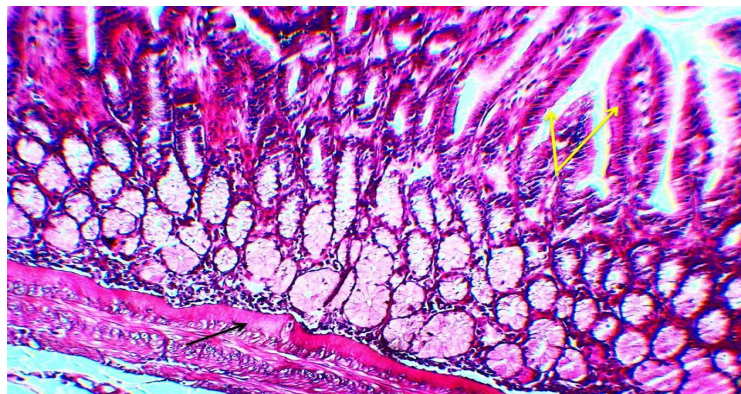


**Fig, 21. Pyloric region of stomach explained shape of gastric pits (yellow arrows) and stratum compactum extend in to pyloric region (black arrow). H&E stain. 100X**
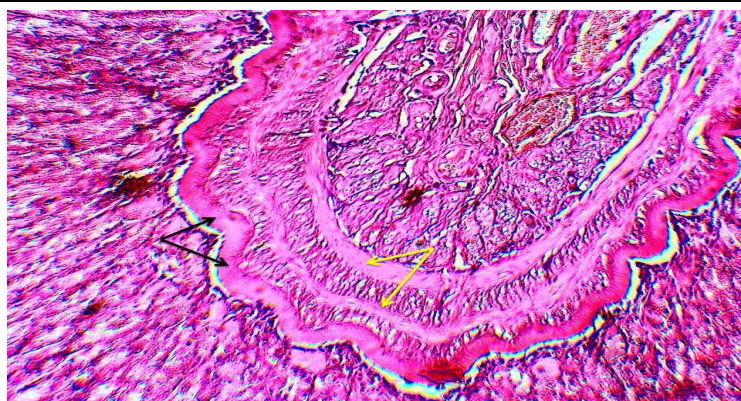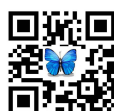


**Fig. 22. Fundic region showing, mucosa resting on the thick layer of stratum compactum (black arrows) and two strip of muscular mucosa (yellow arrows). H&E stain.100X**

**Fig,23. Cardiac region of stomach showing, simple columnar epithelia (red arrows) and simple short coiled gastric glands (yellow arrows). H&E stain.400X**
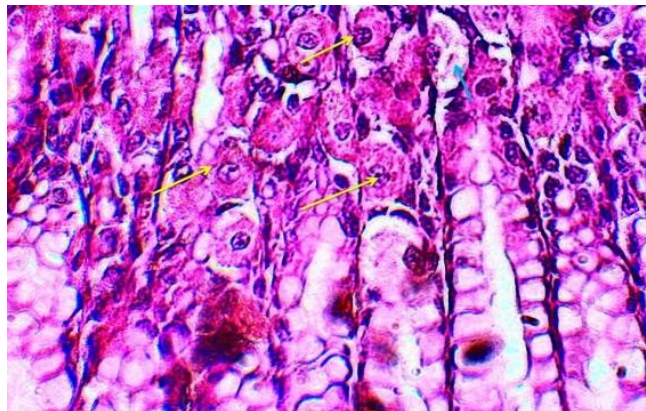


**Fig.24. Fundic region showing, rounded-pyramidal parietal cell (yellow arrows) and great spindle- shape of clear cell (blue arrow). H&E stain.400X**
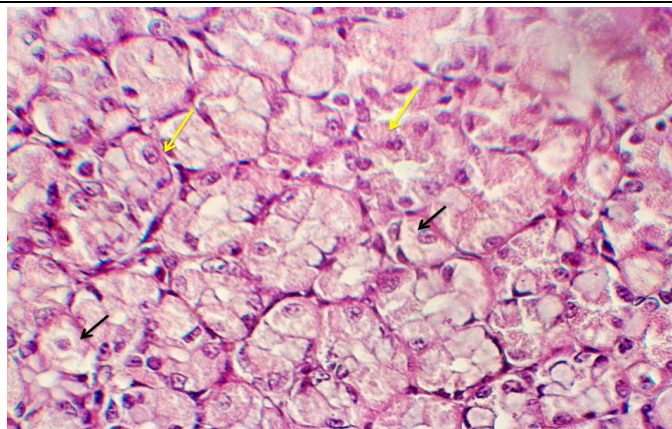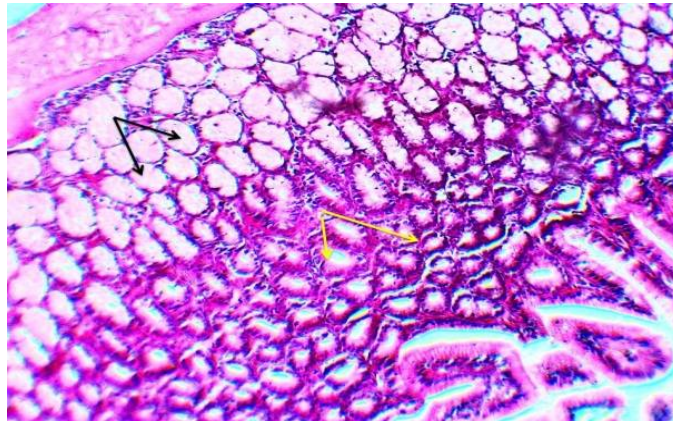


**Fig. 25. Stomach (fundic region) of grey mongoose show chief cells (yellow arrows) and clear cell black arrow).H&E stain. 400X**
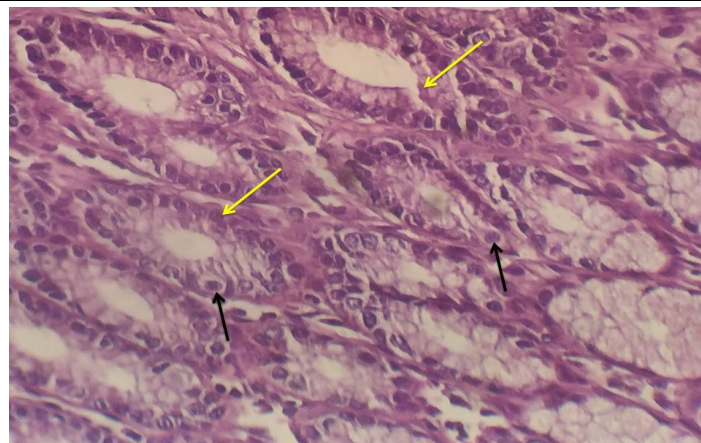
**Hussein Bashar Mahmood and Khalid.K.Kadhim**

**Fig,26 Pyloric region showing two types of gastric glands, deep mucous glands (black arrows) and superficial serous glands (yellow arrows). H&E stain. 100X.**



**Fig,27. Pyloric region of stomach showing, gastric glands (yellowarrows) and G-cell as fried egg-appearance (black arrows).H&E stain.400X**
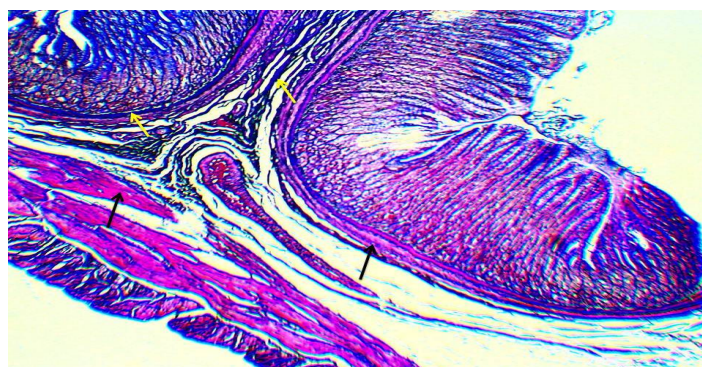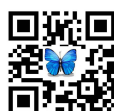


**Fig.28. Stomach of grey mongoose showing collagen fibers in lamina propria and submucosa appeared blue in color (yellow arrows) and smooth muscle fibers red in color (black arrows).Masson's trichrome stain.40X**
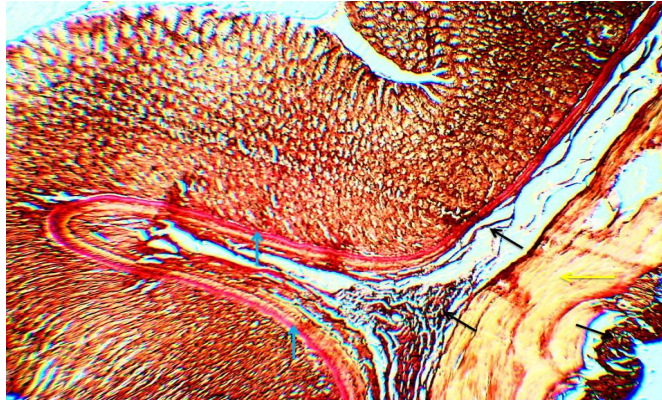
**Fig.29. Stomach (cardiac region) of gray mongoose showing, elastic fibers in submucosa and serosa black color (black arrows), stratum compactum red in color (blue arrows) and smooth muscle yellow in color (yellow arrows). Verhoeff's stain.100X**
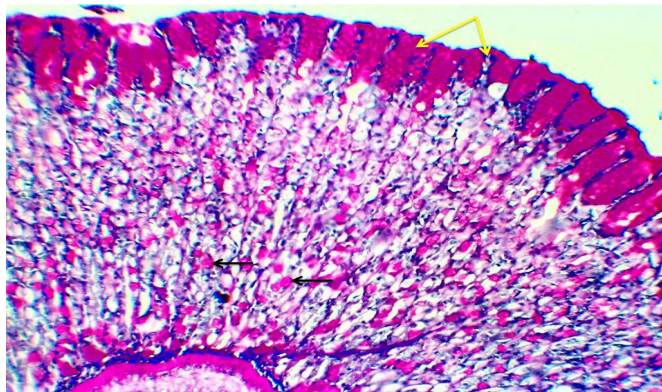


**Fig.30.Fundic region showing red color of gastric pits (yellow arrows) and interstitial space red secretions (black arrows).Ab+PAS stain.100X.**
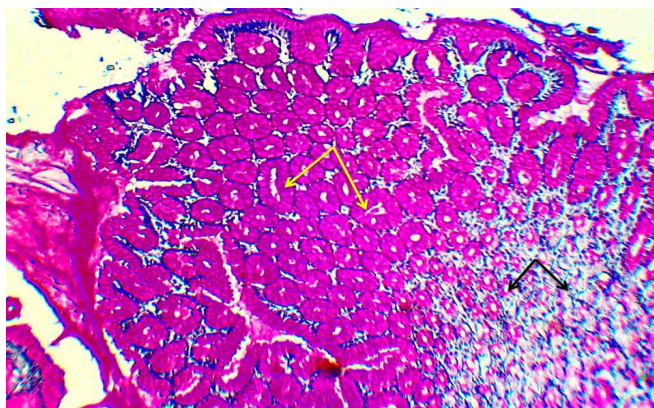


**Fig. 31. Cardiac region showing gastric glands, superficial glands magenta in color (yellow arrows) and deep glands small in size and purple in color (black arrows). Ab+PAS stain.100X.**

**RESEARCH ARTICLE**

# CME Analysis Using cmeDetect Code

Zeinab F.Hussein

Department of Space and Astronomy, College of Science, University of Baghdad, Baghdad, Iraq.

*Address for Correspondence
**Zeinab F. Hussein**
Department of Space and Astronomy,
College of Science,
University of Baghdad,
Baghdad, Iraq.

**ABSTRACT**

In the present work, a selected CMEs events forming a group of 2 events from the year 2002 was analyzed using the *cmeDetect* code previously written for this purpose. The code was able to detect and recognize well-defined CMEs mainly, which was explained if the outer CME edge part was about 3 to 7% further than the actual edge. The results showed that there is a general good agreement with CDWA listings of the MPA. Less agreement is found in height measurements and little agreement is found with speed and acceleration measurements; yet some of the present values were in perfect agreement with CDAW values.A remarkable behavior seen from few results was that the altitude region 5 to 15 $R_{sun}$acted as an acceleration area. Such behavior, however, did not repeat for other CME examples. The CME height results were fitted linearly utilizing a least square fitting and the calculated values of speed were improved. The shorthand of some of the results were discussed and the conclusion from these discussions was that the present code should be developed to include few modifications.

**Keywords:** Coronal Mass Ejections, CDWA, LASCO, SOHO .

## INTRODUCTION

There is a continuous need for an automated, computer based detection code that is able to isolate Coronal Mass Ejections (CME) from various observatories. Being bright, hot and fast plasma with large masses, CMEs are ejected from active regions of the solar corona in a variety of directions with an occurrence that implies that the solar corona is changing continuously. It is thought that CMEs are ejected into free space due to a sudden instability. Although the exact mechanism of CME generation is not clear yet, many studies focused on their behavior which require development of automatic detection utilities. In the present work, this task has been taken, where a computer code was written that aimed to detect and analyze CME events using images taken from the Large Angle and Spectrometric Coronagraph (LASCO) detector on board the Solar and HeliosphericObservatory (SOHO). Few selected examples of CMEs were studied by means of the present method using LASCO archived images.

16476

**Zeinab F. Hussein**

The detection process was made using a Matlab program called cmeDetect. This program contained various functions that were written during this work for the task of analyzing CME events. The main detection method used in this work was based on bulk detection of CME events then track their motion. Analysis depended on LASCO images with resolution 512x512 pixels. Final analysis included CME heights, velocities, accelerations, masses, energies and directions of the detected events. Comparison with CDAW library was extensively made. In our earlier work [1,2],the *cmeDetect* computer code was described with some details, followed by analysis of the few kinematic properties of Coronal Mass Ejection (CME). A full review of that code, as well as the literature concerning the CME's detection was given. In this paper, a thorough presentation of that code's results are given.

### Data

The computer code uses images from SOHO/LASCO online library [3]. The images were pre-selected,based on large CME events from CDAW CME list [4]. Dates were then used in [3] to acquire images of the relevant events' days and stored on the PC for analysis. The results are listed below.

## RESULTS AND DISCUSSION

### The CME event of 02/12/2002 at time 17:16:00

The results are shown in the Figures (1-a to d). In Figure (1-a), the CME height results showed that this quantity develops almost linearly with time. The same behavior is shown in the rest of all of the examples used in this work. Such behavior is explained to be due to the nature of the CME itself, where it is identified as a mass of plasma leaving the Sun. However, the height development is not the same for every CME event. After about 5 hours of the initial CME detection a sudden increase took place in the height values where the CME jumped from $13R_{sun}$ to $20R_{sun}$ in about an hour. Associated is a sudden jump in the results of the Figure (1-b) for speed measures. This implies that there was a sudden acceleration at these areas which is indeed shown in Figure (1-c). However, the speed and acceleration results in this case, and most cases studied in this work, were fluctuating around a mean value. In order to calculate the CME speed, there are two suggested methods:

(1) by taking the mean average of the results of dividing CME height by time difference, which is shown in Figure (1-b) and in all (b) parts of the results, and  (2) to perform a linear least-square curve fitting to the CME height data obtained from the present code, and deduce the CME speed as the slope of the resultant fit equation. The curve fitting procedure was added in order to determine the speed of the CME more reasonably than just taking the mean average of the CME height development with time which is shown in Figure (1-b). The values of the calculated CME height and their linear fit were also plotted in the same figure with standard height data obtained from CDAW catalog in Figure (1-e). The goodness of the fit was acceptable compared with the present data, however, these data showed only behavior agreement with CDAW data. The error values, although reach considerable values up to 60% of height data, was expected because the present code uses few major approximations as discussed above, therefore adding more corrections is necessary for any future development of the present attempt. Nevertheless, there is a general agreement between the present results and those of CDAW catalog. Speed measurement from the mean average values of Figure (1-b) was  274 km/sec and from CDAW was 867 km/sec; therefore this speed comes with a very high percentage error value of about 68 %. The CME speed from the slope of the fit was a*$R_{sun}$/60000 =~ 338 km/sec. The percentage of error this time was better to reach about 61%, yet it still a value with considerable error. Furthermore, the maximum value of speed from present calculations was 980 km/sec shown in Figure (1-b), and this particular value has an error of ~ 13%.
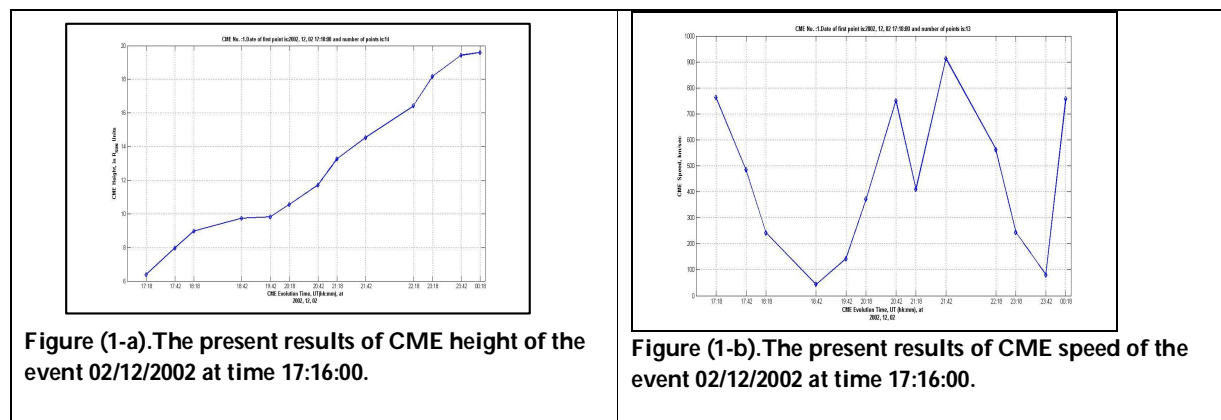
**Zeinab F. Hussein**

**The CME event of 28/12/2002 at time 12:31:00**

The third CME example is the event of mid-day 28-12-2002. This is a good example that can be used to demonstrate the difference between cmeDetect code and CDAW catalog since the results were in remarkable similar behavior yet with different numeric values. Figure (2-a) shows the CME height with time, and in similar behavior yet with different numeric values. the effect seen above in the region 10-15$R_{sun}$ was not seen. The linearity of this figure is clear for almost all values. The angular direction was at 315 degrees with error of less than 1%. Before the consistency of present results is discussed in this case, it should be mentioned that the fluctuating behavior of speed and acceleration curve takes place in particular CME cases when the same images contain more than one detectable event. This reveals the high instability of the procedure used in this code, that is to estimate speed by determining the height derivative with time directly. Thus it is left as a future work to develop a built-in function that directly computes the appropriate values of speed and acceleration. Speed and acceleration shown in Figures (2-b and c) also did not show any significant acceleration behavior at the time of these heights. Speed results in special showed a general increasing behavior yet interrupted with sudden drops, and this might be due to the effect of coronal part of the solar magnetic field which holds in a resistive way the development of the CME plasma.

CDAW [4]. Figure (2-d) shows that CME speed was decreasing. This phenomenon will be discussed briefly in the results of CME event at 01/03/2003 at time 12:21:00. The mean average of the calculated acceleration in this work was ( -2.5) m/sec$^2$, with about 12% error from acceleration found in CDAW which has the value of (-2.84) m/sec$^2$. The results of height are also compared with a figure plot at Figure (2-e) in this example. The figure clearly shows about the exact behavior with almost fixed difference of about 1.5$R_{sun}$. Speed calculation in this example was in a good agreement with CDAW value, it was 354 km/sec from the average of Figure (2-b), and 432 km/sec from the curve fitting; with associated percentage of error 11% and 8% from the CDAW value 399 km/sec.

## REFERENCES

1. Hussein, Zeinab F., "Detection and Analysis of Coronal Mass Ejection (CME) from SOHO/LASCO Coronagraphs Data", M.Sc. Thesis, Department of Astronomy and Space, College of Science, University of Baghdad (2015).
2. Selman, Ahmed A., andHussein, Zeinab F., "The cmeDetect Computer Code for CME Analysis", International Journal of Scientific & Engineering Research (IJSER), Vol.6, Issue 2, February – 2015, p.782.
3. The official website of SOHO from NASA (accessed 2-12-2014):
4. http://sohowww.nascom.nasa.gov/
5. CDAW Catalog from ALSCO/SOHO website (accessed 2-12-2014):
6. http://cdaw.gsfc.nasa.gov/CME_list/

**Figure (1-a).The present results of CME height of the event 02/12/2002 at time 17:16:00.**



**Figure (1-b).The present results of CME speed of the event 02/12/2002 at time 17:16:00.**

**Figure (1-c).The present results of CME acceleration of the event 02/12/2002 at time 17:16:00.**



**Figure (1-d). Height and its derivative results of the event 02/12/2002 at time 17:16:00 from CDAW [4].**



**Figure (1-e). Height and its derivative results of the event with onset 02/12/2002 at time 17:16:00 from present and CDAW data. Blue circles illustrate present data, red diamonds is their linear fit, and black squares are the CDAW data [4].**
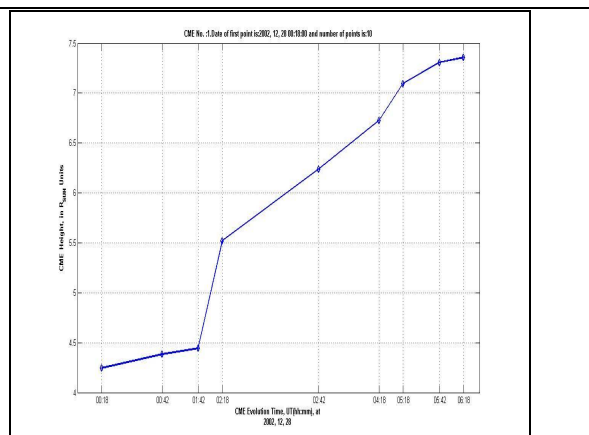


**Figure (2-a).The present results of CME height of the event 28/12/2002 at time 12:31:00.**



**Figure (2-b).The present results of CME speed of the event 28/12/2002 at time 12:31:00.**
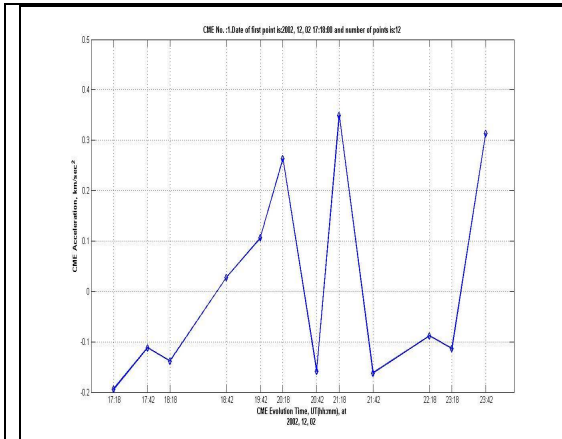


**Figure (2-c).The present results of CME acceleration of the event 28/12/2002 at time 12:31:00.**
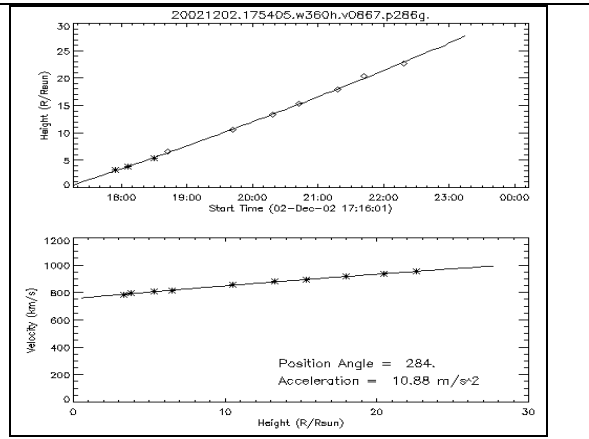
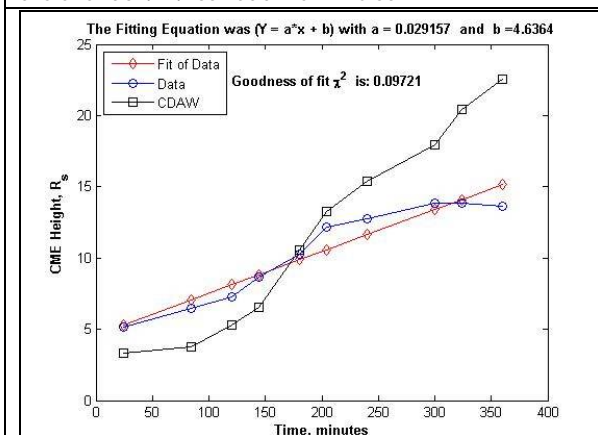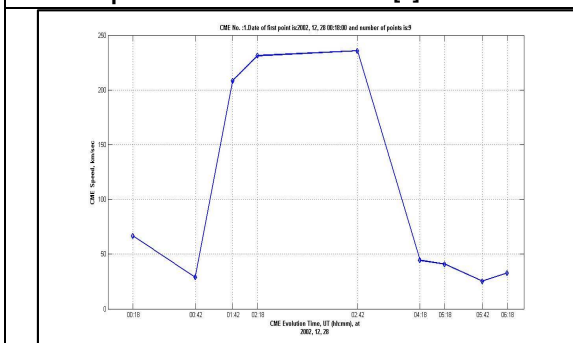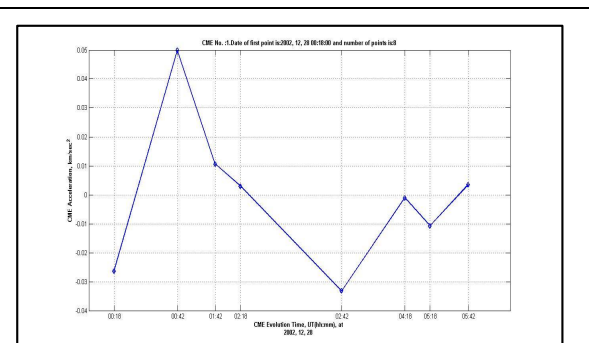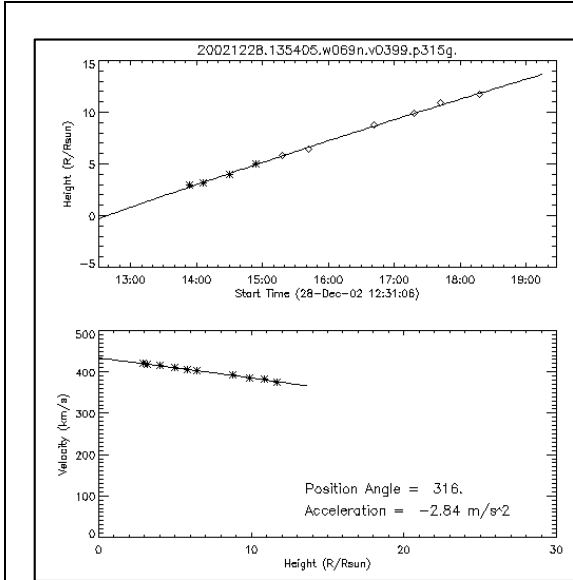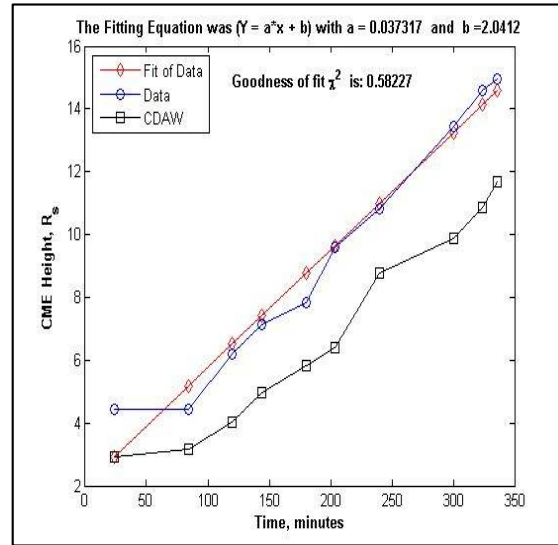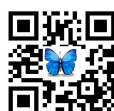**Figure (2-d). Height and its derivative results of the event 28/12/2002 at time 12:31:00 from CDAW [4].**



**Figure (2-e). Height and its derivative results of the event 28/12/2002 at time 12:31:00 compared with CDAW results.**

**RESEARCH ARTICLE**

# Experimental Hypo-Magnesemia Induced in Awassi Lambs Using Potassium Chloride

Ali Mohammed Aboud*and Wasan A. Gharbi

College of Veterinary Medicine, University of Baghdad, Iraq.

*Address for Correspondence
**Ali Mohammed Aboud**
College of Veterinary Medicine,
University of Baghdad, Iraq
Email: dr.ali.alzuhairy@gmail.com dr.wasan.vet.77@gmail.com

**ABSTRACT**

This study conducted to inducethehypomagnesemiain Awassi lambs using of high oral sub-lethal doses potassium chloride (KCL) solution, and measurement the levels of serum magnesium (Mg), calcium (Ca), potassium (K), and acetylcholine esterase (AChE) in blood of study animals. For this purpose, a totally of 12 male Awassi lambs were submitted firstlytoa preparatory period for one month,and then divided into two equal groups (control group Aand experimental groupsB). During study's period continued for 7 weeks, diets of both groups changed and only lambs ofgroupB were drenched with oral KCL solution.Under aseptic conditions, blood samples collectedonce weekly from all study lambs using of anticoagulant vacutainer tubes.Statistical significant decreases (P≤0.05) were encountered in Mg, Ca, and AChElevelsat 5th, 6th and 7th weeks of study. However, significant increase (P≤0.05) in Kvalues was reported among allperiods of study particularly at the last three weeks (5th, 6th, and 7th). Clinically, results showed thatthe lambs of experimental group B were observed variable abnormalities includedanorexia, arrhythmia and tachycardia, shallow and rapid respiration, constipation or diarrhea, salivation, ruminal tympany, nervous signs, general weakness, visible pale and/or anemic mucous membranes, wool affections (loss of wool crimp, steely appearance withwool loss and depigmentation), and enlargement of knee or hock joints. At last 7th week of study, it showed that 3 lambs of experimental group B were found died. It have been concluded that high levels of K could affect Awassi lamb resulting in significant variation in blood levels ofMg, Ca, AChE and K, and causing clinical abnormalities and mortalities;therefore, affect of K on other blood parameters should be screened.

**Keywords**: Hypomagnesemia, Awassi, Lambs, KCL

## INTRODUCTION

Inadequate nutrition is a major factor contributing to the low productivity and product quality of sheep herds under different conditions. In most countries, the major source of feeding is the rangeland forages that their quantity and quality can be influenced directly by the seasonal changes (29, 48). To optimize the livestock performance, diets should contain sufficient levels of proteins, carbohydrates, vitamins, in addition to minerals as magnesium (Mg), calcium (Ca), phosphorus (P), sodium (Na) and potassium (K) (42). Mg is one of the most essential macro-minerals, which play an important role the growth, health, reproduction and immune system. As well as, it required for many

**Ali Mohammed Aboud and Wasan A. Gharbi**

body functions and biochemical processes for both humans and animals (15, 49). However, several factors can affect on Mg absorption and/or utilization which increased the risk of hypomagnesemia in ruminants as high dietary intakes of K or low levels of Mg and Ca in rapidly growing spring grass (27, 40). In ruminant, high plasma K can reduce retention of Mg irrespective of Mg intakewhereas the availability of serum Mg is correlated negatively with the high levels of dietary K intake (28). Among different animals, there is positive association between Mg and Ca as the Mg stimulates Ca re-uptake by Ca activated ATPase (10). It's shown that Mg plays a great role in regulation of membrane channels and excitation-contraction coupling in muscles (3, 33). Also, Mg has an effect on impulse transmission in the neuromuscular system as it interfering with the releasing of acetylcholine, sensitivity of motor end plate, threshold of muscle membrane, and activation of cholinesterase system (11). However, there are two common clinical forms of Mg deficiency were reported in ruminants including the grass tetany that occurs at spring to animals grazing only gasses, and the winter tetany that occurs in animals consuming only cereal forages (31, 46). The clinical signs of Mg deficiency are dramatic, and the affected sheep mostly becomes unable to walk or appear uncoordinated, collapse and sensitive to touch (4, 6). It seems that there are no wide studies related to Mg deficiency in sheep or lambs at different regions in Iraq. Hence the present study is targeted for:

1.  Induction of hypomagnesemia in Awassi lambs using oral doses of KCL solution.
2.  Biochemical analysis of serum Mg, K, Ca, and AChE for study lambs.
3.  Clinical examination of lambs to detecting the abnormal symptoms during periods of study.

## MATERIALS AND METHODS

### Study Animals

The present study was involved a totally of 12 male Awassi lambs that aged 6-8 (5.9 ± 1.04) months and weighted 23-29 (26.20 ± 2.86) Kg. Prior to study, all lambs were submitted firstly for preparation period (one month), during which, they drenched and injected with Curafluke 5% (1.5 ml/10 Kg-BW) and Ivermectine 1% (1ml/50 Kg-BW), respectively, twice times at interval of 14 days for controlling of internal and external parasites. Also, they fed sufficient amounts of high quality diets compromised of concentrated (wheat and barley) and green (alfalfa) nutrition. Then, lambs were divided randomly into two equal groups; A as a control group, and B as an experimental group that drenched with KCL solution, weekly, according to their weight. During an experimental period extend 7 weeks (1/1/2018 to 18/2/2018), both groups were fed on grass hay and low amount of barley.

### KCL Preparation

According to manufacturer instructions (*Science Lab, Sarjapur, India*), KCL solution was prepared as weighting of KCL powder carefully using an electronic analytical balance and put the powder in a flask, dissolving 100 g of KCL powder in 1 liter of distilled water, completely, and transferring the solution into dark bottle and keep it at room temperature until be used. Lambs of group B were drenched weekly with oral KCL solution at a dose of 1.35 mg/kg using of stomach tube (1).

### Sample Collection and Clinical Examination

Under aseptic conditions, all study lambs of both groups were submitted, weekly, for collecting of venous blood samples from jugular vein using of free-anticoagulant vacutainers. Blood samples transferred to the lab using of ice-box, centrifuged at 4000 rpm for 10 minutes at room temperature. Sera samples were kept at -20$^o$C into numbered eppendorfs until be used. Also, the study lambs were examined, daily, for detection of abnormal clinical symptoms among the experimental period of study.

### Biochemical Analysis

According to manufacture instructions of Mg (*BioVision / USA*), K (*Crest Biosystem / India*), Ca (*Caymanchem / USA*), and AChE (*BioVision / USA*), the sera of all study lambs were examined biochemically.

**Ali Mohammed Aboud and Wasan A. Gharbi**

### Statistical Analysis

Two programs were used; Microsoft Office Excel (*2013*) and IBM/SPSS (*V$_{23}$*). The obtained data were tabled, classified and subjected to descriptive and *t-test*. Significant differences for values that included the mean ± SE (range)of experimental group B compared and control group Awere detected at a level of (P≤0.05).

## RESULTS

### Biochemical Analysis

Results revealed a significant decreasing (P≤0.05) in levels of serum Mg among all weeks of study particularly at 5$^{th}$, 6$^{th}$ and 7$^{th}$ weeks (Table 1). A significant (P<0.05) elevation in levels of serum K was detected among lambs of group Bstarted from the 2$^{nd}$to the 7$^{th}$ weeks (Table 2).The levels of serum Ca were reduced significantly (P≤0.05) at 3$^{rd}$, 4$^{th}$, 5$^{th}$, 6$^{th}$ and 7$^{th}$weeks, (Table 3). The measuring of serum AChE in lambs of group B was revealed on significant reduction (P≤0.05) among most weeks of study particularly at 4$^{th}$, 5$^{th}$, 6$^{th}$ and 7$^{th}$ weeks, (Table 4).

### Abnormal Clinical Symptoms

Various abnormal symptoms were showed during the daily clinical examination of lambs (Table 5), which involved the following: anorexia, arrhythmia and tachycardia, shallow and rapid respiration, constipation or diarrhea, salivation, ruminal tympany, nervous signs, general weakness, visible pale and/or anemic mucous membranes, wool affections (loss of wool crimp, steely appearance and loss of wool with depigmentation), and enlargement of knee or hock joints. In addition, 3 lambs were found dead at the last 6$^{th}$ week of a study.

## DISCUSSION

Nutrition quality, absorption and bioavailability of minerals are depending mainly on the chemical form, digestibility of a mineral and the interactions between minerals with other dietary components (20). Sub-optimal imbalance or mineral deficiencies might be considered as more risk in reducing performance than the visible minerals deficiency that can be detected and rectified (5). Among the experimentally period of this study, the levels of serum Mg in blood of Awassi lambs were decreased, significantly, at the same time with increased the levels of K. These results were in agreement with those reported by (28, 41) as the high levels of plasma K reduce the retention of Mg. As well as, the process of Mg absorption is K concentration-dependant, so that, any increasing in K intake can reduce markedly the absorption of Mg (12). Although, sheep need to consume Mg regularly to prevent Mg deficiency, it is difficult to define the accurately what the exact optimal intake should be (16). The recommended daily allowance for Mg intake varied between animals in depending on the animal's species, sex, age, health status, and management factors such as region, herd, source feeding and water drinking, weather and medication or prevention schedules (13, 24, 37). Also, there are number of factors that interact, markedly, with the absorption of Mg from reticulo-rumen and/or intestinal mucosa (8, 21).

It's noteworthy that the processed foods have much lower Mg content than unrefined grain products (25). Regarding to serum Ca, the results of this study were detected a significant decreasing (P≤0.05) in its levels among the period of study. Interrelationship between different minerals might influence on absorption and utilization of each other as Mg that has nearly correlation with the Ca, phosphorus, manganese, and zinc (23, 47). In cow, (18) were demonstrated that the high dietary K content in forage is more predispose cows to hypocalcemia as it interfere with the ruminal absorption of Ca and increasing the risk of milk fever. Also, they indicated that the most constructive step to prevent milk fever is to reduce the dietary K content in nutrition of prepartum cows. On the other hand, hypocalcemia could be resulted due to influencing of hypomagnesemia on parathyroid hormone (PTH) synthesis, secretion with decreasing the responsiveness of tissue to this hormone (30).  Normally, the concentration of Ca in plasma is maintained within very narrow limits, and the PTH probably, might the important factor in maintaining of Ca hemostasis, increases the concentration of Ca in extracellular fluid and plasma (36, 38). Suh *et al.,* (1973) demonstrated

that the restriction of dietary Mg produced hypomagnesemia and this was companied by a decrease in the concentration of total and ionized calcium in the plasma and an increase in the concentration of plasma phosphate that a picture pointing to derangement in parathyroid physiology (43).The levels of serum AChE, measured in this study, reported a markedly reduction in most weeks of study. AChE have consist mainly of two enzymes that catalyst the hydrolysis of cholinergic neurotransmitters by breaking of ACh into Choline and acetic acid (45). As reported previously, Mg plays an important role in several intracellular processes in addition in a number of the sequential enzymatic reactions of glycolysis (22, 44). Moreover, Mg is known to activate cholinesterase and to enhance the ability of metabolic processes to increase the L fraction of the membrane potential of the nerve fiber. It maintains and balances the electrical signals in the body; however, Mg deficiency certainly qualifies as a principle cause of disease (14). Ca, also, is required for neuronal release of neurotransmitter, thus, Ca depletion can hamper the signal transmission at the level of synaptic cleft of neuromuscular junctions (2).  In regard to abnormal clinical symptoms associated with hypomagnesemia, the results of clinical examination were showed variable clinical symptoms. The abnormal signs could be the first indicator to existence of a problem in individual sheep or among the whole flock.

Although, hypomagnesemia is well recognized in sheep as being characterized by nervous system signs of excitability and recumbency with titanic spasms or fits, most of these signs are non-specific and associated usually with additional abnormalities such as hypocalcemia or metabolic acidosis (34, 50). Most evidence points to hypomagnesemia as the cause of tetanic signs observed, nonetheless, the concurrent hypocalcemia may have a contributory effect to be even as a dominant factor in many instances (17). The affected animals might develop the paddling convulsions, tachypnea, tachycardia, and fever due to any type of stimuli, after severe muscle exertion or due to acute changes in weather patterns (9). Mg deficiency is more incidences in ewes, 2-4 weeks, after lambing at cool and wet season, and the affected sheep may simply found dead in pasture particularly those that loss their weight during winter, or lambs that being anorexic (26, 35). Generally, hypocalcemia is typical in severe hypomagnesemia, and the degree of severity is related to level of Mg depletion (19). High doses of dietary supplements or drugs are often resulting in diarrhea that accompanied by tympany or abdominal cramping (32). The most commonly minerals are reported to be caused diarrhea include carbonate, chloride, gluconate, and oxide (7). However, diarrhea and laxative effects of various salts occur due to the osmotic activity of unabsorbed salts in intestine or colon, and stimulation of gastric motility (39).

## REFERENCES

1. Abd El-Maksoud H, Tahia E, El-Kharadly W (2012). Biochemical alteration of experimentally induced hypomagnesaemia in male baladi goats. Benha VMJ., 23 (1): 19-25.
2. Agulhon C, Petravicz J, McMullen AB, Sweger EJ, Taves SR, McCarthy KD (2008). What is the role of astrocyte calcium in neurophysiology?. Neuron, 59 (6): 932-946.
3. Bara M, Guiet-Bara A, Durlach J (1993). Regulation of sodium and potassium pathways by magnesium in cell membranes. Magnesium Research, 6(2), 167-177.
4. Bayomi YH., Mohamed WA., and Morsi, AM. (2017). Oxidative Stress Biomarkers in Dystrophic Lambs and Kids in Relation to Body Condition Scores. Zagazig Veterinary Journal, 45 (S1), 189-200.
5. Cabrita AR, Maia MR, Oliveira HM, Sousa-Pinto I, Almeida AA, Pinto E, Fonseca AJ (2016). Tracing seaweeds as mineral sources for farm-animals. Journal of applied phycology, 28(5), 3135-3150.
6. Caple, IW. (1989). Nutritional problems affecting calcium and magnesium metabolism in grazing ruminants. Recent Advances in Animal Nutrition in Australia, 7, 37-46.
7. Cotruvo JA, Costello R, Weglicki WB (2017). Magnesium, Hard Water, and Health. JournalAmerican Water Works Association, 109 (11): 62-68.
8. Coudray C, Demigne C, Rayssiguier Y (2003). Effects of dietary fibers on magnesium absorption in animals and humans. Journal of nutrition, 133 (1): 1-4.

9.  Daly R, Faux CM (2018). Blizzards and Range Cattle: Management Before, During, and After the Storm. Veterinary Clinics of North America, 34 (2): 265-275.

10. D'Angelo EK, Singer HA, Rembold CM (1992). Magnesium relaxes arterial smooth muscle by decreasing intracellular Ca2+ without changing intracellular Mg2+. Journal of clinical investigation, 89 (6): 1988-1994.

11. De Baaij JH, Hoenderop JG, Bindels RJ (2015). Magnesium in man: implications for health and disease. Physiological reviews, 95 (1): 1-46.

12. Ding Y, Luo W, Xu G (2006). Characterisation of magnesium nutrition and interaction of magnesium and potassium in rice. Annals of Applied Biology, 149(2): 111-123.

13. Dodic M, Abouantoun T, Connor A, Wintour EM, Moritz KM (2002). Programming effects of short prenatal exposure to dexamethasone in sheep. Hypertension-Dallas, 40 (5): 729-734.

14. Elkhashab RA (2013). Activation of butyrylcholinesterase enzyme by magnesium ions. ESJ, 9 (18): 303-310.

15. Faye B, Konuspayeva G (2012). The sustainability challenge to the dairy sector–The growing importance of non-cattle milk production worldwide. Inte Dairy J, 24 (2): 50-56.

16. Georgievskii VI, Annenkov BN, Samokhin VT (2013). Mineral nutrition of animals: studies in the agricultural and food sciences. Elsevier: 69-77.

17. Ghanem MM (2013, January). Comparative Study on the Clinical and Subclinical Hypomagnesemia in Calves with Evaluation of Therapeutic Response. Assiut Uni, 19 (22): 123-135.

18. Goff JP, Horst RL (1997). Effects of the Addition of Potassium or Sodium, but Not Calcium, to Prepartum Rations on Milk Fever in Dairy Cows. J Dairy Sci, 80 (1): 176 – 186.

19. Goff JP (2006). Macromineral physiology and application to the feeding of the dairy cow for prevention of milk fever and other periparturient mineral disorders. Animal feed science and technology, 126 (3- 4): 237-257.

20. Goff JP (2018). Invited review: Mineral absorption mechanisms, mineral interactions that affect acid–base and antioxidant status, and diet considerations to improve mineral status. Journal of dairy science, 101(4), 2763-2813.

21. Hardwick LL, Jones MR, Brautbar N, Lee DB (1990). Site and mechanism of intestinal magnesium absorption. Miner Electrolyte Metab, 16 (2): 174-180.

22. Hartwig A (2001). Role of magnesium in genomic stability. Mutation Research/Fundamental and Molecular Mechanisms of Mutagenesis, 475 (1): 113-121.

23. Hunt JR (2003). Bioavailability of iron, zinc, and other trace minerals from vegetarian diets. American journal of clinical nutrition, 78(3): 633S-639S.

24. Jáuregui BM, García U, Osoro K, Celaya R (2009). Sheep and goat grazing effects on three Atlantic heathland types. Rangeland ecology & management, 62 (2): 119-126.

25. Karppanen H, Karppanen P, Mervaala E (2005). Why and how to implement sodium, potassium, calcium, and magnesium changes in food items and diets ?. J H Hyper, 19 (S3): S10-S19.

26. Khan ZI, Hussain A, Ashraf M, Ashraf MY, Yousaf M, Akhtar M, Maqbool A (2004). A review on mineral imbalances in grazing livestock and usefulness of soil, dietary components, animal tissues and fluid analysis in the assessment of these imbalances. J Anim Vet Adv, 3(1): 394-412.

27. Lechartier C, Peyraud JL (2011). The effects of starch and rapidly degradable dry matter from concentrate on ruminal digestion in dairy cows fed corn silage-based diets with fixed forage proportion. Journal of dairy science, 94(5), 2440-2454.

28. Martín-Tereso J, Martens H (2014). Calcium and magnesium physiology and nutrition in relation to the prevention of milk fever and tetany (dietary management of macrominerals in preventing disease). Veterinary Clinics: Food Animal Practice, 30 (3): 643-670.

29. Minson DJ (1990). Forage In Ruminant Nutrition. 1st edition, Academic Press, Queensland, Australia. Pp: 275.

30. Moe SM (2008). Disorders involving calcium, phosphorus, and magnesium. Primary Care: Clinics in Office Practice, 35 (2): 215-237.

31. Norvell TM (2011). Effects of increasing tetany risk ratio and magnesium supplementation on mineral balance and feeding behavior by ruminants. Doctoral thesis, dissertation, College of Agriculture, Montana State University-Bozeman: 11.

32. Papaioannou D, Katsoulos PD, Panousis N, Karatzias H (2005). The role of natural and synthetic zeolites as feed additives on the prevention and/or the treatment of certain farm animal diseases: a review. Microporous and mesoporous materials, 84 (1-3): 161-170.

33. Payandeh J, Pfoh R, Pai EF (2013). The structure and regulation of magnesium selective ion channels. Biochimica et Biophysica Acta (BBA)-Biomembranes, 1828(11), 2778-2792.

34. Radostits OM, Gay CC, Hinchcliff KW, Constable PD (2006). Veterinary Medicine E-Book: A textbook of the diseases of cattle, horses, sheep, pigs and goats. 10th Edition, Elsevier Health Sciences: 1656.

35. Rook JS (2000). Pregnancy toxemia of ewes, does, and beef cows. Veterinary Clinics: Food Animal Practice, 16(2): 293-317.

36. Rude RK, Gruber HE (2004). Magnesium deficiency and osteoporosis: animal and human observations. J Nutr Bio, 15 (12): 710-716.

37. Sampelayo MS, Chilliard Y, Schmidely P, Boza J (2007). Influence of type of diet on the fat constituents of goat and sheep milk. Small Ruminant Research, 68 (2): 42-63.

38. Saris NL, Karppanen H, Lewenstam A (2000). Magnesium: an update on physiological, clinical and analytical aspects. Clinica chimica acta, 294 (2): 1-26.

39. Schiller LR (2001). The therapy of constipation. Alim Pharm & Therap, 15(6): 749-763.

40. Schonewille JT, Van't Klooster AT, Beynen AC (1999). Effects of Intrinsic Potassium in Artificially Dried Grass and Supplemental Potassium Bicarbonate on Apparent Magnesium Absorption in Dry Cows1. J Dairy Sci, 82 (8): 1824-1830.

41. Schonewille JT (2013). Magnesium in dairy cow nutrition: an overview. Plant and soil, 368 (2): 167-178.

42. Soetan KO, Olaiya CO, Oyewole OE (2010). The importance of mineral elements for humans, domestic animals and plants-A review. Afri J Food Sci, 4 (5): 200-222.

43. Suh SM, Tashjian A, Matsuo N, Parkinson DK, Fraser D (1973). Pathogenesis of hypocalcemia in primary hypomagnesemia: normal end-organ responsiveness to parathyroid hormone, impaired parathyroid gland function. J Clin Invest, 52(1): 153-160.

44. Takaya J, Higashino H, Kobayashi Y (2004). Intracellular magnesium and insulin resistance. Magnesium research, 17(2): 126-136.

45. Taylor P, Radic Z (1994). The cholinesterases: from genes to proteins. Annual review of pharmacology and toxicology, 34(1), 281-320.

46. Underwood WJ, Blauwiekel R, Delano ML, Gillesby R, Mischler SA, Schoell A (2015). Biology and Diseases of Ruminants (Sheep, Goats, and Cattle). In Laboratory Animal Medicine, 3rd Edition. Elsevier Health Sciences: 623.

47. Weiss WP (2004). Macromineral digestion by lactating dairy cows: Factors affecting digestibility of magnesium. J Dairy Sci, 87 (7): 2167-2171.

48. Yadav S, Singh A, Singh Y (2016). Advances in Sheep and Goat production and management. National Livestock Mission, GOI Directorate of Animal Husbandry, Lucknow, India. Pp: 18

49. Yanuartono Y, Indarjulianto S, Nururrozi A, Purnamaningsih H (2016). The role of macrominerals on ruminants reproduction. J Sain Vet, 34 (2): 155-165.

50. Zein-Eldin MM, Ghanem MM, El-Raof AY, El-Attar HM, El-Khaiat HM (2014). Clinical, haematobiochemical and ruminal changes during the onset and recovery of induced lactic acidosis in sheep. Biotech Ani Husb, 30 (4): 647-659.

**Table 1. Mg Level in study groups**

| Week | Control Group A | Experimental Group B |
|------|------------------|------------------------|
| 1 | 1.24 ± 0.13 (1.19 – 1.31) | 1.16 ± 0.61 (0.97 – 1.23) |
| 2 | 1.22 ± 0.22 (1.18 – 1.30) | 1.09 ± 0.43 (0.88 – 1.15) |
| 3 | 1.21 ± 0.14 (1.18 – 1.28) | 0.96 ± 0.28 (0.81 – 1.07) |
| 4 | 1.21 ± 0.29 (1.17 – 1.27) | 0.83 ± 0.52 (0.76 – 0.92) |
| 5 | 1.19 ± 0.31 (1.14 – 1.26) | 0.71 ± 0.29 (0.62 – 0.83) |
| 6 | 1.18 ± 0.18 (1.11 – 1.23) | 0.64 ± 0.14 ** (0.57 – 0.51) |
| 7 | 1.15 ± 0.13 (1.08 – 1.21) | 0.53 ± 0.1** (0.50 – 0.57) |

Values are mean ± standard error (range),(Unit: mg/dl), ** ($P \leq 0.05$).Results revealed a significant decreasing ($P \leq 0.05$) in levels of serum Mg among all weeks of study particularly at 5th, 6th and 7th weeks (Table 1).

**Table 2. K Level in study groups**

| Week | Control Group A | Experimental Group B |
|------|------------------|------------------------|
| 1 | 3.51 ± 0.42 (3.44 – 3.57) | 3.86 ± 1.13 (3.73 – 4.02) |
| 2 | 3.53 ± 0.81 (3.48 – 3.58) | 4.43 ± 0.54 (3.34 – 4.60) |

| 3 | 3.57 ± 0.95 (3.52 – 3.60) | 4.91 ± 0.92 (4.78 – 5.04) |
| 4 | 3.61 ± 1.12 (3.56 – 3.64) | 5.49 ± 1.03 (5.23 – 5.68) |
| 5 | 3.64 ± 0.98 (3.59 – 3.69) | 6.24 ± 0.73(6.11 – 6.38) |
| 6 | 3.67 ± 0.72 (3.62 – 3.75) | 8.06 ± 1.16 (7.84 – 8.41) |
| 7 | 3.81 ± 0.85 (3.69 – 3.88) | 10.19 ± 1.04 (9.76 – 10. 48) |

Values are mean ± standard error (range),(Unit: mmol/L), ($P \leq 0.05$).A significant ($P < 0.05$) elevation in levels of serum K was detected among lambs of group Bstarted from the $2^{nd}$to the $7^{th}$ weeks (Table 2).

**Table.3. Ca Level in study groups**

| Week | Control Group A | Experimental Group B |
|---|---|---|
| 1 | 2.87 ± 0.09 (2.84 – 2.96) | 2.83 ± 0.17 (2.80 – 2.86) |
| 2 | 2.86 ± 0.17 (2.83 – 2.95) | 2.81 ± 0.41 (2.77 – 2.84) |
| 3 | 2.84 ± 0.16 (2.82 – 2.91) | 2.77 ± 0.09 (2.72 – 2.81) |
| 4 | 2.82 ± 0.21 (2.79 – 2.87) | 2.73 ± 0.16 (2.70 – 2.76) |
| 5 | 2.81 ± 0.06 (2.77 – 2.85) | 2.68 ± 0.64 (2.63 – 2.71) |
| 6 | 2.79 ± 0.15 (2.74– 2.84) | 2.61 ± 0.1 (2.56– 2.68) |
| 7 | 2.78 ± 0.24 (2.69 – 2.84) | 2.56 ± 0.31 (2.49 – 2.64) |

Values are mean ± standard error (range),(Unit: mmol/L), ($P \leq 0.05$). The levels of serum Ca were reduced significantly ($P \leq 0.05$) at $3^{rd}$, $4^{th}$, $5^{th}$, $6^{th}$ and $7^{th}$weeks, (Table 3).

**Table (4): AChE Level in study groups**

| Week | Control Group A | Experimental Group B |
|---|---|---|
| 1 | 0.41 ± 0.027 (0.39 – 0.43) | 0.38 ± 0.031 (0.35 – 0.41) |
| 2 | 0.41 ± 0.029 (0.38 – 0.43) | 0.35± 0.025 (0.31 – 0.37) |
| 3 | 0.40 ± 0.034 (0.36 – 0.42) | 0.31 ± 0.034 (0.27 – 0.35) |
| 4 | 0.39 ± 0.028 (0.35 – 0.42) | 0.25 ± 0.022 (0.22 – 0.28) |
| 5 | 0.38 ± 0.031 (0.35 – 0.40) | 0.19 ± 0.018 (0.16 – 0.24) |
| 6 | 0.38 ± 0.027 (0.34 – 0.39) | 0.16 ± 0.029 (0.12 – 0.19) |
| 7 | 0.37 ± 0.022 (0.33 – 0.38) | 0.13 ± 0.028 (0.09 – 0.15) |

**Values are mean ± standard error (range),(Unit: mU/ml), ($P \leq 0.05$).** The measuring of serum AChE in lambs of group B was revealed on significant reduction ($P \leq 0.05$) among most weeks of study particularly at $4^{th}$, $5^{th}$, $6^{th}$ and $7^{th}$ weeks, (Table 4).

**Table 5. Abnormal behaviors observed in lambs of experimental group B**

| Symptoms | Lambs No. (Study's week) |
|---|---|
| Anorexia | 1($2^{nd}$), 2 ($3^{rd}$), 2 ($4^{th}$), 3 ($5^{th}$), and 3 ($6^{th}$) |
| Arrhythmia & tachycardia | 2 ($1^{st}$), 4($2^{nd}$), 5 ($3^{rd}$), 5 ($4^{th}$), 6 ($5^{th}$), 6 ($6^{th}$), 3 ($7^{th}$) |
| Constipation | 1 ($1^{st}$), and 1($2^{nd}$) |
| Diarrhea | 1 ($3^{rd}$), 2 ($4^{th}$), 2 ($5^{th}$), and 3 ($6^{th}$) |
| Salivation | 1 ($3^{rd}$), 2 ($5^{th}$), 3 ($6^{th}$), and 2 ($7^{th}$) |
| Ruminal Tympany | 1 ($1^{st}$), 3($2^{nd}$), 2 ($3^{rd}$), 2 ($4^{th}$), and 1 ($5^{th}$) |
| Nervous Signs | 1 ($3^{rd}$), 2 ($4^{th}$), 3 ($5^{th}$), 5 ($6^{th}$), and 3 ($7^{th}$) |
| Shallow Respiration & Tachypnea | 2 ($1^{st}$), 4($2^{nd}$), 5 ($3^{rd}$), 5 ($4^{th}$), 6 ($5^{th}$), 6 ($6^{th}$), 3 ($7^{th}$) |
| General Weakness | All |
| Pale and /or Anemic M.M | 3($2^{nd}$), 3 ($3^{rd}$), 5 ($4^{th}$), 6 ($5^{th}$), and 3 ($7^{th}$) |
| Wool Affection | 2 ($5^{th}$), 3 ($6^{th}$), and 2 ($7^{th}$) |
| Joint Enlargement | 2 ($5^{th}$), and 3 ($6^{th}$) |
| Mortalities | 3 ($7^{th}$) |

# A Study on the Effect of Very Fast Halo CME on Behind Shock Wave in the MESEP Events

Dhuha Ryadh Majeed* and Amjad Al-Sawad

Department of Astronomy and Space, College of Science, University of Baghdad, Baghdad, Iraq.

*Address for Correspondence
**Dhuha Ryadh Majeed**
Department of Astronomy and Space,
College of Science,
University of Baghdad,
Baghdad, Iraq.

**ABSTRACT**

We investigate 18 MESEP events during 1997 until the end of 2013. Events duration were not less than two days and consisting of at least two fast wide CMEs from the same active region and associated with intense X-ray flares and clear type II&IV emissions. We selected three simple events to explain the data which is the 7-10 March 2011, 18-20 July 2012, and 28-29 October 2013. All the events were associated with halo CMEs and solar flare of class X- or M. In all cases, type II, which were with or without type IV radio emissions were observed, indicative that the CMEs were driving coronal shocks. The period of the observation was taken in order to compare the results of CMEs observed by LASCO/SOHO and STEREO. CMEs were chosen with speeds above 500 km/s, and a halo type followed by another CME with speed more than 500km/s and angular width above 60º considering the association with a solar flare. The intensity-time profile for the energetic protons detected by ERNE/SOHO was used as indication for effectiveness of the coronal and IP shocks driven by the CMEs. The study used multispectral data from multi-spacecraft observing the sun in order to complete the tracking of the accelerator of the SEPs observed in situ by ERNE. The parameters of the accelerators, like CME speed, acceleration, location, radio emission type and shock wave parameter like solar wind speed, Mach number, Alfven wave and the associated flare, like $H_\alpha$ location, class, and duration regarding soft X-ray emission were studied.

**Keywords:** halo CME, Shock Wave, Solar Wind, MESEP.

## INTRODUCTION

The Sun loses constantly mass and this mass misfortune is called solar wind. The presence of the solar wind was first proposed to comprehend magnetic tempests on the Earth. Amid magnetic tempests, the properties of the World's ionosphere are changed and radio correspondence can genuinely wind up upset for quite a while (around 36 hours)

after the perception of some rough movement on the Sun (flare). Such an irritation can't be caused by electromagnetic radiation from the Sun since it takes 8 minutes to achieve the Earth. Therefore, it was proposed that the Sun was emanating particles which caused magnetic tempests when they achieve the area of the Earth [1].Coronal Mass Ejections (CMEs) are large-scale eruptions of plasma and magnetic field which propagate from the Sun into the Heliosphere. Post-eruption, CMEs are driven by the release of energy carried by the magnetic fields advocated by the CME. However, the CME is an observable change in coronal structure that shock waves assume a critical part in the solar corona and interplanetary space since they can accelerate SEPs up to high energies. Therefore, shock waves joined by eruptive solar events are for the most part considered as one wellspring of SEP events. In the solar corona, shock waves can be produced by two distinct systems, more often than not called the cylinder instrument and the impact wave component. CMEs can go about as a cylinder, driving bow-shock waves in the corona and into the IP medium [2]. Full halos refer to CMEs that appear to surround the occulting disk within the coronagraphic field of view [3].

CMEs that are wide (width > 120º, but < 360º) are known as partial halos. Some researchers collectively refer to all CMEs with ≥ 120º as halo CMEs. Here we consider only those completely surrounding the occulting disk as full halos. Among full halos, those appearing close to the central meridian either in the front-side or in the back-side generally appear symmetric around the occulting disk. Shock waves play an important role in the solar corona and interplanetary space, since they are able to accelerate particles (electrons, protons and heavy ions) up to high energies. Presently there are two kinds of shock [4]. The prompt impact wave starts in the magnetic-rebuilding aggravation at the beginning of the flare impulsive stage as it moves outward and forms into a quick mode MHD shock wave and associated with type II burst at metric wavelengths [5]. In the meantime, the CME, in the IP medium, moves outward and drives an IP shock in front of it. This wave, dissimilar to the impact wave, can proceed as long as the CME proliferates supersonically; when it touches base at the earth it makes a reasonable mark in the geomagnetic field (SSC).

## Data selection

Our basic selection criteria for the analyzed events were had to be two CMEs within two-three days and that each of the CMEs associated with coronal metric and D-H radio type II&IV burst. The Wind/WAVES type II bursts and CMEs list at http://cdaw.gsfc.nasa.gov/CME_list/radio/waves_type2.html was used to find event sequences that matched these requirements. The preliminary candidate list consisted of 18 sequences of consecutive events. Further requirements were that the CMEs were chosen considering the association with a shock wave .must be associated to shock wave to be separable from each other so that their associated features could be investigated and that energetic protons associated with the first two CMEs were observed. Data gaps in the in situ particle data made the analysis impossible for some events. Eventually, three triple-events remained for analysis. The CME speed, height-time evolution, and width for the selected events were obtained from the SOHO/LASCO CME Catalog at http://cdaw.gsfc.nasa.gov/ [6]. The data for the associated IP radio type II events were taken from the Wind/WAVES [7] catalog at http://lep694.gsfc.nasa.gov/waves/data_products.html. Flares locations were checked from the NOAA/NGDC flare listings at http://www.ngdc.noaa.gov/stp/ spaceweather.html. The SOHO/ERNE [8] proton data were then investigated at http://www.srl.utu.fi/ernedata/main_english.html, to find the associated proton events.

## Event analysis and results

The three sequences of multiple CME events that fulfilled our selection criteria occurred on 7-10 March 2011, 18-20 July 2012 and 28-29 October 2013. Their main properties are presented in Table 1. All the CMEs were fast, halo type CMEs.

### Events 7-10 March 2011

On the 7-10 March 2011an MESEP event was seen on 72 MeV channel of ERNE/SOHO. First event (CME1) was halo with FC2AT at 20:00UT on 7th March 2011. The proton injection time was calculated at 20:47 UT while the CME was at a heliocentric location of $10.33R_\Theta$. The CME was with Iinear speed of 2125 km/s and deceleration of 63.1 m/s$^2$ and associated with M3.7 solar flare on H$\alpha$ location N24W58 in AR 1165 and associated with DH radio emissions type II started at 20:00-2012UT. Second event (CME2) was AW 99º with FC2AT at 20:12UT on 8th March 2011. The proton injection time was calculated at 20:47UT while the CME was at a heliocentric location of $4.089R_\Theta$ and CAP 236º with a linear speed of 702km/s and acceleration of 4.1m/s$^2$ and associated with M5.6 solar flare on H$\alpha$ location S19W87 in AR 1165 and association with DH radio emissions type II started at 20:16-21:35UT as we see in figure (1). A shock wave arrival was observed by SOHO/CELIAS/MTOF on 10 March 2011at5:45UT caused by CME1 with 58 hours traveling time. From the figures below you can see the intensity profile and the characteristics of shock wave (solar wind, mach no, Alfven wave)

### Events 18-20 July 2012

An MESEP event was seen on 23.3 MeV channel of ERNE/SOHO on the 18-20 July 2012. First event (CME1) was halo with FC2AT at 6:24 UT on 18th July 2012. The proton injection time was calculated at 6:18UT while the CME was at a heliocentric location of $3.43R_\Theta$ table (3.2). The CME was with Iinear speed of 873 km/s and deceleration of 10.9 m/s$^2$ with C3.0 solar flare H$\alpha$ location N17W75 on AR 1520. Second event (CME2) was halo with FC2AT at 5:24UT on 19th July 2012. The proton injection time was calculated at 5:49UT while the CME was at a heliocentric location of $5.002R_\Theta$ with a linear speed of 1631 km/s and deceleration of 8.0m/s$^2$ and associated with M7.7 solar flare H$\alpha$ location S17W89 on AR 1520, The DH radio emissions were observed in association with previous eruptions as Type II started on 18 July 2012 at 6:15-6:40UT in association with CME1. Type II started on 19 July 20012 at 5:30-6:20-1:30 UT and Type IV at 5:23-5:30i UT in association with CME2 fig (3). A shock wave arrival was observed by SOHO/CELIAS/MTOF on 20 July 2012 at4:00 UT caused by CME2 with 24.5 hours traveling time. From the figures below you can see the intensity profile and the characteristics of shock wave (solar wind, mach no, Alfven wave)

### Events 28-29 October 2013

An MESEP event was seen on 18.9 MeV channel of ERNE/SOHO on the 28-29 October 2013. First event (CME1) was halo with FC2AT at 2:24 UT on 28th October 2013. The proton injection time was calculated at 2:33UT while the CME was at a heliocentric location of $4.65R_\Theta$ table (3.2). The CME was with Iinear speed of 695 km/s and deceleration of 12.1m/s$^2$ with X1.0 solar flare H$\alpha$ location N17W72 on AR 1875. Second event (CME2) was Aw 156º with FC2AT at 4:84UT on 28th October 2013. The proton injection time was calculated at 5:03UT while the CME was at a heliocentric location of $6.416R_\Theta$ and CAP 315º with a linear speed of 1201 km/s and deceleration of 45.2m/s$^2$ and associated with M5.1 solar flare H$\alpha$ location N07W51 on AR 10798, The DH radio emissions were observed in association with previous eruptions as Type II started on 28 October 2013 at 4:45UT in association with CME1. Type II started on 28 October 2013at 4:41UT with type IV at 4:37-10:16UT in association with CME2, fig (5).A shock wave arrival was observed by SOHO/CELIAS/MTOF on 29 October 2013 at9:62UT caused by CME1 with 31 hours traveling time. From the figures below you can see the intensity profile and the characteristics of shock wave (solar wind, mach no, Alfven wave)

## DISCUSSION AND CONCLUSIONS

It has been well known by the current time that solar shock waves are developing in different mechanism according to the ambient medium which is the solar wind. In fact any driven shock wave by solar blast will not be considered as an effective one, unless it is powerful enough to accelerate SEPs. The differences in the ambient parameters have

created a debate about the two phases of the shock wave, which is the coronal and IP shock. For long time the researchers were sometimes go for coronal shock as main accelerator and for some others the IP shock was the main accelerator. Still as we know the magnetic field in the corona is perpendicular with the shock front and parallel in the IP medium. This will cause a difference in the energy sum since the inhalation of the magnetic collision will be transferred to the SEPs. On the other hand the solar wind can be much faster near corona than IP which will be in the favor of the IP shock acceleration. Anyhow, if there is an effect on the solar wind speed or magnetic disturbance in the corona or IP it will be effective on the efficiency of the shock wave, thus in the multiple CME SEP events, the first CME will for sure speed up the solar wind and disturb the magnetic field behind it. This can play a major role in changing the shock parameters for the second CME. In this thesis we studied the possibility for this effectiveness and the associated phenomenon and we found the following:

1. All the CME1 were associated with SEP but the effective shock wave (coronal and IP) were observed in 14 events only.
2. About 50% (9/18) of CME2 were associated with SEP and their coronal shock waves were effective, while the rest have no shock observation and no SEP signals.
3. In the events were the speed of the CME1 was higher in 50% (9/18) the solar wind was effected and led to alter the Mach number and p and for the CME2 so no shock observed, which it means that the speed play as a major role in this case.
4. we found that 17%(3/18) the CME2 driven a shock wave with CME1 shock wave
5. all events were associated with solar flare in class C,M and X. There are 11% of CMEs1 were not associated with solar flare and 11% of CMEs2 were associated.
6. In some other studies there was indication of penetrating for the SEPs accelerated by CME2 for the decelerating shock of the CME1, which it means effectiveness for the acceleration. While in our study we found the speed is the affective parameter according to the data that we observed.

## REFERENCES

1. A. Hanslmeier (2002 ),The Sun and Space Weather ,Astrophysics and Space Science Library , Springer.
2. Forbes T. G., Linker J. A. , Chen J., Cid C., Ko´ Ta J., Lee M. A., Mann G., Miki´C Z., Potgieter M. S., Schmidt J. M., Siscoe G. L., Vainio R., Antiochos S. K. and Riley P., ―CME theory and models‖, Space Science Reviews , DOI: 10.1007/s11214-006-9019-8, Volume. 123, pp.251–302, 2006.
3. N. Gopalswamy, A. Lara, S. Yashiro, S. Nunes, S., R. A. Howard, in: Wilson, A. (ed.) Solar Variability as an Input to the Earth's Environment SP-535, ESA, Noordwijk,2003, p.403.
4. N. Gopalswamy, S. Yashiro, M. L. Kaiser, R. A. Howard, and J. L. Bougeret; Characteristics of coronal mass ejections associated with long-wavelength type II radio bursts; Journal of Geophysical Research A, Vol. 106, no. 12, pp. 29219–29229; 2001.
5. B. Vršnak,; Dynamics of solar coronal eruptions; Journal of Geophysical Research, Vol., 106, Issue A11, pp. 25249-25260, 2001.
6. S. Yashiro, N. Gopalswamy, G. Michalek, O.C. St. Cyr, S. Plunkett, N.B. Rich, and R.A. Howard, A catalog of white light coronal mass ejections observed by the SOHO spacecraft, J. Geophys. Res. 109,A07105, 2004.
7. J.-L. Bougeret, M.L. Kaiser, P.J. Kellogg, et al., Waves: The Radio and plasma wave Investigation on the Wind spacecraft, Space Sci. Rev 71, 231, 1995.
8. J. Torsti, E. Valtonen, M. Lumme et al., Energetic particle experiment ERNE, Solar Phys. 162, 505,1995.

**Dhuha Ryadh Majeed and Amjad Al-Sawad**

**Table 1. show the CMEs properties**

| CME1 | 7.3.11 | 18.7.12 | 28.10.13 |
|---|---|---|---|
| FC2AT(UT) | 20:00 | 6:24 | 2:24 |
| CPA(deg.) | HALO | HALO | HALO |
| AW(deg.) | …… | ……… | |
| Speed(km/s) | 2125 | 873 | 695 |
| Solar flare SXR(UT) | M3.7 | C3.0 | X1.0 |
| Solar flare Hα | N24W58 | S17W75 | N05W72 |
| Solar flare active region | 1165 | 1520 | 1875 |
| Solar Radio emission II type | 20:00-20:12 | 6:15-6:40 | 4:45 |
| Solar Radio emission IV type | ……. | ……. | ……. |
| **CME2** | **8.3.11** | **19.7.12** | 28.10.13 |
| FC2AT(U-T) | 20:12 | 5:24 | 4:48 |
| CPA(deg.) | 236 | HALO | 315 |
| AW(deg.) | 99 | | 156 |
| Speed(km/s) | 702 | 1631 | 1201 |
| Solar flare SXR(UT) | M1.7 | M7.7 | M5.1 |
| Solar flare Hα | S19W87 | S17W89 | N07W51 |
| Solar flare active region | 1165 | 1520 | 1875 |
| Solar Radio emission II type | 20:16-21:35 | 5:30-6:20 | 4:41 |
| Solar Radio emission | ……… | 5:23-5:30 | 4:37-10;16 |
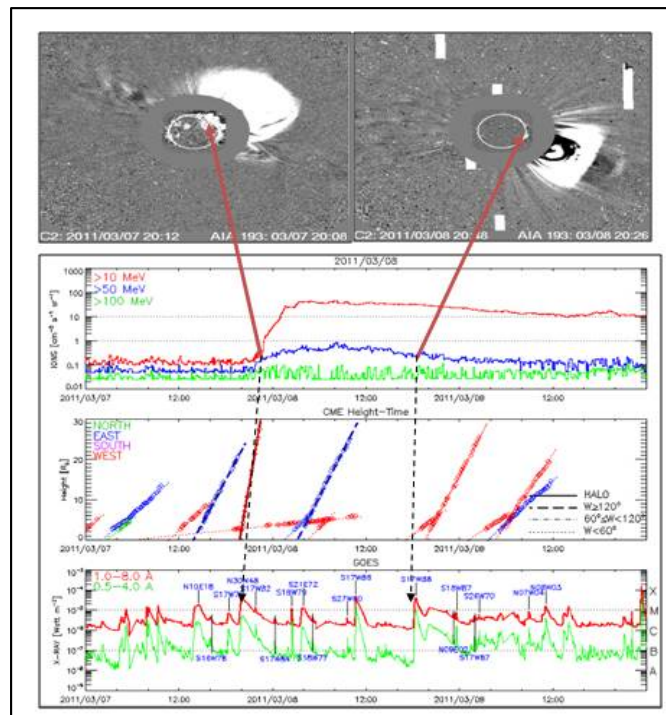


**Figure 1. the 7-10 March 2000 event: the top panel show the first C2 appearance of CME1 (red arrow) and CME2 (red arrow). Lower panel shows the height and direction of CMEs. Bottom shows the associated soft X-ray flare**

16492

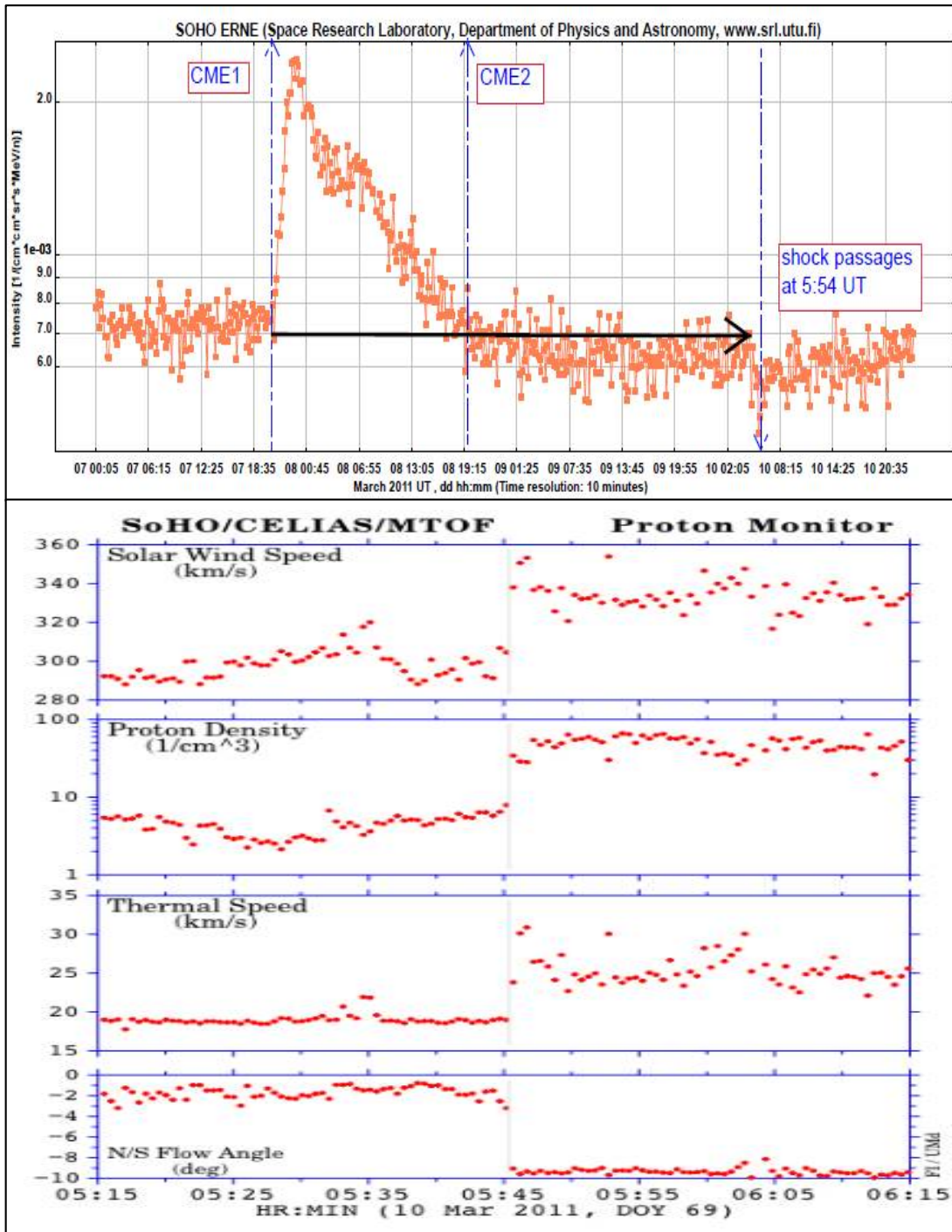**Dhuha Ryadh Majeed and Amjad Al-Sawad**



**Figure 2a. The event 7-10 March 2011. Top panel shows the intensity-time profile from SOHO/ERNE with 10-hour time resolution . Lower panel shows the behave(solar wind, proton density, thermal speed and flow angle) of a particle in shock wave from SOHO/CELIAS/ MTOF.**
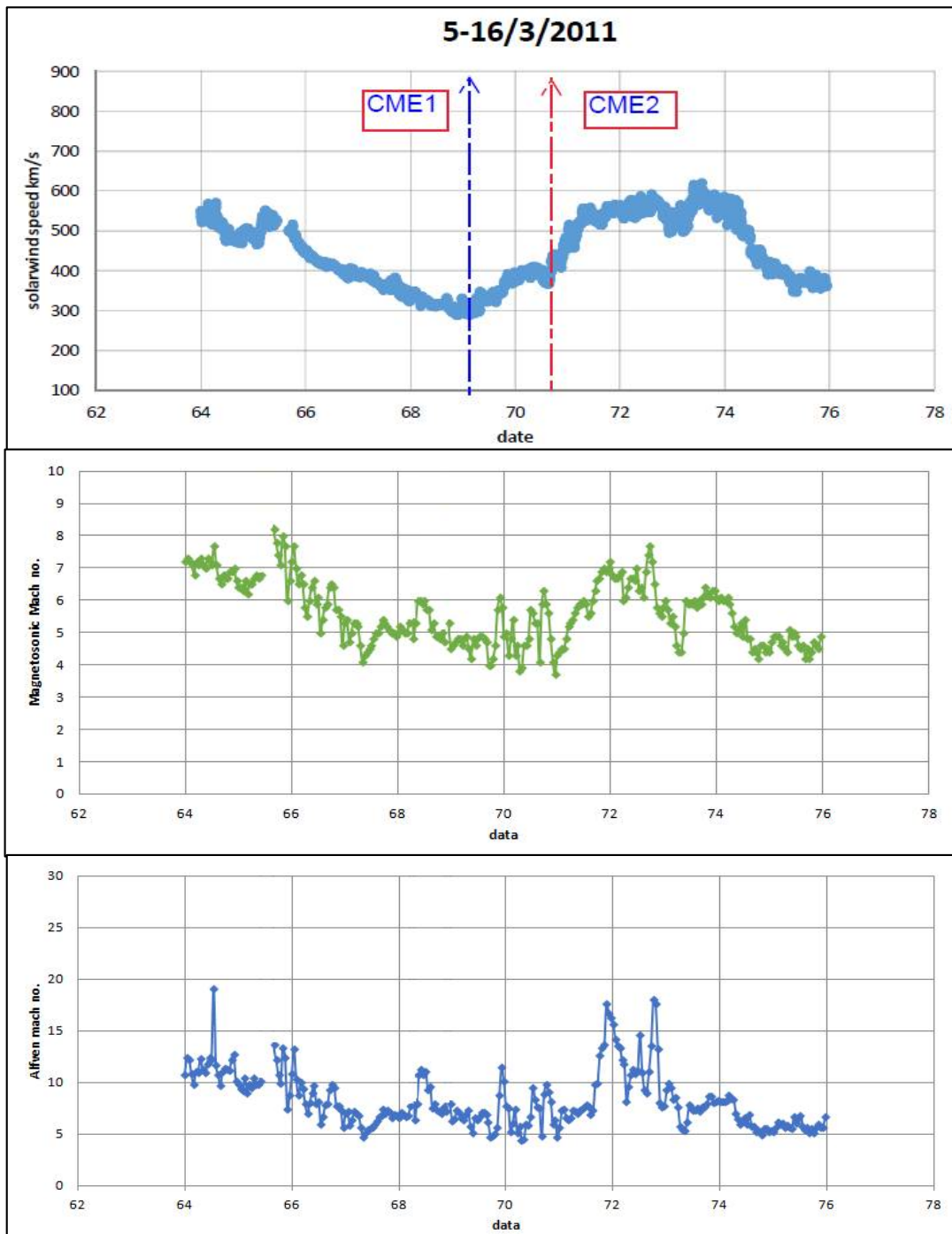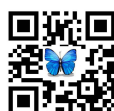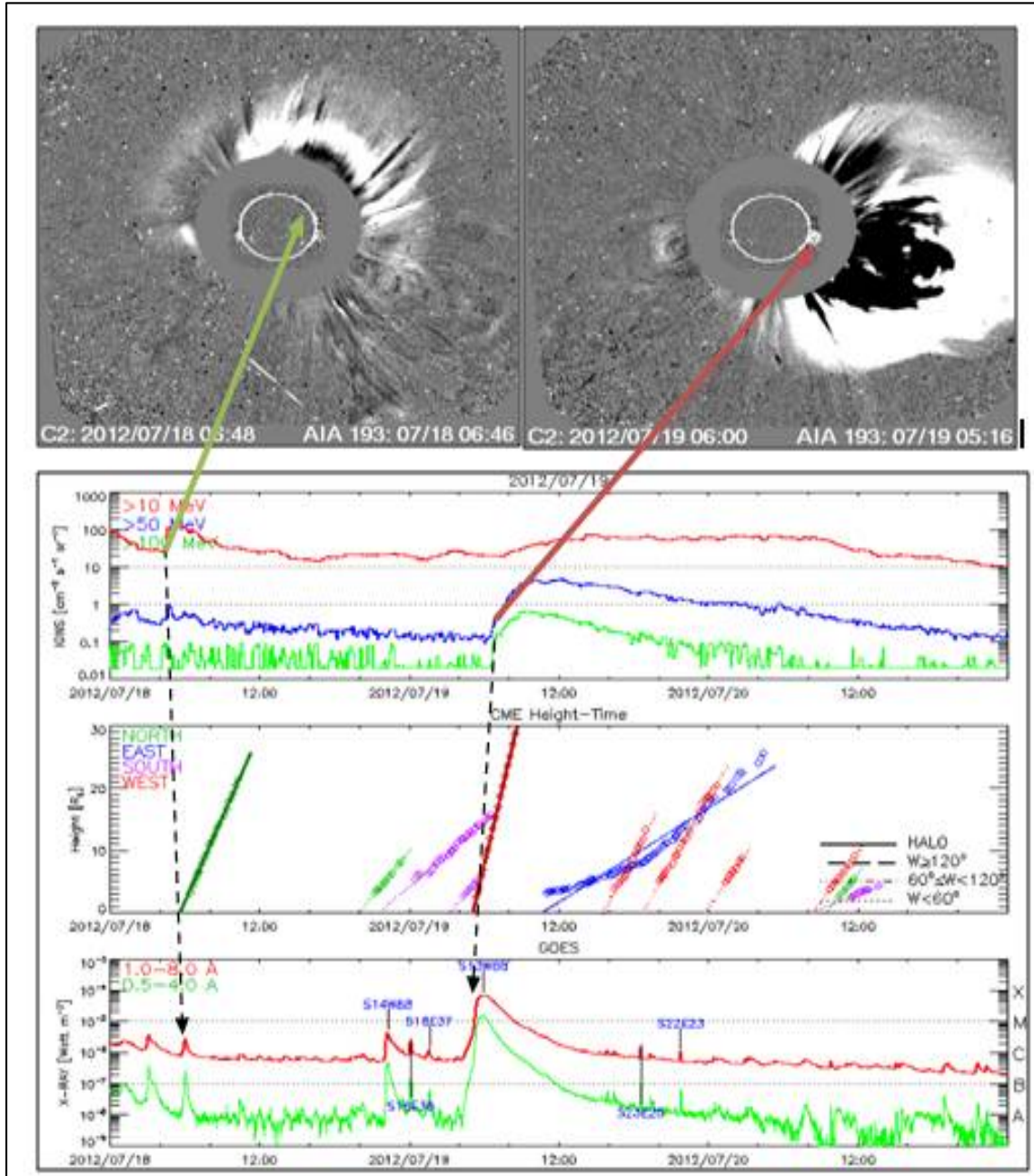
**Dhuha Ryadh Majeed and Amjad AI-Sawad**



**Figure 2b. The characteristic of the shock wave (the uppre panel represant the solar wind speed,the mid panel represent the mach number and the lower panel represent the Alfven speed) blue arrow represent CME1,red arrow represent CME2.**

**Dhuha Ryadh Majeed and Amjad Al-Sawad**



**Figure 3. the 19-21 July 2012 event: Top panel show the first C2 appearance of CME1 (green arrow) and CME2 (red arrow). Lower panel shows the height and direction of CMEs. Bottom shows the associated soft X-ray flare.**
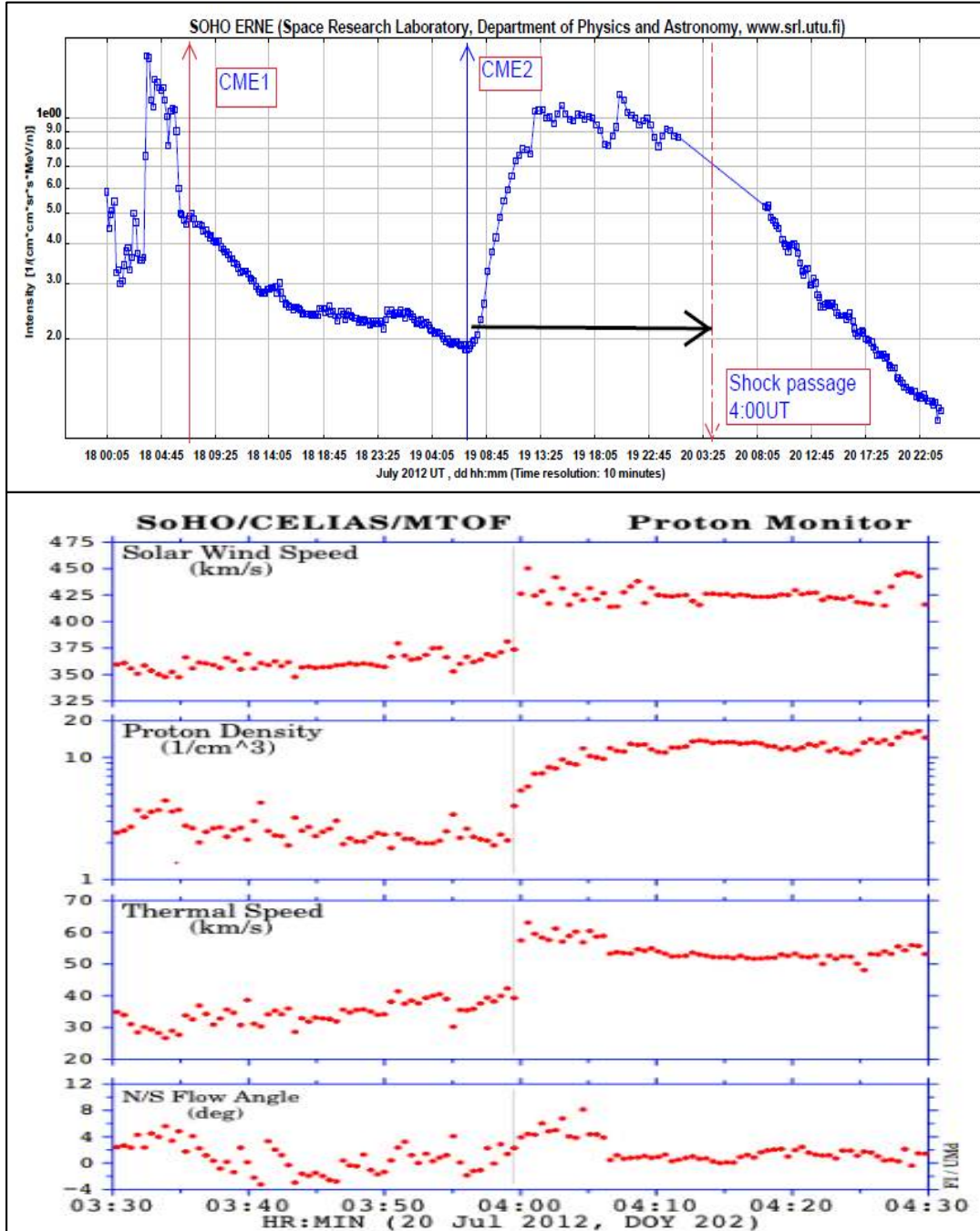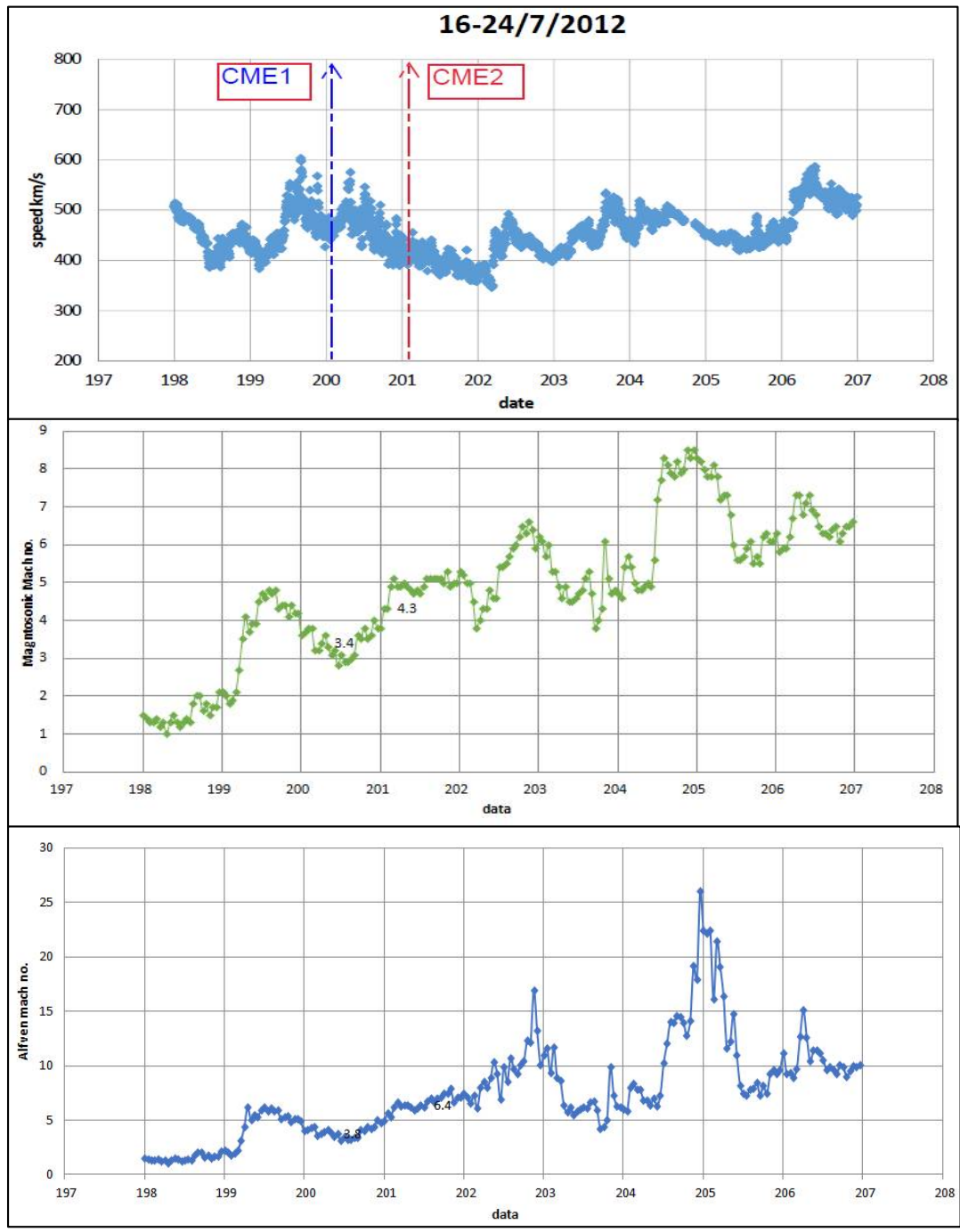
**Dhuha Ryadh Majeed and Amjad Al-Sawad**



**Figure 4a. The event 18-20 July 2012. Top panel shows the intensity-time profile from SOHO/ERNE with 10-hour time resolution. Lower panel shows the behave(solar wind, proton density, thermal speed and flow angle) of a particle in shock wave from SOHO/CELIAS/ MTOF**

16496

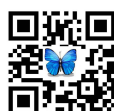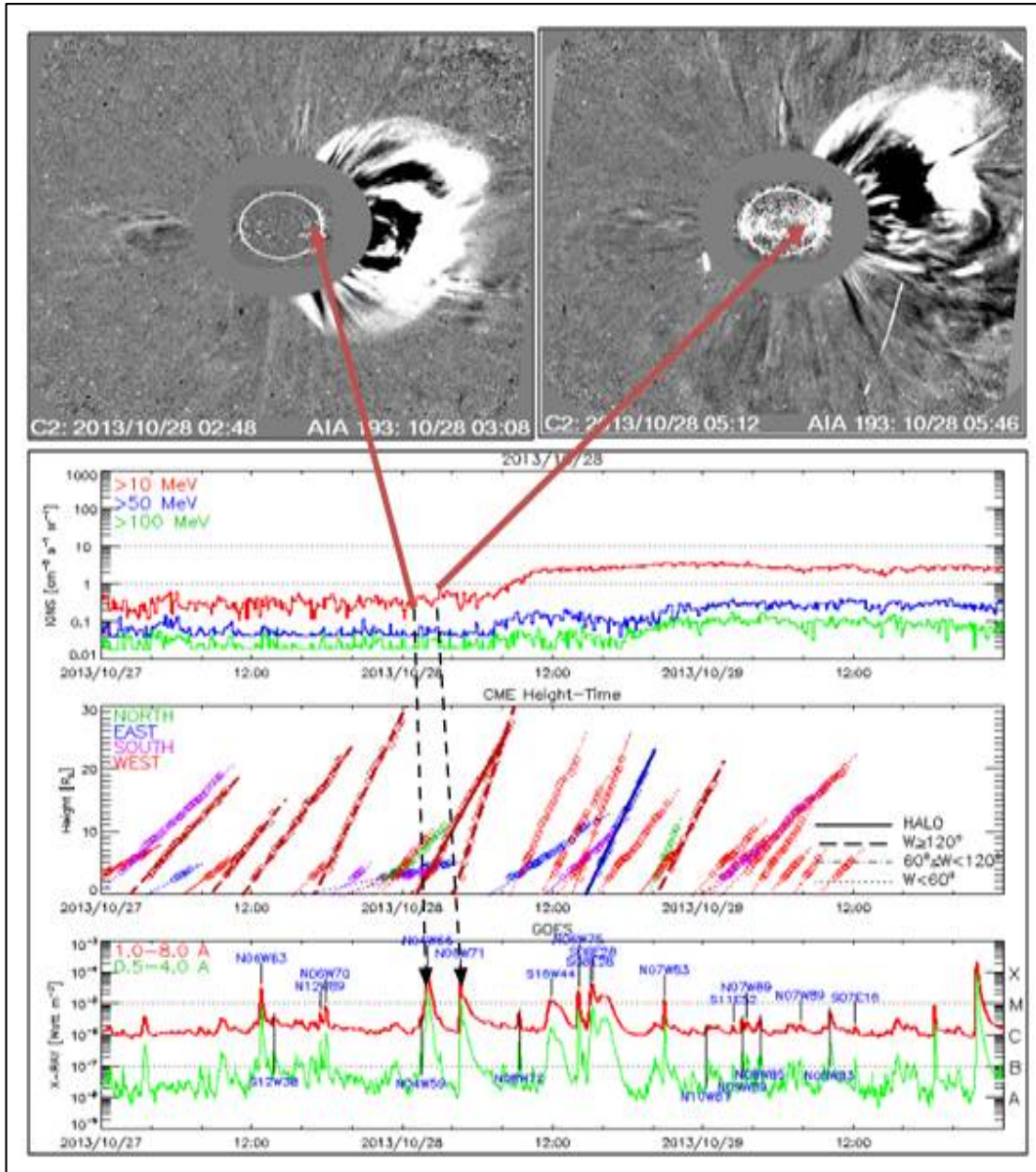**Dhuha Ryadh Majeed and Amjad Al-Sawad**



**Figure 4b. the characteristic of the shock wave (the uppre panel represant the solar wind speed,the mid panel represent the mach number and the lower panel represent the Alfven speed) blue arrow represent CME1, red arrow represent CME2.**

**Dhuha Ryadh Majeed and Amjad Al-Sawad**



**Figure(5) the 28-30 October 2013 event: Top panel show the first C2 appearance of CME1 (red arrow) and CME2 (green arrow). Lower panel shows the height and direction of CMEs. Bottom shows the associated soft X-ray flare.**
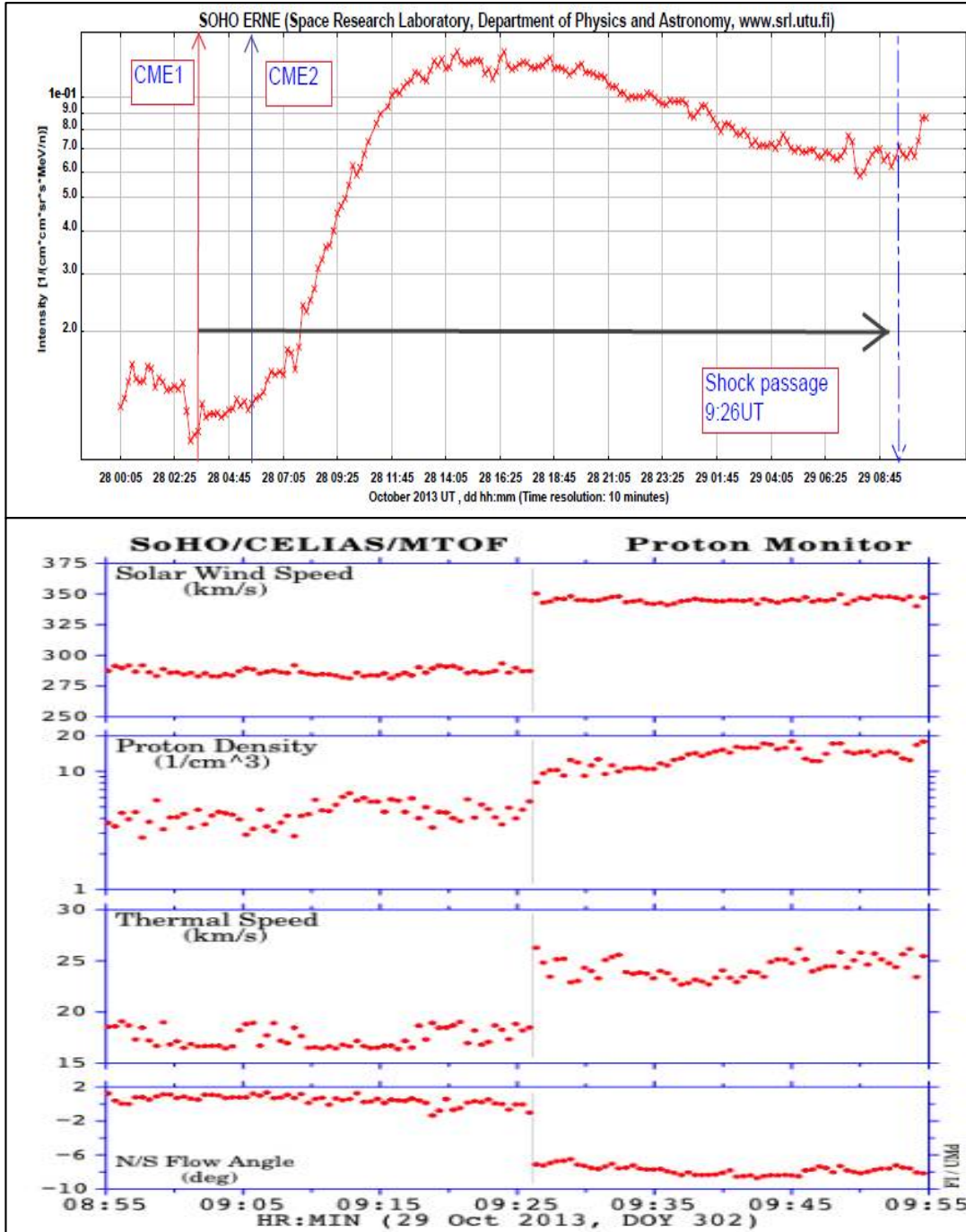
16498

**Dhuha Ryadh Majeed and Amjad Al-Sawad**



**Figure 6a. The event 28 October 2013. Top panel shows the intensity-time profile from SOHO/ERNE with 10-hour time resolution. Lower panel shows the behaver (solar wind, proton density, thermal speed and flow angle) of a particle in shock wave from SOHO/CELIAS/ MTOF.**
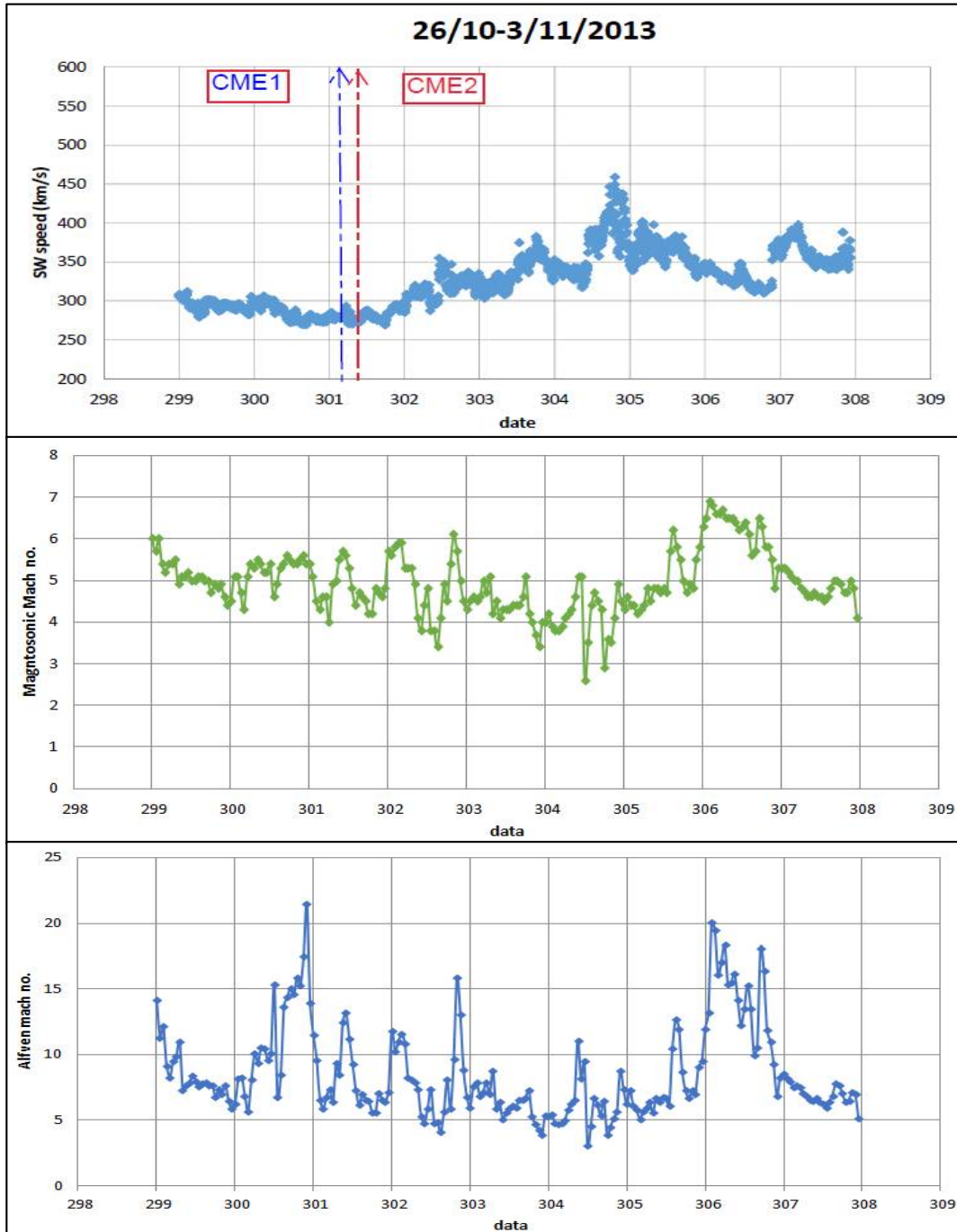
**Dhuha Ryadh Majeed and Amjad Al-Sawad**



**Figure 6b. the characteristic of the shock wave (the uppre panel represant the solar wind speed,the mid panel represent the mach number and the lower panel represent the Alfven speed) blue arrow represent CME1, red arrow represent CME2**

**RESEARCH ARTICLE**

# Effect of Polychromatic Light on Image Performance of Human Eye with Polythiourethane Contact Lens

Ali H. Al-Hamdani and Halah A.Hashim*

Laser and Optoelectronics Engineering Department, University of Technology, Baghdad, Iraq.

*Address for Correspondence
**Halah A.Hashim**
Laser and Optoelectronics Engineering Department,
University of Technology,
Baghdad, Iraq.
Email:halahabdullah941@gmail.com

**ABSTRACT**

The human eye, as our vision organ, is affected by optical aberrations, which are optical defectsthat influence vision. Such defectsinvolve the formationof low-quality images on the retina. This phenomenoncan be described as the failure to obtain a faithful representation of an object in the image plane. These aberrations come in different forms, namely, monochromatic and polychromatic aberrations. In this work, we conducted quantitative comparisons of the human eye performance at a range of fields of view for different entrance pupil diameters.To evaluate such performance, the difference in image quality under monochromatic and polychromatic aberrations was observed with the use of the software Zemax-EE (2005)and the Liou and Brennan human eye model.The modulation transfer function, blur spot size (RMS) and the type and amount of aberrations were used as criteria in analyzing retinal image degradation.

**Keywords:** Human eye, Liou and Brennan model, Zemax, aberration, PTU polymer.

## INTRODUCTION

The human eye is considered one of the most important organs due to its major function. It generally receives more than 80% of the details of the surrounding area [1]. The optical function of the human eye is to form an image of an object on the retina,which is a highly complicated and sensitive process [2]. A good optical eye produces an object image with fine quality [3].However, this biological vision instrument experiences an essential optical defect called optical aberration [4]. Thus, the quality of formed imagesare affected by optical system defects.These errors are classified as monochromaticand polychromaticaberrations[5].Monochromatic aberration results from the geometry of the optical system [6]. This aberration is also known as third-order aberration and classified into five types, namely,spherical aberration, coma, astigmatism, field curvature and distortion[7]. Polychromatic aberration results

**Ali H. Al-Hamdani and Halah A.Hashim**

due to the optical system dispersion of the refractive media[8].The refractive index of the eye is a function of the wavelength $n(\lambda)$[9]. As explained according to Snell's law, the ray of light with an angle of incident $i$ passing into the eye is refracted at an angle of $i'$ inside the eye, commonly referred to as dispersion phenomenon[10].

$$sin i = n(\lambda) sin i' \quad (1)$$

## MATERIALS

Material selection is the first and most important step in design[11]. Polymers are the most suitable materials currently available for producingcontact lenses [12]. In this study,polythiourethane (PTU) polymer,an optical plastic material,is used for this specific calculation. This material has good optical characteristics (refractive index of 1.67 and Abbe number of 28), thereby becoming qualified foruse in this design[13]. The refractive index, which measures the propagation of a ray of light through a substance [14],isdefined as

$$n = \frac{c}{v} \quad (2)$$

where $n$is the refractive index,$c$ is the velocity of light in free space and $v$is the velocity at a particular medium.The Abbe number $(v_d)$represents the dispersion of a transparent material[14] and is expressed as

$$v_d = \frac{n_d - 1}{n_f - n_c} \quad (3)$$

where$v_d$is the Abbe number and$n_d$, $n_f$and$n_c$are the refractive indexes at wavelengths of 550, 470 and 650 nm, respectively.

## METHODS

A contact lens was designed from PTU polymer, a new type of optical polymer used in the ophthalmicfield, due to thematerial's high refractive index, low dispersion characteristicsand good impact strength.The software program Zemax and the Liou and Brennan human eye model were used to preciselycompare the performance of the human eye between monochromatic and polychromatic conditions[15]. To distinguish the most efficient model,we aimed to identify the results with the highest accuracy, which symbolised semblance with biological eye results. Different criteria were used, such as the tangential modulation transfer function (MTFT), sagittal modulation transfer function (MTFS), the type of aberrations that affect and degrade the retinal image and root mean square (RMS).

### Modulation Transfer Function

The modulation transfer function (MTF) indicates the distinctness and difference of an imaging system and measures the quality of the retinal image[16].

$$MTF(v) = \frac{C'}{C} \quad (4)$$

where $C$is the contrast in the target and defined as the ratio of the amplitude of the sine-wave $A$ to its average value $B$,and $C'$ is the corresponding contrast in the image.

$$C = \frac{A}{B} \quad (5)$$

where
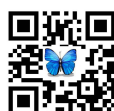
**Ali H. AI-Hamdani and Halah A.Hashim**

$$A = \frac{Max - Min}{2} \text{ and } D = \frac{Max + Min}{2}. \qquad (6)$$

The contrast can be expressed as

$$C = \frac{Max - Min}{Max + Min}. \quad (7)$$

**Root Mean Square**

The spot radius is another measurementof retinal image quality, and it relies on the spot diagram. It is computed as the RMS of all the distances between each marginal ray intersection $(x_i, \ y_i)$ with the image plane and a reference point $(x_0, \ y_0)$ generated by the chief ray intersection[17].

## RESULTS AND DISCUSSION

Images formed on the human eye retina vary in quality under two conditions, namely, monochromatic and polychromatic aberrations.In this research, we studied the difference in performance of the optical system and compared the obtained results. We observed the effect of an FOV increase range of 5°–60° for entrance pupil diameters of1.5 and 2mm on image quality under both conditions.The analysis criteria used were MTFT, MTFS, wave aberration and RMS. Figures 1–4 present the performance of the human eye in cases of monochromatic and polychromatic aberrations. Figures 1-aand 1-b indicate that the MTFS differed from the MTFT due to differences in the image plane.However, both MTFs were degrading, with the MTFS becoming affected more than the MTFT. Meanwhile, Figure 1-c shows that when the FOV was increased, the distortion aberration was also increased, thereby affecting the quality of the formed image. Figure 1-dshows that the RMS increased as the FOV increased. Figure 2 explains other results at EPD=2mm at a different FOV. Figures 2-a and 2-b show the degradation of MTFT and MTFS, respectively, with increasing EPD. Figure 2-c provides the amount of Seidel aberration that increased with EPD and FOV, and Figure 2-d illustrates an increase in RMS.

Figures 3 and 4 present the polychromatic performance. Given the differencein the image quality introduced by the MTF performance, in which the polychromatic MTFT presented an inferior performance compared with monochromatic MTFT (This difference was due to the wide band of wavelength in the case of the polychromaticaberration and the variation in the wave aberrations obtained from the polychromatic and monochromatic PTUs.). Given the amount of aberration that affected on the overall optical system performance.It is polychromatic,so considerable aberration would enter the optical system due to the different wavelength band.The RMS in the polychromatic PTU gradually increased under the effect of FOV.Given that it is polychromatic, the more the FOV increased, the more the band size of the incoming aberration affected the formed image. Figure 5 compares the monochromatic and polychromatic performance for different FOVs at an entrance pupil diameter of 1.5 mm.

## CONCLUSION

We measured the monochromatic and polychromatic aberrations for several FOVs at different iris and pupil diameters. The quantitative comparison conducted in this work for the human eye performance under both conditionsdepicted tolerances in image quality. The optical system produced considerably better image quality under the monochromatic condition than under the polychromatic condition.Monochromatic aberration is a single wavelength that affects the formed image,thus resulting in less aberration and degradation in image quality than does polychromatic aberration,which has multiple wavelengthsthat affect the performance and quality of the retinal image. These findings illustrated the difference in performance and how it affected the overall system.
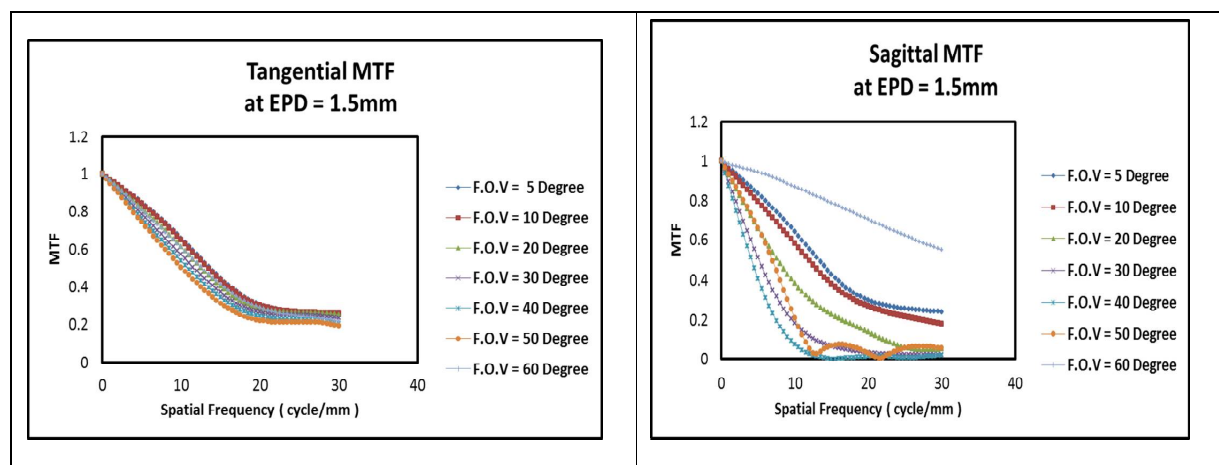
**Ali H. Al-Hamdani and Halah A.Hashim**

**Ethical approval**

This article does not contain any studies with human participants or animals performed by any of the authors.

## REFERENCES

1.  D. Mcbride, *Modern Miracle Medical Machines THE HUMAN EYE AND VISION A Quick Review of Waves Modeling the Eye as an Optical System.* 2010.
2.  J. C. He, S. A. Burns, and S. Marcos, "Monochromatic aberrations in the accommodated human eye," *Vision Res.*, vol. 40, no. 1, pp. 41–48, 2000.
3.  N. Yu, F. Fang, B. Wu, L. Zeng, and Y. Cheng, "State of the art of intraocular lens manufacturing," pp. 3–4, 2018.
4.  L. A. V de Carvalho and J. C. de Castro, "Preliminary results of an instrument for measuring the optical aberrations of the human eye," *Brazilian J. Phys.*, vol. 33, no. 1, pp. 140–147, 2003.
5.  L. N. Thibos, A. Bradley, D. L. Still, X. Zhang, and P. A. Howarth, "Theory and measurement of ocular chromatic aberration," *Vision Res.*, vol. 30, no. 1, pp. 33–49, 1990.
6.  Y. U. Ogboso and H. E. Bedell, "Magnitude of lateral chromatic aberration across the retina of the human eye," *JOSA A*, vol. 4, no. 8, pp. 1666–1672, 1987.
7.  D. A. Atchison, G. Smith, and G. Smith, "Optics of the human eye," 2000.
8.  D. Atchison, "Optics of the Human Eye," pp. 1–19.
9.  M. Rynders, B. Lidkea, W. Chisholm, and L. N. Thibos, "Statistical distribution of foveal transverse chromatic aberration, pupil centration, and angle ψ in a population of young adult eyes," *JOSA A*, vol. 12, no. 10, pp. 2348–2357, 1995.
10. B. Daemi, "How to measure the Transverse Chromatic Aberration of the human eye in off-axis angles," 2011.
11. M. F. Ashby, "Materials selection in mechanical design," *MRS Bull*, vol. 30, no. 12, p. 995, 2005.
12. K. Kogler, "Selection of plastics for optical applications," *Adv. Mater. Process.*, pp. 6–9, 1999.
13. B. Jaffrennou, N. Droger, F. Méchin, J. Halary, and J. Pascault, "Characterization , structural transitions and properties of a tightly crosslinked polythiourethane network for optical applications," no. 082, pp. 1–19, 2005.
14. G. S. Jha, G. Seshadri, A. Mohan, and R. K. Khandal, "Development of High Refractive Index Plastics," no. 120, pp. 1–25, 2007.
15. D. A. Atchison, "Optical models for human myopic eyes," *Vision Res.*, vol. 46, no. 14, pp. 2236–2250, 2006.
16. O. Corporation, "How to Measure MTF and other Properties of Lenses," pp. 1–64, 1999.
17. O. D. Program and U. Guide, "ZEMAX ® Optical Design Program User ' s Guide," 2005.

16504

**Ali H. Al-Hamdani and Halah A.Hashim**



**Figure 1. a)Tangential modulation transfer function (MTFT), b) sagittal modulation transfer function (MTFS), c) wave aberration with field of view (FOV), d) root mean square (RMS).**
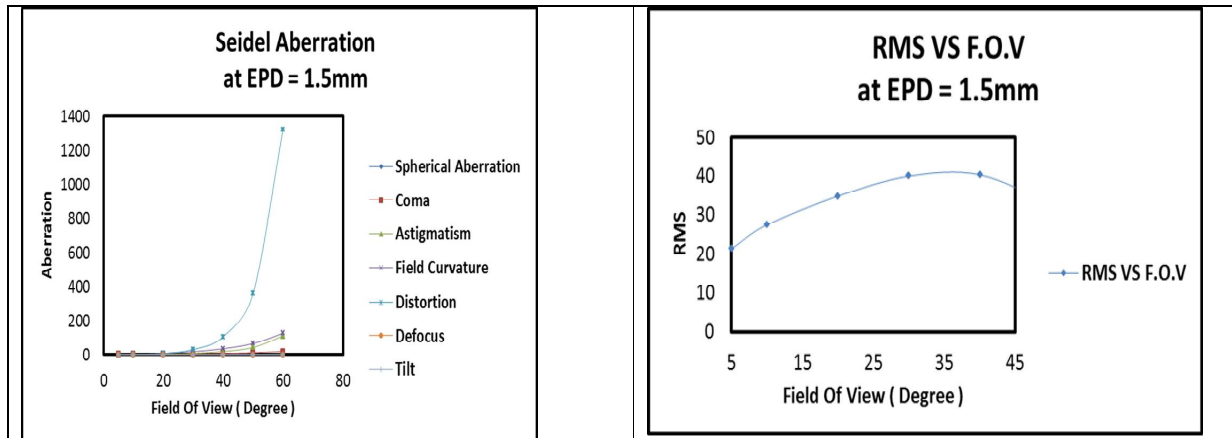


**Figure 2. a) Tangential modulation transfer function (MTFT), b) sagittal modulation transfer function (MTFS), c) wave aberration with field of view (FOV), d) root mean square (RMS).**

## Ali H. Al-Hamdani and Halah A.Hashim



**Figure 3: a) Tangential modulation transfer function (MTFT), b) sagittal modulation transfer function (MTFS), c) wave aberration with field of view (FOV), d) root mean square (RMS).**
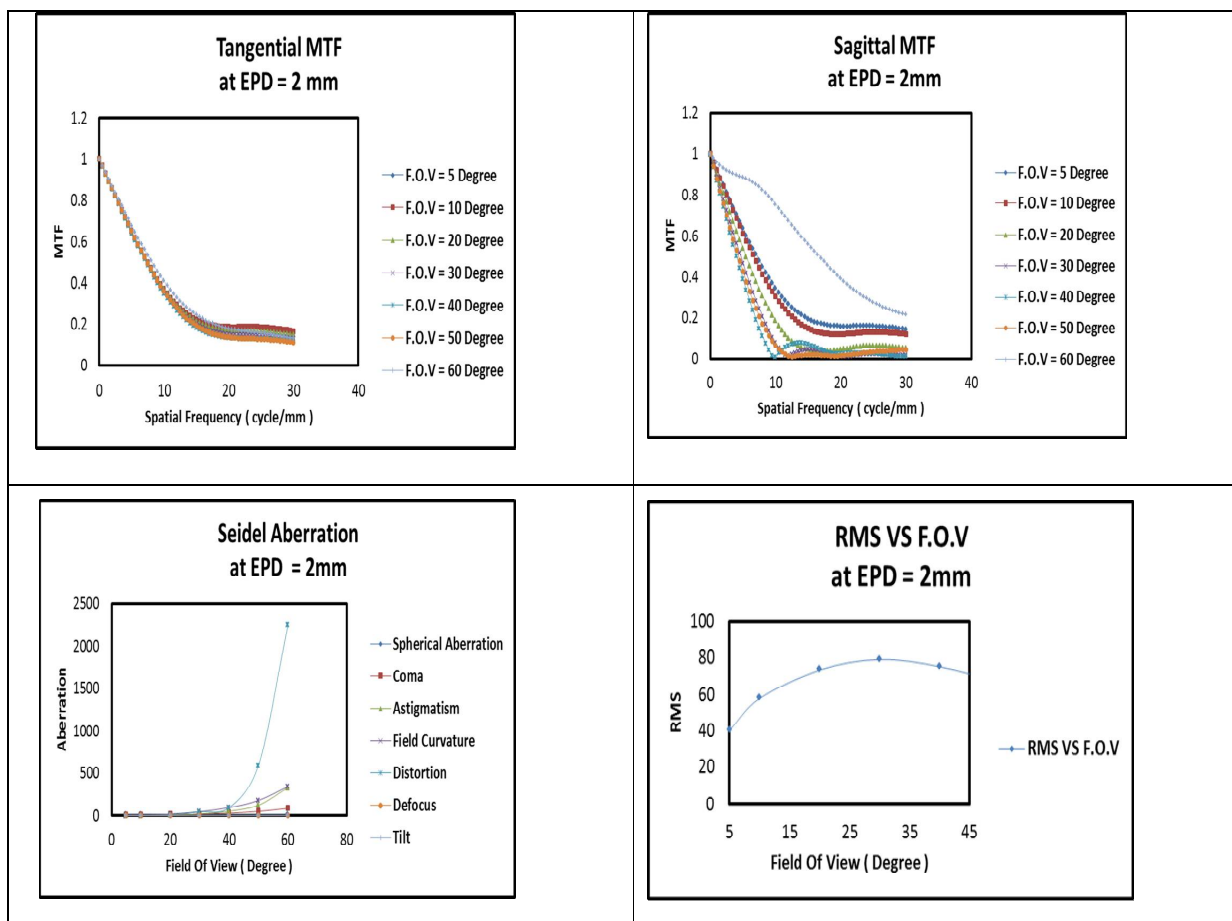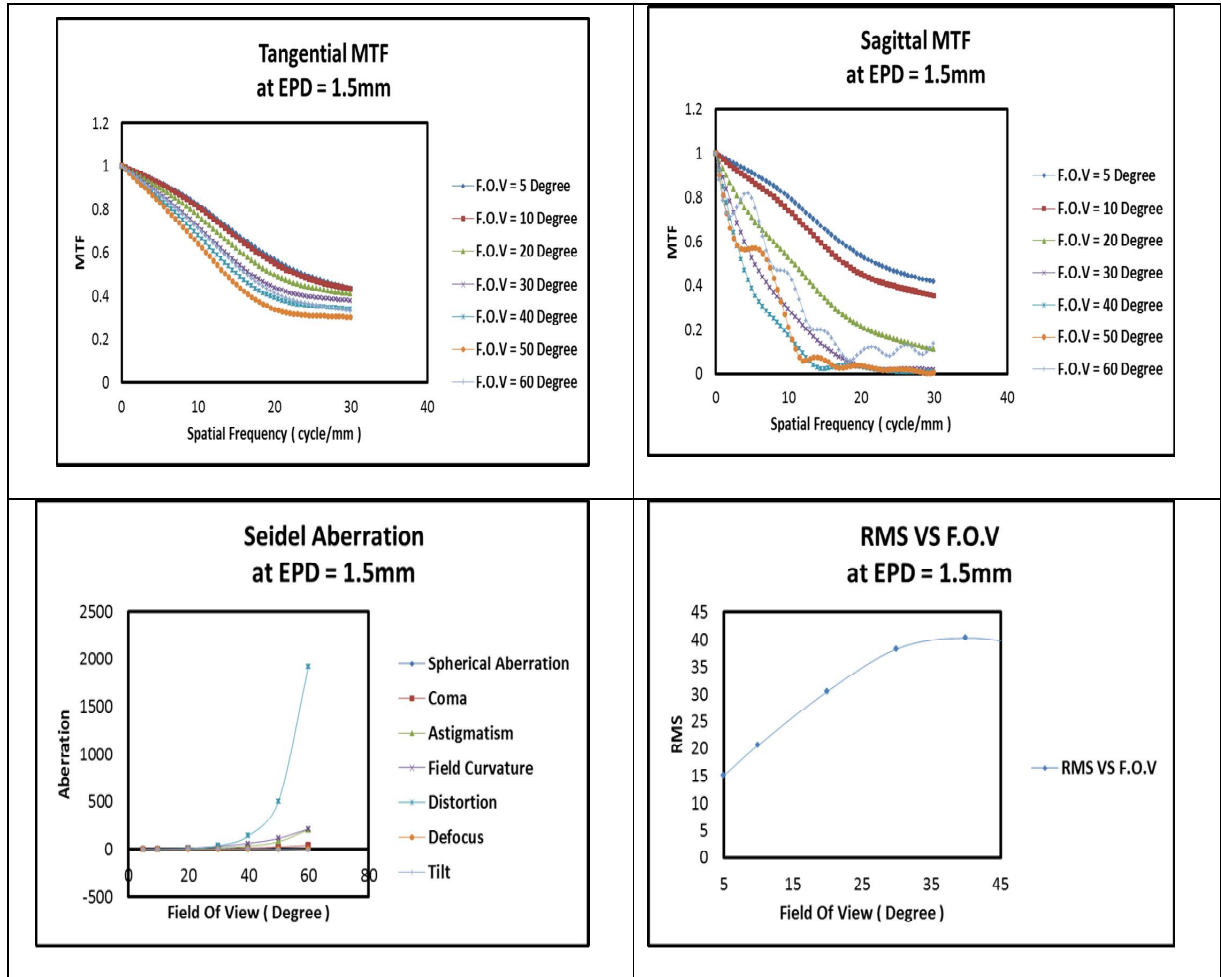
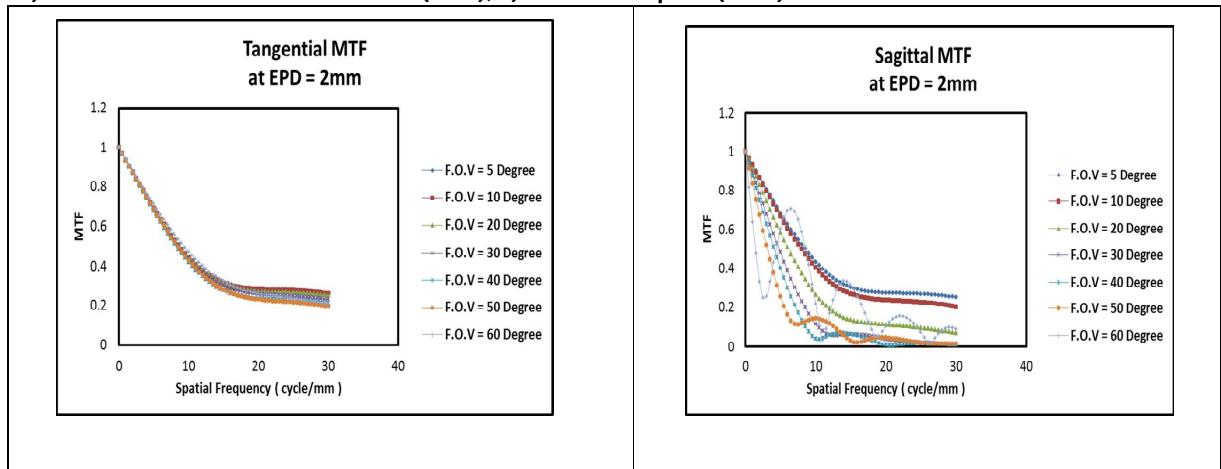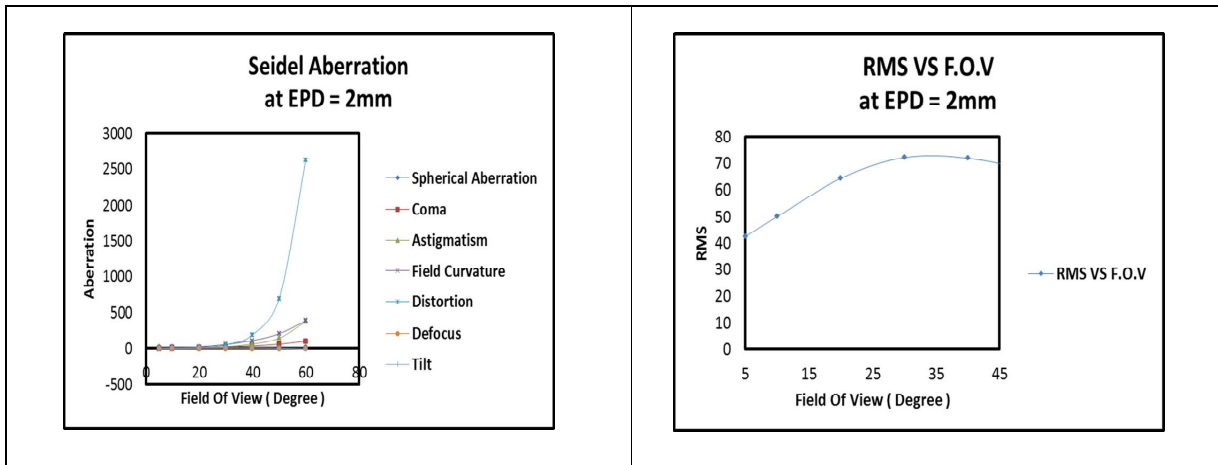**Ali H. Al-Hamdani and Halah A.Hashim**



**Figure 4: a) Tangential modulation transfer function (MTFT), b) sagittal modulation transfer function (MTFS), c) wave aberration with field of view (FOV), d) root mean square (RMS).**
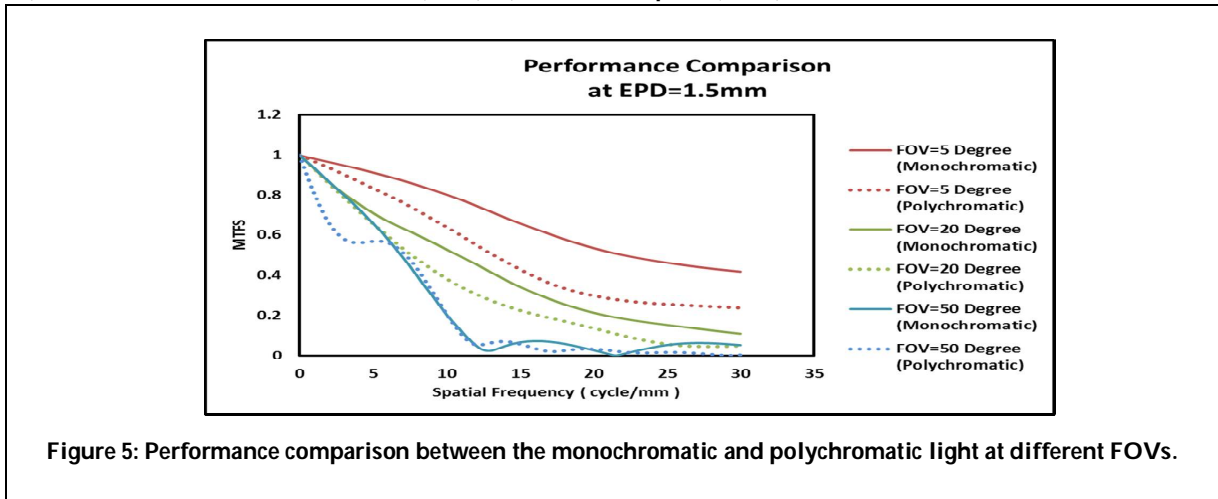


**Figure 5: Performance comparison between the monochromatic and polychromatic light at different FOVs.**

16507

**RESEARCH ARTICLE**

# Histopathological Study of Some Knee Tissues and Correlation between Serum and Synovial Fluid in Rheumatoid Arthritis of Iraqi Patients

Ola A. Jassim[1*], Sahar A. H. Al-Sharqi [2], Mahmood Shihab Wahab [3] and Sammir Rasmy Almousawi[4]

[1,2]Dept. of Biology, College of Science, Musatnsirihya University, Baghdad, Iraq.
[3]Nursing Home Hospital, Medical City Complex, Baghdad, Iraq.
[4]Ministry of Health, Baghdad, Iraq.

*Address for Correspondence
**Ola A. Jassim**
Dept. of Biology,
College of Science,
Musatnsirihya University,
Baghdad, Iraq.

**ABSTRACT**

Rheumatoid arthritis (RA) is one of chronic autoimmune disease leading to extensive changes of the joint resulting in cartilage damage and bone erosion. The present study focuses on some histopathological change in knee of the RA patients in hematological and biochemical testes of patients and control. The samples were taken (synovial membrane, anterior cruciate ligament, and meniscal cartilage) from 30 knees of rheumatoid arthritis patients (20 females and 10 male) during total knee replacement and kept in formalin (10%) for histological study. Blood sample were obtained from 30 RA patients and 20 controls. The tissue, blood samples were collected during period from October 2016 to June 2017.The histopathological study of knee tissue with RA (synovial membrane, anterior cruciate ligament, and meniscal) show many histopathological changes such as congestion blood vessels, fibrin deposition and infiltration of inflammatory cells. There was signification elevation (p< 0.05) in serum total protein, albumin and globulin in rheumatoid arthritis patients group compared to healthy controls groups. There was significate elevation (p< 0.05) of total protein, albumin and globulin in serum of rheumatoid arthritis patients when compared with synovial fluid of rheumatoid arthritis patients. The results of CRP, ASOT and RF were positive in 76.7% of rheumatoid arthritis patients, while, it was negative in 23.3% of patients with RA.

**Keywords:** Rheumatoid arthritis, synovial fluid, synovial membrane, knee joint.

# INTRODUCTION

Rheumatoid arthritis (RA) is a chronic autoimmune disease characterized by inflammation of the synovial, which outlines the inner cavity of synovial joints except for cartilage surfaces. It is a heterogeneous disease straddling several disease subsets with possible different pathogenic pathways (Van der Helm and Huizinga, 2008). Findings of population-based studies show that RA affects around 0.5–1.0% of adults in developed countries. (Symmons *et al.*, 2002). RA manifests in a polyarthritis, predominantly affecting the small joints of the hands and feet (Cojocaru *et al*., 2010).Another very severe consequence of RA can be additional organ manifestation, like skin, eyes, lungs, heart and even accelerated atherosclerosis (Gabriel and Michaud, 2009). The knee consists of combination of bones, articular cartilage, menisci, ligaments, and tendons are the essential internal parts of the knee which help in distributing the load and in providing stability to the knee (Sheng, 2008), and synovial membrane which is the delicate, vascularized tissue that covers the non-articular surfaces of the synovial joint cavity and the intra-capsular bone surfaces it is composed of an epithelial-like cell lining facing the joint cavity, Synovial functions include innate immune surveillance, lubrication, and intra articular joint tissue nutrition, representing a metabolic protection of joint function (Berumen *et al.*, 2002).

Knee has four primary ligaments, anterior cruciate ligaments ACL, posterior cruciate ligaments PCL, lateral collateral ligament LCL and medial collateral ligament MCL and one secondary ligament, the anterolateral ligament ALL. The function of ligaments is to stabilize the knee by resisting forces and moments (Claes *et al.*, 2013). There are two types of cartilage in the knee, the hyaline and the fibrous cartilage called the menisci for protect knee (Werner, 2004).

# MATERIALS AND METHODS

The study included 30 patients with RA and range in age 40-80 year were obtained from Nursing home hospital, Ghazy Al-hariri hospital for surgical specialties / Medical city and AI- Tage hospital, in addition 20 sample as control. The histopathological and biochemical study were conducted at Mustansiriyah University in the laboratories of Biology department during the period from October 2016 to June 2017.

### Tissue collection

The tissue specimens and synovial fluid were obtained during operations involving total knee replacement, from 30 patients with RA, which is diagnosed by specializes doctor. The tissue specimens were kept in the fixative solution (formalin10%) for histopathological study. After the fixation, sections are processed, embedded in paraffin and 5μm thick glass mounted sections are prepared, which are routinely stained with Hematoxylin and Eosin according to (Suvaran *et al.,* 2013).

### Serum and synovial fluid collection

From each 30 patients and 20 control, 5 ml of venous blood was collected from a suitable vein was used to obtain serum which separated by centrifugation 3000 r.p.m
for 5 min, then they were kept in -20ºC until the time for using. Synovial fluid was kept in plane tube then stored at -20ºC until assayed.

**Biochemical test**

**A- Detection of C reactive protein (CRP), Rheumatoid factor (RF) and Anti streptolysin O Titer (ASOT)**

These assay were done by using a rapid latex slide test for the detection of CRP, RF and ASOT in serum, according to SPECTRUM Company kit.

**B- Determination of total protein, albumin and globulin in serum and synovial fluid**

This assay was done by using Spectrophotometer test for determination of total protein, albumin and globulin in serum and synovial fluid according to AGAPPE company kit.

**Calculation of the results**

- Total protein conc. (mg / dl) = $\dfrac{\text{Absorbance of sample}}{\text{Absorbance of standard}} \times 6$
- Albumin conc. (mg / dl) = $\dfrac{\text{Absorbance of sample}}{\text{Absorbance of standard}} \times 3$
- Globulin conc. (mg / dl) = Total protein – Albumin

**Statistical Analysis**

Differences between groups were calculated by T-test where appropriate using (Minitab Version 11) values were expressed as mean ± standard deviation. A p-value of less than 0.05 was considered statistically significant.

# RESULTS AND DISCUSSION

**A-Synovial membrane**

Histologic studies showed different proportions and changes that:

- The synovial lining cells and villous more hyperplasia in knee specimens of RA patients (Figure 1).
- The inflammatory cell infiltrate showed a significantly higher in knee tissues of RA patients, these histologic changes are illustrated in (Figure 2).

In addition, many subepithelial area replaced by mature adipocytes (Figure 3).

- Also different degrees of fibrosis, increase of neo-formation vessels and mononuclear infiltration were present in the synovial tissue (Figure 4).
- Light microscope showed hydropic changes in large area of synovial membrane (Figure 5)

Synovial tissue sampling can be performed safely in both large joints (knee, ankle) and small joints like wrist. It has been shown that inflammation in one joint is similar to inflammation in other joints (Kraan *et al.*, 2002). The synovial membrane is made up of a cellular inner layer, the synovial lining (synovium), mainly composed of macrophage and fibroblast-like synoviocytes (Iwanaga *et al.*, 2000). Expansion of the synoviocytes leads to thickening of the joint lining and formation of the pannus tissue, which invades and destroys local articular structures and bone (See and Janet, 2004). Inflamed synovial membrane displays three major histological alterations: hyperplasia of the intimal lining

16510

layer due to accumulation of macrophages and proliferation of fibroblast-like synoviocytes that are in an altered activation state; neoangiogenesis with endothelial activation in the synovial sublining; and a vast influx of inflammatory cells such as macrophages, dendritic cells, lymphocytes and mast cells in the synovial sublining (Marleen and Dominique, 2015). These infiltrating leucocytes are activated and produce a vast amount of pro-inflammatory and destructive mediators that contribute to synovitis as well as to cartilage and bone destruction (Gerlag and Tak, 2009). Inflammation of the synovium has been seen primarily as a lymphocytic phenomenon, and the accumulation of lymphocyte aggregates in the synovium is considered to be the hallmark of RA (John, 2004).

Study of Manzo and Pitzalis, (2007) show that three types of lymphocyte infiltration patterns are observed in synovitis: diffuse infiltration of lymphocytes, aggregates of B cells and T cells, and ectopic lymphoid neogenesis such as the presence of follicular dendritic cells and high endothelial venules. Synovial ectopic lymphoid neogenesis may play a role in mounting immune responses, and in particular the autoimmune responses observed in RA (Humby *et al.*, 2009). Hyperplasia of synovial membrane leads to increase of accumulation of macrophages and this lead to increase of joint destruction in patients of RA (Haringman *et al.*, 2005). Kinne *et al.*, (2000) reported that various pathogenetic mechanisms might lead to a final common pathway resulting in synovial macrophage activation. This may cause increased production of a variety of proinflammatory cytokines and chemokines, which play a part in the development of symptoms like pain and swelling (Vervoordeldonk and Tak, 2002).Most of the macrophages in actively inflamed joints are localised by far in the synovial sublining rather than in the intimal lining layer (Smeets *et al.*, 2003). The current result was in agreement with David and Michael (2001) who observed Synovial-vessel endothelial cells transform into high endothelial venules and more blood vessels proliferation in the early course of the disease high endothelial venules facilitate the transit of leucocytes from the bloodstream into tissues

## B-Anterior cruciate ligament (ACL)

Histological examination for ACL biopsy of knee RA patient is degeneration changes with proliferation of fibrocystic (Figure 6). On the other hand, all sections illustrate large areas of fibrosis and numerous new formations of blood vessels (Figure 7). In addition, disorder in formation of collagen fibers and deposition of fibrin around blood vessels is revealed (Figure 8). The ACL disruption is one of the most common and destruction of knee. It is mainly sustained as a result of sports participation. These injuries often result in joint effusion, altered movement, muscle weakness, reduced functional performance ACL injuries are also associated with long-term clinical sequelae that include meniscal tears, and also associated with RA and other diseases (Levine *et al.*, 2013). ACL injuries affect the surrounding structures of the knee and are associated with a decrease in the patients' life quality. It has been demonstrated that ACL traumas affect the meniscus, induce cartilage damage (Arner *et al.*, 2016). It is well known that ligaments are active structures that possess the ability to undergo modifications in different pathologic conditions. Tissue destruction may be positively correlated with the remodeling response after injury matrix metalloproteinases appear to stimulate angiogenesis (increase in blood vessels) and inflammatory reactions in the synovium of patients with RA. These metalloproteinases are not expressed in the synovial tissue in normal conditions (Jitariu *et al.*, 2017). Also various metalloproteinases play a critical role in the process of ligamentization. In case of ligament reconstruction, they seem to facilitate cell migration, proliferation and angiogenesis in the synovium (Raif, 2008).

The RA ligaments showed a thickened hyperplastic synovial cell layer, vascular proliferation, hemosiderin deposition, lymphoid aggregates, and histiocytes dispersed between the collagen fibers (Nelissen and Hogendoorn, 2001). These rustles might be related to current results that report histopathological changes in ALC tissues. Study of Mattiello *et al.* (2008) reported that the acute phase of ACL tissue injury the concentration of the synovial fluid increases due to the presence of ma-cromolecules and fragments of macromolecules such as cartilage oligomeric matrix protein (COMP), stromelysin, proteins and proteoglycan (PG) fragments such as sulfated glycosaminoglycans (GAGs), as well as inflammatory cells, synoviocytes

and free chondrocytes derived from destructive processes in the cartilage. Macromolecular changes in SF content can be observed, since under normal conditions they are absent.Experimental models have shown that ACL rupture leads to an increase in the joint destruction along with motion reduction too. It appears that a greater anterior knee laxity may represent a risk factor for ACL traumas depending on different particularities of ACL and bone geometry (Wang *et al.*, 2016).

## C- Knee menisci

All fields of the knee menisci sections of RA patients were examined using Hematoxylin and Eosin stain. Extensive chondrocytes death in many area was noticed, also abnormal controlling and proliferation of chondrocyte in patients who underwent total knee replacement with RA (Figure 9). In addition, large areas of fibrosis illustrates with proliferation and disorientation of chondrocytes (Figure 10). On the other hand, all sections demonstrated abnormal proliferation of chondrocytes and inflammatory cells infiltration in different areas of menisci tissues (Figure 11). The knee joint meniscus is fibrocartilage in nature and is designed to provide stability of the knee, load distribution, shock absorption. The functions of the menisci are facilitated by proteoglycans and collagen type I and type II, proteoglycans enable the matrix to absorb shock, whereas collagens provide the rigidity (Englund *et al.*, 2003). Meniscal Cartilage is the important part of synovial joints. It consists of chondrocytes that are embedded in a dense and highly organized extracellular matrix (ECM) (Pap *et al.*, 2013). Any damage to cartilage integrity not only affects its function and the ability to move a damaged joint, but can also result in profound effects on the state and metabolic activities of the chondrocytes themselves, as well as on neighbouring cells and tissues, such as the synovium. In turn, any changes to chondrocyte phenotype and metabolism will change the composition of the sur-rounding ECM (O'Conor *et al.*, 2014). Joints suffering of RA increase meniscal matrix degradation (Mario *et al.*, 2005). Evidences suggest that RA is initiated by a sustained antigenic stimulus that induces perpetual activation of inflammatory and resident cells of the joint and results in the production of proinflammatory mediators that initiates progressive erosion of cartilage (Vervoordeldonk and Tak, 2002).

## Biochemical test

## 1- Protein analysis in serum and synovial fluid

The data that present in table (1) and figure (12) show that mean ± SD of serum total protein in control were (7.5 ±0.59 mg /dl) while the mean ±SD level of patient RA were (7.6±0.6 mg /dl). The result showed increase significant difference ($p < 0.05$) of serum total protein in RA patient compared with control. This result agrees with Cylwik *et al.*, (2010) which reported signification difference in level of total protein in RA patients. Study of Rall and Roubenoff, (2004) shows that in RA increase of proteins breakdown compared with healthy persons, the proteins breakdown rates are directly associated with TNF-$\alpha$ productions by peripheral blood monocular cell. While the level of total albumin that is present in table (1) and figure (12).

The rustle showed signification difference ($p < 0.05$) in total albumin level of RA patients were (3.07±0.3 mg /dl) compared with controls were (4.27±0.2 mg /dl). The study of Sezgin *et al.*, (2005) is agreement with this result which found signification difference in albumin with RA patients. Inflammatory illnesses (acute and chronic) are the major causes of albumin concentration decline in RA serum albumin levels were lower because higher TNF-$\alpha$ levels, lead to hypoalbuminemia, which is a consequence of inflammation due to suppression of albumin synthesis and transfer of albumin from the vascular to the extravascular space (Bożena and Majdan, 2011).The level of total globulin that present in table (1) and figure (12) the rustle showed signification difference ($p < 0.05$) in total globulin level of RA patients (3.8±0.7 mg /dl) were compared with control were (3.2±0.7 mg /dl). The present study was in agreement with the study of Ahmet *et al.*, (2007) which reported signification difference in total globulin level of RA patients.

Globulin as another major protein also plays a part in chronic inflammation. Some components of globulin would increase under the condition of inflammation. The high level of globulin is considered to be a marker of activation of inflammation Adly *et al*, (2006) Increased globulin level have been reported to reflect chronic inflammation Because systemic inflammation has been shown to cause an increase in the levels of various proinflammatory cytokines (Azab *et al.*, 2013). The data that present in table (2) and figure (13) show mean ± SD of serum total protein level in RA patients were (17.6±0.6 mg/dl) while the mean± SD level of synovial fluid total protein in RA patients were (4.02±0.8 mg/dl).The result showed signification difference (p<0.05) between serum total protein level and synovial total protein.

While the level of serum total albumin (3.07±0.3 mg/dl) and synovial total albumin (2.14±0.7mg/dl) that present in table (2) and figure (13). The rustle showed difference (p<0.05) between serum total albumin level and synovial total albumin.Also the level of serum total globulin (3.8±0.7mg/dl) and synovial total globulin (2.11±0.8 mg/dl) that present in table (2) and figure (13) The rustle showed difference (p<0.05) in serum total globulin level and synovial globulin. Synovial fluid is containing many of potential biomarkers because the synovial fluid is in direct contact with articular cartilage, synovium, ligament, meniscus and joint capsule. Alterations in metabolism of any of these tissues during disease progression are reflected as alterations in the profile of synovial fluid (Duan, *et al.,* 2012). The higher levels of proteins in synovial fluids of RA patients have been observed to induce the expression of cytokines in mononuclear cells, and it is involved in regulating bone formation and promotes angiogenesis (Mitali, *et al.,* 2016). There are so many proteins in synovial fluid particular attention is given to albumin and globulin, which are the main proteins in the synovial fluid. Albumin and globulin typically account for 60-75 % the synovial fluid proteins (Maria, 2014).

### 2- C - reactive protein, Anti-Streptolysin-O and Rheumatoid Factor level in serum

The study in table (3) shows that CRP was positive in 76.7% of RA patients, where it was negative in 23.3%

The CRP an acute phase protein is synthesized by hepatocytes in response to pro-inflammatory cytokines in particular IL-6. It has been shown to be of great value as an inflammatory marker in RA and has been suggested to mediate part of the complement activation in RA (Molenaar *et al.*, 2001). On the other hand, it also has anti-inflammatory properties, such as reducing neutrophil adhesion to endothelium (Christopher and Paul, 2005). The result showed agreement with the study of Surekha *et al*, (2006) which is found elevatione in CRP levels. This study explains that ASOT in this test is positive in 76.7% of RA patients, where it was negative in 23.3%.of RA patients shows in table (3). The study showed that ASO test was positive in RA patients, are in conflicting with (Tikly and Makda, 2009), and it may have been associated with past or present Streptoccoi infection (Ferri, 2009), that's in turn assumed that those patients may be infected with rheumatic fever instead of RA Gerber, (2007).

Table (3) shows that RF was positive in 76.7% of RA patients, where it was negative in 23.3% of RA patients. It has long been recognized that RFs play a pivotal role in the differential diagnosis of polyarthritis because they make it possible to identify RA patients (Miller *et al.*, 2013) It has also been shown that RFs are useful in predicting the development of RA, as the detection of IgM, IgA, and IgG RFs may predate its onset by years (Nielsen *et al.*, 2012), and it has been reported that their appearance in serum is sequential before diagnosis: first IgM RF, then IgA RF, and finally IgG RF (Deane *et al.*, 2010). It has also been suggested that RFs potentiate the presentation of antigens to T cells by means of the dendritic cell uptake of immune complexes with exogenous antigens and by means of RF B cells, which seems to be more efficient APCs than other B cells (Stewart *et al.*, 1997). This result agree with the previous studies (Francesca *et al.*, 2013) and (De Rycke *et al.,* 2004) who have also found elevation in RF in patients of RA. Study of Wilusz *et al.* (2008) shows that Inflammatory cytokines that produced by synovial macrophage appear to have a positive effect on meniscal degradative which active the pro-inflammatory pathways in the meniscus and joint tissues consequently. The meniscal matrix begins to degrade and progressively loose its crucial role in load distribution and joint lubrication. Cartilage is largely considered a target tissue in RA, which becomes damaged as a

**Ola A. Jassim *et al.***

result of the inflamed and hyperplastic synovial membrane, which is itself caused by the manifestation of systemic autoimmunity in the articular joints (Rommel *et al.*, 2007). And it has been well known that in the course of the disease cells of the inflamed synovium, particularly activated fibroblast-like synoviocytes (FLS), attack the cartilage and lead to its progressive destruction (Bottini and Firestein, 2013).

## REFERENCES

1. Adly, L., Hill, D., Sherman, M. E., Sturgeon, S. R., Fears, T., Mies, C., and Schairer, C. (2006). Serum concentrations of estrogens, sex hormone-binding globulin, and androgens and risk of breast cancer in postmenopausal women. International journal of cancer, 119(10): 2402-2407.
2. Ahmet, I., Suleyman, S. K., Abdullah, O., and Osman, M. (2007). Anxiety and depression in patients with rheumatoid arthritis. Clinical Rheumatology, 26:872–878.
3. Arner, J.W., Irvine, J.N., Zheng, L., Gale, T., Thorhauer, E., Hankins, M., Abebe, E., Teshman, S., Zhang, X., and Harner C.D. (2016). The Effects of Anterior Cruciate Ligament Deficiency on the Meniscus and Articular Cartilage: A Novel Dynamic in Vitro Pilot Study. Orthopaedic journal of sports medicine, 4(4): 2325967116639895.
4. Azab, B. N., Bhatt, V. R., Vonfrolio, S., Bachir, R., Rubinshteyn, V., Alkaied, H., and Bloom, S. W. (2013). Value of the pretreatment albumin to globulin ratio in predicting long-term mortality in breast cancer patients. The American Journal of Surgery, 206(5): 764-770.
5. Berumen-Nafarrate, E., Leal-Berumen, I., Luevano, E., Solis, F. J., and Munoz-Esteves, E. (2002). Synovial tissue and synovial fluid. The journal of knee surgery, 15(1): 46-48.
6. Bottini, N. and Firestein, G. S. (2013). Duality of fibroblast-like synoviocytes in RA: passive responders and imprinted aggressors. Nature Reviews Rheumatology, 9(1): 24-330.
7. Bottini, N. and Firestein, G. S. (2013). Duality of fibroblast-like synoviocytes in RA: passive responders and imprinted aggressors. Nature Reviews Rheumatology, 9(1): 24-330.
8. Bozena T, S. and Maria, M. (2011). Associations between parameters Cardiovascular events in early RA are a result of inflammatory burden and traditional risk factors: a five year prospective study. Arthritis research and therapy, 13(4), 131.
9. Christopher, L.C. and Paul, G. S. (2005). Laboratory Testing in the Rheumatic Diseases: A Practical Review. Southern Medical Journal, 98:185-191.
10. Claes, S., Vereecke, E., Maes, M., Victor, J., Verdonk, P., and Bellemans, J.(2013). Anatomy of the anterolateral ligament of the knee. Journal of anatomy, 223: 321–328.
11. Cojocaru, M., Cojocaru, I. M., Silosi, I., Vrabie, C. D., & Tanasescu, R. (2010). Extra-articular manifestations in rheumatoid arthritis. Maedica, 5(4): 286.
12. Cylwik, B., Chrostek, L., Gindzienska-Sieskiewicz, E., Sierakowski, S., and Szmitkowski, M. (2010). Relationship between serum acute-phase proteins and high disease activity in patients with rheumatoid arthritis. Advances in medical sciences, 55(1): 80-85.
13. David M Lee, Michael E Weinblatt .(2001). Rheumatoid arthritis. 358 (9285) :903– 911.
14. De Rycke, L., Peene, I. S. A. B. E. L. L. E., Hoffman, I. E. A., Kruithof, E., Union, A., Meheus, L., and Boullart, L. (2004). Rheumatoid factor and anticitrullinated protein antibodies in rheumatoid arthritis: diagnostic value, associations with radiological progression rate, and extra-articular manifestations. Annals of the rheumatic diseases, 63(12): 1587-1593.
15. Deane, K. D., Norris, J. M., and Holers, V. M. (2010). Preclinical rheumatoid arthritis: identification, evaluation, and future directions for investigation. Rheumatic Disease Clinics, 36(2): 213-241.
16. Duan, Y., Hao, D., Li, M., Wu, Z., Li, D., Yang, X., and Qiu, G. (2012). Increased synovial fluid visfatin is positively linked to cartilage degradation biomarkers in arthritis. Rheumatology international, 32(4): 985-990.

17. Englund, M., Roemer, F. W., Hayashi, D., Crema, M. D., and Guermazi, A. (2012). Meniscus pathology, osteoarthritis and the treatment controversy. Nature Reviews Rheumatology, 8(7): 412.

18. Ferri, F. F. (2009). Ferri's Clinical Advisor 2010 E-Book: 5 Books in 1 Elsevier Health Sciences.

19. Francesca, I., Roberto, C., and Roberta, G., (2013). Rheumatoid Factors: Clinical Applications, 35(6): 727-734.

20. Gabriel, S. E., and Michaud, K. (2009). Epidemiological studies in incidence, prevalence, mortality, and comorbidity of the rheumatic diseases. Arthritis research and therapy, 11(3): 229.

21. Gerber, M.A. Kliegman, R.M.; Behrman, R.E.; Jenson, H.B.; Stanton, B.F. (2007). Nelson Textbook of Pediatrics Group. 18th edition Philadelphia Saunders.

22. Gerlag, D. M., and Tak, P. P. (2009). How to perform and analyse synovial biopsies. Best Practice & Research Clinical Rheumatology, 23(2): 221-232.

23. Haringman, J. J., Gerlag, D. M., Zwinderman, A. H., Smeets, T. J., Kraan, M. C., Baeten, D., McInnes, I.B., Bresnihan, B., and Tak, P. P. (2005). Synovial tissue macrophages: a sensitive biomarker for response to treatment in patients with rheumatoid arthritis.Annals of the rheumatic diseases, 64(6): 834-838.

24. Humby, F., Bombardieri, M., Manzo, A., Kelly, S., Blades, M. C., Kirkham, B., and Pitzalis, C. (2009). Ectopic lymphoid structures support ongoing production of class-switched autoantibodies in rheumatoid synovium. PLoS medicine, 6(1): e1.

25. Iwanaga, T., Shikichi, M., Kitamura, H., Yanase, H., and Nozawa-Inoue, K. (2000). Morphology and functional roles of synoviocytes in the joint. Archives of histology and cytology, 63(1): 17-31.

26. Jitariu, A. A., Trocan, I., Ceaușu, A. R., Hărăguș, H., Damian, G., and Raica, M.( 2017). Morphologic changes in the injured anterior cruciate ligament (ACL) correlated with the expression of protein s100 and NFAP major therapeutic implications or a wrong getaway towards improving ACL reconstruction. Research and Clinical Medicine, 1:2.

27. John, R. K. (2004). The synovium in rheumatoid arthritis: evidence for (at least) two pathologies. Arthritis & Rheumatology, 50(1): 1-4.

28. Kinne, R. W., Bräuer, R., Stuhlmüller, B., Palombo-Kinne, E., and Burmester, G. R. (2000). Macrophages in rheumatoid arthritis. Arthritis Research & Therapy, 2(3): 189-202.

29. Kraan, M. C., Reece, R. J., Smeets, T. J., Veale, D. J., Emery, P.,and Tak, P. P. (2002). Comparison of synovial tissues from the knee joints and the small joints of rheumatoid arthritis patients: Implications for pathogenesis and evaluation of treatment. Arthritis & Rheumatology, 46(8): 2034-2038.

30. Levine, J. W., Kiapour, A. M., Quatman, C. E., Wordeman, S. C., Goel, V. K., Hewett, T. E., and Demetropoulos, C. K. (2013). Clinically relevant injury patterns after an anterior cruciate ligament injury provide insight into injury mechanisms. The American journal of sports medicine, 41(2): 385-395.

31. Manzo, A. and Pitzalis, C. (2007). Lymphoid tissue reactions in rheumatoid arthritis . Autoimmunity reviews, 7(1), 30-34.

32. Maria, P. (2014).A Study of lubrication Mechanisms of Lipids and Proteins in Model Synovial Fluids. College of London. Thesis.

33. Mario, F., Abiraman, S., James, D., Robert, G., Frank, B., Nicholas, P., and Robert. S.(2005).Anti-inflammatory effects of continuous passive motion on meniscal fibrocartilage. Journal of Orthopaedic Research, 23(5): 1165-1 171.

34. Marleen, G. S., and Dominique L. B. (2015). Immunopathology of synovitis: from histology to molecular pathways. Rheumatology, 55(4): 599-606.

35. Mattiello-Rosa, S. M. G., Cintra Neto, P. F. A., Lima, G. E. G., Pinto, K. N. Z., Cohen, M., and Pimentel, E. R. (2008). Glycosaminoglycan loss from cartilage after anterior cruciate ligament rupture: influence of time since rupture and chondral injury. Brazilian Journal of Physical Therapy, 12(1): 64-69.

36. Miller, A., Mahtani, K. R., Waterfield, M. A., Timms, A., Misbah, S. A., and Luqmani, R. A. (2013). Is rheumatoid factor useful in primary care? A retrospective cross-sectional study. Clinical rheumatology, 32(7): 1089-1093.

37. Mitali, B., Lavanya, B., Santosh, R., Jayshree, A., Renu, G., Gajanan, S., Bipin, N., Ramesh, J., Subramanian, S., and Pandey, A. (2016). Synovial fluid proteome in rheumatoid arthritis. Clinical proteomics, 13(1): 12.

**Ola A. Jassim *et al.***

38. Molenaar, E. T., Voskuyl, A. E., Familian, A., van Mierlo, G. J., Dijkmans, B. A., and Hack, C. E. (2001). Complement activation in patients with rheumatoid arthritis mediated in part by C-reactive protein. Arthritis & Rheumatology, 44(5): 997-1002.

39. Nelissen, R. G. H. H., and Hogendoorn, P. C. W.(2001). Retain or sacrifice the posterior cruciate ligament in total knee arthroplasty? A histopathological study of the cruciate ligament in osteoarthritic and rheumatoid disease. Journal of clinical pathology, 54(5): 381-384.

40. Nielsen, S. F., Bojesen, S. E., Schnohr, P., and Nordestgaard, B. G. (2012). Elevated rheumatoid factor and long term risk of rheumatoid arthritis: a prospective cohort study. Bmj, 345:5244.

41. O'Conor, C. J., Leddy, H. A., Benefield, H. C., Liedtke, W. B., and Guilak, F. (2014). TRPV4-mediated mechanotransduction regulates the metabolic response of chondrocytes to dynamic loading. Proceedings of the National Academy of Sciences, 111(4): 1316-1321.

42. Pap, T., Korb-Pap, A., Heitzmann, M. and Bertrand, J.(2013). in Oxford Textbook of Rheumatology 4th edition : 409–414.

43. Raif, E. M. (2008). Effect of cyclic tensile load on the regulation of the expression of matrix metalloproteases (MMPs-1,-3) and structural components in synovial cells. Journal of cellular and molecular medicine, 12(6): 2439-2448.

44. Rall ,L. C., Roubenoff. R. (2004). Rheumatoid cachexia: metabolic abnormatilitis, mechanisms and intervention .Marshfield Clinic Research Foundation, 43:1219-1223.

45. Rommel, C., Camps, M., and Ji, H. (2007). PI3Kδ and PI3Kγ: partners in crime in inflammation in rheumatoid arthritis and beyond?. Nature Reviews Immunology, 7(3): 191-201.

46. Rommel, C., Camps, M., and Ji, H. (2007). PI3Kδ and PI3Kγ: partners in crime in inflammation in rheumatoid arthritis and beyond?. Nature Reviews Immunology, 7(3): 191-201.

47. See, H. W., and Janet M. L. (2004). Factors underlying chronic inflammation in rheumatoid arthritis. Archivum Immunologiae Therapiae Experimentalis, 52(6): 379-388.

48. Sezgin ,S., Abdurrahim, K., Mithat, Y., and Ugur, E. I. (2005) . Plasma total and erythrocyte antioxidant enzyme arthritis and osteoarthritis .Clinical antioxidant capacity, lipid peroxidation, activities in patients with rheumatoid Biochemistry, 38(11): 981 – 986

49. Sheng , P. (2008). Study on Revision Total Knee Arthroplasty. Clinical, Radiological and Survival Patterns PhD Thesis Finland: University of Tampere.

50. Smeets, T. J. M., Barg, E. C., Kraan, M. C., Smith, M. D., Breedveld, F. C., and Tak, P. P. (2003). Analysis of the cell infiltrate and expression of proinflammatory cytokines and matrix metalloproteinases in arthroscopic synovial biopsies: comparison with synovial samples from patients with end stage, destructive rheumatoid arthritis. Annals of the rheumatic diseases, 62(7): 635-638.

51. Stewart, J. J., Agosto, H., Litwin, S., Welsh, J. D., Shlomchik, M., Weigert, M., and Seiden, P. E. (1997). A solution to the rheumatoid factor paradox: pathologic rheumatoid factors can be tolerized by competition with natural rheumatoid factors. The Journal of Immunology, 159(4): 1728-1738.

52. Surekha, R. H. Madhavi, G., Srikanth, B.M.V., Jharna, P., Rao U.R.K., and Jyothy A. (2006). Serum ADA and C-reactive protein in rheumatoid arthritis. International Journal of Human Genetics, 6(3), 195-198.

53. Symmons, D., Turner, G., Webb, R., Asten, P., Barrett, E., Lunt, M., Scott, D., and Silman, A. (2002). The prevalence of rheumatoid arthritis in the United Kingdom: new estimates for a new century. Rheumatology, 41(7): 793-800.

54. Tikly, M., and Makda, M. A. (2009). A diagnostic approach to the common arthritic conditions. South African Family Practice, 51(3):188-193.

55. Van der Helm-van, A. H., and Huizinga, T. W. (2008). Advances in the genetics of rheumatoid arthritis point to subclassification into distinct disease subsets. Arthritis research & therapy, 10(2): 205

56. Vervoordeldonk, M.J., and Tak, P.P. (2002). Cytokines in rheumatoid arthritis. Current Rheumatology Reports ,4:208-17

57. Wang, H. M., Shultz, S. J., and Schmitz, R. J. (2016). Association of Anterior Cruciate Ligament Width with Anterior Knee Laxity. Journal of athletic training, 51(6): 460-465.
58. Werner, P. (2004) Color Atlas of Human Anatomy, volume 1: Locomotor System. 5th edition.
59. Wilusz, R. E., Weinberg, J. B., Guilak, F., and McNulty, A. L. (2008). Inhibition of integrative repair of the meniscus following acute exposure to interleukin-1 in vitro. Journal of Orthopaedic Research, 26(4): 504-512.
60. Wilusz, R. E., Weinberg, J. B., Guilak, F., and McNulty, A. L. (2008). Inhibition of integrative repair of the meniscus following acute exposure to interleukin-1 in vitro. Journal of Orthopaedic Research, 26(4): 504-512.

**Table 1. Protein analysis of serum of RA patients and control**

| Test type mg/dl | Control | (RA) patients | P- value |
|---|---|---|---|
| Total protein | 7.5±0.59 | 7.6±0.6 * | 0.02 |
| Total albumin | 4.27±0.2 | 3.07±0.3 * | 0.001 |
| Total globulin | 3.2±0.7 | 3.8±0.7 * | 0.007 |
| *Signification differences between patients and control (p< 0.05). Results are expressed as mean ±Standard deviation. RA: Rheumatoid arthritis | | | |

**Table 2. Effect of study Protein analysis in serum and synovial fluid of RA patients**

| Test type   mg/dl | Serum | Synovial fluid | P- value |
|---|---|---|---|
| Total  protein | 17.6±0.6* | 4.02±0.8 | 0.001 |
| Total  albumin | 3.07±0.3* | 2.14±0.7 | 0.01 |
| Total  globulin | 3.8±0.7 * | 2.11±0.8 | 0.01 |
| *Signification differences between groups (p< 0.05). Results are expressed as mean ±Standard deviation. | | | |

**Table 3. CRP, ASOT, RF analysis in serum of RA patients**

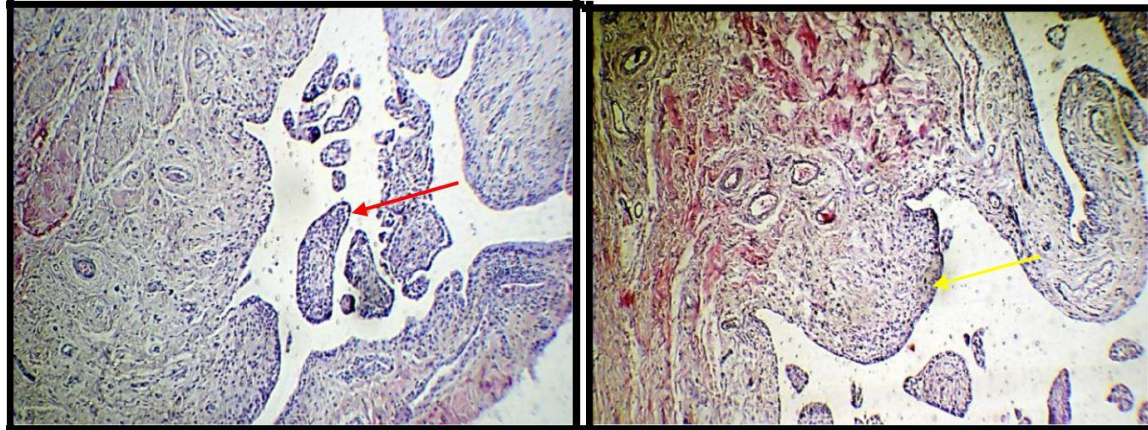| Test type | Negative Number (%) | Positive Number(%)titer | Total |
|---|---|---|---|
| CRP NV: | 7(23.3) | 15(50) =6 | 23(76.7) |
|  |  | 8(26.7)=12 |  |
| ASOT NV: | 7(23.3) | 15(50) =200 | 23(76.7) |
|  |  | 8(26.7)=400 |  |
| RF NV: | 7(23.3) | 15(50) =6 | 23(76.7) |
|  |  | 8(26.7)=12 |  |
| Results are expressed as percentage (%). CRP:C- Reactive Protein, ASOT: Anti-Streptolysin-O and RF:Rheumatoid factor | | | |
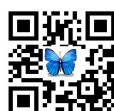
**Figure 1. Cross section in synovial membrane of knee RA patient show synovial lining hyperplasia (yellow arrow) and villous hyperplasia (red arrow) (Hematoxylin and Eosin staining, x10).**
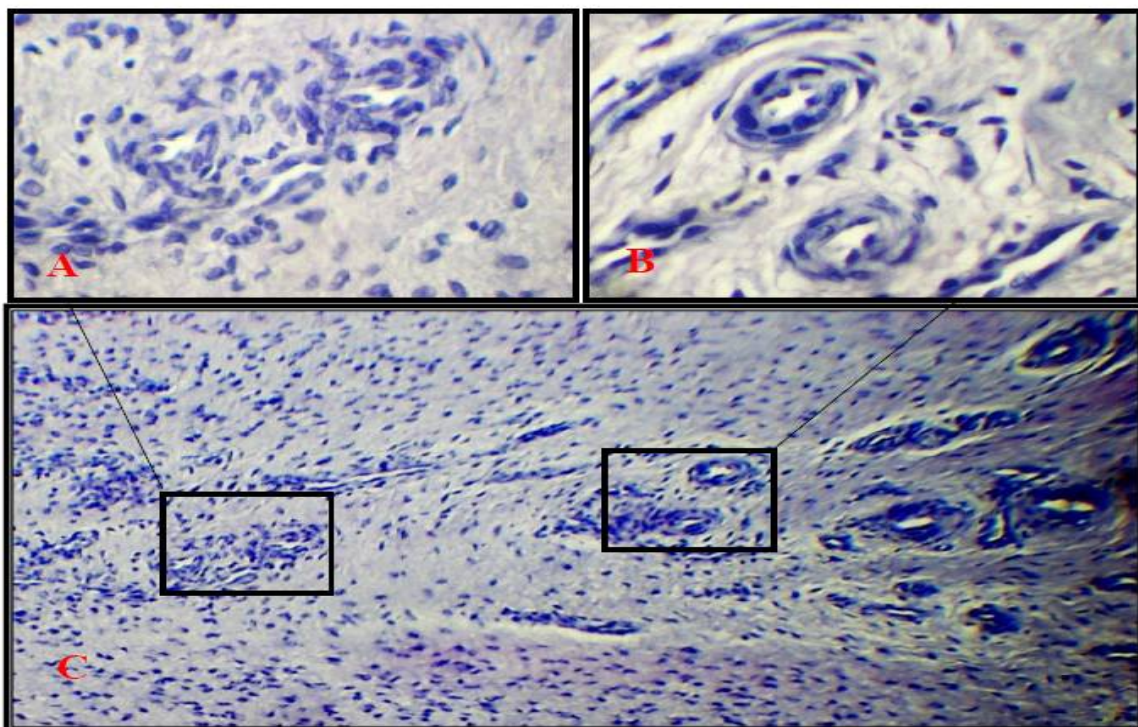


**Figure 2. Cross section in synovial membrane of knee RA patient show inflammatory cells infiltration in many area especially around blood vessels (Hematoxylin and Eosin staining, A and B x40, C x10)**
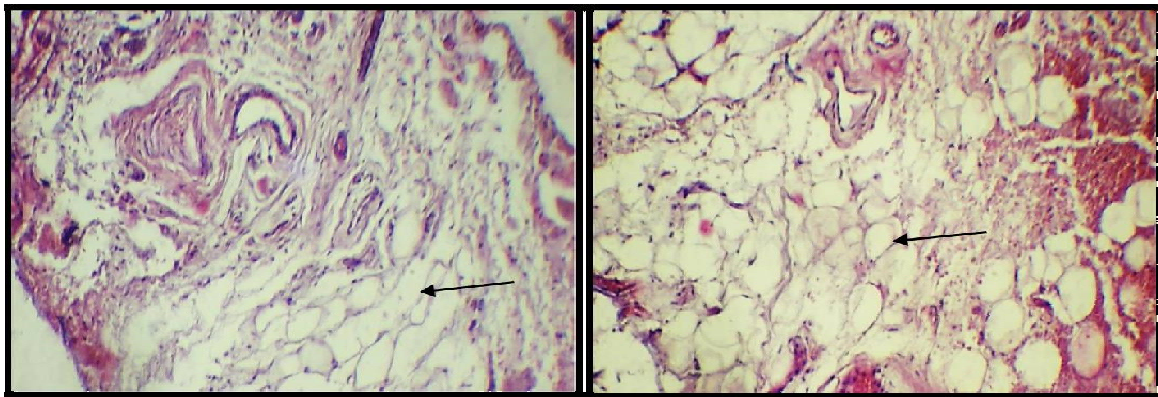
Ola A. Jassim *et al.*



**Figure 3. Cross section in synovial membrane of knee RA patient show subepithelial area replaced by mature adipocytes (arrow) (Hematoxylin and Eosin staining, x40).**
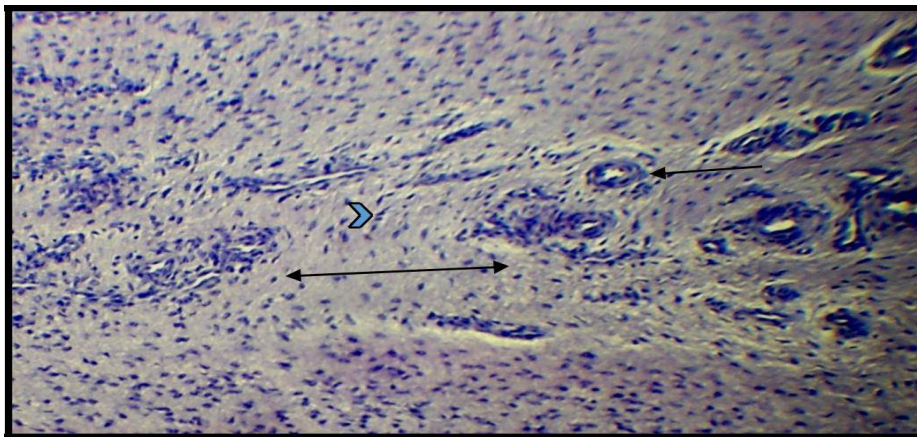


**Figure 4. Cross section in synovial membrane of knee RA patient reveal to fibrosis (↔), proliferation of fibroblasts (➘) and perivascular inflammatory cell infiltrates (˥) (Hematoxylin and Eosin staining, x10).**
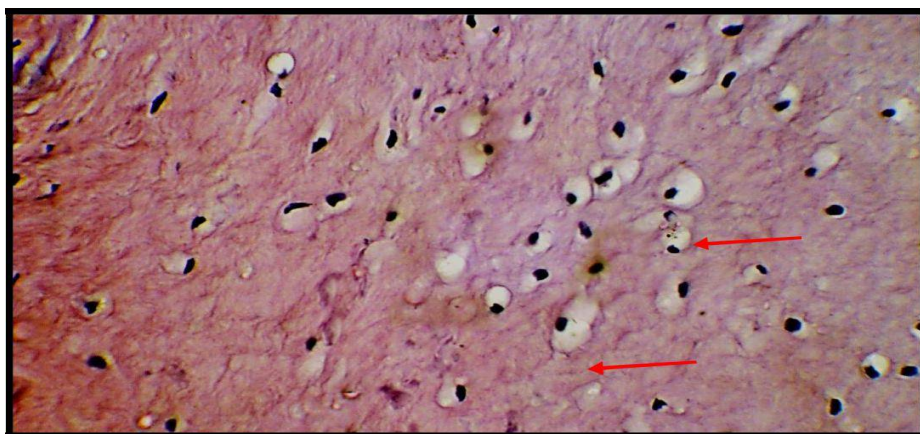


**Figure 5. Cross section in synovial membrane of knee RA patient reveal to hydropic changes in large area of tissue (Hematoxylin and Eosin staining, x40).**
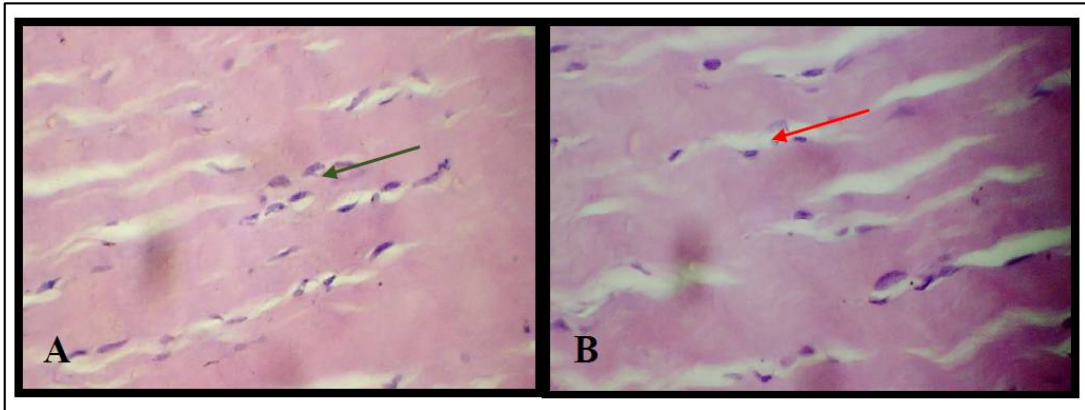
**Figure 6. Cross section in ACL of knee RA patient show degeneration (red arrow) and proliferation of fibrocystic (green arrow) (Hematoxylin and Eosin staining, x10).**
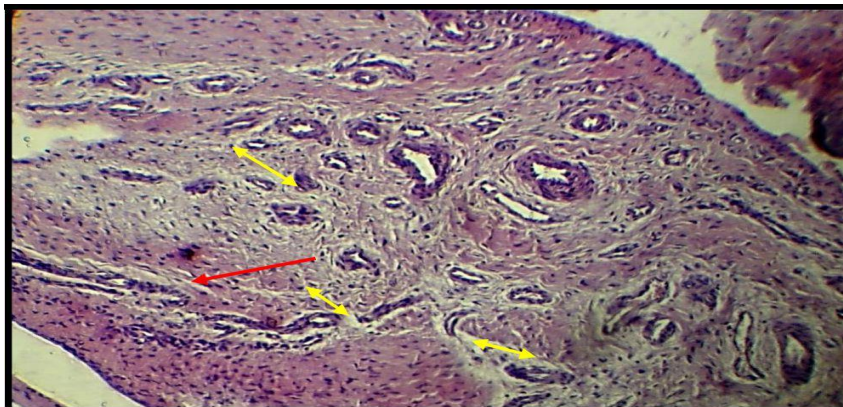


**Figure 7. Cross section in ACL of knee RA patient illustrate large areas of fibrosis (red arrow) and neo-formation of blood vessels (yellow arrow) (Hematoxylin and Eosin staining, x10).**
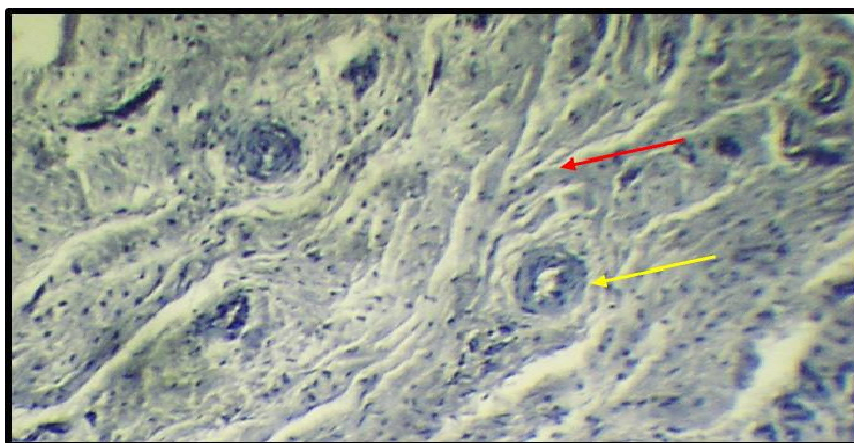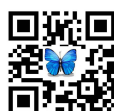


**Figure 8. Cross section in ACL of knee RA patient show disorder in formation of collagen fibers (red arrow) and deposition of fibrin around blood vessels (yellow arrow) (Hematoxylin and Eosin staining, ×40).**
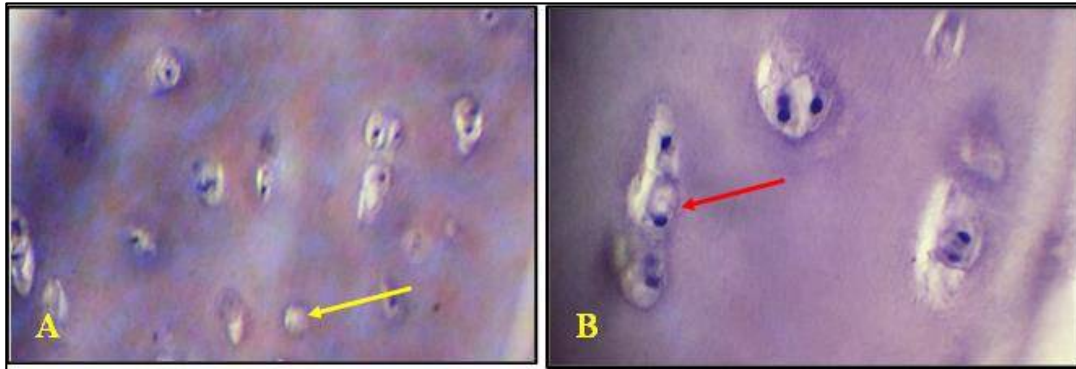
**Figure 9. Cross section in menisci of knee RA patient show: A- chondrocytes death in many area B- abnormal controlling and proliferation of chondrocyte (Hematoxylin and Eosin staining, x40).**



**Figure 10. Cross section in menisci of knee RA patient illustrate large area of fibrosis (red arrow), proliferation and disorientation of chondrocytes (green arrow) (Hematoxylin and Eosin staining, x10)**
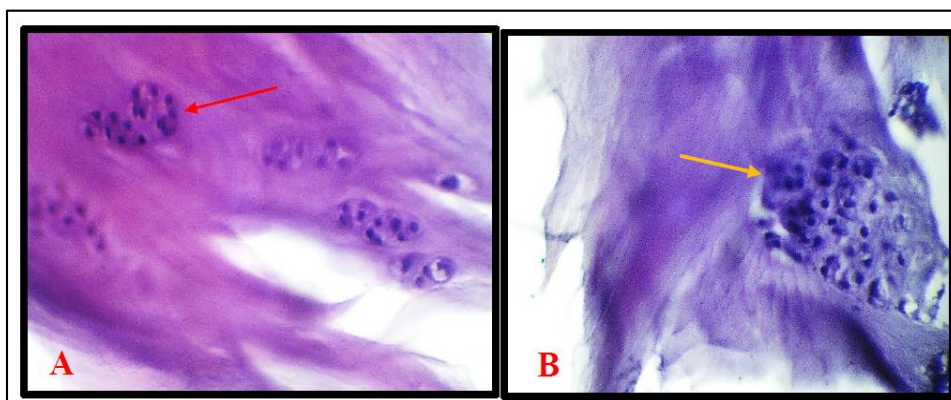


**Figure 11. Cross section in menisci of knee RA patient reveal to: A- abnormal proliferation of chondrocytes B- inflammatory cells infiltration (Hematoxylin and Eosin staining, x40).**
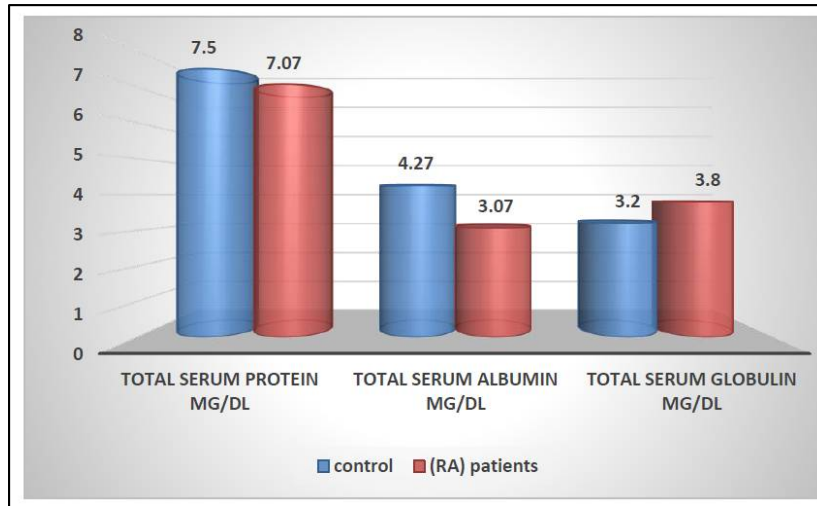
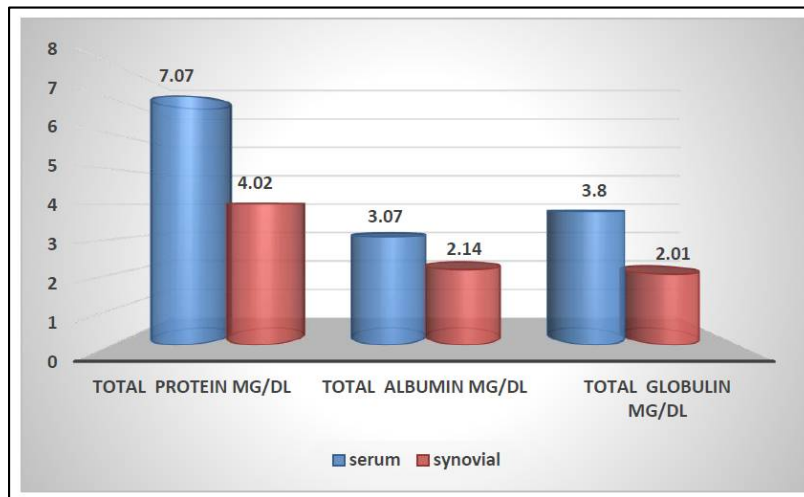**Figure 12. Effect of study total protein analysis in serum of RA patients and control**



**Figure 13: Effect of study Protein analysis in serum and synovial fluid of RA patients.**

**RESEARCH ARTICLE**

# Guess Solar Radiation Energy on Iraq by using DEMS and ArcGIS Techniques

Ayatf. Abed* and Ebtesam F.Khanjer

Department of Astronomy and Space, College of Science, University of Baghdad, Iraq.

*Address for Correspondence
**Ayatf. Abed**
Department of Astronomy and Space,
College of Science,
University of Baghdad, Iraq.

**ABSTRACT**

The radiation from the sun is the primary natural energy source of the planet Earth. Other natural energy sources are the cosmic radiation, the natural terrestrial radioactivity and the geothermal heat flux from the interior to the surface of the Earth, but these sources are energetically negligible as compared to solar radiation. In developing countries, such as Iraq, interest in solar energy applications has been growing in providing electricity and water supply in different areas Understanding solar radiation data is essential for modeling solar energy systems. Solar radiation is used directly to produce electricity for photo voltaic (PV) systems and solar thermal systems.The development of solar energy will have in the next years needs a reliable estimation of available solar energy resources.  In theglobel scales, topography is the most important factor in determining the distribution of solar radiation at the surface of the Earth. In this paper the Benefit from Digital Elevation Model (DEM) at (1-7-2017)  from satellite ( Landsat-8) , providing topographic information of Iraq. By using spatial analysis in  Arc _GIS  software to estimation the solar radiation energy in  complex topography areas in Iraq. The results gave us maps of distributions of solar radiation energy Per three-hour map

**Keywords**: solar radiation, DEM, Arc _GIs.

## INTRODUCTION

### Solar radiation

The radiation from the sun is the primary natural energy source of the planet Earth. Other natural energy sources are the cosmic radiation, the natural terrestrial radioactivity and the geothermal heat flux from the interior to the surface of the Earth, but these sources are energetically negligible as compared to solar radiation. When the spoken is of solar radiation, it means the electromagnetic radiation of the Sun. The energy distribution of electromagnetic radiation

over different wavelength is called Spectrum. The electromagnetic spectrum is divided into different spectral ranges (Figure 1)[1] The quantity of solar radiation reaching the earth's surface varies dramatically as a function of changing atmospheric condition as well as the changing position of the sun through the day, [3].

**The Elevation Concept**

The elevation of  a geographic location is  its height above or  below a fixed reference point, most commonly a reference geoid, a mathematical model of the Earth's sea level as an equipotential  gravitational surface. Elevation, or geometric height, is mainly used when referring to points on the Earth's surface, while altitude or geo-potential height is used for points above the surface, such as an aircraft in flight or a spacecraft in orbit, and depth is used for points below the surface. Less commonly, elevation is measured using the center of the Earth as the reference point. Due toequatorial bulge, there is debate as to which of the summits of Mount Everest or Chimborazo is at the higher elevation, as the Chimborazo summit is further from the Earth's center, while the Mount Everest summit is higher above mean sea level see figure (2)[5]

**Digital Elevation Models (DEMs)**

Elevation model are created from point data that samples the x,y,and z coordinates of locations on the earth's surface. Two main type elevation models exist: DEMs, which are raster datasets depicting the earth's topography as a regularly spaced grid, and triangular irregular networks, which connect irregularly spaced elevation points with triangular surfaces. Ingeneral, DEMs tend to be created from imagery, with triangular irregular networks created from survey data. The earth's topography forms the natural foundation for working in three dimensions, where objects are placed above, on, or below the terrain surface.To work in 3D, the GIS analyst must have a model of the earth's topography. By representing topography, elevation models provide a 3D context for mapping and analysis and are an indispensable tool for the GIS analyst.[6]

**Study area**

is located in the Middle East between latitudes 29° 5' and 37° 22' N and longitudes 38° 45' and 48° 45' N. Iraq as a Middle Eastern country is one of those countries which are situated on yellow belt of earth that can receive the maximum light during the day and different months in the year. Iraq climate describe as hot weather in summer and cold in the winter season..[9]

## EXPERIMENTAL WORK

The method were obtained by using the ArcMap GIS 10.3 to calculate the solar radiation of Iraq in July fromSRTM DEM for a pixel area 90X90 meter by applying two steps:

## CONCLUSIONS

The use of DEMs allows obtaining better estimates of the solar radiation in Iraq areas, by taking into account the topographic parameters in  radiation transfer models.The  Arc- GIs technique  has been  evaluated by using experimental data collected in an area of complex topography in Iraq provides good estimates of the solar radiation.

## REFERENCES

1.  E. O. Falayi, A. B. Rabiu,"*Solar Radiation Models and  Information for Renewable Energy Applications*, pp:112 -125, 2012.

**Ayatf. Abed and Ebtesam F.Khanjer**

2. Ahmed A. Hameed, Neamah Mohsen Al-Fatlawy and Ali M. Al-Salihi," *Estimation Of Hourly Global Solar Radiation Incident On Inclined Surfaces In Iraq At Different Sky Condition*", International Journal of Research in Applied Vol. 5, 2017.

3. Spokas and Forcella,"*Estimating Hourly Incoming Solar Radiation from Limited Meteorological Data*",pp:182-189, 2006

4. M. Santamouris , G. Mihalakakou, B. Psiloglou , G. Eftaxias and D. N. Asimakopoulos,"*Modeling the Global Solar Radiation on the Earth's Surface Using Atmospheric Deterministic and Intelligent Data-Driven Techniques*", journal ofclimate,1999

5. Li, Z., Zhu, Q. and Gold, C. "*Digital terrain modeling: principles and methodology*", 2005.

6. Kass Green, Russell G. Congalton, and Mark Tukman, "*Imagery and GIS*",pp:92373-8100,2017

7. Saddam RazakAbboud, "*Spatial variation of thermal anomalies in Iraq*", Journal of the Faculty of Education,2018
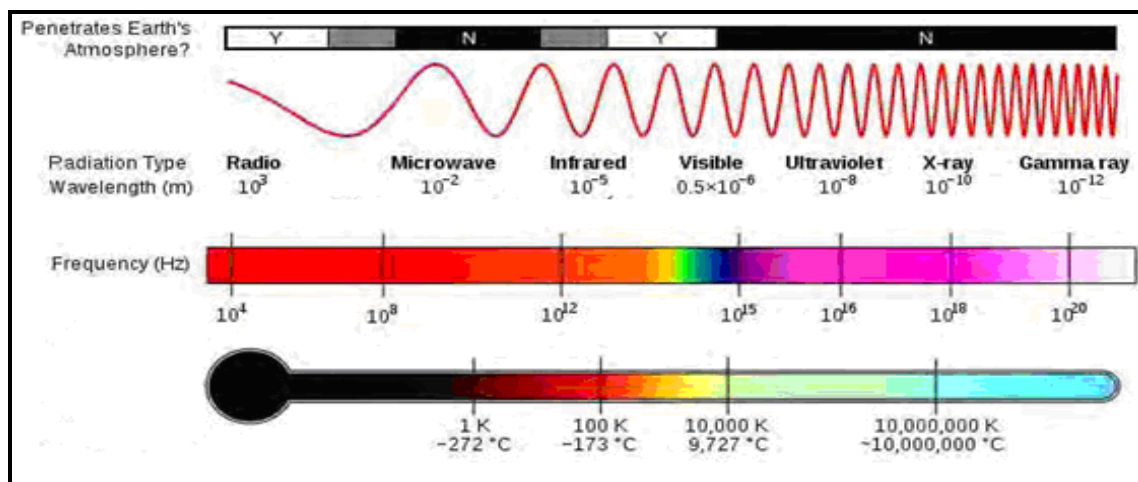
**Figure.1. Spectral ranges of electromagnetic radiation, [2].**
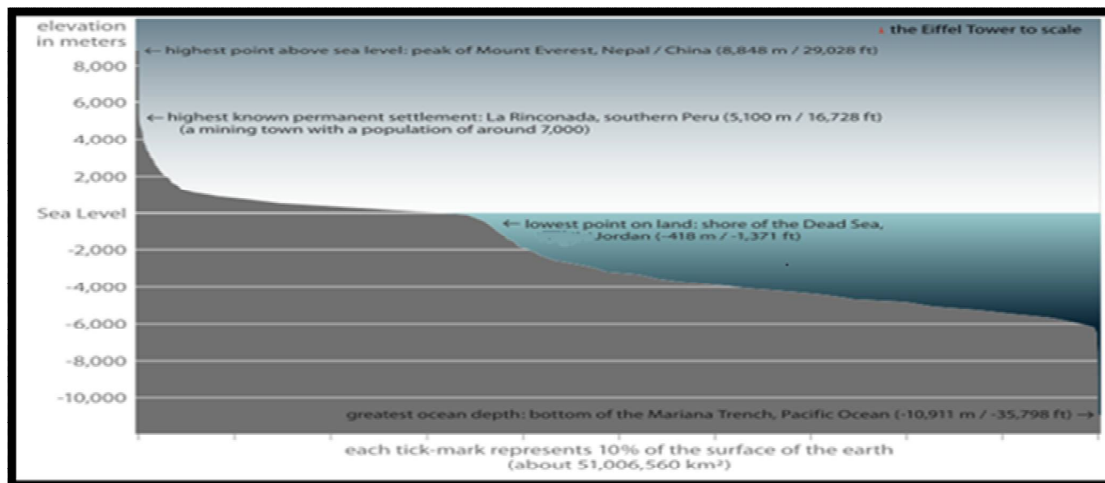


**Figure 2.Elevation histogram of the Earth's crust, [4]**

**Ayatf. Abed and Ebtesam F.Khanjer**

**Figure 3.Iraq country region and Baghdad city location [7]**



**Figure 4. SRTM DEM images**

**Ayatf. Abed and Ebtesam F.Khanjer**



**Figure 5. Grouping of DEMS images**

**Figure 6.DEMS after mosaic images**



**Figure 7. DEMS of Iraq**

16527

**Ayatf. Abed and Ebtesam F.Khanjer**



**Figure 8. solar radiation of Iraq in July**

**RESEARCH ARTICLE**

# Molecular Comparison of Adhesins of Uropathogenic *Escherichia coli* Isolates from Patients with First Episode and Recurrent Urinary Tract Infections

Zainab Ali Bachai* and Sareaa Maseer Gatya Al-Mayahie

Microbiology, Department of Biology, College of Science, University of Wasit, Iraq.

*Address for Correspondence
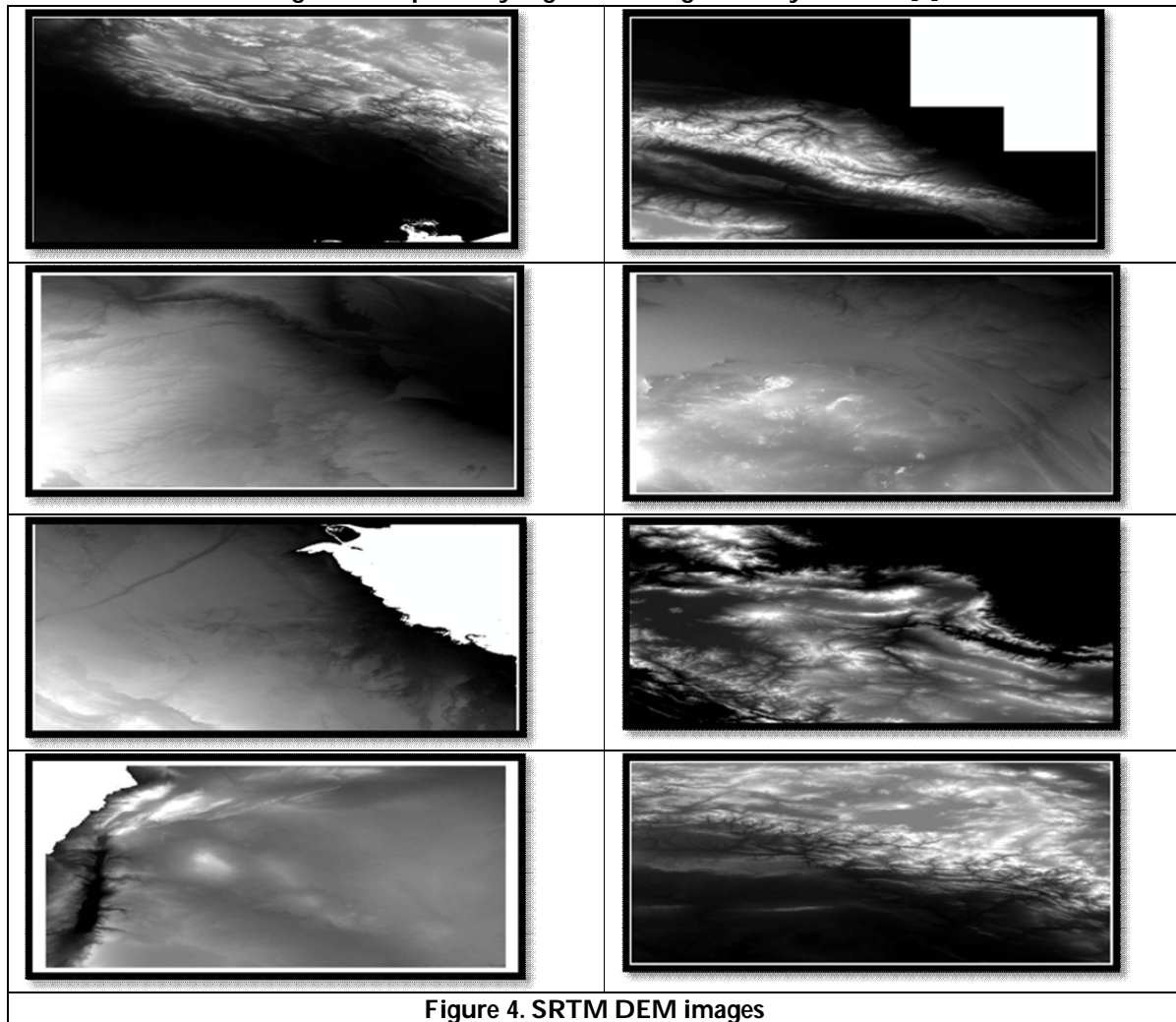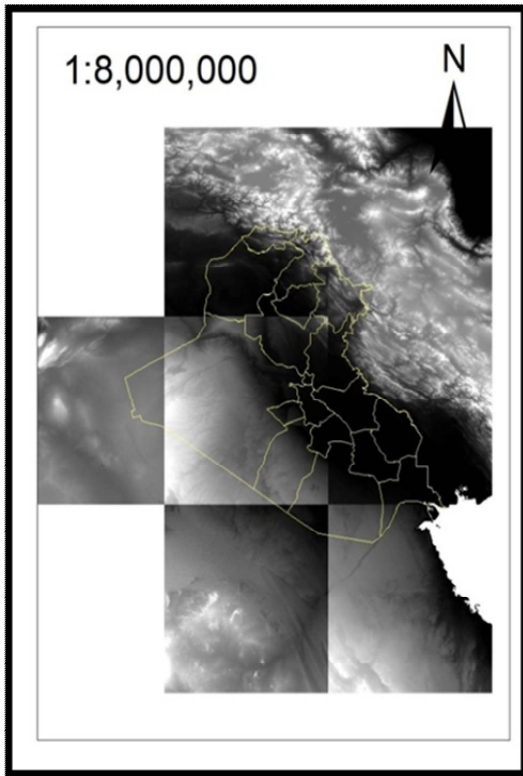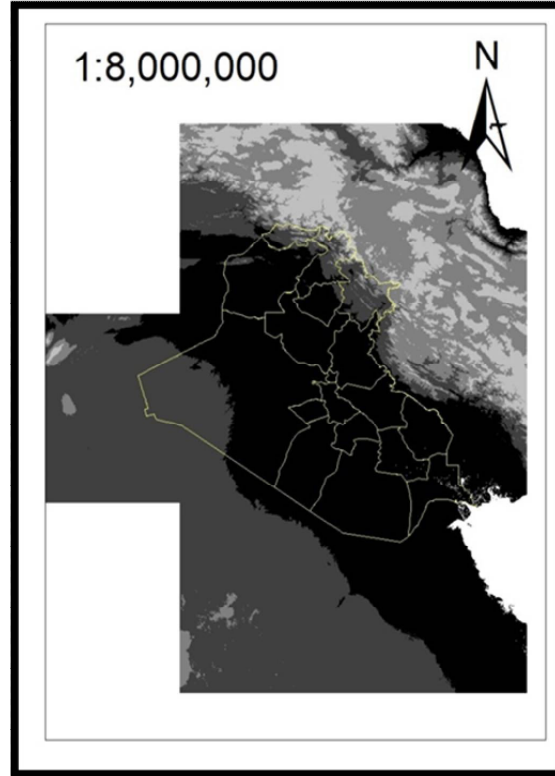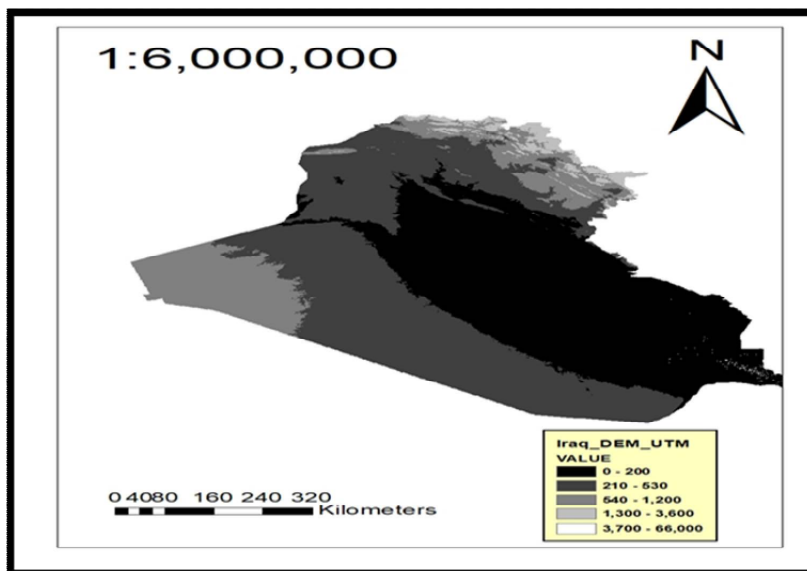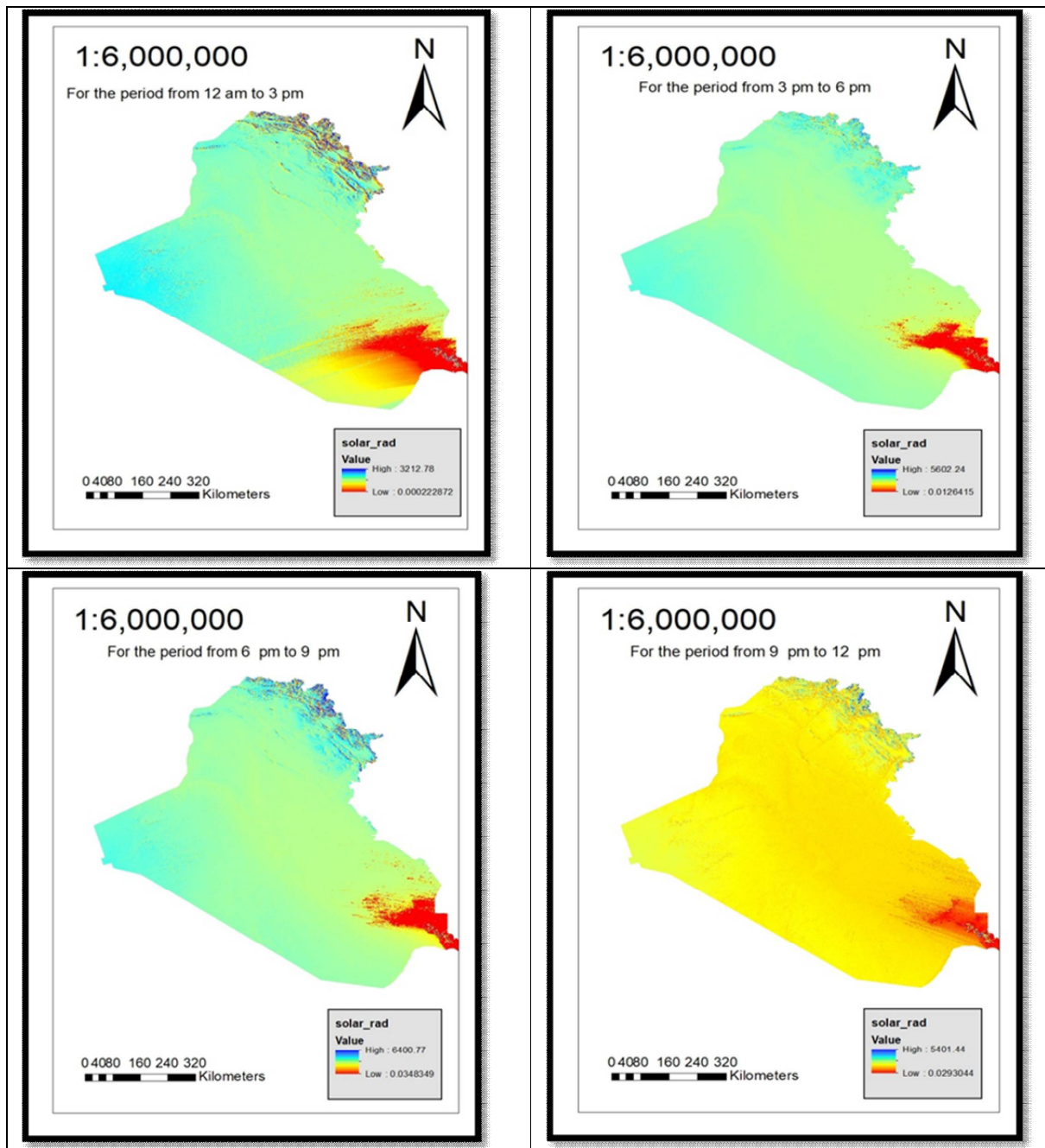**Zainab Ali Bachai**
Microbiology,
Department of Biology,
College of Science,
University of Wasit, Iraq.

### ABSTRACT

Worldwide, 30-44% of women withacute uncomplicated cystitis has a recurrence. *Escherichia coli* (*E. coli*) is the most common organism, causing 68-77% of recurrences. Varied results were obtained regarding the pattern of distribution of virulence genes in *E. coli* and their association with recurrent urinary tract infection (RUTI). So that, uropathogenic *E. coli* (UPEC) isolates from first episode UTI (FUTI) and RUTI were comparedby PCR protocols for distribution of adhesins'genes including: *fimH*; *papC*and *papG allels I,II,III*; *iha*; *sfa/focDE*;*afa/drab*;*bmaE* and *nfaE* and common UPEC virulence factors (VFs) namely *hlyA*; *fyuA* and*kpsMII*. Also, quadraplex PCR was applied to determine *E. coli*phylogroups. Statistically, there were no significant differences between FUTI and RUTI isolates for all of the studied VFs and phylogroups except *fimH*which was significantly (P≤ 0.05) more prevalent among FUTI than RUTI isolates(97.2% vs. 79.5%). Although the differences were not significant, RUTI isolates seemed to be more virulent than FUTI isolates in whichthe most frequent associations of adhesins with other VFs were observed represented by *fimH* +*papC* + *iha* + *kpsMII* + *hlyA* + *fyuA* (13.6%) and *fimH* + *papC* + *iha* + *kpsMII* + *fyuA*(9.0%). Also, in both FUTI and RUTI high frequency of the isolates clustered in *E. coli* phylogroup B2 followed by groups A and D. Moreover, concentration of VFs' genes was higher in phylogroups B2, D, and F. From this study's results it seems likely that bacterial factors have no apparent effect on predisposition to RUTI.

**Keywords:** recurrent UTI, first episode UTI, *E. coli*, virulence factors.

**Zainab Ali Bachai and Sareaa Maseer Gatya Al-Mayahie**
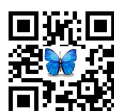
# INTRODUCTION

Recurrent urinary tract infections (RUTIs) are symptomatic UTIs that follow recovery of an earlier infection after appropriate treatment [1]. This infection is defined as 3 UTIs with 3 positive urine cultures throughout a 12-month period, or 2 infections throughout the last 6 months [2]. Worldwide, 50-80% of women have acute uncomplicated cystitis, of whom 30-44% will have a recurrence. *Escherichia coli* (*E. coli*) is the most common organism, causing 68-77% of recurrences[3]. Because *E. coli* causes 90% of UTIs among ambulatory patients [2], both first and second UTIs may be caused by it. These bacteria possess a range of virulence genes that facilitate their adherence and survival in the urinary tract and allow them to establish infection [4]. Moreover, *E. coli* strains differ in their ability to cause infection due to different phylogenetic groups to which they belong [5]. These phylogroups were described by Clermont *et al.* in 2013 and included: A, B1, B2, D, C, E, F, and clade I [6]. Worldwide, phylogenetic analyses have demonstrated that virulent extraintestinal *E. coli* strains belong mainly to group B2 and, to a lesser extent, to group D. In contrast, most of the commensal strains are associated with group A or group B1 [7].

Bacterial adherence to uroepithelial cells is an essential stage for the initiation and development of UTI. This process allows bacteria to resist the flushing action of the urine flow and bladder emptying, promoting bacterial persistence and activation of the host signaling pathways [8]. The important question is that: why in some people the infection persisted and reoccurred after treatment? To partially answer this question, this project was proposed to find out if there is any difference in bacterial virulence factors (especially adhesins) that may contribute in predisposition to this state. To achieve this aim, UPEC isolates from patients with FUTI and RUTI were compared for the possession of UPEC adhesins and phylogroups by PCR protocols and the differences were then analyzed statistically.

# MATERIALS AND METHODS

### Bacterial isolates

In this study, 80 UPEC isolates were collected from outpatients with FUTI(n = 36) and RUTI (n = 44) attended Al-Karama hospital and Al-Kut hospital for Gynecology and Obstetrics and Pediatrics in Al-Kut/Wasit Province/Iraq, during the period from July 1st. to December 30th., 2017. Isolates were grown on standard culture media and identified by conventional biochemical methods [9]. Positive urine samples were described by a bacterial growth of ≥ $10^5$ CFU/ml.

### Molecular detection of UPECs' VFs and phylogroups by PCR

### DNA extraction

DNA extraction was done by boiling method according to Yamamoto *et al.* [10] with modification which included suspending 24 hr. old bacterial culture (3 loopfulls) on TSA in 1 mlof sterile 1X TE buffer (pH 8.0) instead of sterile D.W

### Detection of UPECs' VFs

The isolates were screened by multiplex-PCR for UPEC adhesins' genes and common UPEC VFs. The reactions were analyzed in 3 pools, as follows: pool1: *fyuA*, *bmaE* and *sfa/focDE*; pool2: *hlyA*, *kpsMII* and *nfaE*and pool3: *afa/drab*, *iha*, *fimH* and *papC*. Primers sequences and amplification procedures were carried out according to Yamamoto *et al.* [10] and Johnson and Stell [11].

**Zainab Ali Bachai and Sareaa Maseer Gatya Al-Mayahie**

**Phylogenetic grouping of the isolates**

In this study, Quadraplex PCR [6] was used to determine the distribution of phylogenetic groups among UPEC isolates based on the presence of *chuA, yjaA,* and *arpA* genes and TspE4.C2 DNA fragment.

**Statistical analysis**

Differences in the distributions of the studied determinants were tested by Chi square [12]. A P value of ≤ 0.05 was considered to indicate statistical significance.

# RESULTS

### Distribution of virulence factors' genes

Statistically, there were no significant differences in distribution of adhesins genes and other UPEC VFs among FUTI and RUTI isolates, except *fimH* which was significantly (P≤ 0.05) more prevalent among FUTI than RUTI isolates (97.2% vs. 79.5%). Distribution of these genes was summarized in Table 1. Analyses of association of adhesins with each other (Table 2) in an isolate revealed that *fimH+iha* had the highest association (13.8%) among FUTI isolates, followed by *fimH+sfa/focDE* and *fimH+papC(papGII) +iha* (11.1% foreach). On the other hand, among RUTI isolates the highest association was *fimH+papC(papGII)+iha* (25.0%), followed by *fimH+iha* (9.0%). Regarding the association of adhesins with other VFs,the majority of *kpsMII* was positively associated with *fyuA* and *papC* among both FUTI and RUTI isolates. Also, s*fa/focDE* occurred almost in *papC*-positive isolates and was associated with *hlyA*. Combination of *fimH + papC* (*papGII*) + *iha* + *kpsMII* + *hlyA+fyuA* occurred in 2.7% and 13.6% of FUTI and RUTI isolates, respectively. Whereas, *fimH + papC + iha + kpsMII+fyuA*were in 5.5% of FUTI and 9.0% of RUTI isolates.

### Phylogenetic groups of UPEC

High frequency of this study's isolates clustered in *E. coli* phylogroup B2 (30.5% of FUTI vs. 34.0% of RUTI isolates), followed by groups: A (22.2% vs. 27.2%), D (22.2% vs. 18.1%), F and C (each 5.5% vs. 4.5%) and B1(2.7% vs. 2.2%), whereas phylogroup E was not detected in any isolate (Table 3). In addition, 5.5% and 9.0% of FUTI and RUTI isolates were nontypable, respectively. There was no significant differences in distribution of all of these phylogroups among FUTI and RUTI isolates.

### Phylogenetic distribution of virulence factors

This study's results revealed that there was no significant difference in phylogenetic distribution of VFs among FUTI and RUTI isolates. Moreover, VFswere concentratedin phylogroups B2, D, and F (Table 4), which had the highest rates of multiple virulence factors possession (three or more virulence factors/isolate): 96.1%, 94.1% and 75%, respectively. While, 20% and 16.6% of group A and nontypable isolates had multiple virulence factors, respectively. No isolate of both groups C and B1 had multiple virulence factors.

# DISCUSSION

Survey of previous studies [13-15]about the importance of a virulence factor as a predisposing factor to recurrent UTI revealed a controversial results. To our best knowledge, there were few studies regarding this subject, worldwide. So that this project was proposed to make our inspection of which factors (especially adhesins ) that might be more prevalent among *E. coli* isolates from cases of RUTI than those from cases of FUTI.

In this work, the patterns of virulence genes' distribution in UPEC and its association with recurrent UTI were consistent with previous studies [13-15]. Statistically, only *fimH* (adhesin of type 1 fimbriae) was more prevalent among FUTIthan RUTI isolates. This result disagreed with Foxman *et al.* [13] who showed that the *fimH* occurred in 100% of each FUTI and RUTI isolates. Also, Agarwal *et al.* [15] reported *fimH* in 87.5% of FUTI isolates and 90.9% of RUTI isolates and showed that the difference was not significant. This disagreement of this study's results with these researchers may be attributed to the low numbers of isolates (n=80: 36 FUTI and 44 RUTI isolates) obtained in this study, especially if we know that almost all *E. coli* isolates contain*fimH* and express type 1 fimbriae [16]. Moreover, although highly prevalent in commensal *E.coli* as well as UPEC, Type 1 fimbriae are considered to be one of the most important VFs involved in establishment of a UTI mediating extracellular binding to the host urothelium and invasion [17-18]. Furthermore, type 1 fimbriae was reported to be necessary for intracellular aggregation into intracellular bacterial communities and thus possibly the pathogenesis of RUTI [16].Although the differences were not significant statistically,  RUTI isolates seemed to be more virulent than FUTI isolates (Tables 1 and 2). Other studies revealed that RUTI isolates have virulence score higher than that of FUTI isolates [14-15].

High frequency of this study's isolates clustered in *E. coli* phylogroup B2 (both FUTI and RUTI isolates). No significant differences in distribution of all phylogroups among both groups of this study included isolates and this was in agreement with previous studies [14-15]. In the present study, the prevalence of other virulence genes was higher in phylogenetic groups B2, D, and F (Table 4) and this agreed with previous studies [19-21]. What is worth to note here in this study is that group F had a virulence that is comparable to that of groups B2 and D in which the highest rates of multiple virulence factors possession (three or more virulence factors/ isolate) were observed (96.1% of group B2 isolates, 94.1% of group D isolates and 75.0% of group F isolates). These results supported the crucial role of groups B2, D, and F in UTI causation. The high virulence of group F isolates may be explained by the fact that phylogroup F consists of strains that form a sister group to phylogroup B2 [22-23]. It is closely related to both group B2 (the origin of most human clinical *E.coli* isolates) and group D (the origin of most non-B2 extraintestinal pathogenic *E. coli*: ExPEC) [6,24]. Worldwide and to our best knowledge, this was the first time that the new *E. coli* phylogroup F been investigated for possession of virulence factors of UPEC and that it had virulence that was comparable to that of groups B2 and D which were best known as  including the virulent UPEC strains. In conclusion, it seems likely that bacterial factors has no apparent effect on predisposition to RUTI compared with previously known host predisposing factors. Biochemical and anatomical studies are required to investigate these host predisposing factors to RUTI in order to design suitable management procedures.

## REFERENCES

1. Kodner, C. M.; Gupton, E. K. T. (2010). Recurrent urinary tract infection in women: diagnosis and management. American Family Physician. 82: 638-643.
2. Epp, A.; Saskatoon, S. K.; Larochelle, A.; Lambert, S. T. (2010). Recurrent urinary tract infection. SOGC clinical practice guideline. 250: 1082-1090.
3. Gupta, K. and Trautner, B. W. (2013). Diagnosis and management of recurrent urinary tract infections in non-pregnant women. British Medical Journal. 346:f3140.
4. Totsika, M.; Moriel, D. G.; Idris, A.; Rogers, B. A.; Wurpel, D. J.; Phan, M. et al. (2012). Uropathogenic Escherichia coli Mediated Urinary Tract Infection. Current Drug Targets. (13): 1386-1399.
5. Moreno, E.; Johnson, J. R.; Pe´rez, T. P; Prats, G.; Kuskowski, M. A.; Andreu, A. (2009). Structure and urovirulence characteristics of the fecal Escherichia coli population among healthy women. Microbes and Infection. 11: 274-280.
6. Clermont, O.; Christenson, J. K.; Denamur, E.; Gordon, D. M. (2013). The Clermont Escherichia coli phylo-typing method revisited: improvement of specificity and detection of new phylo-groups. Environ. Microbiol. Rep. 5:58-65.

7.  Iranpour, D.; Hassanpour, M; Ansari, H.; Tajbakhsh, S.; Khamisipour, G.; and Najafi A. (2015). Phylogenetic groups of Escherichia coli strains from patients with urinary tract infection in iran based on the new Clermont phylotyping method. BioMed Research International. 2015: 1-7.

8.  Bahalo, S.; Tajbakhsh, E.; Tajbakhsh, S.; Momeni, M.; and Tajbakhsh, F. (2013). Detection of some virulence factors of Escherichia coli isolated from urinary tract infection isolated of children in shahrekord iran by multiplex PCR. Middle-East Journal of Scientific Research. 14 (1): 29-32.

9.  MacFaddin, J. F. (2000). Biochemical Tests for Identification of Medical Bacteria (3rd ed.). Lippincott Williams and Wilkins, London.

10. Yamamoto, S.; Terai, A.; Yuri, K.; Kurazono, H.; Takeda, Y.; Yoshida, O. (1995). Detection of urovirulence factors in Escherichia coli by multiplex polymerase chain reaction. FEMS Immunology and Medical Microbiology. 12: 85–90.

11. Johnson, J. R. and Stell, A. L. (2000). Extended virulence genotypes of Escherichia coli strains from patients with urosepsis in relation to phylogeny and host compromise. The Journal of Infectious Diseases. 181: 261–272.

12. Ross, S. M. (2009). Introduction to probability and statistics for Engineers and Scientists. (4thedn), Elsevier, London.

13. Foxman, B.; Zhang, L.; Tallman, P.; Palin, K.; Rode, C.; Bloch, C. et al. (1995). Virulence characteristics of Escherichia coli causing first urinary tract infection predict risk of second infection. The Journal of Infectious Diseases. 172: 1536-1541.

14. Johnson, J. R.; O'Bryan, T. T.; Delavari, P.; Kuskowski, M.; Stapleton, A.; Carlino, U.; and Russo, T. A. (2001). Clonal relationships and extended virulence genotypes among Escherichia coli isolates from women with a first or recurrent episode of cystitis. The Journal of Infectious Diseases. 183: 1508–1517.

15. Agarwal, J.; Mishr, B.; Srivastava, S.; Srivastava, R.; Pandey, A. (2014). Virulence determinants in Escherichia coli associated with recurrent cystitis in sexually active women. Microbial Pathogenesis. 74: 38-41.

16. Ejrnæs, K. (2011). Bacterial characteristics of importance for recurrent urinary tract infections caused by Escherichia coli. Danish medical bulletin. 58(4): B4187.

17. Chen, S. L.; Hung, C. S.; Pinkner, J. S.; Walker, J. N.; Cusumano, C. K.; Li, Z.; et al. (2009). Positive selection identifies an in vivo role for fimH during urinary tract infection in addition to mannose binding. PNAS. 106. (52): 22439–22444.

18. Schwartz, D. J.; Kalas, V.; Pinkner, J. S.; Chen, S. L.; Spaulding, C. N.; Dodson, K. W.; et al. (2013). Positively selected FimH residues enhance virulence during urinary tract infection by altering FimH conformation. Proceedings of the National Academy of Sciences of the United States of America. 110(39): 15530–15537.

19. Abdi, H. A. and Rashki, A. (2014). Comparison of virulence factors distribution in uropathogenic E. coli isolates from phylogenetic groups B2 and D. International Journal of Enteric Pathogens. 2(4): e21725.

20. Lee, J. H.; Subhadra, B.; Son, Y. J.; Kim, D. H.; Park, H. S.; Kim, J. M. et al. (2016). Phylogenetic group distributions, virulence factors and antimicrobial resistance properties of uropathogenic Escherichia coli strains isolated from patients with urinary tract infections in South Korea. Letters in Applied Microbiology. (62): 84-90.

21. Najafi A. ,Hasanpour M. ,Askary A. ,Aziemzadeh M. , and Hashemi N. (2017). Distribution of pathogenicity island markers and virulence factors in new phylogenetic groups of uropathogenic Escherichia coli isolates. Folia Microbiologica.

22. Jaureguy, F.; Landraud, L.; Passet, V.; Diancourt, L.; Frapy, E.; Guigon, G. *et al.* (2008). Phylogenetic and genomic diversity of human bacteremic *Escherichia coli* strains. BMC Genomics. 9: 560.

23. Clermont, O.; Olier, M.; Hoede, C; Diancourt, L; Brisse, S.; Keroudean, M. et al. (2011). Animal and human pathogenic Escherichia coli strains share common genetic backgrounds. Infection, Genetics and Evolution. 11: 654–662.

24. Johnson, J. R.; Johnston, B. D.; and Gordonc, D. M. (2017). Rapid and specific detection of the Escherichia coli sequence type 648 complex (STc648) within phylogroup F. JCM01949-16, version 2.

**Zainab Ali Bachai and Sareaa Maseer Gatya Al-Mayahie**

**Table 1: Percentage frequency of UPEC adhesins and other VFs' genes among *E. coli* isolates from patients with FUTI and RUTI**

| VF's gene | No. (%) of *E. coli* isolates | | |
|---|---|---|---|
| | FUTI (n = 36) | RUTI (n = 44) | Total (n = 80) |
| *fimH** | 35 (97.2) | 35 (79.5) | 70 (87.5) |
| *Iha* | 14 (38.3) | 18 (40.9) | 32 (40.0) |
| *papC* | 10 (27.7) | 17 (38.6) | 27 (33.7) |
| *papGI* | 0 | 0 | 0 |
| *papGII* | 9 (25.0) | 16 (36.3) | 25 (31.2) |
| *papGIII* | 1 (2.7) | 1 (2.2) | 2 (2.5) |
| *sfa/focDE* | 9 (25.0) | 6 (13.6) | 15 (18.7) |
| *afa/drab* | 2 (5.5) | 5 (11.3) | 7 (8.7) |
| *bmaE* | 0 | 0 | 0 |
| *nfaE* | 0 | 0 | 0 |
| *hlyA* | 10 (27.7) | 11 (25.0) | 21 (26.2) |
| *fyuA* | 23 (63.8) | 29 (65.9) | 52 (65.0) |
| *kpsMTII* | 20 (55.5) | 23 (52.2) | 43 (53.7) |

* Statistically *fimH* was more prevalent (P ≤ 0.05) among FUTI than RUTI isolates.

**Table 2. Patterns of distribution of adhesive genes among FUTI and RUTI *E.coli* isolates (n=80).**

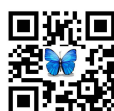| Adhens' pattern | No. (%)of *E. coli* isolates | |
|---|---|---|
| | FUTI (n=36) | RUTI (n=44) |
| Null | 0 | 6 (13.6) |
| *fimH* only | 14 (38.8) | 10 (22.7) |
| *afa/draB* only | 0 | 1 (2.27) |
| *papC (papGII)*only | 0 | 1 (2.27) |
| *iha* only | 1 (2.7) | 0 |
| *sfa/focDE* only | 0 | 1 (2.27) |
| *fimH + sfa/focDE* | 4 (11.11) | 2 (4.5) |
| *fimH + afaE* | 1 (2.7) | 1 (2.27) |
| *fimH + iha* | 5 (13.8) | 4 (9.09) |
| *fimH + papC(papGII)* | 1 (2.7) | 1 (2.27) |
| *fimH + papC(papGII) + iha* | 4 (11.11) | 11 (25) |
| *fimH + papC (papGII)+ sfa/focDE* | 1 (2.7) | 1 (2.27) |
| *fimH + papC (papGIII)+ sfa/focDE* | 1 (2.7) | 1 (2.27) |
| *fimH + afaE + iha* | 0 | 1 (2.27) |
| *fimH + afaE + papC (papGII)* | 0 | 1 (2.27) |
| *fimH + iha + sfa/focDE* | 1 (2.7) | 0 |
| *fimH + afaE + papC (papGII) + iha* | 1 (2.7) | 0 |
| *fimH + iha + papC (papGII) + sfa/focDE* | 2 (5.5) | 1 (2.27) |

**Table 3. Distribution of FUTI and RUTI UPEC isolates among *E. coli* phylogroups.**

| Phylogroup | No. (%) of *E. coli* isolates | | |
|---|---|---|---|
| | FUTI (n=36) | RUTI (n=44) | Total (n=80) |
| B2 | 11 (30.5) | 15 (34) | 26 |
| B1 | 1 (2.7) | 1 (2.27) | 2 (2.5) |
| A | 8 (22.2) | 12 (27.27) | 20 (25) |
| D | 8 (22.22) | 8 (18.18) | 16 (20) |
| F | 2 (5.5) | 2 (4.5) | 4 (5) |
| C | 2 (5.5) | 2(4.5) | 4 (5) |
| E | 0 | 0 | 0 |
| Nontypeable(NT) | 2 (5.5) | 4 (9) | 6 (7.5) |

**Table 4. Percentage of VFs' genes among Phylogroupsof*E coli* isolates from cases of FUTI and RUTI.**

| VFs' gene | % of positive *E. coli* isolates | | | | | | | | | | | | | |
|---|---|---|---|---|---|---|---|---|---|---|---|---|---|---|
| | B2 (n=26) | | D (n=17) | | F (n=4) | | A (n=20) | | B1 (n=2) | | C (n=5) | | NT (n=6) | |
| | F | R | F | R | F | R | F | R | F | R | F | R | F | R |
| *fimH* | 100 | 93.3 | 100 | 100 | 100 | 50 | 100 | 75 | 100 | 100 | 100 | 100 | 50 | 0 |
| *papC* | 45.4 | 73.3 | 44.4 | 62.5 | 50 | 50 | 0 | 0 | 0 | 0 | 0 | 0 | 0 | 0 |
| *afa/drab* | 0 | 13.3 | 22.2 | 12.5 | 0 | 50 | 0 | 8.3 | 0 | 0 | 0 | 0 | 0 | 0 |
| *Iha* | 36.3 | 60.0 | 44.4 | 62.5 | 100 | 50 | 25 | 25 | 100 | 0 | 0 | 0 | 50 | 0 |
| *nfaE* | 0 | 0 | 0 | 0 | 0 | 0 | 0 | 0 | 0 | 0 | 0 | 0 | 0 | 0 |
| *sfa/focDE* | 81.8 | 33.3 | 0 | 0 | 0 | 0 | 0 | 0 | 0 | 0 | 0 | 0 | 0 | 25 |
| *bmaE* | 0 | 0 | 0 | 0 | 0 | 0 | 0 | 0 | 0 | 0 | 0 | 0 | 0 | 0 |
| *fyuA* | 90.9 | 93.3 | 100 | 100 | 100 | 100 | 12.5 | 25 | 0 | 0 | 0 | 0 | 50 | 50 |
| *hlyA* | 63.6 | 46.6 | 33.3 | 37.5 | 0 | 0 | 0 | 8.3 | 0 | 0 | 0 | 0 | 0 | 0 |
| *kpsMII* | 100 | 86.6 | 55.5 | 100 | 100 | 50 | 12.5 | 8.3 | 0 | 0 | 0 | 0 | 50 | 0 |

**F: FUTI**; **R: RUTI.**

**RESEARCH ARTICLE**

# The Nanocomposite Film of Polypyrrole and Functionalized Single Walled Carbon Nanotubes as Gas Sensor of NO₂ Oxidizing Gas

Ghada Ayad Kadhim[1]* and Mahdi Hasan Suhail[2]

[1]Department of Physics, College of Science, University of Wasit, Iraq.
[2]Department of Physics, College of Science, University of Baghdad,Iraq.

*Address for Correspondence
**Ghada Ayad Kadhim**
Department of Physics,
College of Science,
University of Wasit, Iraq.

**ABSTRACT**

The nanocomposite of polypyrrole (PPy) and functionalizedsingle wall carbon nanotube (fSWCNT)as a gas sensor for oxidizing gas (NO₂) were synthesized by in electrochemical polymerization.nanocomposite were deposited onto (Indium tin oxide) ITO coated glass for pyrrole  monomer with oxalic acid and different concentration  from fSWCNTs(0.015, 0.02) in the 150 mL from distilled water.the response of these films for NO₂ gas was estimated by monitoring the change in electrical resistance at different temperature (20,50,100,150 and 200)ºC. it is observed that the PPy/fSWCNT  nanocomposite had greater sensitivity  than  pure  polypyrrole.X-Ray diffraction (XRD),Atomic Force  Microscope (AFM),Field Emission Scanning Electron microscopy (FE-SEM)and Fourier Transform Infrared (FT-IR) Spectroscopy, were used to characterize the synthesized PPy-SWCNT nanocomposite.The XRD showed that the prepared films have *polycrystalline*structure at 2θ=(24, 43)º.Surface morphology of nanocomposites was investigated by (FE-SEM). AFM result showed that nanocomposite have uniform granular structure with average grain size of (40.75, 47.07 and96.74) nm. The FTIR spectroscopy the spectra give prominent and thedistinct bonds.

**Keywords:** gas, polypyrrole, X-Ray, nanocomposite, SEM, XRD, FT-IR

## INTRODUCTION

Nitrogen Dioxide (NO₂) is one of a group of gases called nitrogen oxides (NOx).Acute harm due to NO₂ exposure is only likely to arise in occupational settings. Direct exposure to the skin can cause irritations and burns. Only very high concentrations of the gaseous form cause immediate distress: 10–20 ppm can cause mild irritation of the nose and throat, 25–50 ppm can cause edema leading to bronchitis or pneumonia, and levels above 100 ppm can cause death due to asphyxiation from fluid in the lungs[1,2].Hence, the detection of NO₂gas is very important in terms of

both environmental as well as health monitoring sectors. There is a plethora of number of gas sensing techniques availablefor the proper control and detection of $NO_2$ which vary in their concentration ranges and sensing mechanisms [3,4].Awide variety of materials, such as, metal oxides, polymers and carbon based materials have been used as sensing elements for various $NO_2$ gas sensor applications [5,6].Materials such as conducting polymers (CPs) and carbon nanotube (CNT)are chief candidates when considering high-speed response and high-strain properties, respectively, as necessary attributes of a composite[7].

Conducting polymers(CPs) such aspolypyrrole (PPy) ,polythiophene (PTh), polyaniline (PANI) and their derivatives are widely used in sensing material due to its high sensitivity, cost effectiveness, room temperature operation and fast response [8].One of the important conductive polymers is polypyrrole and its derivatives have attracted a great deal of attention because of its good environmental stability, high electrical conductivityand simple processing and synthesis. Furthermore, PPy is among a little number of materials demonstrating gas sensing features at room temperature, a fascinating prospect for developing practical applications [9].the polypyrrole consists of a 5-membered ring, containing a nitrogen (N) heteroatom, the same as with other organic molecules, PPy polymerisation occurs upon oxidation of the monomer, which forms a CP backbone chain with overlapping $\pi$-orbitals and a positive charge along the polymer backbone[10].

The use of single-walled carbon nanotubes(SWNTs ) in biological sensors and effective ultrasensitive chemical because of their high surface-to-volumeratio and their excellent electrical properties [5].numerous approaches have been developed to functionalize (SWNTs), including covalent and noncovalent chemicalfunctionalization, and in studies these have revealed enhancedperformance as gas sensors[11]For instance. (PPy/fSWCNT ) nanocomposites formed via electrochemical polymerization of SWCNT in an pyrrole mixture demonstrated enhanced sensitivity to $NO_2$gaspharmaceutics [12].

The electrochemical approach for making electroactive/conductive films is very versatile and provides a simplistic way to differ the film properties via simply varying the electrolysis conditions in a controlled way. Or the variations in the properties of polymer can be made in the selection of the electrolyte or the monomer. also, the electro synthesis allows an easy control of the thickness of the polymers. Preparation of CPs electrochemically is a complex method and the quality and yield of the resulting polymer thin films is affected by different factors. The concentration and nature of monomer/electrolyte, cell conditions, electrode, the solvent, temperature and applied potential, pH all have a strong effect on the quality and the electro-oxidation reaction of the film [13].

## EXPERIMENTAL

Polyppyrroleand functionalizedsingle wall carbon nanotube nanocomposites were prepared from pyrrole (Py) monomer in acid medium at room temperature by usedtitaniumas working electrode andIndium tin oxideas a reference electrode.ITO has been chemically and ultrasonically cleaned via typical methods. solution of PPy is prepared via using0.1M of pyrrole monomer was doping with oxalic acid (0.1M) with different concentration of(fSWCNT) (0.015 and 0.02) in 150 mL from distilled water. The synthesized electrodes were thoroughly washed by water to avoid the possible presence of electrolyte species on the surface of polymer. nanocomposite thin films were deposited at ( 4.9 and 4) V with variousconcentration of CNT wthin 3 minutes. The prepared thin film wasgreen,uniform, and strongly adherent to substrate. The thickness of the nanocomposite was100nm measured using an optical interferometer via using He-Ne laser (0.632μm). Mask on the films surface from Aluminum of 100 nm thickness was deposited using thermal evaporation. from $NO_2$was introduced(10,20 and 30) ppm in this paper we used only 30% and the other percentages we will publish with other research at differentoperation temperature beginning from room temperature (20ºC) up to 200ºC with step of 50ºC.The characterization of structural properties for samples were investigated by X-ray diffractometer (XRD, Shimadza-6000) using CuK$_\alpha$ radiation. The morphology

**Ghada Ayad Kadhim and Mahdi Hasan Suhail**

of the nanocomposite films was studied using atomic force microscope (AFM) (Angstrom AA3000), Fourier Transform Infrared Spectroscopy (FTIR) was studied by using solid KBr discs Maximum Resolution 0.5cm and the microstructure film study via Hitachi FE-SEMmodel S-4160.

# RESULTS AND DISCUSSION

### XRD Analysis

Figure(1)show analyze the structural characteristics of the pure polypyrrole and nanocomposite films via X-ray diffraction. Diffraction pattern of sample has *Polycrystalline* structure at diffraction angles 2θ=24,43º which is a distinguishing peaks of (PPy/fSWCNTs)[8,14]. The peaks increase in intensity and become sharp with increasing the ratio of CNT.and have different average grain size are calculated by using Debye – Scherer equation.

$$D - \frac{K\lambda}{\beta \cos\theta}$$

Where k is shape factor for average crystallite, β is full width at half maxima (FWHM) of crystalline planes in radians, θ is the angle between incident and reflected rays and λ is the wavelength of the X-ray which is 1.54Å for Cu target. The average grain size increase with increasing concentration of CNT.

### AFM Analysis

The morphology of samples were examined using an (AFM). Figure (2) AFM results showed homogenous andsmooth the PPy and (PPy/fSWCNT) films in (3D) images and granularity distribution films. AFM have different average grain size with different concentration from CNT.The increase of the crystallite size may be caused by columnar grain growth in the structurethrough increasing concentration of fSWCNTAs shown in Figure 2.The results of crystallite size obtained from XRD are in good agreement with those obtained from AFM shown in Table1.

### SEM analysis

The Field Emission Scanning Electron Microscopy (FE-SEM) images of pure PPy, and PPy/SWCNT nanocomposites using different concentrations of SWCNTs suspended in the polymerization electrolyte on ITO substrate interactive 3D surface of films at the operating voltage of 30kV and 60,000 times magnification are shown in Fig.(3). the pure PPy has a granular structure with a verage grain size 33.24nm, but in the nanocomposite we can be observed that many nanotubes with number of granular because presence of CNTs. Increasing the concentration of CNTs lead to increase the average grain size as well as increase of nanotubs and appearance of typical 'cauliflower' structures as shown in fig.(3.b).

### FTIR analysis

Spectroscopy was determined The chemical structures of nanocomposite thin films.The FTIR spectra of PPy and PPy/fSWCNTs at(0.015 and 0.02) from CNTs are shown in Figure 4.In the spectra of Purepolypyrrole, a broad absorption band obtained a stretching N-H band at 3416.21 cm$^{-1}$.The bands at (1558.52 and 1452.82) cm$^{-1}$ is related to the C=Cstretching mode, and the bands at 1176 cm$^{-1}$ is associated to the C-H bending modes while the band for C-H out-of-plane deformation vibration was observed at 875.799 cm$^{-1}$after add 0.02 CNT,After addition we note a slight change in bonds values and a decrease in intensity and this is attributed to the presence of CNTs,which are coincident with the literature[8,14] as shown in Table 2.

16538

**Ghada Ayad Kadhim and Mahdi Hasan Suhail**

**Sensor measurements**

The change in the resistance of the sensing elements PPy films as a function of time for both cases open and closed gas with different concentration of CNT and operation temperature at 30% $NO_2$ displayed in Figure (5). It was found that, the samples resistance decrease with temperature, i.e. behave as a semi-conductor and it decrease with increase the concentration CNT. Also, to exposure the oxidizing $NO_2$ gas molecules with films produced the sudden decrease in the value of resistance.The original resistance value achieved when the $NO_2$ gas had been turned off and fresh air is introduced into the test chamber. The observed change in the resistance of sensor with $NO_2$ gas molecules is due to the adsorption of gas on the surface of films as well as the response for a particular gas or vapor is mainly related to adsorption kinetics of gas on active sensing layer. PPy and (PPy/fSWCNT) are a p-type material in which majority charge carriers are holes. On the other hand, $NO_2$ is an oxidizing gas (electron accepter) and when it interacts with the p-type polypyrrole then it capture electrons from the polymer matrix resulting in the decrease of the resistance. Since the majority carriers (holes) density gets increased due to electron accepting nature of NO2gas. This results in increasing the conductivity of material and film resistance decreases. This result is agree with [15].

The variation of $NO_2$ gas sensitivity, response time and recovery time versus operating temperature for samples with (0.015 and 0.02) of CNT at 30% $NO_2$ as shown from Figures (6 to 8). It can be observed in pure polypyrrole case the high sensitivity at (50or 100)°C, but when we add and increase the concentration of CNT and 30% $NO_2$ be the best sensitivity at room temperature. The concentration of $NO_2$ gas increased then increases active sites for adsorption, causing the increase in response. Over room temperature, sensor sensitivity decreases with the increasing temperature. The response and recovery times are depends on the rate of adsorption and desorption respectively. The response and recovery times were obtained from Figures(7and 8).Such a decrease in response time when concentration of CNT and increase the operation temperature.The temperature increases the holes in the material that act on the gas response speed and also improve the surface properties that make it respond at a lower temperature.

## CONCLUSIONS

In concluding remarks, We have synthesized polypyrrole and (PPy/fSWCNT) nanocomposite via electrochemical polymerization method. From X-ray studies revealed that thin films are polycrystalline. Weillustrate increase grain size with increase the ratio of CNT and showed the less aggregation of the polymer from AFM. Proper formation of all thin films in a conducting form was established by FTIR.The SEM of surface morphology and also studied. Gas sensing characteristics shows response for $NO_2$ gas with operated temperature at room temperature after add CNT.

## REFERENCES

1. G. Pershagen, E. Rylander, S. Norberg, M. Erikssons and L.Nordvall,"Air pollution involving nitrogen dioxide exposure and wheezing bronchitis in children. International journal of epidemiology", 24, pp. 1147–1153 ,1995.
2. R. Kurtenbach, K. Vaupel, J. Kleffmann, U. Klenk, E.Schmidt and P.Wiesen," Emissions of NO, NO2 and PM from inland shipping", Atmos. Chem. Phys., 16,PP. 14285–14295, 2016.
3. E. Zampetti, A. Macagnano, S. Pantalei and A. Bearzotti, "PEDOT: PSS coated titania nanofibers for $NO_2$ detection: study of humidity effects "Sens. Actuators, B, 179,pp. 69-73,2013.
4. P. Zhu, F. Song, P. Ma, Y. Wang,C. Chen and J. Feng, "Morphology-controlled self-assembly of ferrocene-porphyrin based $NO_2$ gas sensor: tuning the semiconducting nature via solvent-solute interaction ",Journal of Materials Chemistry C, 00, pp.1-9,2016.

**Ghada Ayad Kadhim and Mahdi Hasan Suhail**

5.  J.Hong , N.Phiboolsirichit, S. Mubeen, M. Deshusses, A. Mulchandani and N. Myung"Electrical and gas sensing properties of polyaniline functionalized single-walled carbon nanotubes"Nanotechnology21, 075502 (7pp),2010.

6.  J. Li, Y. Lu, Q. Ye, M. Cinke, J. Han, M. Meyyappan, Carbon Nanotube Sensors for Gas and Organic Vapor Detection, Nano Letters, 3,pp.929-33,2003.

7.  M. R. dos Santos and H. P. de Oliveira," simple method for mass production of polypyrrole /carbon nanotubes hybrid artificial muscle", Quim. Nova,Vol. 37, No. 6, pp.1000-1003, 2014.

8.  S. G. Bachhav, D. R. Patil"Study of Polypyrrole-Coated MWCNT Nanocomposites for Ammonia Sensing at Room Temperature",Journal of Materials Science and Chemical Engineering, 3, pp.30-44,2015.

9.  R.L.Whitby, A. Korobeinyk,S.V. Mikhalovsky, T.Fukuda and T.Maekawa," Morphological Effects of Single-Layer Graphene Oxide in the Formation of Covalently Bonded Polypyrrole Composites Using Intermediate Diisocyanate Chemistry", Journal of Nanoparticle Research, 13, 4829-4837,2011.

10. A. Hamilton, " The Formation  and Characterisation of a Polypyrrole Based Sensor for the Detection of Urea", National University of Ireland Maynooth,2012.

11. T. Zhang, M. Nix, B.Yoo, M. Deshusses and N. Myung, "Electrochemically Functionalized Single-Walled Carbon Nanotube Gas Sensor",Electroanalysis 18, No. 12, pp.1153 – 1158,2006.

12. K. H. An, S. Y. Jeong, H. R. Hwang, Y. H. Lee," Enhanced Sensitivity of a Gas Sensor Incorporating Single-Walled Carbon Nanotube–Polypyrrole Nanocomposites" Adv.Mater., 16, pp. 1005–1009,2004.

13. N. R. Stradiotto, H. Yamanaka, M. Valnice and B. Zanoni," Electrochemical sensors: A powerful tool in analytical chemistry", J. Braz. Chem. Soc. ,14 no.2 . 2003.

14. R. A. Mohammed," An investigation of electropolymerization  and corrosion protection properties  of polypyrrole coating on carbon steel and  stainless steel", Scientific Research University of Baghdad,2014.

15. S.T. Navale, A.T. Mane, M.A. Chougule, R.D. Sakhare, S.R. Nalage and V.B. Patil, " Highly selective and sensitive room temperature NO2gas sensor based on polypyrrole thin films", Synthetic Metals 189 ,pp. 94–99,2014.

**Table 1.Values of the grain size (GS) calculated from XRD and AFM investigations**

| Sample | 2θ(Deg.) | GS (XRD measurement ) (nm) | Average GS (AFM investigation ) (nm) |
|---|---|---|---|
| Pure PPy | 24.6 | 36.0 | 40.75 |
| | 43.0 | 25.1 | |
| PPy/0.015 CNT | 25.0000 | 42.0 | 47.07 |
| | 43.0000 | 48.5 | |
| PPy/ 0.02CNT | 24.8500 | 60.3 | 96.74 |

**Table 2. shows the value of bonds for nanocomposite films through a FTIR analysis**

| Sample | N-H | C=C | C-H |
|---|---|---|---|
| Pure PPy | 3416.21 | 1558.52 1452.82 | 1176 |
| PPy/0.015 CNT | 3415.5 | 1561.87 1458.22 | 1174 877.761 |
| PPy/0.02 CNT | 3416.6 | 1564.52 1460.37 | 1176.22 880 |

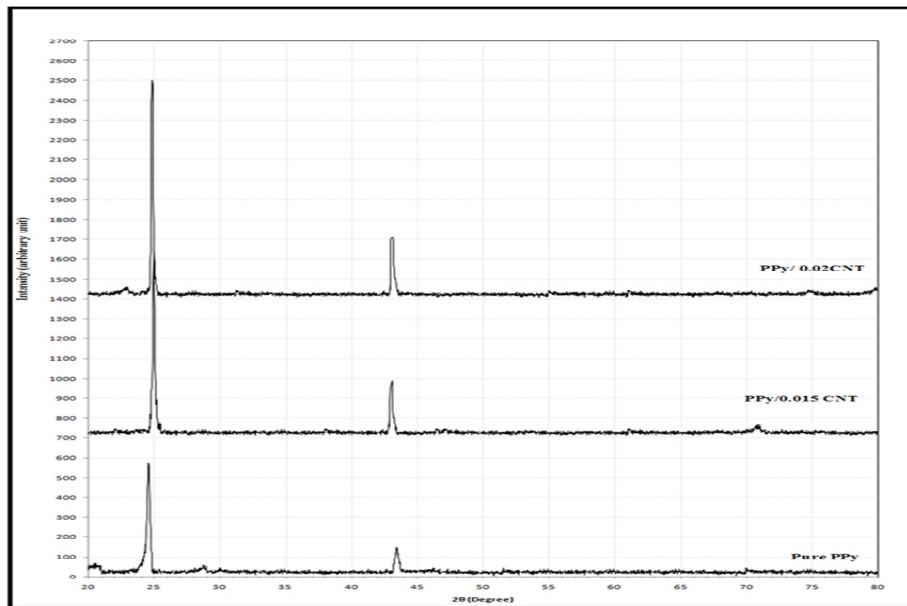**Ghada Ayad Kadhim and Mahdi Hasan Suhail**



**Figure 1.  XRD pattern of PPy and ( PPy/fSWNT) films**
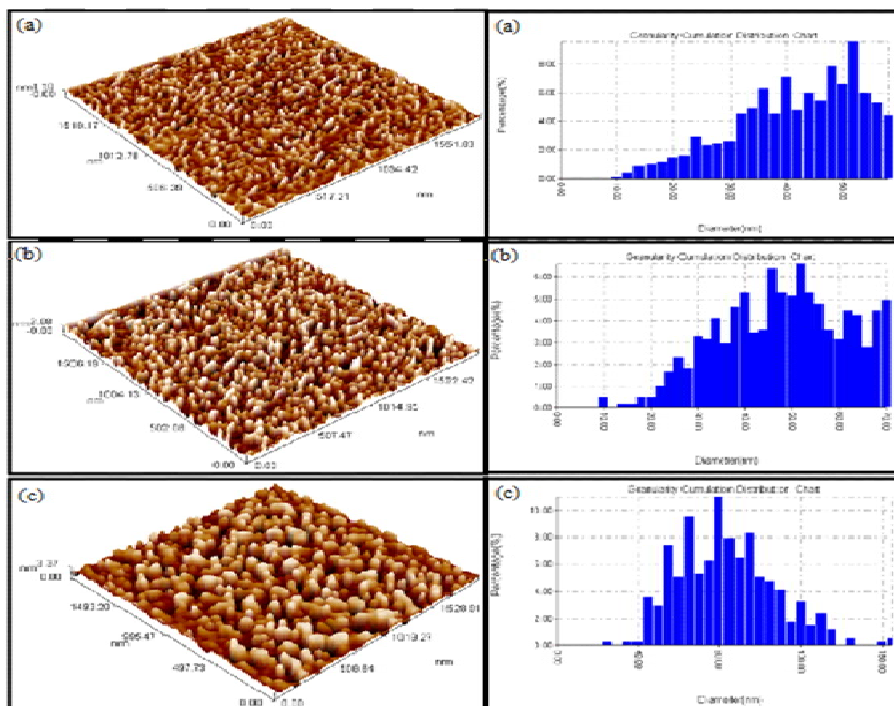


**Figure 2.3D imagesAFM and granularity distribution of nanostructured PPy and (PPy/fSWCNT) films**
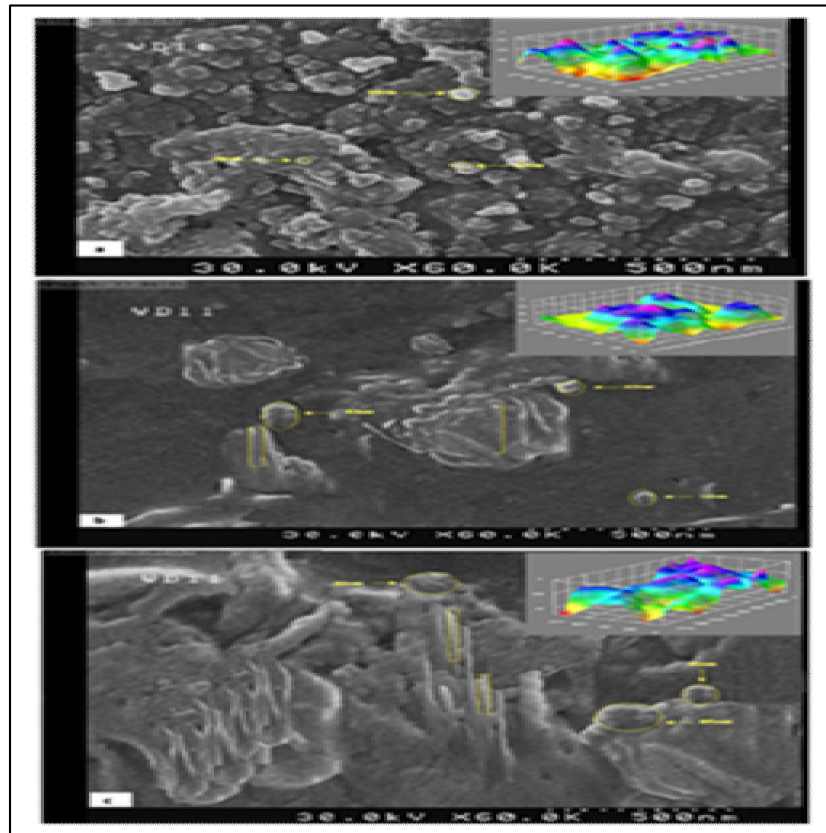
**Ghada Ayad Kadhim and Mahdi Hasan Suhail**



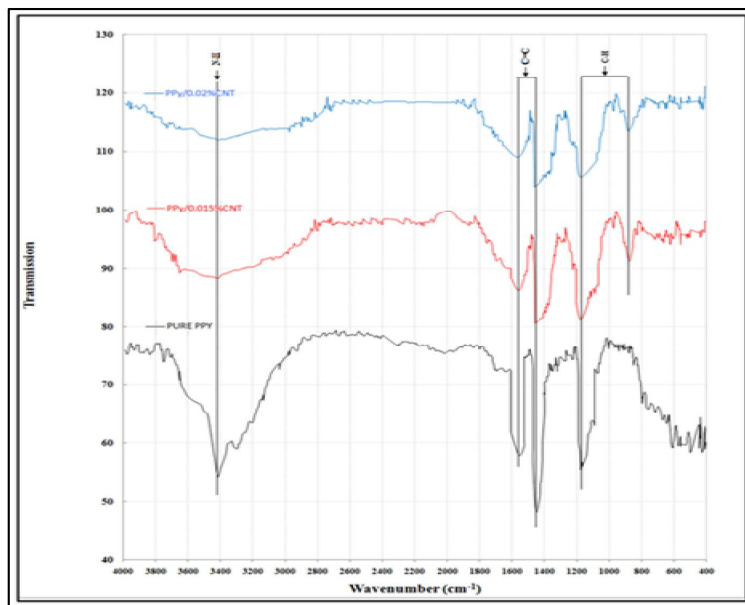**Figure 3.FESEM images of PPy and(PPy/f SWCNTs, scale bar 500 nm.**



**Figure 4. FTIRspectra of the PPy and (PPy/fSWCNT) films**

16542

**Ghada Ayad Kadhim and Mahdi Hasan Suhail**



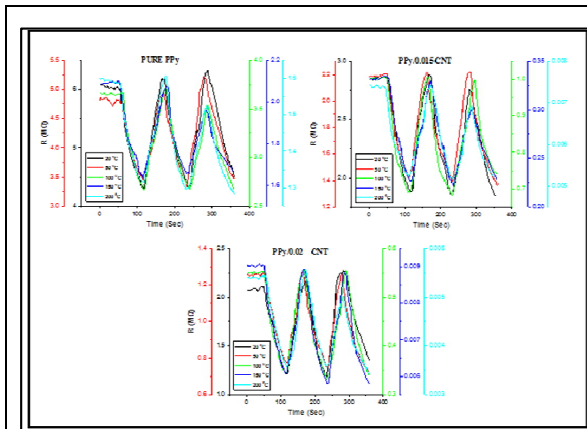**Figure 5. The Variation of resistance with time of PPy and (PPy /fSWCNT with (0.015 and 0.02)% CNT and different operation temperature at 30%NO₂**



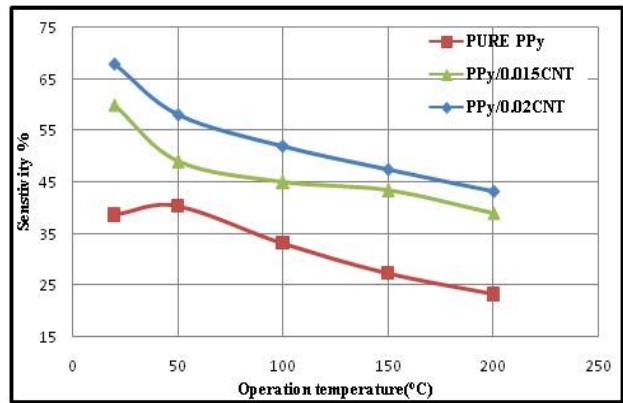**Figure 6. NO₂ gas sensitivity different operating temperature for PPy and (PPy/fSWNT) films with (0.015 and 0.02) CNT at 30%NO₂**
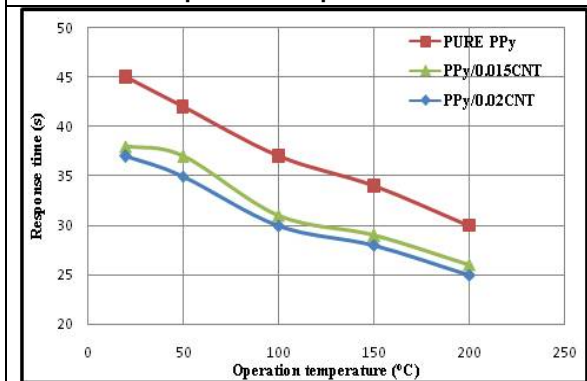


**Figure 7. response time different operating temperature for PPy and (PPy/fSWCNT) films with (0.015 and 0.02) CNT at 30%NO₂.**
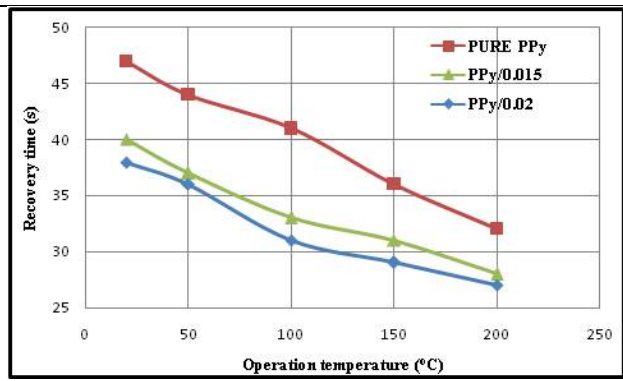


**Figure 8. NO₂ recovery time different operating temperature for PPy and (PPy/fSWNT) films with (0.015 and 0.02) CNT at 30%NO₂**

16543

**RESEARCH ARTICLE**

# Morphological and Morphometrical Characteristics of Lacrimal Apparatus in Adult Iraqi Local Breed Goat *(Caprus hircus)*

Nabeel Abd Murad AL-Mamoori[1*] and Mahdi Abdul-Kareem Atyia[2]

[1]Department of Anatomy & Histology, College of Veterinary Medicine, University of Al-Qadisiyah, Iraq.
[2]Department of Anatomy & Histology, College of Veterinary Medicine, University of Baghdad, Iraq.

*Address for Correspondence
**Nabeel Abd Murad AL-Mamoori**
Department of Anatomy & Histology,
College of Veterinary Medicine,
University of Al-Qadisiyah, Iraq.
Email:Nabeel.almamorri@qu.edu.iq

**ABSTRACT**

In the present study used ten fresh heads of adult indigenous goat *(Caprus hircus)* to study the lacrimal apparatus. The lacrimal apparatus divided into glandular part & ducts system. The glandular part consist of right & left lacrimal glands that produce tear. Whilst duct system consists of excretory duct, dorsal & ventral puncta, dorsal & ventral lacrimal canaliculi & the nasolacrimal duct.The lacrimal gland was elongated,oval, flattened, smooth & light brown in color. Each gland consist of body & appendage. The excretory ducts not easily noticed but could be recognized by using magnified.The dorsal & ventral puncta show in the medial canthus of the eyeball. It has slit-like opening with grayish black in color. Lacrimal canaliculi is start from the lacrimal puncta in the medial canthus of the eyeball & lead into two conical dilatation, which ended by short narrowing canaliculi.The Lacrimal sac consist from joined two lacrimal canaliculi together in the distal end to formation it.The nasolacrimal duct divided into three regions according to course of ducts.

**Keywords:** goat, lacrimal apparatus, lacrimal gland, lacrimal sac, nasolacrimal duct.

## INTRODUCTION

Goat is one types of ruminants, most important provide milk, meat, hair &leather. It spread in different region of the Iraq especially in north region(1). The eyeswere the sensory organ responsible for eyesight. It is well protected from damage by the bone which formed the orbit. It has accessory structures important in the process of maintaining eye, including the lacrimal gland, 3rd eyelid gland (2).The lacrimal apparatus in mammalian consist of many structures can be classify into production tear (lacrimal gland) & drain away tears (lacrimal puncta, lacrimal duct, lacrimal sac, nasolacrimal duct & nasolacrimal puncta)(2&3). The lacrimal fluid is maintaining the cornea & kept clear by diffusion

16544

tear on the corneal surface which act as nutrients of cornea, moisture & lubricate inner surfaces conjunctiva in upper & lower eyelids. Also act as protection of the eye from pathogens (4&5). The lacrimal gland is brown to pink in colour. It islocated on the dorsolateral side of the eyeball. The lacrimal fluid transport about duct system afterwashing the eye, into the nasal cavity& exit through the nasolacrimal punctum (2,3 &6). This study design to providing anatomical & morphometric information about the lacrimal apparatus in Iraqi local breed goat *(Caprus hircus).*

## MATERIALS AND METHODS

### Anatomical & morphometric Studies

In the present study used ten fresh heads of adult goat *(Caprus hircus).* It is collect immediately after slaughtering. The specimens inspection before & after slaughtering to insure the specimen healthy. After collection the specimen clean by washing in running tap water. It is kept in clean plastic containers & transport into the research laboratory to record the required relationship & measurement of the lacrimal apparatus. Make dissected to easy exposure lacrimal gland & duct system. It is described & record appearance features of lacrimal apparatus including the relationship, location, shape &colour. The finally step record the measurements by using electronic vernia, sensitive balance & snapshot the specimens by using Canon digital camera.

## RESULTS

The lacrimal apparatus in the adult indigenous goat *(Caprus hircus)* consists of glandular part & ducts system. The glandular part consists of right & left lacrimal glands. Whilst duct system consists of excretory duct, dorsal & ventral puncta, dorsal & ventral lacrimal canaliculi & the nasolacrimal duct.

### Lacrimal glands

The lacrimal glands locatedon the dorsolateral side of the eyeball. It is extend above dorsal rectus muscle & lateral rectus muscle. The lacrimal glandwas elongated,smooth (non-lobulated), flattened& light brown in color. Each gland was consist of two parts body&appendage. It has dorsal & ventral surfaces, cranial & caudal extremities, medial & lateral borders. The dorsal surface was convex. It is opposite the inner surface of the orbit & it takes the shape of the inner surface of it. Whereas the ventral surface was concave. It is opposite the convexity of dorsal surface of the eyeball (Fig.1&2 ). The body of lacrimal gland was flattened, elongated oval in shape & the cranial end narrowing than the caudal end (Fig.1&2 ). The mean weight, length, width, thickness & volume of body the right lacrimal gland was 1.121±0.181gm, 32.598±1.777mm, 17.015±1.040mm, 3.38±0.303mm & 1.5±0.182mm$^3$ respectively, while the mean weight, length, width, thickness & volume of body the left lacrimal gland was 1.138±0.140gm, 32.047±0.931mm, 16.278±0.869mm, 3.283±0.307mm & 1.5±0.182mm$^3$ respectively. The appendage of lacrimal gland was small rod elongated shape. It has dorsal & ventral surfaces, medial & lateral borders & cranial & caudal extremities(Fig.1&2 ). The mean weight, length, width, thickness & volume of appendage of the right lacrimal gland was 0.03±0.007gm, 11.738±2.137mm, 4.088±0.975mm, 1.704±0.137mm & 3±0.158mm$^3$ respectively, while the mean weight, length, width, thickness & volume of appendage the left lacrimal gland was 0.026±0.006gm, 11.184±1.602mm, 3.018±0.739mm, 1.394±0.245mm & 3±0.158mm$^3$ respectively.

### excretory ducts

The excretory ducts not easily noticed but could be recognized by using magnified. It is origin from the lacrimal glands. It is open in the conjunctival mucous membrane of the upper eyelids in the lateral canthus of the eyeball. The

ducts origin from the lateral border of the caudal part of the of body gland near from beginning of appendage part & the mean number of ducts were 1-2 ducts(Fig.3&4).

### Lacrimal puncta

We observeddorsal & ventral puncta in the medial canthus of the eyeball. It has slit-like opening with grayish black in color(Fig.5).The diameter & distance of punctum from medial canthus of right & left dorsal puncta were 1.121±0.071mm, 1.16±0.114mm, 3.961±0.177mm, 4.086±0.151mm respectively, while the right & left ventral puncta were 1.16±0.062mm, 1.205±0.093mm, 4.053±0.379mm & 4.218±0.361mm respectively.

### Lacrimal canaliculi

It is start from the lacrimal puncta in the medial canthus of the eyeball & lead into two conical dilatation, which ended by short narrowing canaliculi (dorsal & ventral) (Fig.6).The mean length of the right & left dorsal lacrimal canaliculi were 8.555±0.481mm & 8.361±0.516mm respectively, whereas the right & left ventral lacrimal canaliculi were 11.045±0.438mm & 11.48±0.925mm respectively.

### Lacrimal sac

We observed the two lacrimal canaliculiin each side joined together in the distal end to formation thelacrimal sac. It wassituated in the small depression the lacrimal fossa in lacrimal bone. The distal end continuous with nasolacrimal duct(Fig.6). The mean length of right & left lacrimal sac were 23.676±1.436mm & 19.645±1.909mm respectively.

### Nasolacrimal ducts

The nasolacrimal ducts was beginning from the distal end of the lacrimal sac. It extend ventrally on the medial side of the lacrimal, maxillary & incisive bones.  Itpass on the medial side of the lateral wall of the nasal cavity.  The mean total length of the right & left nasolacrimal duct in was 89.71±3.260mm & 91.953±2.983mm respectively. The nasolacrimal duct could be divided into three regions according to course of ducts(Fig.7).The proximal part runin osseous canal that formed by lacrimal & maxillary bone. The mean length of the right & left the proximal part was 26.178±3.188mm & 30.411±2.182 respectively. The middle part was consist of mucous membrane. It extend after the duct leave the osseous region into the junction with the skin of the vestibule of the nasal cavity. The mean length of the right & left the middle part in goat was 40.553±1.915mm & 38.556±1.813mm respectively. The distal part was referred to cutaneous part supported by nasal cartilage. It was smaller part of the nasolacrimal duct ended by the external orifice of the nasolacrimal duct. The mean length of the right & left the distal part in goat was 22.941±1.696mm & 22.983±2.481mm respectively. The external orifice of the nasolacrimal duct has slit-like shape & located ventral to the alar fold of the ventral nasal concha. The mean diameter of right & left was 2.813±0.225mm & 2.876±0.097mm respectively.

## DISCUSSION

In the current study the lacrimal glands in goat located on the dorsolateral aspect of the eyeball. The lacrimal gland limited between the two bones of the orbit & the eyeball. This results agree with the findings (3;7;8;9;10 & 11) that found the lacrimal gland situated in the dorsolateral area eye ball. The lacrimal glands in goat take light brown in color. This results accordance with (12;13;14;15 & 16) incamel, goat, sheep & donkey the lacrimal gland hasbrown in color. Butdiffer with (17; Diesem, (1968)& Elmahadi, (2017)show the color of lacrimal gland in camel, horse & dog was light red. Whilst Maala, et al., (2007)reported the lacrimal gland of the buffalo was red to pink in colour.

**Nabeel Abd Murad AL-Mamoori and Mahdi Abdul-Kareem Atyia**

This difference in the color of the lacrimal glands among the animals because of differ the species of animals. Also the amount of blood remaining in the blood vessels that supply the gland effect on the colour of gland. We observed the lacrimal gland consist of two parts body&appendage. This results accordance with (3;7;11;12;13;15;19;20 &21) show the lacrimal glands in goat, cattle, buffalo, camel & dog were divided into two parts main body& accessory appendage. While differ with (22)reported the lacrimal gland in sheep & goat undivided. It was consist of one compact part. Also (23 & 24)explain the lacrimal gland inEuropean bison & alpaca was undivided & uniform in shape.This alterationmay be because ofdiffer species of animal.

Our results in goat reported thatthe mean weight, length, width, thickness & volume of body the left lacrimal gland was 1.138±0.140gm, 32.047±0.931mm, 16.278±0.869mm, 3.283±0.307mm & 1.5±0.182mm$^3$ respectively. Whilst the mean weight, length, width, thickness & volume of body the right lacrimal gland was 1.121±0.181gm, 32.598±1.777mm, 17.015±1.040mm, 3.38±0.303mm & 1.5±0.182mm$^3$ respectively,This results agreement with (16) show the lacrimal gland in sheep  has 3.58mmthickness, while (15) explain the length of lacrimal gland in donkey was 32 mm.  But differ with While (15) show the lacrimal gland in goat has mean width & length 20mm & 26.5mm respectively. Whilst (25)reported that the mean weight, width, length, thickness & volume of the lacrimal gland in goat was about 1.63 gm, 25mm, 20 mm. 4 mm& 22 mm$^3$ respectively.Also dispute  with (16) reported the lacrimal gland in sheep the mean of weight 1.48gm, length 26.98mm& width20.11mm.

Dispute with (11 & 26) reported that  the lacrimal gland in dog  the mean weight 1.4-1.2 gm. The mean length, width, thickness of lacrimal gland was 14 mm, 2.42mm, & 0.49 mm respectively. Whilst (27) described the lacrimal gland in dog had mean length15.2mm & width 13.8mm.This alteration may becaused by species, genus & age of the animals. We observed the appendage of lacrimal gland in a goat have mean 0.03±0.007gm weight, 11.738±2.137mm length, 4.088±0.975mm width, 1.704±0.137mm thickness &3±0.158mm$^3$volume.This results differ with (15)show the appendage of lacrimal gland in goathas10mm length &7mm width. The presentstudy find the excretory ducts of lacrimal gland in goat had a slit-like opening & take the same color of the conjunctival mucosa of upper eyelids. This results agreement with (16)show the excretory duct of the lacrimal gland in sheep opens in mucous membrane of conjunctiva on the internal surface of the upper eyelid. (28)reported in camel the main lacrimal ducts were small & open into the superior conjunctiva. But differ with (29)in camelseem the excretory ducts of lacrimal gland difficult to find but were noticed by black color. The current study finds that the puncta in goat had slit-like opening & take grayish black in color. This result was accordance with (10;16;22 & 30)explain most mammalshave two lacrimal puncta in the medial canthus of eyes & the colour of puncta differs. But differ with (28;31 & 32)showthe lacrimal puncta in camel was absent & the lacrimal ducts start blindly.

In the present study observed the mean diameter & distance of puncta from medial canthus of right & left dorsal puncta were 1.121±0.071mm, 1.16±0.114mm, 3.961±0.177mm & 4.086±0.151mm respectively, while the right & left ventral puncta were 1.16±0.062mm, 1.205±0.093mm, 4.053±0.379mm & 4.218±0.361mm respectively.This result agreement in some measurements & differ in other with (22)show that in goat the diameter & distance of punctum from medial canthus of right & left dorsal puncta were 1.21±0.13mm, 1.08±0.06mm, 4.94±0.22mm & 4.81±0.27mm respectively, while the right & left ventral puncta were 1.54±0.15mm, 1.50±0.14mm, 3.63±0.16mm & 3.75±0.16mm respectively. In the present study seen the lacrimal ducts in goat, the lacrimal ducts were started from the lacrimal puncta in the medial canthus of the eyeball & reached into the lacrimal sac. This resultsaccordance with(16) in sheep reported that there were two lacrimal canals begin from ventral & dorsal lacrimal puncta. Whiledispute with (16 & 31) showin goat, sheep &donkey have two lacrimal ducts starts by a small dorsal & ventral openings, but in camel, the lacrimal ducts start blindly. We observed  the dorsal canaliculi were similar to that explained by (30) in goat explain  that the dorsal & ventral canaliculi were 8 mm in length. But disagreement with (22) reported that in goat & sheep the mean length of right & left ducts (dorsal & ventral) were 13.64mm, 13.71mm, 10mm & 10.07respectively. Whereas(33) in catshow the length of dorsal 2.5mm &4.5mm ventral lacrimal ducts.

The lacrimal sac was situated in the small depression of lacrimal fossa of the lacrimal bone. This resultssimilar with (22) explain that in goat the two lacrimal canaliculi merged together during course to formation the lacrimal sac. (10;22;30 &34) explain that in sheep, goat & buffalo the dorsal & ventral canaliculi were join into formation a small dilatation lacrimal sac. It was situated in the orbit on the fossa of the lacrimal bone in the medial angle of the eyeball. The nasolacrimal duct was divided into three parts proximal, middle & distal. This resultsaccordance with(30;35;36 & 37)in goat & horse show the nasolacrimal duct extended from the lacrimal sac into the nasal cavity & divided into three parts, while dispute with(10) show the nasolacrimal duct divided into two parts inside & outside osseous canals. Whilst (38) explain the nasolacrimal duct in dog divided in four regions. The current study see that the mean total length of the right & left nasolacrimal duct in goat was 89.71±3.260mm & 91.953±2.983mm respectively. This finding disagreement with (10) in buffalo show the total length left & right nasolacrimal duct was about 232 mm and 235 mm, whilst (16) in sheep explain the mean length of duct was 125.7mm, (28) in camel reported mean length of nasolacrimal duct was 210-230 mm.

# REFERENCES

1- AL-Sadi, H I. *Animal wealth in Iraq and means of improving it.* University of Mosul press: 203-204, 1980.

2- Akers, R M, and D M Denbow. *Anatomy and physiology of domestic animals.* 2nd Ed. Wiley Blackwell, 2013.

3- Dyce, K M, W O Sack, and C J G Wensing. *Textbook of Veterinary 4th edition.* Philadelphia. London. New: W.B. Saunders Company, 2010.

4- Cochran, P E. *Veterinary anatomy and physiology: A clinical laboratory manual.* 2nd Ed. Delmar, Cengage Learning, 2011.

5- Davidson, H J, and V J Kuonen. "The tear film and ocular mucins." *Vet Ophthal*, 7 2004: 71-77.

6- Pasquini, C, T Spurgean, and S Pasquini. *Anatomy of domestic animal.* 7th Ed. SUDZ publishing, 1997.

7- Sisson, S, and J D Grossman. *The anatomy of domestic animals.* Philadelphia. London. Toronto: W.B. Saunders Company, 1975.

8- Getty , R. *The anatomy of domestic animals.* Philadelphia. London. UK: W.B. Saunders Company, 1975.

9- Maala, Ceferino P, Ruth A Cartagena, and Grace D Ocampo. "Macroscopic, histological and histochemical characterization of the lacrimal gland of the Philippine Water Buffalo (Bubalus bubalis)." *Philipp. J. Vet. Med*, 44 2, 2007: 69-75.

10- Al-Bayati, Mustafa kamal. *Aanatomical and histological study of the lacrimal gland and nasolacrimal apparatus in indigenous buffalo (bubalus bubalis).* thesis: vet. Med. Baghdad university, 2015.

11- AL-Obeady, Walaa Fadil. *Morphometrical and histochemical comparative study of lacrimal gland and conjunctival glands between dog (Canis familaris) and ram (Ovis aris).* Thesis: Vet Med University of Baghdad, 2016.

12- Aslan, Kadir, Ibrahim Kurtul, Gursoy Aksoy, and Sami Ozcan. "Gross anatomy of the lacrimal gland (gllacrimalis) and its arterial vascularization in the fetus of zavot-bred cattle." *Kafkas Univ. Vet. Med. J*, 11 1, 2005: 47-49.

13- Ibrahim, Z H, A B Abdalla, and D I Osama. "A gross anatomical study of the lacrimal apparatus of the camel (Camelus dromedarius)." *Sudan Journal of science and technology*, 2006: 1-8.

14- Chengjuan, G, M Jinghong, Y Shiyuan, and W Jianlin. "Anatomical and histochemical characteristics of the lacrimal glands in bactrian camels." *Chinesejournalof Anatomy*, 2008.

15- Alsafy, M A. "Comparative morphological studies on the lacrimal apparatus of one humped camel, goat and donkey." *Journal of Biological Sciences* , 10(3) 2010: 224-230.

16- Abbasi, Mohsen , Hamid Karimi, and Ahmad Gharzi. "Preliminary anatomical and histological study of lacrimal gland in Lori sheep." *Journal Veterinary Science & Technology*, 5 1, 2014: 154-158.

17- Bradley, O C. *The topographical anatomy of the dog.* 5th Ed. Edinburgh. Tweeddale Street,: Oliver and, 1948.

18- Diesem, D V. "Gross anatomic structure of equine and bovine orbit and its contents." *American Journal of Veterinary Research*, 29 1968: 505-510.

19- Pinard, C L, M L Weiss, A H Brightman, B W Fenwick, and H J Davidson. "Normal anatomical and histochemical characteristics of the lacrimal glands in the american bison and cattle." *Anat. Histol. Embryol*, 32 2003: 257-262.

20- Budras, K D, P R Greenough, R E Habel, and C K Mulling. *The atlas of bovine anatomy.* 2nd Ed. Schlutersche.Germany: Hans-BOckler Allee, 2011.

21- Almamoori, N A & Atyia M A "Anatomical & Morphometrical Study of the Lacrimal Apparatus in Adult Iraqi Local Breed Cattle (Bos taurus)"I*ndian Journal of Natural Sciences* 9  51, 2018: 15634-15644.

22- Daryuos, M M, and N S Ahmed. "Comparative morphological and morphometrical study of lacrimal apparatus of Awasi sheep and black goat." *AL-Qadisiyah Journal of Veterinary Medicine Sciences*, 1 11, 2012a: 123-133.

23- Klećkowska-Nawrot, J, R Nowaczyk, K Goździewska-Harłajczuk, K Krasucki, and M Janeczek. "Histological, histochemical and fine structure studies of the lacrimal gland and superficial gland of the third eyelid and their significance on the proper function of the eyeball in alpaca (Vicugna pacos)." *Folia Morphol Via Medica*, 4 2, 2015: 195-205.

24- Kleckowska-Nawrot, Joanna, Renata Nowaczyk, Hariajczuk Gozdziewska, Tomasz Szara, and Katarzyna Olbrych. "Histology, histochemistry and fine structure of the Harderian gland,lacrimal gland and superficial gland of the third eyelid of the Europeanbison, Bison bonasus bonasus (Artiodactyla: Bovidae)." *Zoologia*, 32 5, 2015: 380-394.

25- Al-ramahei, M A. "Anatomical and histological study of lacrimal and nictitans glands in black goat (capius hircus)." *Baghdad Vet. Med.*, 2008: 1-150.

26- Mirhish, Shaker M, and Walaa F AL-Obeady. "Anatomical and histological study of the lacrimal gland of the adult male dog (Canis familaris)." *Global Journal of Bio-science & Biotechnology*, 5 4, 2016: 520-524.

27- El-naseery, Nesma I, Eman I El-behery, Hanaa M El-Ghazali, and Enas El-Hady. "The structural characterization of the lacrimal gland in the adult dog (Canis familiaris)." *BENHA VETERINARY MEDICAL JOURNAL*, 31 2, 2016: 106-116.

28- Elmahadi, Huyam Elmahadi Mustafa. *Studies on morphological and histochemical seasonal changes on the lacrimal apparatus of the One-humpedcamel (Camelusdromedarius).* Thesis: Vet Me Sudan University of Science and Technology, 2017.

29-Elmahdi, Huyam-Elmahdi M, Tahany M Elnagy, and Zarroug H Ibrahim. "Anatomical and morphometric studies on the dromedary camel lacrimal gland in relation to seasonal environmental changes." *Journal of Agricultural and Veterinary Sciences*, 10 1, 2017: 27-38.

30- Shadkhast, M, A S Bigham, N Vajdi, and Z Shafiei. "Lacrimal apparatus system in goat (Capra aegagrus hircus): Anatomical and radiological study." *Asian Journal of animal and veterinary advances*, 3 6, 2008: 2008.

31- Saber, A S, and F M Makady. "Anatomy and clinical studies on the lacrimal system in camel (Camelus dromedarius)." *Assuit Veterinary Medical Journal*, 19 1987: 12-17.

32- Sadegh, Amin Bigham, Mohammad Shadkhast, Siavash Sharifi, and Ahmadreza Mohammadnia. "Lacrimal apparatus system in One-humped camel of iran (Camelus dromedarius): Anatomical and radiological study." *Iranian Journal Of Veterinary Surgery*, Vol.: 2 No.: 5 2007: 75-80.

33- Breit, S, W Kunzel, and M Oppel. "The course of the nasolacrimal duct in brachycephalic cats." *Anat. Histol. Embryol*, 32 2003: 224-227.

34-Ali, mohammad Abbas. *Anatomical and histological study of local buffalos eye (Bubalus bubalis).* thesis: Vet Med University of Basrah, 2009.

35- Seo, Kang-moon, Tae-cheon Kang, Heungshik S Lee, In-se Lee, and Tchi-chou Nam. "Anatomic and radiographic studies of the lacrimal drainage system in Korean native goat." *Korean J Vet Res*, 36(1) 1996: 23-29.

36- Claudia Noller, Claudia, Wolfgang Henninger, Dietrich Gronemeyer, Ruth Hirschberg, and Klaus Budras. "Computed tomography anatomy of the normal feline nasolacrimal drainage system." *Veterinary Radiology & Ultrasound*, 47 1, 2006: 53-60.

37- Spadari , A, G Spinella , A Grandis , N Romagnoli , and M Pietra . "Endoscopic examination of the nasolacrimal duct in ten horses." *Equine vet. J.*, 43 2, 2011: 159-162.

38- Vieira, Nivea M, et al. "Epiphora assessment of dogs with dacryocystography and computed tomography." *Pesq. Vet. Bras.*, 35 12, 2015: 989-996.

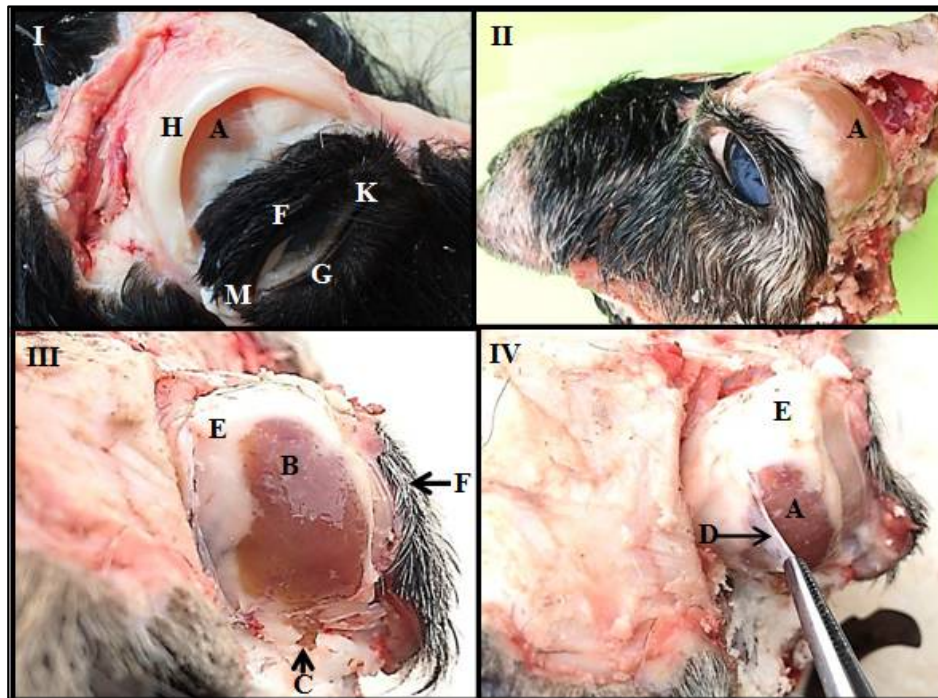**Nabeel Abd Murad AL-Mamoori and Mahdi Abdul-Kareem Atyia**

**Fig.1. I Lateral, II caudolateral, III caudal &caudodorsal views of the Head goat Show: A-** Lacrimal gland. **B-** Body of lac. gland. **C-** Appendage of lac. gland. **D-**Periorbital connective tissue. **E-**Adipose tissue. **F-** Upper eyelid. **G-** Lower eyelid. **H-** Frontal cartilage. **K-** Medial canthus. **M-** Lateral canthus
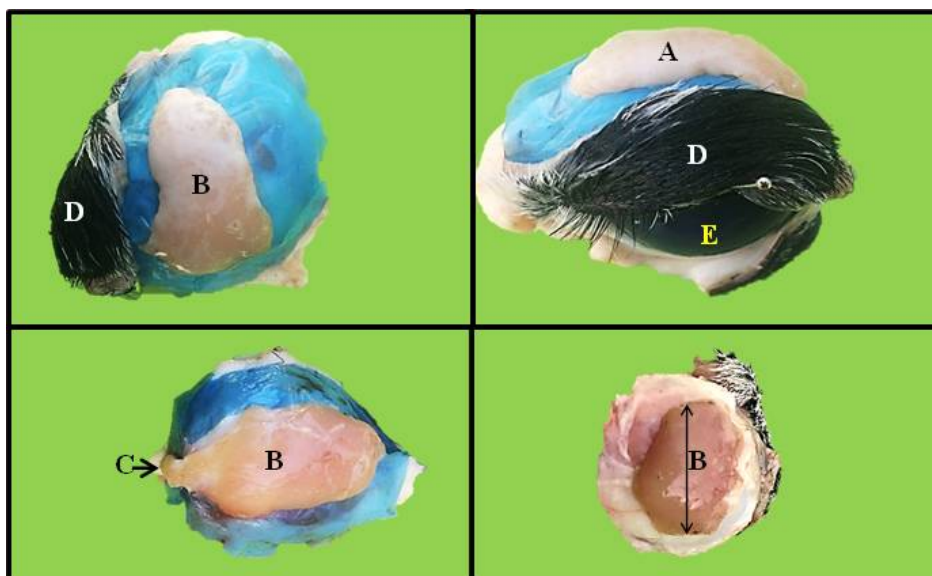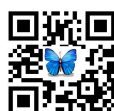


**Fig .2. Lacrimal gland in goat Show:A-**Lacrimal gland.**B-**Body of lacrimal gland. **C-** Appendage of lacrimal gland.**D-**Upper eyelid. **E-**Eyeball

**Nabeel Abd Murad AL-Mamoori and Mahdi Abdul-Kareem Atyia**
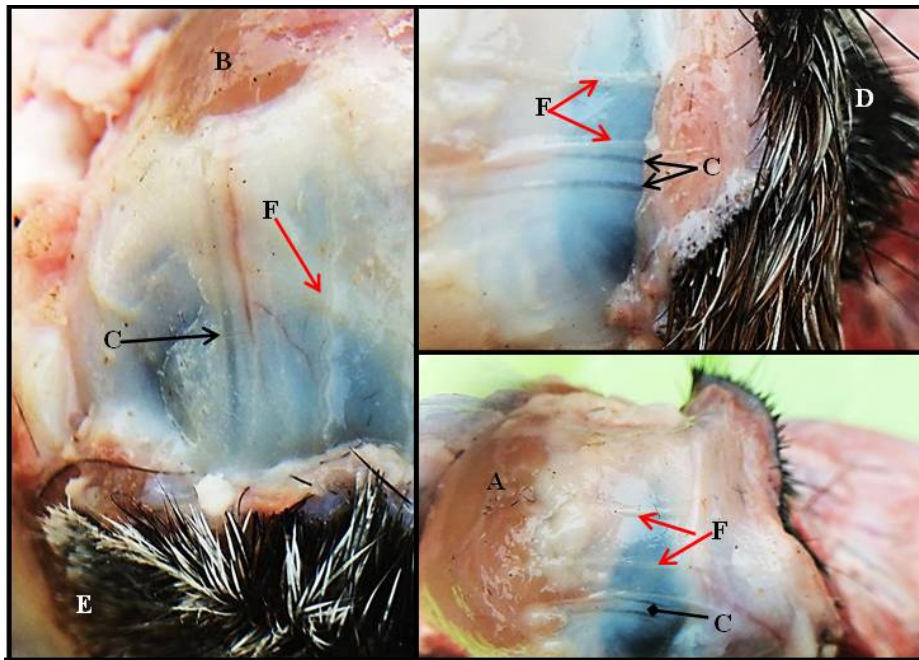
**Fig.3. Major excretory ducts of lacrimal gland in goat Show: A-**Lacrimal gland. **B-**Caudal part of body lacrimal gland. **C-**Major excretory duct of lac. gland. **D-**Upper eyelid. **E-** Lateral canthus. **F-** Nerve supply



**Fig. 4. Conjunctival surface of the upper eyelid (Fornix) in goat Show: A-**One opening of the major excretory duct of lacrimal gland. **B-**Conjunctival surface of upper eyelid (Fornix). **C-**Upper eyelid. **D-**Medial canthus. **E-** Lower eyelid. **F-** eyeball.
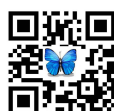
**Nabeel Abd Murad AL-Mamoori and Mahdi Abdul-Kareem Atyia**
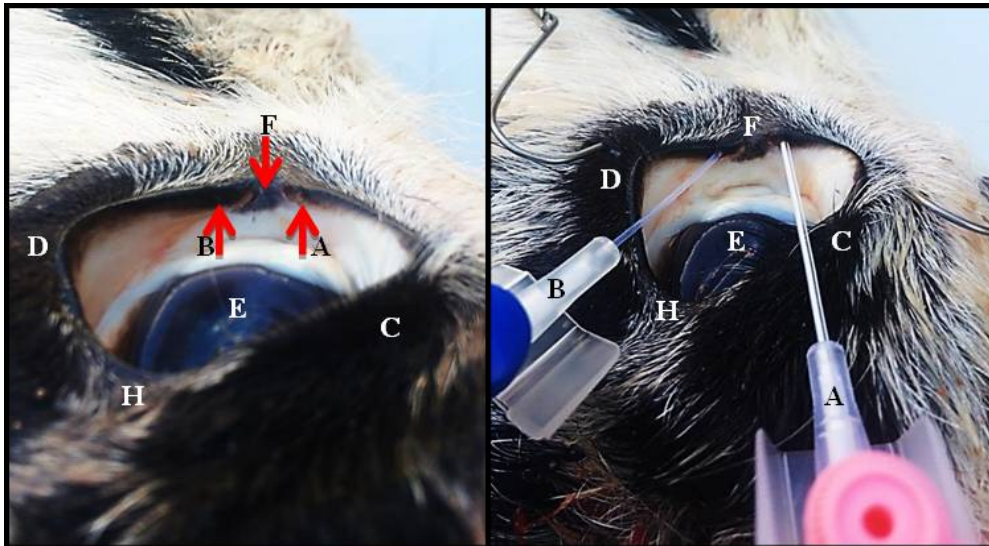
**Fig.5. Lateral view of the eye goat Show: A-** Dorsal punctum, **B-** Ventral punctum. **C-** Upper eyelid. **D-** Lower eyelid, **E-** Eyeball, **F-** Medial canthus,  **H-**Lateral canthus.
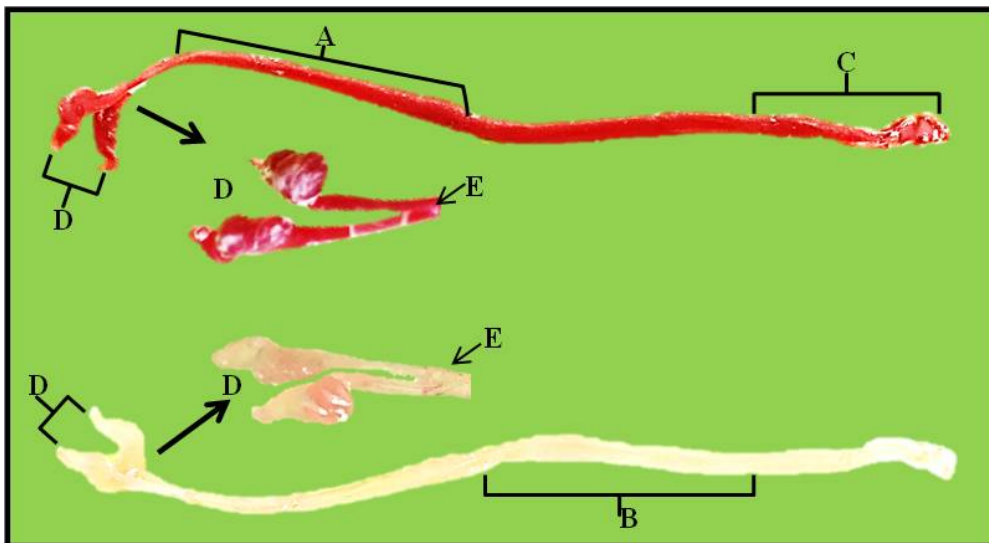


**Fig.6.Resin cast of nasolacrimal duct in goat Show:A-**Proximal part(bony part).**B-**Middle part(Mucous part). **C-** Distal part(Cutaneous part).**D-**Lacrimal canaliculi**E-**Lacrimal sac.

**Nabeel Abd Murad AL-Mamoori and Mahdi Abdul-Kareem Atyia**



**Fig.7. Course of nasolacrimal duct in goat Show:A-**Proximal part(bony part).**B-**Middle part(Mucous part). **C-** Distal part(Cutaneous part).**D-**nasolacrimal opening. **E-**Nasal opening. **F-** Floor nasal cavity. **G-** Roof nasal cavity.

**RESEARCH ARTICLE**

# Physiological Study in *Giardia lamblia* Infected Mice after Oral Supplement with *Cladophora glomerata* Extract

Shatha Khudhaier Abbas*, Ghaidaa Husain Abd – Ali and Firas Salih Abd-Ulhadi

Department of Biology, College of Science, Mustansiriyiah University, Baghdad, Iraq.

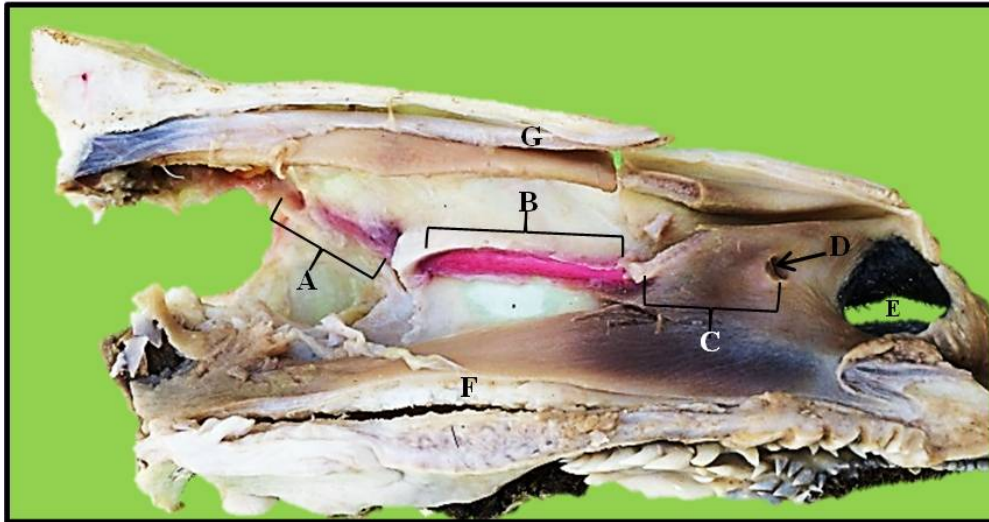*Address for Correspondence
**Shatha Khudhaier Abbas**
Department of Biology,
College of Science,
Mustansiriyiah University, Baghdad, Iraq.
E-mail: dr.Shatha@uomustansiriyah.edu.iq

**ABSTRACT**

This research was conducted to investigate the hematological and hepatic effectsin *Giardia lamblia* infected mice after oral supplement with *Cladophora glomerata* extract (CGE). The parasite was obtained from the stool samples of the patients who visited AL-Kadimiya teaching hospital after verifying their parasite infection with laboratory samples. Freshwater *Cladophora glomerata* was collected of October 2017 from bottom of AL-Najaf sea zone .Eighteen white Swiss mice (male and female) each weighing (16–22 gm) were obtained from the national center for research and drug control with average age between (5-12 weeks).All mice given $1 \times 10^3$ cell of cyst and trophozoite, after (4-8 hours) the stool of al mice were examined and after sure infected by *Giardia* mice were divided into four groups each group contain 20 mice then inoculated as follow: Group 1: inoculated with 1ml from metronidazole orally by using stomach tube (St) at single dose per/ day.Group 2: inoculated with 1ml of the 128 mg/ml of the CGE extract orally by using (St) at single dose per/ day.Group 3: inoculated with 1ml of the 256 mg/ml of the CGE extract orally by using (St) at single dose per/ day.Group 4: inoculated with 1ml of (PBS) orally by using (St) at single dose per/ day (positive control). Each mouse was anaesthetized with chloroform vapour and pooled blood from mice in each group, was collected by cardiac puncture  into heparinized tubes for haematological studies – packed cell volume  (PCV), Haemoglobin (Hb), number of leukocytes (WBC), neutrophil, lymphocyte, eosinophil and monocyte . Serum was separated from the blood by centrifuging (3000 rpm) for a period 15 minute. Liver enzyme determinations in serum for GOT and GPT; and ALK. The results of present study show that therapeutic substances caused all effective in the treatment, that best effect was full killed of flaggy to parasite on the sixth day followed by an 256 mg/ml CGE extract and 128 mg/ml CGE extract full killed on the seventh day was compared with control positive .The results also showed a significant increased  (P< 0.05) in the mean of W.B.C. ,P.C.V and Hb in all infected group in compare with positive control. On other hand, there was no significant difference (P>0.05) in men of W.B.C., P.C.V and Hb in group 2 and 3 in compare with group 1 (Metronidazole

16554

group). The results of Differential white blood cell showed a significant increased (p≤0.05) in the mean of Lymphocyte, Neutrophil, Eosinophil and Monocyte in mice supplement with Metronidazole (500mg/ gm) and mice supplement with CGE extract (128 mg/ml) compared with mice in control positive and CGE extract (256 mg/ml) groups.The results of biochemical tests showed a significant decreased (p≤0.05) in mean of liver enzymes GPT, GOT and ALK in infected mice compared with positive control group. Our findings lead us to propose that bioactive materials of the *C. glomerata* was responsible for the anti-giardial activity and  have potential for use as therapeutic agents against giardiasis.

**Keywords:** *Cladophora glomerata*, *Giardia lamblia,* biochemical, mice, laboratory.

## INTRODUCTION

*Giardia lamblia* (syn. *Giardia duodenalis*, *Giardia intestinalis*) is a protozoan parasite which replicates exclusively in the lumen of the small intestine of a wide variety of mammalian hosts (1,2). Giardiasis is a protozoal disease caused by many species of Giardia one of them is Giardia lamblia (Syn. G. Duodenalis or G. Intestinalis), is one of the most common causes. World wide of intestinal infection in human and domestic animals like dairy calves, dog and cats associated with substantial economic losses (3).Life cycle of *Giardia lamblia* consisting of two stages , the infective stage cyst is resistant to environmental factors and responsible for the transmission of *Giardia lamblia* , and trophozoit is appear- shaped cited by Espelage (4).The specific mechanism of *Giardia lamblia* pathogenesis lead to diarrhea causing symptoms there are associated diarrhea including vomiting, dehydration, malabsorption and malnutrition , the nutritional stages of *Giardia* in the host is very imptant in young children with poor nutrition who was suffering failure tothrine(5). Cladophora is one of the largest filamentous green-algal genus and has a widespread distribution in Caspian Sea Coast(6). freshwater alga *Cladophora glomerata* may be a good source of fatty acids and others bioactive agents(7). Extract of *Cladophoraglomerata*have showed some activity against bacteria fungi and parasite (8,9).The aims of this study was to find out substance efficient for the infection of Giardiasis.

## MATERIALS AND METHODS

### Sours of access to parasite

The parasite was obtained from the stool samples of the patients who visited AL-Kadimiya teaching hospital after verifying their parasite infection with laboratory samples. Methods was used to isolated the parasite then cysts and trophozoits were suspended in phosphate buffer saline (PBS.7.2) and the final concentration was attended (10).

### Culture media

The media (HSP-1) was prepare according to (11) add penicillinb500 mg/ ml and streptomycin 50 mg/ml then add 0.05 ml from serum of human to the media . Put in each tube 5ml of sterile culturemedia (HSP-1). Then add 0,1 ml of stook that have $1\times10^3$cell of cyst and trophozoite.

### Collection and diagnosis of *Cladophora glomerata*

Freshwater *C.glomerata* was collected of October 2017, Collected manually from the water channel around Al-Jadriya camp University of Baghdad. The harvested macro algaewere stored in plastic bags and transported to thelaboratory. Biomass was rinsed with fresh water to eliminatethere materials such as sand, shells, etc. Themacroalgae were stored in the laboratories and dried at50 °C under ventilation in an oven and then groundedto powder form by the blender, and stored in the refrigerator at a temperature of  (4C°) until the will be used.

### Preparation of *Cladophora glomerata* extract (CGE)

The method (12) was depended on the preparation of the extracts of green algae.20 gram of dried weight sample was put in the thimble that was transferred to specific cylinder in the soxhlet apparatus and extracted with 250ml of methanol  solvent at the temperature of 64.7 °C for 3-4 hours until the become the solvent colorless. The extract and filter was taken with the filter paper. After that drain the residual leach ate in the incubator at 37 C °for 48 hours to obtain the dry powder and store in the refrigerator until the used.

### Preparation of laboratory animals

Eighteen white Swiss mice (male and female) each weighing (16–22 gm) were obtained from the national center for research and drug control with average age between (5-12 weeks).All mice given $1 \times 10^3$ cellof cyst and trophozoite, after (4-8 hours) the stool of al mice were examined and after sure infected by*Giardia* mice were divided into four groups each group contain 20 mice then inoculated as follow:

Group 1: inoculated with 1ml from metronidazole orally by using stomach tube (St) at single dose per/ day for seven days.
Group 2: inoculated with 1ml of the 128 mg/ml of the CGEextract orally by using (St) at single dose per/ day for seven days.
Group 3: inoculated with 1ml of the 256 mg/ml of theCGE extract orally by using (St) at single dose per/ day for seven days.
Group 4: inoculated with 1ml of (PBS) orally by using (St) at single dose per/ day (positive control) for seven days.

### Hematological test

Each mouse was anaesthetized with chloroform vapour and pooled blood from mice in each group, was collected by cardiac puncture (12) into heparinized tubes for haematological studies – packed cell volume (PCV), Haemoglobin (Hb), number of leukocytes (WBC), neutrophil, lymphocyte, eosinophil and monocyte according to the method described by Dacie and Lewis (1991) (13).

### Biochemical assays

Serum was separated from the blood by centrifuging (3000rpm) for a period 15 minute.Liver enzyme determinations in serum were based on the methods OF Reitman and Frankel (14)1F for GOT and GPT; and Bessey, *et al.* (15)for AlkP.

### Statistical analysis

Data were expressed as mean ± standard deviation. Student's t-test and one-way analysis of variance test were employed for statistical comparison at (P=0.05).

## RESULTS AND DISCUSSION

The results of present study show that therapeutic substances caused all effective in the treatment, Table (1) showed thenumber of cysts raised in mice during different time period. We conclude from table (1) that best effect was full killed of flaggy to parasite on the sixth day followed by an 256 mg/ml CGEextract and 128 mg/ml CGEextract full killed on the seventh day was compared with control positive.Laungsuwon&Chulalaksananukul2014(16)indicate that extracts of C. glomerata and M. floccosa exhibited appreciable antimicrobial activity and could be a source of

valuable bioactive materials for health products.Orhan*et al.*(17)  reports for the first time antiprotozoal activity of some Turkish marine and freshwater algae, as well as a target-based antiplasmodial screening for the identification of *P. falciparum* FabI inhibitors from aquatic and marine macrophytes. The extracts of *C. glomerata* and *U. lactuca* efficiently inhibited the FabI enzyme (a crucial enzyme of the fatty acid system of *P. falciparum*, to find out whether FabI was their target. None of the extracts were cytotoxic towards mammalian cells.

The results also showed a significant increased ($P < 0.05$) in the mean of W.B.C. , P.C.V and Hbin all infected group in compare with positive control as shown in table (2). On other hand, there was no significant difference ($P > 0.05$) in man of W.B.C., P.C.V and Hb in group 2 and 3 in compare with group 1 (Metronidazole group). This results is agree with Prannapus*et al.* 2006 (18) who reviled that  packed cell volume of the male rats treated with 1.0 g/kg CGE extract was significantly lower than the controls (p 0.05), the level was in the standard range for rat hematocrit.  The results of Differential white blood cell showed a significant increased ($p \le 0.05$) in the mean of Lymphocyte, Neutrophil, Eosinophil and Monocyte in mice supplement with Metronidazole (500mg/ gm) and mice supplement withCGE extract (128 mg/ml) compared with mice in control positive and CGE extract (256 mg/ml) groups table (2). Prannapus*et al.* 2006 (18)  also showed that numbers of white blood cells were not significantly different in the male rats treated with 1.0 g/kg CGE extract from the controls, and this revealed normal function of the hematological system in male rats treated with CGE extract. So we suggest that the increased in differential white blood cell cause by immune response to antigen of parasite. The results of biochemical tests showed a significant decreased ($p \le 0.05$) in mean of liver enzymes GPT, GOT and ALK in infected mice compared with positive control group and this results may be due to the Giardiasis.Saeid*et al.* (19) suggest the possibility of using the *Cladophoraglomerata*as a novel source of natural antimicrobial and antioxidant agents for pharmaceuticalindustries.Our findings lead us to propose that bioactive materials of the *C. glomerata* was responsible for the anti-giardial activity and  have potential for use as therapeutic agents against giardiasis.

# REFERENCES

1.  Faubert, G. 2000. Immune response to Giardia duodenalis. Clin. Microbiol. Rev. 13:35–54.
2.  Espelegye, W.; Heiden,M.; Stark,k. &Alpers,k.(2010).Characters and risk factors for symptomatic Giardia Lamblia infection in Germany. Bio.Med. Cent. Publ. Health.10: 41-49.
3.  Thompson, R. C. A., (2000). Giardiasis as are emerging infectous disease and its zoonotic pontential. Int. J. Parasitol,  30:1259-1267.
4.  Espeleye ,W.; Hiden,M.; Stark,K. &Alpers,K. (2010). Characters' and risk factors for symptomatic Giardia Lamblia infection in germany . Bio.Med.Cent.publ.Health.41-49.
5.  FAO(2014). Multicriteriaanagement of based ranking for risk management of food borne parasites , microbiological risk assessment series 23, food safety and codex unit food and agriculture organization of the united nation Rome Italy
6.  SaeidSoltani, Sara Saadatmand, RamzanaliKhavarinejad and TaherNejadsattari(2011). Antioxidant and antibacterial activities of Cladophora glomerata (L.) Kütz. in Caspian Sea Coast, Iran. African Journal of Biotechnology Vol. 10(39), : 7684-7689.
7.  Joanna, F.; Alicja, K.; Bous£awa, S. ; Katarzyna,F.&  Izabela N. (2017). In vivo studies and stability studyof CLADOPHORA GLOMERATA extract asa cosmetic active ingredient . ActaPoloniaePharmaceutica ñ Drug Research, Vol. 74 No. 2 pp. 633-641.
8.  Rag A.; Hemaiswarya ,S.; Kumar, N.; Sribhar, S.&Rengasamy, R.( 2002). A perspective on the biotechnological potential of micro algae j. Crit. Rev. Microbial. 34(2):77-88.
9.  John,P.B.; Microslan,F.; Mario, H.P.; Cerald, B. & Fernand, G.N.( 2008). Cyan bacterialtoxin as allochemia with potential application as algaecides herbicides and insecticides .Mar .Drugs 6: 117-146.
10. Robert-thompson,I.C.; Stevens,D.P.; Mahmoud,A.A, & Warren, K. (1976). Giardiasis in mouse an animal modle. Gastroenterology, 71:57-61.

11. Meyer,E.A.( 1976). Giardia Lamblia isolation and axenic cultiration . Exp. Parasitol. 39:101-105.

12. Deshmuk,S.D. &Borle, M.N.( 1975). Studies on the insecticidal properties of Enthno. Pharmacol. 37(1):11-18.

13. Dacie, J.V. and& Lewis, S.M. (1991). In Practical Haematology 7th edition ELBS with Churchill Livingstone. Longman group UK 1991. : 5 – 82.

14. Reitman, S. & Frankel, S. A . (1957). Colorimetric method for the determination of serum glutamic oxalacetic and glutamic pyruvic transaminases. Am. J. Clin. Pathol. 28 : 56-63.

15. Bessey, 0. A., Lowry, 0. H. & Brock, M. J. (1946).Method for rapid determination of alkaline phosphatase with 5 cubic millimeters of serum. J. Biol. Chem. 164 : 321-329.

16. Laungsuwon R. &Chulalaksananukul W. (2014). Chemical composition and antibacterial activity of extracts from freshwater green algae, CladophoraglomerataKützing and Microsporafloccosa (Vaucher) Thuret. J. BioSci. Biotech. 3(3): 211-218.

17. Orhan, I.;Sener, B.; Atıcı, T. ; Brun, R.;Perozzo,R.&Tasdemir, D.(2006).  Turkish freshwater and marine macrophyte extracts show in vitro antiprotozoal activity and inhibit FabI, a key enzyme of Plasmodium falciparum fatty acid biosynthesis. Volume 13, Issue 6: 388-393.

18. Prannapus F., Kanokporn S., YuwadeeP.I&Salika A. (2006). Toxicological evaluation of C. glomerata and M. floccosa in a albino rats . SOUTHEAST ASIAN J TROP MED PUBLIC HEALTH. Vol 37 (suppl 3).

19. Saeid S.; Sara Saad A.; Ramzan A.;  Khavari N.&Taher N. (2011). Antioxidant and antibacterial activities of Cladophora glomerata (L.) Kütz. in Caspian Sea Coast, Iran. African Journal of Biotechnology . 10(39): 7684-7689,

**Table 1. The number of cysts raised in mice during different time period**

| Group | Time period ( days)/ Mean ± SD | | | | | | | |
|---|---|---|---|---|---|---|---|---|
| | 1 | 2 | 3 | 4 | 5 | 6 | 7 | 8 |
| Metronidazole | 37±0.6 | 26±1.38 | 14.5±1.26 | 7.0±0.67 | 2.4±0.31 | 0.0±0.00 | 0.0±0.0 | 0.0±0.0 |
| CGE extract (128 mg/ml) | 40±0.43 | 35±0.30 | 26±0.37 | 17.0±0.47 | 9±0.31 | 4±0.3 | 0.00±0.0 | 0.0±0.0 |
| CGE extract (256 mg/ml) | 37.5±0.3 | 29±0.57 | 21±0.37 | 13±0.6 | 6±0.36 | 2,3±0.66 | 0.00±0.0 | 0.0±0.0 |
| Positive control | 39 ± 0.37 | 40 ± 0.41 | 42 ± 0.35 | 44 ± 0.32 | 45.9± 0.29 | 46.5 ±0.37 | 47±0.23 | 47.9 ±0.01 |

**Table.2.Hematological values of infected mice treated with Metronidazole andextract of *C. glomerata*at doses of 128 and 256 mg/kg for seven days compared with positive controls.**

| Groups | Hb gm/dl | P.C.V. (%) | Total white blood cell count(cell/mm3) | Differential white blood cell (%) | | | |
|---|---|---|---|---|---|---|---|
| | | | | Lymphocyte | Neutrophil | Eosinophil | Monocyte |
| Metronidazole (500mg/ gm) | 12.5 ± 0.5 | 39.0 ± 0.01 | 9.31 ± 0.31 | 5.80±0.21 | 5.01±0.21 | 0.49±0.08 | 0.51±0.05 |
| CGE extract (128 mg/ml) | 11.0 ± 0.3 | 36.0 ± 0.01 | 10.94 ± 0.08 | 5.90±0.22 | 4.61±0.14 | 0.41±0.02 | 0.50±0.05 |
| CGE extract (256 mg/ml) | 11.7 ± 0.16 | 37.0 ± 0.05 | 9.65 ± 0.45 | 4.70±0.28 | 3.01±0.15 | 0.31±0.01 | 0.31±0.02 |
| Positive control | 10.5 ± 0.02* | 33.0 ±0.06* | 8.01 ± 0.54* | 4.60±0.26 | 3.97 ±0.21 | 0.38±0.09 | 0.41±0.02 |

* = significant difference at $p < 0.05$

**Table .3. Biochemical values of infected mice treated with Metronidazole and extract of** *C. glomerata* **at doses of 128 and 256 mg/kg for seven days compared with positive controls.**

| Groups | ALK (IU/L) | GPT(IU/L) | GOT(IU/L) |
|---|---|---|---|
| Metronidazole(500mg/ gm) | 6.9±61 | 0.39±80 | 0.38±9.0 |
| CGE extract (128 mg/ml) | 6.30±97.5 | 0.36±10.7 | 0.37±10.5 |
| CGE extract (256 mg/ml) | 6.0± 109 | 0.30±9.6 | 0.30±9.6 |
| Positive control | 8.50±132* | 0.45±15.3* | 0.45±15.3* |

* = significant difference at $p < 0.05$

**RESEARCH ARTICLE**

# Comparative Histomorphological and Histochemical Study of Thyroid Gland in Adult Males of Guinea Pigs (*Cavia porcellus*) and Albino Rats (*Rattus norvegicus*)

Abbas. L. Batah[1] and Shakir. M. Mirhish[2] *

[1]Department of Anatomy and Histology, College of Medicine, University of Misan, Iraq.
[2]Department of Anatomy and Histology, College of Veterinary Medicine, University of Baghdad, Iraq.

*Address for Correspondence
**Shakir. M. Mirhish**
Department of Anatomy and Histology,
College of Veterinary Medicine,
University of Baghdad, Iraq.

**ABSTRACT**

The present study was carried on twenty adult males of each Albino Rats and Guinea pigs to study the histomorphological and histochemical features of thyroid gland.Morphologically the thyroid gland was consisted of two lobes of reddish brown in color; in Albino Rats, the lobes were located on ventrolateral side of trachea connected caudally with isthmus, appeared as conical or oval in shape. In Guinea pigs were situated laterally on each side of trachea without isthmus and appeared as elongated or oval in shape. Histologically and Histochemical, the thyroid gland in both animals was surrounded by capsule, in Albino Rats; capsule was composed of one layer and in Guinea pigs it was composed of two layers of collagens fibers. Each lobe of thyroid gland was consisted of different size and shape of follicles (large, medium size and small follicles). In Albino Rats the lining epithelium of follicles was ranged from simple cuboidal in rest state to columnar epithelium in active state. In Guinea pigs it was ranged from simple cuboidal to squamous in rest state and cuboidal in active state. The Parafollicular cells in thyroid gland of Albino Rats were concentrated in the center of the lobe, appeared as oval or rounded in the shape, located interfollicular in position and some located between the basement membrane and follicular cells but not contact with colloid. In Guinea pigs, Parafollicular cells were appeared in all parts of the thyroid gland, located between the multiple follicles (interfollicular position) and few number of Parafollicular cells were located between the follicular cells (intrafollicular position)reach to lumen of the follicle. The Parafollicular cells and the colloid in lumen of follicles were exhibited moderate to strong PAS reaction.The statistical analysis revealed that there is significant deference at (p < 0.05) in the mean thickness of capsule and diameters of different follicles between the left and right lobe of thyroid gland in the Albino Rats and Guinea pigs, and there is significant deference at (p < 0.05) in the mean thickness of capsule, diameters of different follicles and height of epithelium between Albino Rats and Guinea pigs.

**Keywords:** Histological, histochemical, thyroid gland, Guinea pigs, Albino Rats.

**Abbas.L. Batah and Shakir. M. Mirhish**

# INTRODUCTION

Rodents are one of the largest orders of mammals, most rodents are herbivorous but some are omnivorous and some prey on insects. Guinea pigs (*Cavia porcellus*) are small laboratory animals, which constitutes a small suborder (Hystricomorphic)belong to the family Caviidae and the genus Cavia were probably first introduced into Europe from SouthAmerica [1].The Guinea pigs are excellent experimental subjects for physiological and histological studies due to many reasons, their body weight, size, ease to be handled and they adapt rapidly in laboratory situation. The main diet of Guinea pigs is the grass [2]. A laboratory rats (*Rattus norvegicus*) belong tosuborder Myodonta, family Muroidea and the genus Rattus,have served as an important animal model for research in psychology and biomedical sciences. The diet of Rats is dried food,berries, nuts, fresh fruits, and vegetables[3]. The thyroid gland is the largest and the first recognized endocrine glands during development in vertebrates [4]. It is an unique among the endocrine gland in that it stores large amount of hormone in an intact form within extracellular compartments in the center of follicles and small quantities of hormones in intracellular site[5]. The thyroid gland exhibits similar follicular structure, although there are certain gross, histological and ultrastructural variations amongst the species. Thyroid responses to environmental and nutritional influences do differ amongst domestic animals [6].

The thyroid gland consists of numerous follicles of various sizes which form thefunctional and histological unit of the thyroid gland. It iscomposed of three principal components; the lining follicular, parafollicular cells and the luminal colloid,The follicular cells vary in height, depending on the state of activity of the follicle. The lining epithelium changes from squamous or low cuboidal in the resting state and to cuboidal or columnar in the active state [7].The follicular cells produce thyroid hormones (triiodothyronine, T3 and tetraiodothyronine,T4which playing an important roles for reproduction, differentiation and migration of cells during embryonic stages[8]. The parafollicular cells are secreted mainly calcitonin hormone which regulate the calcium level in the blood and few other regulatory peptide of the thyroid such as somatoststin, chromogranin A and neuron specific enolase that are involved in intrathyroidal regulation of follicular cells[9]. According to these functions and others, a lot of studies had been done on this gland of different species of mammals despite of this fact, Therefore the present investigation was aimed to: Throw a spot of light on the histological structure of the thyroid gland in Guinea pigs ((*Cavia porcellus*) and Albino Rats(*Rattus norvegicus*)and to compare between them.

# MATERIALS AND METHODS

Twenty healthy adult males of eachGuinea pigs (*Cavia porcellus*) and Albino Rats ((*Rattus norvegicus*) were used in the present study,the mean weight of albino Rats was 347.60 ± 4.21 gm and the guinea pigs was712.90 ± 13.01 gm.The animals were brought from the animal house of veterinary medicine of Basra University, the animals were kept alive in plastic cage, given feed and water ad libitum and acclimated for two weeks before the research.The animals euthanized byusing inhalation of chloroform in a closed container [10]. Guinea pigs and Albino Rats were humanly sacrificed and thyroid gland was dissected out.The shape, color and location were recorded before the fixation and the photographs of the thyroid was taken to depict the gross anatomy by using digital camera Sony cyber-shot (14.2 mega pixel).For histological and histochemical study samples of thyroid gland was fixed in 10% neutral buffered formaldehyde and sectioned serially at 5µm. Sections were stainedwith Hematoxylin and eosin and forhistochemical studies PAS and Masson Trichrome stain [11].The histological sections of this study were examined by using light microscope type (Olympus/ Japan), with different magnifications (X4; X10 and X40),then the sections were photographed by using (Olympus/ Japan) microscope and digital camera,An ocular micrometercalibrated with stage micrometerwas used for histological parameters which include the thickness of capsule, diameter of different size follicles and the height of lining epithelium [12]. By using the Statistical Analysis Systemprogram, the data were expressed as mean ± standard errors (SE) and p- value < 0.05 was considered statistically significance [13].

**Abbas.L. Batah and Shakir. M. Mirhish**

## RESULTS

Morphologically the thyroid gland was consisted of two lobes of reddish brown in color; in Albino Rats, the lobes were located on ventrolateral side of trachea connected caudally with isthmus, appeared as conical or oval in shape. In Guinea pigs were situated laterally on each side of trachea without isthmus and appeared as elongated or oval in shape (Fig. 1, 2). The histological and histochemical results were showed that the thyroid gland of Albino RatsandGuinea pigs was surrounded by a thin capsule of dense irregular connective tissue, in Albino Rats; the capsule was composed of single layer of fine collagen fibers, fibroblasts with spindleshape, elastic fibers and blood vessels.In Guinea pigs; the capsule composed of two layers; the inner layer was composed of bundles of collagens fibers with spindle-shape fibroblast and the external layer that composed of loose collagens fibers intermixed with adipose tissues (Fig. 3, 4).

From the capsule of the thyroid gland in both Albino Rats and Guinea pigs thin trabeculae contained blood vessels extended into the parenchyma of the gland and divided it into small lobules(Fig. 5, 6).Each lobule was consisted of an aggregation of a various sizes of thyroid follicles and three main sized of follicles were identified; the large, medium and small-sized follicles and the thyroid follicles were appeared with different shapes were found rounded, oval, polygonal and irregular follicles, the oval and rounded follicles were predominated, each follicle was surrounded by a basement membrane, inter follicular connective tissue and a network of capillaries,In Albino Rats the larger follicles tend to be peripherally located while the smallest follicles tend to be centrally,In Guinea pigs; the large follicles interspersed with small and medium-sized follicles were located at peripheral under the capsule, very few number of large follicles intermixed with small and medium sized follicles were distributed in the center of gland(Fig. 7, 8).The connective tissues of the capsule and the trabeculae in the thyroid gland of both animals were exhibited moderate reaction with Periodic Acid Schiff stain (Fig. 9, 10). The mean thickness of capsule and diameters of different follicles in the left and right lobe of thyroid gland of both animals were as in (Table 1).The statistical analysis revealed that there is significant difference at ($p < 0.05$) in themean thickness of capsule and diameters of different follicles between the left and right lobe of thyroid gland in each animal (Table 1). The lining epithelium of folliclesin Albino Rats was ranged from simple cuboidal in rest state to columnar epithelium in active state(Fig. 11, 12). In Guinea pigs it was ranged from simple cuboidal to squamous in rest state and cuboidal in active state(Fig. 13, 14).

The height of epithelium of folliclesin Albino Rats and Guinea pigs were as in (Table 1).The Parafollicular cells in thyroid gland of Albino Rats were concentrated in the center of the lobe, appeared as oval or rounded in the shape, equal or larger than the follicular cells in the size, light stain cytoplasm, spherical nucleus and occur singly or small group, located interfollicular in position and some located between the basement membrane and follicular cells but not contact with colloid. In Guinea pigs, Parafollicular cells were appeared in all parts of the thyroid gland, rounded or ovalin shape, acidophilic cytoplasm, dense nucleus,clearnucleoli, slightly larger than the follicular,located between the multiple follicles (interfollicular position) and few number of Parafollicular cells were located between the follicular cells (intrafollicular position)reach to lumen of the follicle.(Fig.15, 16).The thyroid follicles in the thyroid gland of Guinea pigs and Albino Rats were filled with a variable amount of homogenous eosinophilic colloid substance(Fig. 11, 13).The colloid substances and parafollicular cells were exhibited variable reaction for Periodic Acid Schiffstain(Fig. 9, 10). The statistical analysis revealed that the means thickness of capsule and diameters of different follicles in the right and left lobe of thyroid gland in Guinea Pigs were greater than those of Albino Rats significantly at ($p < 0.05$).The means height of lining epithelium in Albino Rats wasgreater than those of Guinea pigs significantly at ($p < 0.05$)(Table2).

## DISCUSSION

The thyroid gland in both animals was consisted of two lobes of reddish brown in color; in Albino Rats, the lobes were located on ventrolateral side of trachea connected caudally with isthmus, appeared as conical or oval in shape

16562

and extend along the fourth or fifth tracheal rings as described by [14] in Ratand disagree with [15 in mice who showed that the right and left lobe of thyroid gland extended along the first three tracheal rings.In Guinea pigs were situated laterally on each side of trachea without isthmus and appeared as elongated or oval in shape and extend along sixth tracheal rings, these results agree with[16] in adult male mongooses.  The histological results showed that the thyroid gland in Albino Rats and Guinea pigs were basically identical and similar to those found in domestic animals[17]. The thyroid gland in both species was surrounded by a thin capsule of dense irregular connective tissue, in Albino Rats; the thyroid gland was surrounded by single layer of fine collagen fibers, fibroblasts with spindleshape, elastic fibers and blood vessels as described by[18] in Rats. In Guinea pigs; the capsule composed of two layers of collagens fibers intermixed with amount of adipose tissues and fewer elastic fibers these results accord with[19] inWeasel (*Herpestes  javanicus*). From the capsule of the thyroid gland in both Albino Rats and Guinea pigs thin strands of trabeculae which contained blood vessels extended into the parenchyma of the gland and divided it into small lobules, each lobule was consisted of aggregation of three main sized of follicles were identified; the large, medium and small-sized follicles with rounded, oval, polygonal and irregular shape, each follicle was surrounded by a basement membrane, inter follicular connective tissue and a network of capillaries these results coincide with[20] inadult male African giant rat (Cricetomys gambianus) and [21] in grasscutter (*Thryonomys swinderianus*).

The capsule and the trabeculae in both animals were exhibited moderate reaction with Masson's Trichrome, Periodic Acid Schiff stain imply that the capsule is rich in collagen and carbohydrate.  The statistical analysis revealed that the means thickness of capsule in right and left lobes of Guinea pigs were greater than those of Albino Rats significantly at ($p < 0.05$)such differences may be due to the species variation. The statistical analysis revealed that the means diameter of large, medium  and small follicles of  right and left lobes in guinea pigs were greater than those of albino Rats significantly at ($p < 0.05$), this variation may be due to the activity of the thyroid gland in different animal species. The follicular diameter is an indicator of follicular activity, which is inversely proportional to the follicular diameter [22].The histological structure variations of thyroid gland may be related to the physiological adaptation [23]. In this study the isthmus in Albino Rats appeared as glandular tissue and showed various sizes and shapes of follicles this agree with[24] in African Giant Rat and [16]) in adult male mongooses.

While in Guinea pigs,the isthmus was absent, the same result reported by [21]in African grasscutter (*Thryonomys swinder anus*) and [25] in red pandas (*Ailurusfulgens*) this difference may be due to species variation [26].The predominant lining epithelium different follicles in Albino Rats was variable from simple cuboidal epithelium in reststate to low columnar in active state of thyroid gland as described by [27] n Rats. In Guinea pigs lining epithelium of follicles was variable from simple cuboidal epithelium to squamous epithelium in restingstate while was simple cuboidal in active state these results accord with [20] in adult male African giant rat (Cricetomys gambianus).The follicular lining and basement membrane of the follicular cell were positive for Periodic Acid Schiff stains imply that the follicular lining and basement membrane were rich in carbohydrate. The statistical analysis was revealed that the means height of epithelium in right and left lobe of Albino Rats were greater than those of Guinea pigs these differences may be due to that the thyroid gland activity was differ in the two animals Parafollicular cells in thyroid gland of Albino Rats were concentrated in the center of the lobe, appeared as oval or rounded in the shape, equal or larger than the follicular cells in the size, light stain cytoplasm, spherical nucleus and occur singly or small group, located interfollicular in position and some located between the basement membrane and follicular cells but not contact with colloid.

In Guinea pigs, Parafollicular cells were appeared in all parts of the thyroid gland, rounded or ovalin shape, acidophilic cytoplasm, dense nucleus, clearnucleoli, slightly larger than the follicular, located between the multiple follicles (interfollicular position) and few number of Parafollicular cells were located between the follicular cells (intrafollicular position)reach to lumen of the follicle these results accord with [27] in Rats and [21] in African grasscutter (*Thryonomys swinderianus*) and [28] ingolden hamsters.The Parafollicular cells were exhibited moderate to strong reaction to Periodic Acid Schiff stain as described by [20] in African giant pouched rats.  Thyroid follicles in both animals were filled with homogeneous and eosinophilic colloid, the distribution of colloid substance in the

follicles was variable, some follicles were filled completely with colloid; some follicles were filled with small amount and some follicles were devoid the colloid material depend on state of the gland. The colloid substances appeared variable reaction with Periodic Acid Schiff stain, some follicles were exhibited strong reaction with magenta color and some were exhibited weak reaction depend on distribution of the colloid substance and activity of the gland these results coincide with [28] in Rabbits and [24] inAfrican giant pouched rats.

## REFERENCES

1. Wagner, J.E. and Manning, P.J. (1976).The biology of the guinea pig. Academic PresNew York NY.
2. Rowlands, I.W. and Weir, B.J. (1974).The biology of hystricomorph rodents.Symp. Zool. Soc. London UK: 34.
3. Vandenbergh, J. G. (2000). "Use of House Mice in Biomedical Research,*ILAR Journal.* 41 (3): 133–135.
4. Dickoff, W. W. and Darling, D.S.(1983). Evolution of thyroid function and its control in lower vertebrates *Am. Zool.,* 23: 697-707.
5. Braverman,L.E.(1996). Evaluation of thyroid status in patients with thyrotoxicosis,*Clin. Chem.* 42(1):174-178.
6. Bhardwaj, R. L., Rajpu, R; Pathak, V and Thakur, K (2006).Animal ComparativeIndiananatomy of the thyroid gland of small ruminantsJournal of Sciences76(1): 46-47.
7. Louise, T and Waugh. A. (2002).Thyroid gland in veterinary physiology andapplied anatomy ,text book for veterinary nurses and technicians:Pp:70-75.
8. Kress, E., Samarut, J. and Plateroti, M. (2009). Thyroid hormones and the control of cell proliferation or cell differentiation: paradox or duality, *Mol. CellEndocrinol.,*313: 36–49.
9. Sawicki, B. (1995).  Evaluation of the role of mammalian thyroid parafollicularcells(review).  ActaHistochem., 97: 389-399.
10. Adeyemu, O. and Oke, B.O. (1990). Companies of the Testicular and  EpididymisProtein of the AGR(Cricitomysgambians) andLaboratory Rats. Journal of Tropical Vegetarian 8: 17-27.
11. Bancroft, J. D. and Stevens, A. (1990). Theory and Practice of HistologicalTechniques.3rd Ed., Churchill Livingston, London, UK.Pp: 109-121.
12. Luna,L.G.(1968) Manual of Histological ,3rdedition ,Grow-Hill book.
13. Sas. (2012). Statistical Analysis System, User's Guide. Statistical,Version 9.1th ed. SAS.Inst. Inc. Cary.N.C. USA.
14. Dintzis,S.Mand perle,K.M.D.(2018).Endocrine systemin:Treuting,P.M;Dintzis,S.M and Monting.K.S.Comparative Anatomy and Histology .Amouse.Rat and Human Atlas,2end edition,Elsevier,Academic press.uk.Pp:251-271.
15. Choksi, N.Y; Jahnke, G.D; St Hilaire, C and Shelby, M. ( 2003).Role of thyroid hormones in human and laboratory animal reproductive.health Birth Defects Res. B Dev. Reprod. Toxicol.68:479–491.
16. Tadjalli, M and Faramarzi, A.(2016).Gross anatomy of the Thyroid and Parathyroid glands in Indian Gray Mongoose *(Herpestes edwardsii)*.Cibtech Journal ofZoology,5(1):1-5.
17. Dellmann, H. D. (1981).Endocrine system. In: Textbook of Veterinary Histology.Dellmann and Brown (ED). 2nd ed. Lea and Febiger. Pp:83-87.
18. Elkalawy, S. A. M; Abo-Elnour, R. K; El Deeb, D.F and Yousry, M. M. (2013). Histologicaland immunohistochemical study of the effect of experimentally induced hypothyroidism on the thyroid gland and bone of male albino rats.The Egyptian Journal of Histology, 36:92-102.
19. Al-Aamery, R.A and Dauod, H.A. (2016).Anatomical and Histological Study  of  thyroid Gland in Weasel (*Herpestes javanicus*),*Ibn Al-Haitham J. for Pure* and*Appl. Sci,*29(1):40-48.
20. Enemali, F.U; Hambolu,J.O; Alawa,J.N and Anosike,I.V.(2016).Gross anatomical,Histological and Histochemical studies of thyroid gland of African Giant Rat (Cricetomys gambianus-water house). *Journal of Pharmacy and Biological Sciences*, 11(4):40-43.
21. Igbokwe C.O. (2010). Gross and Micoscopic Anatomy of Thyroid Gland of the wild African Grass cutter in Southern Nigerian, *Enviromental Journal of Anatomy* 14 (1): 5-10.
22. Banks, W.J. (1993).Applied Veterinary Histology. "Endocrine System"3rd ed.  Mosby Year Book.Baltimore Boston London.Pp: 408-427.

23. Igbokwe,C.O and Ezeasor,D.N.(2015). Gross and Morphometric Anatomical Changes of the Thyroid Gland in the West African Dwarf Goat (*Capra hircus*) During the Foetal and Post-Natal Periods of Development; Nig.Vet.J. 36(4):1272-1282.

24. Enemali, F.U. (2014).Anatomical Studies on Thyroid, Parathyroid and Adrenal gland of The African Giant Rat(Cricetomys gambianus Water House-1849),M.ScThesis,Faculty of medicine,Ahmudu Bello University,Zaria,Nigeria.

25. Zhi-ping M.I. (2004).An observation on the anatomy and histology of the thyroid gland in red pandas *(Ailurusfulqens)*. Sichuan Journal of Zoology 29(4): 609-611.

26. Dyce, K.M; Sack, W. O. and Wensing, C. J. G. (2002).Text book of Veterinary Anatomy. 3rd ed. Saunders,Philadelphia. Pennsylvania. P:213.

27. Kaufman, M. H; Nikitin. A. Y and Sundberg. J. P. (2010). Histological Basic ofMouse endocrine system,Academic Press, London,Pp:7-81.

28. Parchami,A and Dehkordi,R.F.(2012).Sex Differences in Thyroid GlandStructure ofRabbits.Europ. J. Appl. Sci., 4 (6): 245-248.

**Table 1.Histological parameters of Thyroid gland in Albino Rats and Guinea Pig**s

| Type of animal | Histological parameters(µm) | Right Lobe Mean ± SE | Left Lobe Mean ± SE | T-Test |
|---|---|---|---|---|
| Albino rats | Thickness of capsule | 88.28 ± 1.01 | 98.85 ± 0.85 | 2.89 * |
| | Diameter of large Follicle | 169.42 ± 1.21 | 128.57 ± 0.84 | 3.21 * |
| | Diameter of Medium Follicle | 52.28 ± 1.02 | 59.71 ± 0.68 | 2.66 * |
| | Diameter of small Follicle | 21.71 ± 1.02 | 22.28 ± 0.68 | 2.66 NS |
| | Height of epithelium | 9.28 ± 0.24 | 9.35 ± 0.23 | 0.735 NS |
| Guinea pigs | Thickness of capsule | 242.28 ± 1.01 | 230.85 ± 1.37 | 3.71 * |
| | Diameter of large Follicle | 228.57 ± 0.84 | 213.43 ± 0.84 | 2.59 * |
| | Diameter of Medium Follicle | 94.57 ± 0.84 | 75.14 ± 0.96 | 2.78 * |
| | Diameter of small Follicle | 45.42 ± 0.84 | 43.14 ± 0.96 | 2.78 NS |
| | Height of epithelium | 5.21 ± 0.28 | 5.21 ± 0.28 | 0.880 NS |
| * (P<0.05) significant, NS: Non-Significant. | | | | |

**Abbas.L. Batah and Shakir. M. Mirhish**

**Table 2.Histological parameters of Thyroid gland in Albino Rats and Guinea Pig**s

| Parts of gland | Histological parameters(µm) | Albino rats Mean ± SE | Guinea pigs Mean ± SE | T-Test |
|---|---|---|---|---|
| Right  Lobe | Thickness of capsule | 88.28 ± 1.01 | 242.28 ± 1.01 | 17.06 * |
| | Diameter of large Follicle | 169.42 ± 1.21 | 228.57 ± 0.84 | 21.57 * |
| | Diameter of medium Follicle | 52.28 ± 1.02 | 94.57 ± 0.84 | 13.28 * |
| | Diameter of small Follicle | 21.71 ± 1.02 | 45.42 ± 0.84 | 7.41 * |
| | Height of epithelium | 9.28 ± 0.24 | 5.21 ± 0.28 | 1.87 * |
| Left  Lobe | Thickness of capsule | 98.85 ± 0.85 | 230.85 ± 1.37 | 19.53 * |
| | Diameter of large Follicle | 128.57 ± 0.84 | 213.43 ± 0.84 | 16.30 * |
| | Diameter of Medium Follicle | 59.71 ± 0.68 | 75.14 ± 0.96 | 8.63 * |
| | Diameter of small Follicle | 22.28 ± 0.68 | 43.14 ± 0.96 | 5.77 * |
| | Height of epithelium | 9.35 ± 0.23 | 5.21 ± 0.28 | 2.16 * |
| * (P<0.05) significant. | | | | |
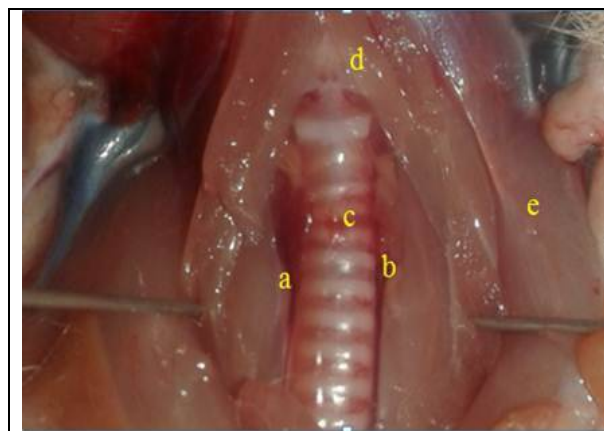


**Figure.1. Shows the anatomical location of thyroid gland in Albino Rats: a- Right lobe, b-Left lobe, c-Isthmus, d-sternothyroideus muscle, e-sternomastoideus muscle**
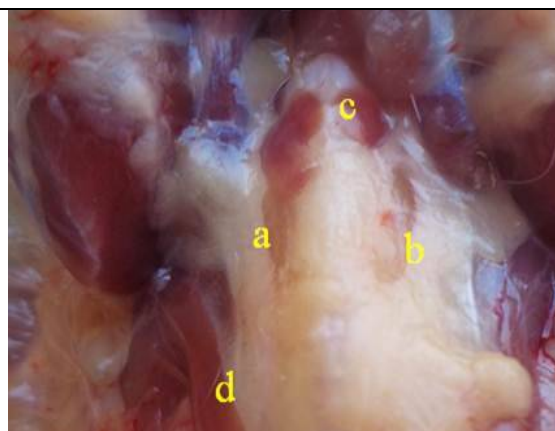


**Figure. 2. Shows the anatomical location of thyroid gland in albino Rats a- Right lobe, b-Left lobe, c-Isthmus, d-Sternomastoideus muscle**
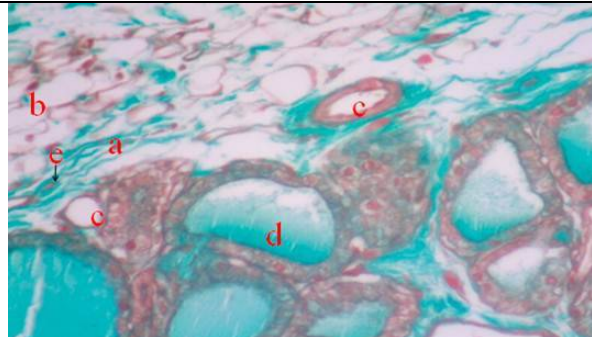
**Abbas.L. Batah and Shakir. M. Mirhish**

**Figure.3. Histological section of thyroid gland in Albino Rats shows: a- Capsule, b- Adipose tissue, c-Blood vessels, d- Thyroid follicles, e-Fibroblast,,MassonTrichrome stain,400 X.**
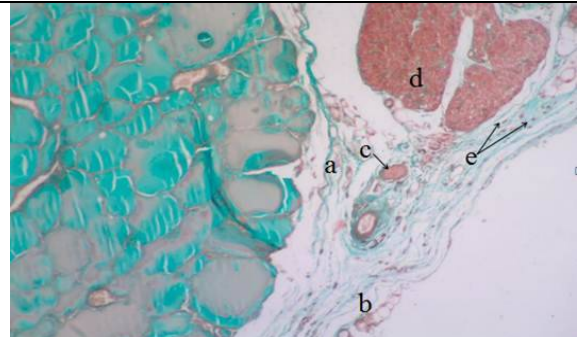


**Figure.4. Histological section of thyroid gland in Guinea pigs shows: a- Inner layer of capsule, b-Outer layer of capsule, c-Nerve, d-Parathyroid gland, e-Fibroblast, Masson Trichrome,100.X**
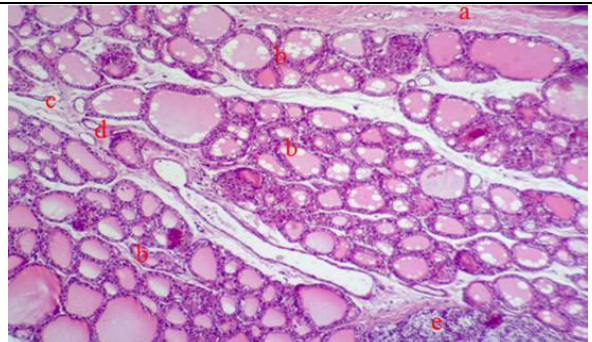


**Figure.5. Histological section of thyroid gland in Albino Rats shows: a- Capsule , b- Lobule, c-Trabeculae, d- Blood vessels, e-Parathyroid gland, H& E stain, 100X**
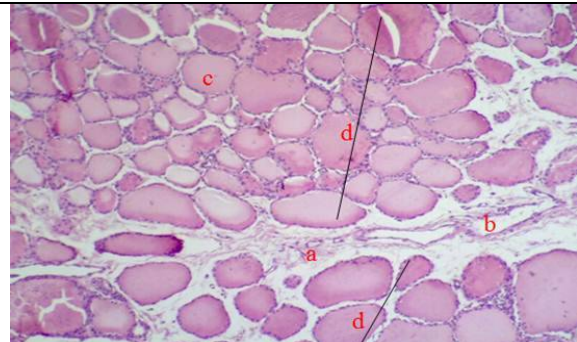


**Figure.6. Histological section of thyroid gland in guinea pigs shows: a- Septa, b- Blood vessels, c-Thyroid follicle, d-Lobule H&E stain, 100 X**
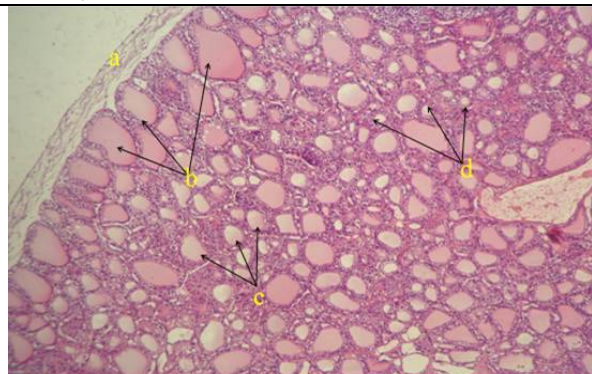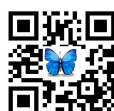


**Figure.7. Histological section of thyroid gland in Albino Rats shows :a- Capsule, b- Large follicles, c-Medium follicles, d-Small follicles, H&E stain, 100 X**



**Figure.8. Histological section of thyroid gland in Guinea pigs shows : a- Capsule, b-.Large follicles, c-Medium size follicles, e-Small follicles, H&E stain, 100 X**
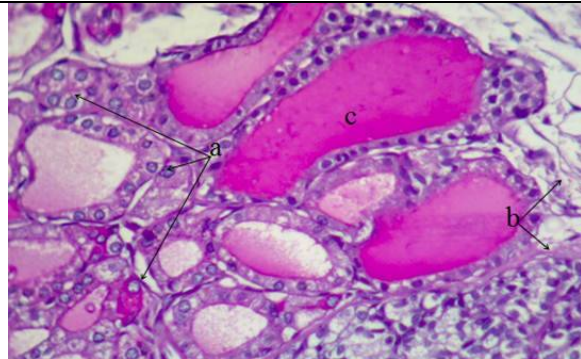
**Figure.9. Histological section of thyroid gland in Albino Rats shows : a-Parafollicular cell (interfollicular position),.b-.Capsule, C-Colloid, H& E stain, 400X**
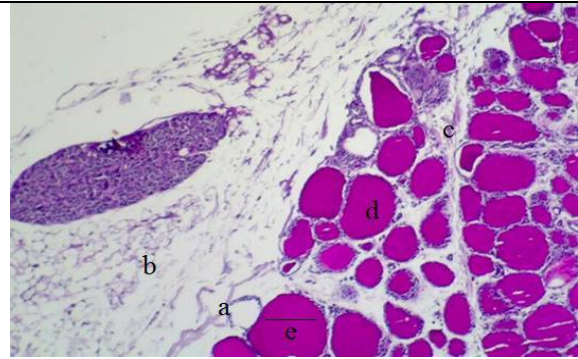


**Figure.10. Histological section of thyroid gland in Guinea pigs shows : a- Inner layer of capsule, b-Outer layer of capsule, c- Septa, d-Colloid, e-Thyroid follicle, PASstain, X100.**
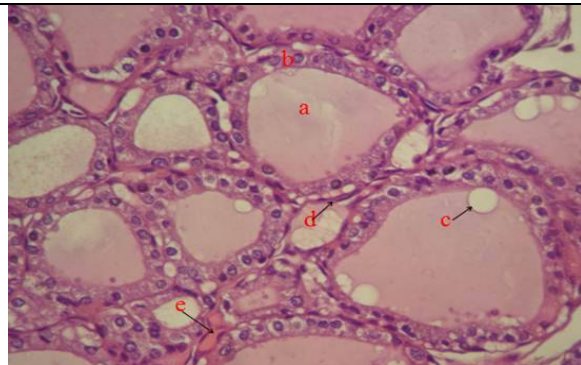


**Figure.11. Histological section in thyroid gland of Albino Rats shows: a-Colloid, b- Lining epithelial, c-Vacuole, d-Fibroblast, e-Sinusoid, H& E stain, 400 X.**
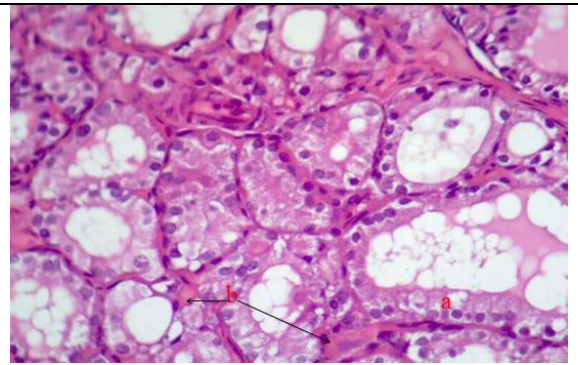


**Figure.12. Histological section of thyroid gland in Albino Rats (active state) shows: a-Lining epithelium, b-Sinusoid, H& E stain, 400X**



**Figure.13. Histological section of thyroid gland in Guinea pigs (inactive state) shows: a, Colloid, b-Simple squamous epithelium, c-Simple cuboidal epithelium, H&E stain, 400 X.**
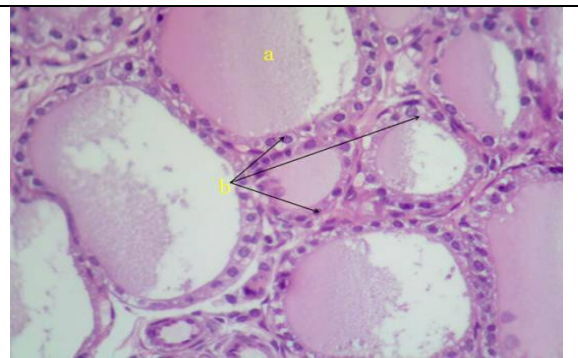


**Figure.14. Histological section of thyroid gland in Guinea pigs (active state) shows: a- Colloid, b-Simple cuboidal epithelium in all follicles, H&E satin,400 X**

16568

**Abbas.L. Batah and Shakir. M. Mirhish**



**Figure.15. Histological section of thyroid gland in Albino Rats shows:a-Parafollicular cell (interfollicular position).b-Parafollicular cell. C-Parathyroid gland H& E stain, 400X**



**Figure.16. Histological section of thyroid gland in Guinea pigs shows : a- Colloid, b-Parafollicular cells, c-Vacuoles, H&E stain, 400 X.**
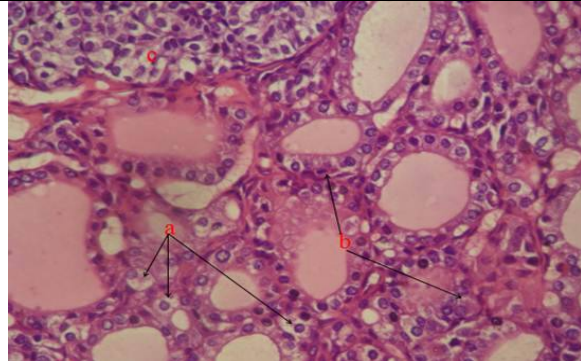
**RESEARCH ARTICLE**

# Influence of γ Al₂O₃ Nanoparticles Addition and Pressure on the Electrical, Structural and Microstructure Properties of Bi-2223 Superconducting System

Bushra A. Aljurani*, Ghazala Y.Hermiz and Khalid A. Shyaa

Physics Department, College of Science, University of Baghdad, Baghdad,Iraq.

*Address for Correspondence
**Bushra A. Aljurani**
Physics Department,
College of Science,
University of Baghdad,
Baghdad- Iraq.

## ABSTRACT

γ Al₂O₃ nanoparticle  ( 10 and 50) nm was added to Bi-2223 superconductor prepared by solid state reaction method with intermediate grinding. A stoichiometric precursor of x=0.2,0.4 and  0.6 wt% Al₂O₃ nanoparticle is systematically added to the well balanced $Bi_{1.7}Pb_{0.3}Sr_2Ca_2Cu_3O_{10+\delta}$ that pressed under different pressures 0.3,0.5,0.7,0.9 and 1.1 GPa. in order to trace the effect of nanoparticles addition and pressure to the system. Microstructure, transitions temperature, phases and cell parameters were investigated. Addition of Al₂O₃ nanoparticle is found to slowly decrease the Bi-2223 phase volume and the resistive transitions for x=0-0.6 wt % samples whereas accelerated formation of the Bi-2212 phase is detected for further additions. Changes in superconducting properties of Al-added Bi-2223 system at different pressure were discussed and the findings were further compared with available literature

**Keywords:** Bi-2223 superconductors, γ (Al₂O₃)nano particles, pressure effect

## INTRODUCTION

Meada et al. [1] was the first who worked with BSCCO superconductors and found its $T_c$ =105 K since then extensive research in this system still continues, BSCCO system has  a layered structure with three identical phases, particularly, $Bi_2Sr_2CuO_6$, $Bi_2Sr_2CaCu_2O_8$ and $Bi_2Sr_2Ca_2Cu_3O_{10}$.Chemical doping and  addition of element are known to affect and control the superconducting and physical properties of layered structure superconductors. The superconducting properties of Bi2223 system are highly related to its hole concentration, pinning ability and its phases structure [2-5]. The addition of nano particles of the size that is between the coherence length (ζ) and penetration depth (λ) to (Bi, Pb)-2223 phase can improve its superconducting properties. A suitable amount of nano particles may cause different effects on the microstructure and pinning properties of high temperature

**Bushra A. Aljurani** *et al.*

superconductors. It has been reported by Annabi et al.[6] and Ghattas et al.[7] that the addition of a small amount of $Al_2O_3$ improve the flux pinning ability and has a little effect on the (Bi,Pb)-2223 formation process. Ben Azzouz et al.[8] studied the effects of $Al_2O_3$ nano particles addition on the fluctuation conductivity of (Bi,Pb)-2223 superconductors .They found an increase of the Ginzburg number on the addition of nano $Al_2O_3$ particles during the final sintering cycle of a multi-step preparation process, to $(Bi,Pb)_2Sr_2Ca_2Cu_3O$ precursor powders .The correlation between fluctuation amplitude and current density ($J_c$) has been discussed. Hermiz et al.[9] examined the effect of pressure on the superconducting and mechanical properties of $Bi_{1.6}Pb_{0.4}Sr_{1.8}Ba_{0.2}Ca_2Cu_{2.2}Ni_{0.8}O_\delta$ system . An improvement of mechanical properties was found when the pressure was increased from 0.3 to 0.9 GPa. The highest critical temperature was 117 K under 0.7 GPa.

Most studies on the nanosized particle addition into (Bi, Pb)-2223 have been carried out with one average size [10,11]. The present work involves studying the effect of $Al_2O_3$ addition with different average sizes (10 and 50) nm in $(Al_2O_3)x$ $Bi_{1.7}Pb_{0.3}Sr_2Ca_2Cu_3O_{10+\delta}$ where x=0.2,0.4 and 0.6.These sizes are large than ($\zeta$) but smaller than ($\lambda$). The objective of this work is to determine the effect of different nanosized $Al_2O_3$ on the phase formation, structure, microstructure, critical temperature of Bi-2223 superconductor pressed under different pressure

## EXPERIMENTAL PART

$\gamma$ $(Al_2O_3)_xBi_{1.7}Pb_{0.3}Sr_2Ca_2Cu_{28}O_{10+\delta}$ samples for x=0.2,0.4 and 0.6 were prepared by conventional solid-state reaction method. Appropriate amounts of $Bi_2O_3$(99.9%), $Pb_3O_4$(99.9%), $SrCO_3$(99.9%), CaO(99.9%), CuO (99.9%) and nano particle of size (10 and 50) nm $Al_2O_3$(99.9%) powders were used as starting materials. .The powders of the precursors were mixed together using agate mortar. The mixture homogenization takes place by adding a sufficient quantity of 2-propanol to form a paste during the process of grinding of about (1 h). In the second step , the materials were grounded to a fine powder and then calcined in air at 800 ℃ for (24)h. The mixture was then pressed into pellets (1.3 cm) in diameter and (0.2) cm thick, using a hydraulic press type (SPECAC), under pressure of 0.3,0.5,0.7,0.9 and 1.1GPa.. The pellets were sintered in air at 830 ℃ for 140 h.The structure of the prepared samples was obtained using X-ray diffraction technique (XRD) (Philips) with $Cu_{K\alpha}$ source. The resistivity and the critical temperature ($T_c$) were measured using the four point probe method. The surface morphology of the samples was examined using Scanning Electron Microscope (SEM ) type VEGA\\TESCAN-SEM (SEM Hv 30.00 kV).

## RESULTS AND DISCUSSION

The resistivity behavior as a function of temperature for $(Al_2O_3)$ $Bi_{1.7}Pb_{0.3}Sr_2Ca_2Cu_3O_{10+\delta}$ with different concentration and for two size of nano- sizes of the $Al_2O_3$ added pressed under different pressures are shown in figure (1) and the values of critical temperature $T_c$ are listed in Tables (1). From this figure and Table, one can see an increase of the critical temperature $T_c$ with the increase of pressure from 0.3 GPa to 0.7 GPa for both nano size of $Al_2O_3$ and for all concentrations. On the other hand, it was found that the resistivity of the samples pressed under 0.3 GPa did not reach to zero even at the boiling point of liquid nitrogen, rather it behaved like a superconductor. While an increase of the pressure above 0.7 GPa,0.9 GPa. and 1.1 GPa, the resistivity increased with the temperature decrease until transition to semiconductor behavior for all concentrations and for both nano sizes. It is believed that the increase of the critical temperature as the pressure increasing up to 0.7 GPa as depict in Table (1) may be due to the increase of the carrier concentration $n_h$ in the $CuO_2$ planes, the change of $n_h$ within the unit cell leads to the improvement of the critical temperature [9,12]. It is noticed from figure (1) and Table (1) that the $(Al_2O_3)_{0.6}Bi_{1.7}Pb_{0.3}Sr_2Ca_2Cu_3O_{10+\delta}$ sample has the highest $T_c$ of 128K, while $(Al_2O_3)_{0.2}Bi_{1.7}Pb_{0.3}Sr_2Ca_2Cu_3O_{10+\delta}$ has the highest $T_c$ of 118K, for the samples with (10) nm and (50) nm of $Al_2O_3$ addition, respectively which were pressed under 0.7 GPa. From the results, it can be concluded that the pressure 0.7 GPa. is the optimum value to get the highest $T_c$ value of superconducting samples. This may be because pressure induced changes in the carrier concentration assuming that the change distribution among the crystallographically in equivalent $CuO_2$ layers is nonhomogenous as referred by Rabinowitz and

**Bushra A. Aljurani** *et al.*

McMullen [13].The crystal structure of the prepared samples of the $\gamma$ $(Al_2O_3)_x Bi_{1.7}Pb_{0.3}Sr_2Ca_2Cu_3O_{10+\delta}$ system with different nanoparticle size (10 and 50) nm of $Al_2O_3$ added and of different concentrations x=0.2, 0.4, and 0.6 wt% that was sintered at 830°C for 140h, and pressed under different pressure (0.3, 0.5 and 0.7) GPa. are shown in Fig.(2-5). The XRD analyses showed an orthorhombic structure for all the samples and most of them showed two main phases: high-$T_c$ phase (2223), and low-$T_c$ phase (2212), in addition to some impurities like $Ca_2PbO_4$. The appearance of more than two phases could be related to the stacking faults along the c-axis as a result of the displacement of an ion or oxygen defect or to the ordering of cations. The indices of reflection were from that reported by Koyama et al. [14] and Silunkeet et al.[15]. It should be mentioned that the position and the relative intensity of the diffraction peaks vary slightly of the prepared samples in different values of pressure. On the other side, peaks corresponding to the $Al_2O_3$ were detected by x-ray diffraction at $2\theta=14.3°$ for (006) Miller indices [16], this indicate that incorporation $Al_2O_3$ in the sample. It is clearly revealed that the pressure will improve the crystallites, the peaks get sharper with an increase of its intensity. The most intense peak pattern of samples belongs to the high $T_c$ phase (Bi-2223) which also indicates are increase in the volume fraction of high superconducting phase with increasing pressure up to 0.7 GPa for both nanoparticle addition as shown in Table (1).

The parameters a, b, c, and c/a, were calculated from the XRD analysis for both sizes of $Al_2O_3$, nanoparticles added as shown in Tables (1). From this Table, one can see an increase in c/a with an increase of pressure from 0.3 to 0.7 GPa for all samples of different concentrations and different nano sizes of $Al_2O_3$ added. It is worth mentioning that the optimum pressure was obtained at 0.7 GPa, which gives us the best structural properties with high volume fraction for the samples of both nano sizes of $Al_2O_3$ added, and different concentrations Surface morphology micrographs obtained with the Scanning Electron Microscope (SEM) for $(Al_2O_3)_x Bi_{1.7}Pb_{0.3}Sr_2Ca_2Cu_3O_{10+\delta}$ samples of different concentrations and different nanosizes of $Al_2O_3$ added which were pressed under different pressures are shown in figures (6-8). It is clear from these figures that the change of grain size and the distribution of grains on the surface of the samples is affect by pressure. The surface area images of the samples show the formation of randomly plate like grains. The occurrence of grains with plate like structure is a signature of Bi-2223 phase formation [17].

At low pressure, the microstructures of the samples reveal a minor difference in the porosity level. Thus, the pressure increasing from 0.3 GPa to 0.7 GPa lead to enhance the sample morphology slightly and have a clear effect on the microstructure by decreasing the porosity level for both sizes (10 and 50) nm of $Al_2O_3$ nanoparticle added as illustrates in figures (6-8).This result is confirmed by XRD and electrical resistivity results.As a result, the best structure regarding the porosity and homogeneity of the material is that for samples pressed under 0.7 GPa. The reaction that took place under this pressure favored the growth of Bi-2223 phase with the improvement of the density of the material. So good connectivity between grain, less porosity and high growth are obtained. Enhancement of $T_c$ was obtained as a result of the good connectivity pressed under this pressure

## CONCLUSIONS

It is worth mentioning that the optimum pressure which gives the best structural properties with high volume fraction for the samples of both nano sizes of the $Al_2O_3$ added, and with different concentrations is 0.7 GPa,. Under this pressure the growth of Bi-2223 phase with improved density is favored. Good connectivity between grains, less porosity and high growth are resulted.

## REFERENCES

1. H. Maeda, Y. Tanaka, M. Fukutomi and T. Asano. "A New High-$T_c$ Oxide Superconductor without a Rare Earth Element" Jpn. J. Appl. Phys.27, L209 (1988).
2. C.Terzioglu, M.Yilmazlar, O.Ozturk and E.Yanmaz. "Structural and physical properties of Sm-doped $Bi_{1.6}Pb_{0.4}Sr_2Ca_{2-x}Sm_xCu_3O_y$ superconductors" Physica C,423,119 (2005).

16572

**Bushra A. Aljurani *et al.***

3.  R.P. Aloysius, P. Guruswamy and U. Syamaprasad." Enhanced critical current density in (Bi,Pb)-2223 superconductor by Nd addition in low percentages"Physica C, 426–431, 556–562(2005).

4.  H.Sozeri, N. Ghazanfari, H.Ozkan and A. Kilic." Enhancement in the high-$T_c$ phase of BSCCO superconductors by Nb addition"Supercond. Sci. Technol., 20, 522–528(2007).

5.  S.A. Halim, S.B. Mohamed, H. Azhan, S.A. Khawaldeh and H.A.A. Sidek. "Effect of barium doping in Bi–Pb–Sr–Ca–Cu–O ceramics superconductors"Physica C, 312, 78–84 (1999).

6.  M. Annabi, A. Mchirgui, F. Ben Azzouz, M. Zouaoui and M.Ben Salem."Addition of nanometer $Al_2O_3$during the final processing of (Bi,Pb)-2223 superconductors" Physica C, 405, 25–33(2004).

7.  A. Ghattas, M. Annabi, M. Zouaoui, F. Ben Azzouz and M. Ben Salem."Flux pinning by Al-based nano particles embedded in polycrystalline (Bi,Pb)-2223 superconductors" PhysicaC, 468, 31–38(2008).

8.  F. Ben Azzouz,M. Annabi, M. Zouaoui,M. Ben Salem. "Effects of $Al_2O_3$ nanometer particles addition on the fluctuation conductivity in (Bi,Pb)-2223 superconductors "Physica status solidi C 3,2978–2981, 2006.

9.  G.Y. Hermiz, B.A. Aljurani, H.A. Thabit ."Effect of Pressure on the Superconducting and Mechanical Properties of $Bi_{1.6}Pb_{0.4}Sr_{1.8}Ba_{0.2}Ca_2Cu_{2.2}Ni_{0.8}O_{10+\delta}$ System "AMPC 3 42-47(2013).

10. B.A. Aljurani and K.A. Shyaa"Superconducting Properties of $Bi_{1.7}Pb_{0.3} Sr_2Ca_2Cu_3 O_{10+\delta}$ Added with Nano Particle $\gamma Al_2O_3$" Australian Journal of Basic and Applied Sciences 9, 54-60 ,( 2015).

11. A. Zelati1, A.Amirabadizadeh1 , A. Kompany, H.Salamati and J. Sonier" Effects of $Dy_2O_3$ Nanoparticle Addition on Structural and Superconducting Properties of BSCCO" Indian Journal of Science and Technology, 7, 123–134, (2014).

12. X. J. Chen, H. Q. Lin and C. D. Gong, "Pressure Dependence of $T_c$ in Y-Ba-Cu-O Superconductors," Physical Review Letter, Vol. 85,2000, 2180-2183.

13. M. *Rabinowitz* and T. *McMullen*, "General model of pressure-induced transition temperature increase with focus on the Hg-Ba-Ca-Cu-O System "Applied Physics Letters 63 ,P.985,(1993)

14. M.Koyama, L. Solymer, and D. Walsh, "Electrical properties of Materials "P. 365-366, Oxford, York, Tokyo, Oxford University, press (1998).

15. S. Silunkeet, V.Z. Kresin and S. A. Wolf, "Fundamentals of Superconductivity", Ch.1, Plenum Press, New York, (1990).

16. K. S. Ghandhi, "Theory and Practice of Microelectronics", Copyright by John Willy and Sons, P. 133 (1968).

17. S.A. Saleh, "Studies on Sintering Effect on the Structural and Transport Properties of (2223) Phase," Physica C, 444, 40–44, (2006).

**Table 1. The variation in lattice parameters, c/a and volume fraction of Bi-2223 and Bi-2212 and transition temperature for $\gamma$ ($Al_2O_3$)$_x$ $Bi_{1.7}$ $Pb_{0.3}$ $Sr_2$ $Ca_2$ $Cu_3$ $O_{10+\delta}$ system for different nanoparticles size of $Al_2O_3$ addition and different nominal composition pressed under different pressure**

| Particles size $Al_2O_3$ | x wt % | P GPa. | a Å | b Å | c Å | c/a | Bi-2223% | Bi-2212% | $T_c$ (K) |
|---|---|---|---|---|---|---|---|---|---|
| 10 nm | 0.2 | 0.5 | 5.46 | 5.28 | 37.50 | 6.87 | 72.94 | 27.06 | 103 |
| | | 0.7 | 5.40 | 5.40 | 37.03 | 6.86 | 74.79 | 25.21 | 112 |
| | 0.4 | 0.3 | 5.44 | 5.10 | 37.11 | 6.72 | 73.84 | 26.16 | 101 |
| | | 0.5 | 5.19 | 5.36 | 37.45 | 6.82 | 75.34 | 24.66 | 104 |
| | | 0.7 | 5.39 | 5.31 | 37.27 | 6.91 | 76.50 | 23.50 | 115 |
| | 0.6 | 0.3 | 5.15 | 5.40 | 37.15 | 6.71 | 85.47 | 14.53 | 102 |
| | | 0.5 | 5.42 | 5.21 | 37.12 | 6.84 | 89.57 | 10.43 | 105 |
| | | 0.7 | 5.43 | 5.41 | 37.48 | 6.90 | 92.75 | 7.250 | 128 |
| 50 nm | 0.2 | 0.5 | 5.49 | 5.32 | 37.05 | 6.74 | 79.21 | 20.79 | 102 |
| | | 0.7 | 5.43 | 5.36 | 37.24 | 6.86 | 81.15 | 18.85 | 118 |
| | 0.4 | 0.3 | 5.34 | 5.42 | 37.10 | 6.19 | 71.27 | 28.73 | semi |

16573

**Bushra A. Aljurani** *et al.*

|  |  |  |  |  |  |  |  |  |
|---|---|---|---|---|---|---|---|---|
|  | 0.5 | 5.15 | 5.29 | 37.60 | 6.30 | 73.87 | 26.13 | 105 |
|  | 0.7 | 5.49 | 5.38 | 37.10 | 6.76 | 77.70 | 22.30 | 113 |
|  | 0.3 | 5.43 | 5.19 | 37.16 | 6.45 | 72.75 | 27.25 | semi |
| 0.6 | 0.5 | 5.34 | 5.01 | 37.82 | 6.68 | 74.45 | 25.55 | 103 |
|  | 0.7 | 5.44 | 5.34 | 37.04 | 6.81 | 78.63 | 21.37 | 108 |
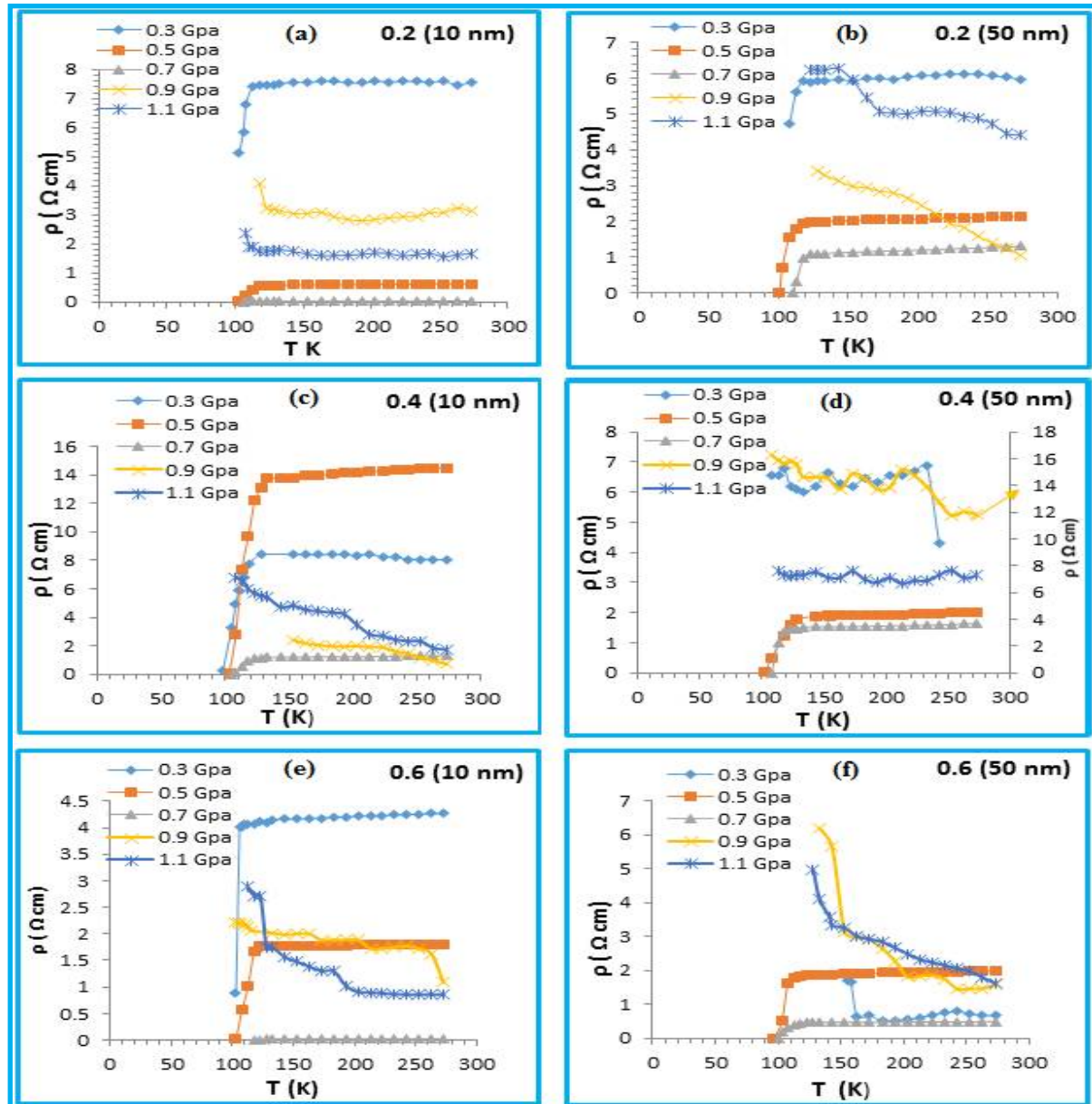


**Figure 1. Resistivity (ϱ) as a function of a temperature for** $\gamma$ **(Al$_2$O$_3$)$_x$Bi$_{1.7}$Pb$_{0.3}$Sr$_2$Ca$_2$Cu$_3$O$_{10+\delta}$ sample with different concentration of** $\gamma$**Al$_2$O$_3$ (10 and 50) nm pressed under different pressure. (a) x=0.2 10 nm (b) x=0.2 50 nm (c) x=0.4 10 nm (d) x=0.4 50 nm (e) x=0.6 10 nm (f) x=0.6 50 nm**
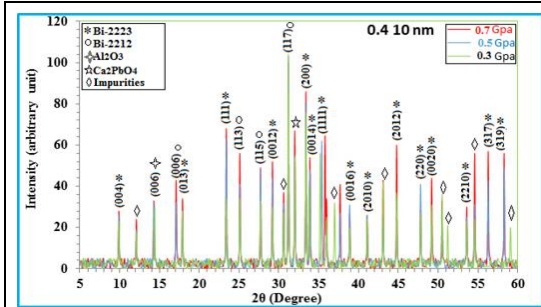
**Bushra A. Aljurani** *et al.*



**Figure 2.** X-ray diffraction patterns of $\gamma$ $(Al_2O_3)_{0.4}Bi_{1.7}Pb_{0.3}Sr_2Ca_2Cu_3O_{10+\delta}$ for (10) nm of $Al_2O_3$ addition under different pressure values

**Figure 3.** X-ray diffraction patterns of $\gamma$ $(Al_2O_3)_{0.4}Bi_{1.7}Pb_{0.3}Sr_2Ca_2Cu_3O_{10+\delta}$ for (50) nm of $Al_2O_3$ addition under different pressure values.
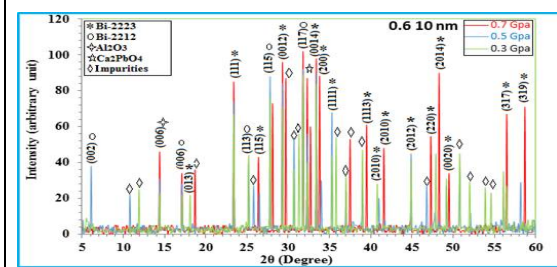
**Figure 4.** X-ray diffraction patterns of $\gamma$ $(Al_2O_3)_{0.6}Bi_{1.7}Pb_{0.3}Sr_2Ca_2Cu_3O_{10+\delta}$ for (10) nm of $Al_2O_3$ addition under different pressure values.
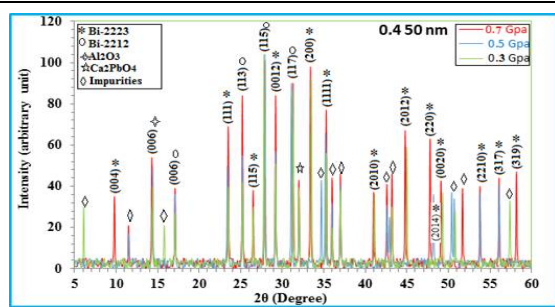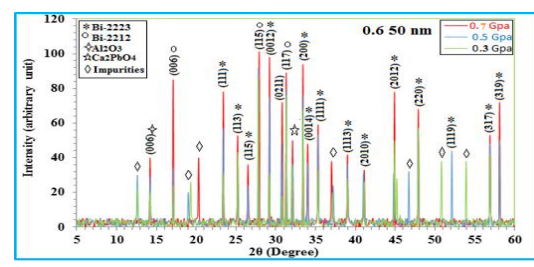
**Figure 5.** X-ray diffraction patterns of $\gamma$ $(Al_2O_3)_{0.6}Bi_{1.7}Pb_{0.3}Sr_2Ca_2Cu_3O_{10+\delta}$ for (50) nm of $Al_2O_3$ addition under different pressure values.



**Figure 6.** SEM micrographs of $\gamma$ $(Al_2O_3)_{0.2}Bi_{1.7}Pb_{0.3}Sr_2Ca_2Cu_3O_{10+\delta}$ samples
(a) For (10) nm of $Al_2O_3$ addition at 0.5 GPa. (b) For (50) nm of $Al_2O_3$ addition at 0.5 GPa.
(c) For (10) nm of $Al_2O_3$ addition at 0.7 GPa. (d) For (50) nm of $Al_2O_3$ addition at 0.7 GPa

**Figure(7):SEM micrographs of** $\gamma$ **(Al$_2$O$_3$)$_{0.4}$Bi$_{1.7}$ Pb$_{0.3}$ Sr$_2$ Ca$_2$ Cu$_3$ O$_{10+\delta}$ samples (a) For (10) nm Al$_2$O$_3$under 0.3GPa. (b) For (50) nm Al$_2$O$_3$under 0.3 GPa. (c) For (10) nm Al$_2$O$_3$under 0.5 GPa. (d) For (50) nm Al$_2$O$_3$under 0.5 GPa. (e) For (10) nm Al$_2$O$_3$under 0.7 GPa.(f) For (50) nm Al$_2$O$_3$under 0.7 GPa.**
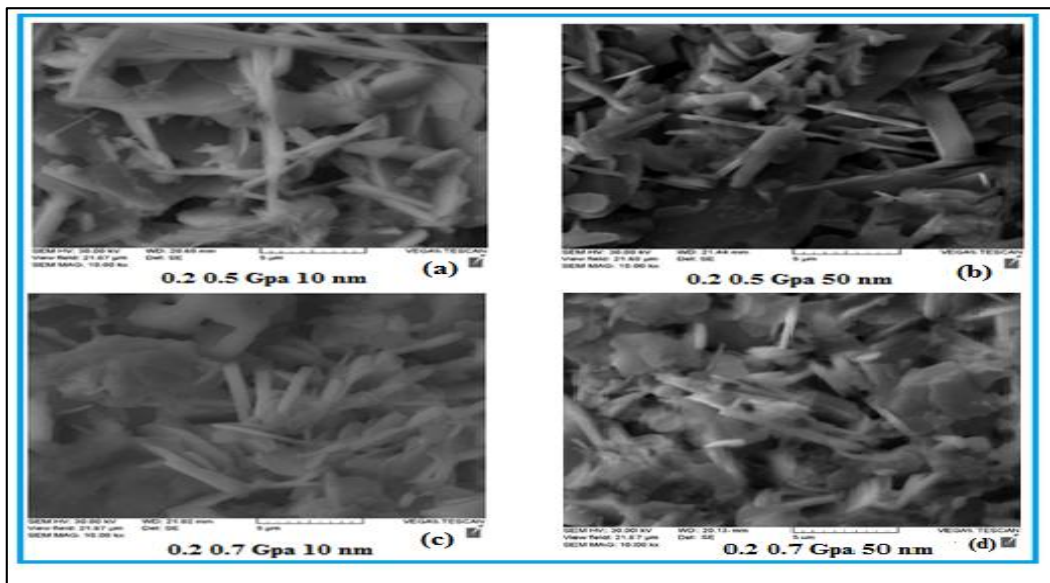
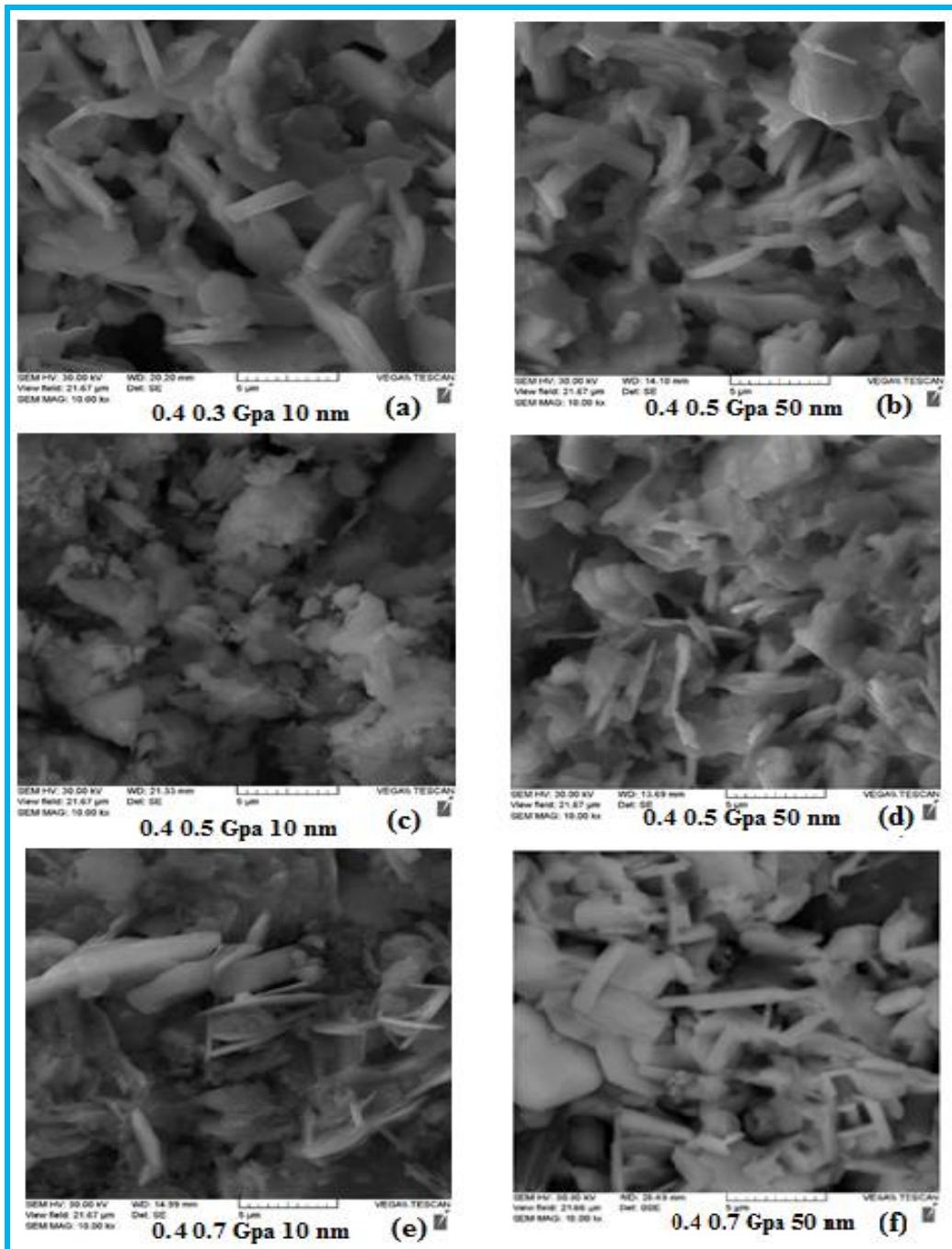**Bushra A. Aljurani** *et al.*
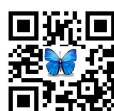


**Figure 8.** SEM micrographs of $\gamma$ $(Al_2O_3)_{0.6}Bi_{1.7}$ $Pb_{0.3}Sr_2Ca_2Cu_3O_{10+\delta}$ samples (a) For (10) nm $Al_2O_3$ under 0.3 GPa.(b) For (50) nm $Al_2O_3$ under 0.3 GPa. (c) For (10) nm $Al_2O_3$ under 0.5 GPa. (d) For (50) nm $Al_2O_3$ under 0.5 GPa. (e) For (10) nm $Al_2O_3$ under 0.7 GPa. (f) For (50) nm $Al_2O_3$ under 0.7 GPa
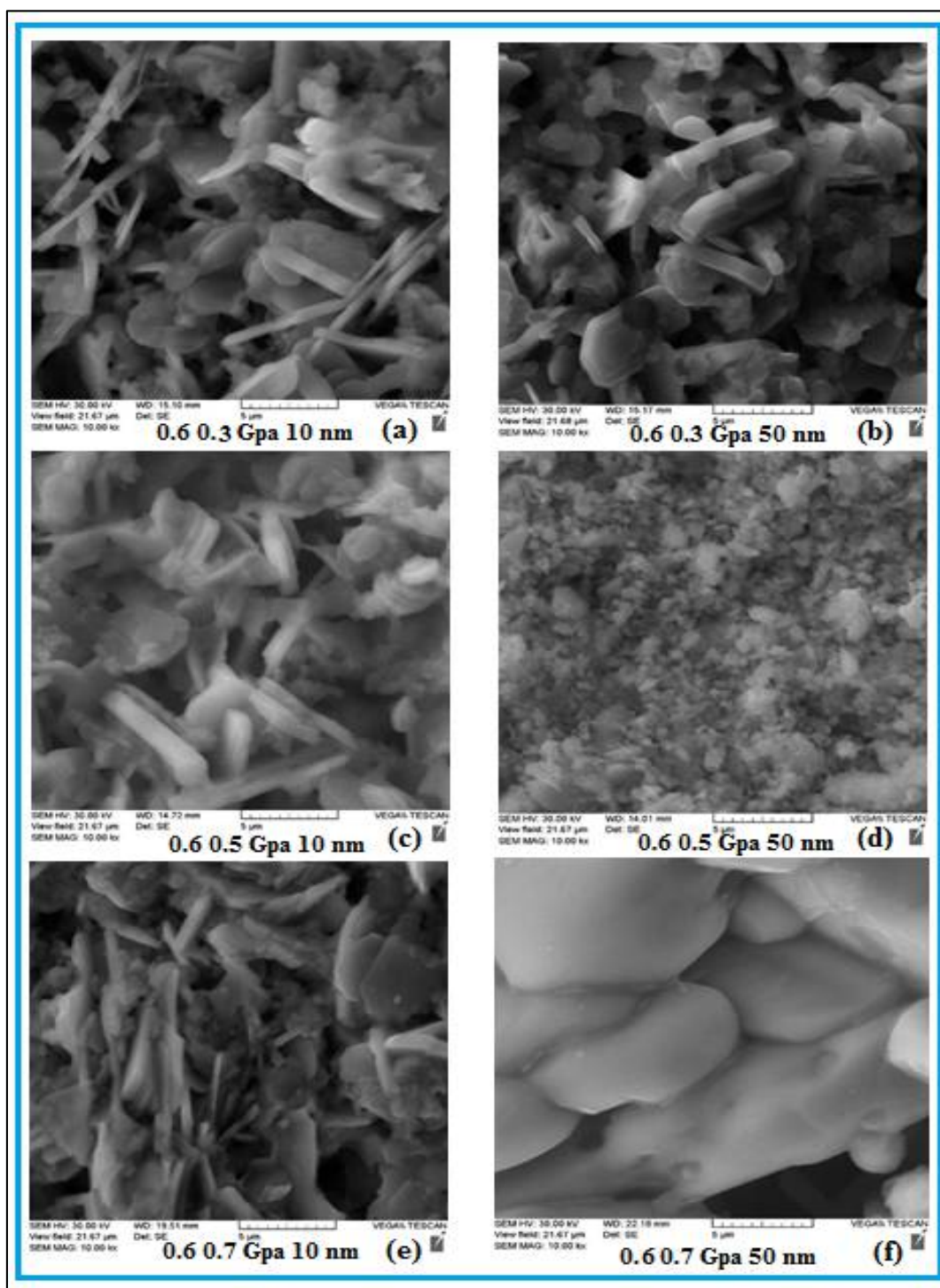
16577

**RESEARCH ARTICLE**

# Fast Search Method by Block Categorization and Multi Codebook Designing Based on Block Edge

Maha A. Hameed

Department of Astronomy, College of Science, University of Baghdad,Iraq.

*Address for Correspondence
**Maha A. Hameed**
Department of Astronomy,
College of Science,
University of Baghdad, Iraq.
Email:Yu96312@gmail.com

## ABSTRACT

While the encoding of a VQ technique requires search in codebook for all input vectors to identify the codeword that achieve best- matched (i.e. this is a time consuming procedure), so, in this search, we have implemented a new block- scanning method to generating sub codebooks by dividing the codebook to categorized the codewords and blocks of input image depending on blocks data into pour, diagonal, vertical and horizontal classes. The categorization process is usually applying before the process those treatments with codebook. In our work, the categorization idea is mostly simple for software performance by reducing the search time, where it generate the same decoded quality as this achieve in the full search method.

**Keywords:** categorization, sub binary codebooks and codewords.

## INTRODUCTION

The Block Truncation coding method preserves spatial information in the image content with low computational complexity but it has a medium compression ratio [1,2]. Therefore, an adaptation (vector quantization method) is required to advance the compressibility of the BTC method to represent binary form (bit map) of the coded image. While the applications of VQ method are limited because the encoding procedure is computational complexity system [3,4], in this paper,  we present a new Fast search method for image compression depending on block classification (multi codebook designing) based on block edge this idea will be used to perform both encoding and decoding phases to decrease the search time of the binary codebook by decreasing the time of matching search, then simplifying in the computational complexity, therefore one can design an efficient blocks classification method and a new different categories codebook ( sub codebooks i.e. empty, diagonal, horizontal and vertical categories) by designing a method for classified VQ based on edge in blocks, where this classification idea is chiefly simple for

16578

software implementation where it could decrease the time of search with same decoded image quality which may be obtained when using full search.

### The Block Truncation Compression technique

Block Truncation Compression (BTC) is a method for grayscale images. This method divides the original image into blocks of "*n*x*n*" pixels then uses a quantize in order to decrease the number of grey levels for each block while preserving the same mean and standard deviation [2,5], where these values is difference from block to another, then this two level quantization for each block is calculate as follows; If a pixel value is greater than or equal to the mean value it is replaced by the value "1", otherwise "0". Reconstruction image is made by these two values that is mean and the standard deviation.

### Vector Quantization (VQ)

Vector quantization (VQ) methods develop the principles of quantization basic.
This method is to extend of fixed- size vectors, this called code vectors, all these vectors input in dictionary called codebook. Then a given image is partitioned into blocks called input image vectors. after that for each input image vector, the code vector that identify closest matching in the codebook is determined and its index in the codebook is used as the encoding of the vector in original image [4,6]. Because of its fast lookup ability at the decoder side, VQ method based coding schemes are mostly attractive to applications

### Multi codebook designing based on edge in block

To decrease the difficulty of computational for VQ method, we have adopted a new scanning method for generating the required code block. The proposed method of scanning is based on classifying the codebook and blocks of input image into horizontal, vertical, empty and diagonal categories. For each block, the direction of the main edge is calculated by computing the totality gradient value in vertical and horizontal directions, as follows, Let *pv(i,j)* represents a *n\*n* element in block of size *n\*n*.

The vertical gradient value is;

$$V_{(i,j)} = pv_{(i,j+1)} - pv_{(i,j)} \ldots\ldots\ldots\ldots(1)$$ , where *i=1……n, j=1…...n-1.*

While, the horizontal gradient value is;

$$H_{(i,j)} = pv_{(i+1,j)} - pv_{(i,j)} \ldots\ldots\ldots\ldots(2)$$ , where *i=1…...n-1, j=1…...n.*

For each block, the special effects of total vertical edge are computed as;

$$E_V = \sum_{i=1}^{n} \sum_{j=1}^{n-1} \left| V_{(i,j)} \right| \ldots\ldots\ldots\ldots\ldots(3)$$

$$E_H = \sum_{j=1}^{n} \sum_{i=1}^{n-1} \left| H_{(i,j)} \right| \ldots\ldots\ldots\ldots\ldots(4)$$

The procedure of classification can be calculate from equations 3 and 4, as follows,

$$\theta = TAN^{-1}(E_V \big/ E_H) \ldots \ldots \ldots (5)$$

For each block, when $E_V$ and $E_H$ are equal to zero (i.e. $\theta = 0$) the block can be classified as empty but it is classified as horizontal if $0 < \theta \leq 30$, or it is classified as vertical class if $60 \leq \theta \leq 90$, else it is diagonal.

In this paper, in order to overcome the connected problem with the codebook search, we use categorization of block (i.e. multi codebook design) depended on the edge involved in each block, this idea lead to decrease in the time of searching which required to search the best matching between vector of input image with codebook vectors.

**The process of fast method**

Block *categorization* and sub codebook designing based on the block edge) in the proposed method is described as follows;

**Step 1**

Initialization, a binary codebook blocks are categorized to involve four codebook (i.e. empty, diagonal, horizontal and vertical categories). Where take a label for each class, for empty "0", horizontal "1", vertical "2" and "3" for diagonal.

**Step 2**

An image is divided into blocks 4x4, and the BTC is implemented then for each block the reconstruction values and bit plan (binary block) are calculated.

**Step 3**

Take each input block from bit map (binary image) then calculate $E_H$, $E_V$ and $\theta$ for its.

**Step 4**

From eq. 5 classify input block as empty when both $E_V$ and $E_H$ values are equal to zero, but when $0 < \theta \leq 30$, it is classified as horizontal, or it is classified as vertical class when $60 \leq \theta \leq 90$, else it is diagonal class and give a label for input block ( index "") of sub class ( where $i_c$= 0, 1, 2 or 3).

**Step 5**

Calculate the matching distortion of input vector with codewords in the corresponding class ( i.e. sub codebook) then give the input block a label ( index "$i_b$") of nearest codeword.

**Step6**

Translate two indexes "$i_c$" and "$i_b$" with two reconstruction values, then go to step 3. This method will be very proficient when we classify a codebook in subs, this idea lead to decreasing in the time of search this simplified a full

16580

codebook search which required to find the best matching for each input vector in order to find the best- matched codeword, where this is because many distortion computations can be eliminated.

## Experimental

We express a new method to reducing the computational complexity time of VQ in encoding and decoding by applying block categorization to present a new high speed search method in VQ method by improving the BTC method which is examined by simulation. The search in main codebook has high computational complexity, therefore the new adopted method of scanning is used for category codebook blocks into sub smaller codebook (i.e. Multi codebook designing) then this leads to decreasing the complexity in computational with more less time in searching in full search method. Initially a binary codebook containing 256 codeword vectors is generated using the universal method then the codebook is categorized to involve four sub codebooks ( i.e. empty, diagonal, horizontal and vertical categories). an image is divided into 4x4 blocks then the BTC and VQ methods are implemented

## CONCLUSION

The efficiency of applying categorized method for an encoding and decoding methods are tested, where, it is listed in table 1. One can see from This table, that the proposed method was very efficient when we categorized codebook into different categories, (multi codebook designing based on edge in each block), this idea was particularly simple for software implementations where this scheme leaded to reducing in the time of searching of best matching processing and simplifying a full codebook search for each input vector to find the best matched codeword. In other word, the elimination efficiencies of encoding and decoding for different images were very good, because many distortion computations can consequently be eliminated when categorizing a codebook.

## REFERENCES

1. Y. - Gi Wu, " Block truncation image bit plane coding", Optical Engineering, Vol. 41, No. 10, pp. 2476-2478, 2002.
2. J. - M. Guo, "Improved block truncation coding using modified error diffusion", Electronics letters, Vol. 44, No. 7, 2008.
3. Sindhu M1 and Rajkamal R2, "Images and Its Compression Techniques – A Review", International Journal of Recent Trends in Engineering, Vol. 2, No. 4, 2009.
4. S. H. Hang and S.H. Chen, "Fast encoding algorithm for VQ based image coding", Electronics letters, No.19 , Vol. 26, pp. 1618-1619,1990.
5. A. S. Devi1, S. S. Priyadharsini2 and S. Athinarayanan3, " A BLOCK BASED SCHEME FOR ENHANCING LOW LUMINATED IMAGES", The International journal of Multimedia & Its Applications (IJMA), Vol.2, No.3, 2010.
6. N.M. Nasrabadi and Y. Feng, "Vector quantization of images based upon a neural-network clustering algorithm", Visual Communications and Image Processing, SPIE Vol. 1001, pp. 207-213, 1988.

**Table 1. The elimination efficiency for encoding and decoding for different images.**

| Image name | Encoding Elimination efficiencies | Decoding Elimination efficiencies |
|---|---|---|
| IMAGE1 | 86.1% | 61.3% |
| IMAGE2 | 76.4% | 43.7% |
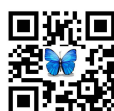
**Maha A. Hameed**
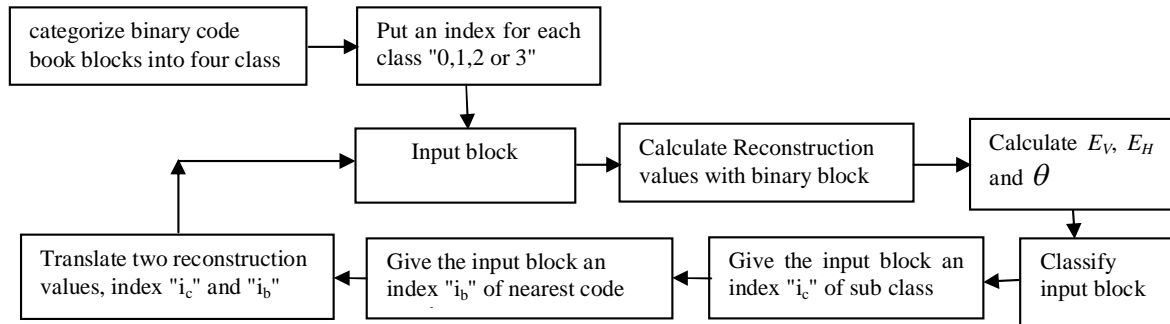


**Fig. 2.The diagram of the mentioned method**

**RESEARCH ARTICLE**

# Stomatal Characteristics in *Phalaenopsis* Orchids

Kaveriamma M M[1]*, P.K. Rajeevan[2] and Nandhini. K[2]

[1]College of Forestry, University of Agricultural and Horticultural Sciences, Kodagu, Karnataka, India.
[2]College of Horticulture, Kerala Agricultural University Thrissur, Kerala, India.

*Address for Correspondence
**Kaveriamma M M**
College of Forestry,
University of Agricultural and Horticultural Sciences,
Kodagu, Karnataka, India.
Email:inkavya@gmail.com

## ABSTRACT

*Phalaenopsis* orchid is one of the most sought after plant in the international flower trade. They are short stemmed epiphytes following a Crassulacean Acid Metabolism pathway of photosynthesis. Stomatal distribution though varying among varieties was maximum in the abaxial surface compared to adaxial or stalk of inflorescence in all the varieties. Stomatal conductance reached peak at 4am and was nil between 10am and 6pm. *S*tomatal conductance of all the varieties gradually increased from 6pm till 4am and the peak was observed between 2am and 4am. Stomatal rhythm was proportional to stomatal conductance..

**Keywords:** *Phalaenopsis,* orchid, flower, *S*tomatal, Metabolism.

## INTRODUCTION

*Phalaenopsis*, commonly called the moth orchid is an important commercial genus of orchids. Species and hybrids in this genus are of high value in Floriculture because of their beautiful and long-lasting flowers. Phalaenopsis are short stemmed monopodial orchids. Plants are slow growing and mature plants attain an average height of twelve to fifteen centimeters, although a few individuals may grow taller.  Aerial roots are fleshy with velamen tissues  at the tip that aid in absorption of moisture. (Sahavacharin, 1981).  Leaves are large, varying in colour, shape and orientation with a Crassulacean Acid Metabolism (CAM) pathway of photosynthesis. Stomata are found on most aerial surface of plants often including the epidermis of leaves, stems and flowers (Esau, 1977). Gaseous exchange of carbon dioxide ($CO_2$) for photosynthesis against the loss of water via transpiration occur through stomata. When a plant encounters adverse environmental conditions, such as drought, abscissic acid triggers stomata to shut tightly in order to prevent plants from dehydration and wilting.  Stomatal conductance, is the measure of the rate of passage of carbon dioxide ($CO_2$) entering, or water vapor exiting through the stomata of a leaf. Stomatal rhythm is directly proportional to stomatal conductance. Many constitutive CAM species fix $CO_2$ almost exclusively at night (Osmond,1978). In *Agave deserti* $CO_2$ uptake extends into the early morning, and also occurs in the late afternoon. The

16583

high intercellular $CO_2$ concentrations associated with malate decarboxylation suppress stomatal opening during the middle of the day (Drennan and Noble, 2000).

## MATERIALS AND METHODS

Stomatal studies were conducted in five different varieties of *Phalaenopsis* viz., Roxanne, Magic Kiss, Pink Magic, Chin Shang Stripe and Kathleen Ai. Stomatal impressions were taken at three different areas using glue (quick fix). These impressions were photographed at a magnification of 10 x using phase contrast microscope. The number of stomata was recorded and expressed as density per square millimetre. Stomatal conductance was studied by using an open system portable infra red gas analyzer, IRGA (model LI-6400) at an interval of 2 hours for a 24 hour cycle and expressed as cm $s^{-1}$. The observation was recorded when the ambient air temperature was 32/21 °C and relative humidity was 64 per cent.

## RESULTS

Stomatal density varied among varieties and is given in Table 1. The stomatal density was more in leaves than on stalk of flower spike.  On abaxial surface of the leaves, the stomatal density was highest in Medium Pink (36.00 per $mm^2$) followed by Roxanne (28.80 per $mm^2$) and Chin Shang Stripe (21.40 per $mm^2$). Density was minimum in Magic Kiss (18.40). On the abaxial surface, stomatal density was on par in all the varieties. In flower spike, stomatal density was on par in Magic Kiss (5.05 per $mm^2$) and Kathleen Ai (5.00 per $mm^2$) and lowest in Medium Pink (3.00 per $mm^2$). Stomatal conductance values are recorded in Table 2 and depicted in Fig. 1. It varied among varieties. Stomatal conductance was maximum at 4 am and was negligible between 10am and 4pm for all the varieties. Chin Shang Stripe recorded the maximum values throughout the period of study reaching a peak of 2.84 mol/$m^2$/s at 4am. Minimum value was recorded in Roxanne 2.03 mol/$m^2$/s at 4am. Stomatal rhythm was proportional to stomatal conductance. The stomata opened wide at 4 am in all the trial varieties. It closed post dawn or was negligible during mid day.

## DISCUSSION

Stomata are the structure through which gaseous exchange takes place between intercellular spaces of subepidermal cells and the atmosphere. Stomata play a key role in the acclimation and adaptation of plants to their environment. Plants may exert control over their gas exchange rates by varying stomatal density. Hew *et al.,* (2005) reported that the stomata of *Arachnis* cv. Maggie Oei, *Aranda* cv. Deborah, *Arundina graminifolia, Bromheadia finlaysoniana, Cattleya browringlana x C. forbesii* and *Spathoglottis plicata* occur only on the lower epidermis of the leaves. The present study in phalaenopsis orchids revealed that the stomatal density was considerably higher in the abaxial surface of leaves and lower but definitely present in adaxial surface and flower spike in all varieties. Highest density (36.00/ $mm^2$ ) of stomata was observed in the abaxial surface of *Phalaenopsis* 'Medium Pink' and minimum in *Phalaenopsis* 'Kathleen Ai' (18.80/$mm^2$ ). Among varieties, the adaxial surface which is exposed to light recorded an almost uniform density ranging between 4.98/$mm^2$ and 5.15/$mm^2$.  A similar observation of 5.33/$mm^2$ on adaxial side and 42.66/$mm^2$ on abaxial surface was reported in orchid species *Aerides lour* by Mulgaonkar (2005). Ferris (2008) reported absence of stomata on the adaxial leaf surfaces of *Spiranthes* orchid. Low stomatal density and low stomatal conductance were related to high water content. In *Phalaenopsis*, being a CAM plant, stomatal conductance of all the varieties gradually increased from 6pm till 4am and the peak was observed between 2am and 4am which is in corroboration with the findings in *Cattleya* sp. (Goh *et al.,* 1977).  The gradual decrease in stomatal opening was observed from 4am to 8am and it completely closed by midday. Gradual opening of stomata was observed after 4pm. The rhythmic opening of stomata was in relation to the stomatal conductance.

## ACKNOWLEDGEMENT

## REFERENCES

1. Dennan, P.M. and Noble,P.S. 2000. Responses of CAM species to increasing   atmospheric CO 2 concentrations. *Plant Cell* and *Environment* (23):767–781.
2. Esau, 1977. *Anatomy of seed plants.* John Wiley & Sons, New York: pp88-99
3. Goh, C.J., Avadhani, P.N.,  Loh, C.S., Hanegraaf, C. and Arditti, J. 1977. Diurnal stomata and acidity rhythms in orchids. *New Phytologist.* 78(2): 365-372.
4. Ferris, M.J.  2008. Stomata, Subsidiary Cells, and Implications. *The McAllen Interrnternational Orchid Society Journal* 9(3): 9-16
5. Hew, C.S., Lee, G.L., Wong, S.C.2005. Occurrence of non functional stomata in the flowers of tropical orchids. Annals of Botany 46(2):195
6. Mulgaonkar, M.S. 2005. Orchid taxonomy studies on dermal anatomy of some terricolous orchids from sahyadri (Western Ghats) *International Journal of    Mendelian Society.* 22(1-2):61-63
7. Osmond C.B. (1978) Crassulacean acid metabolism: a curiosity in context. A*nnual Review of Plant Physiology* 29: 379–414.
8. Sahavachrin, O.1981. Induction of plantlets on inflorescence of *Phalaenopsis* by application of N-6-benzyl adenine. *Kasetsart Journal of  Natural science* 15(2):54-64

**Table 1. Stomatal density in *Phalaenopsis* orchids**

| Variety | Leaf Surface | | Spike |
|---|---|---|---|
| | Adaxial  (per mm²) | Abaxial  (per mm²) | Spike  (per mm²) |
| Roxanne | 28.80$^b$ | 5.10$^a$ | 4.00$^b$ |
| Magic Kiss | 18.40$^c$ | 5.15$^a$ | 5.05$^a$ |
| Medium Pink | 36.00$^a$ | 4.98$^{ab}$ | 3.00$^c$ |
| Chin Shang Stripe | 21.40$^c$ | 5.11$^a$ | 4.10$^b$ |
| Kathleen Ai | 18.80$^c$ | 5.13$^a$ | 5.00$^a$ |

**Table 2. Stomatal conductance (mol/m²/s) in *Phlaenopsis* orchids in a 24 hours cycle**

| Variety | 8pm | 10pm | 12am | 2am | 4am | 6am | 8am | 10am | 12pm | 2pm | 4pm | 6pm |
|---|---|---|---|---|---|---|---|---|---|---|---|---|
| Magic Kiss | 0.20 | 0.83 | 0.72 | 1.36 | 2.08 | 0.95 | 0.14 | 0.03 | 0.00 | 0.00 | 0.01 | 0.01 |
| Medium Pink | 0.28 | 0.91 | 1.19 | 0.85 | 2.07 | 0.51 | 0.02 | 0.04 | 0.00 | 0.00 | 0.01 | 0.02 |
| Kathleen Ai | 0.18 | 0.89 | 1.11 | 1.28 | 2.07 | 0.46 | 0.03 | 0.04 | 0.01 | 0.01 | 0.01 | 0.03 |
| Roxanne | 0.16 | 0.83 | 1.13 | 1.26 | 2.03 | 0.46 | 0.03 | 0.02 | 0.00 | 0.01 | 0.01 | 0.05 |
| Chin Shang Stripe | 0.38 | 1.24 | 1.62 | 1.77 | 2.84 | 0.89 | 0.12 | 0.04 | 0.01 | 0.01 | 0.01 | 0.06 |
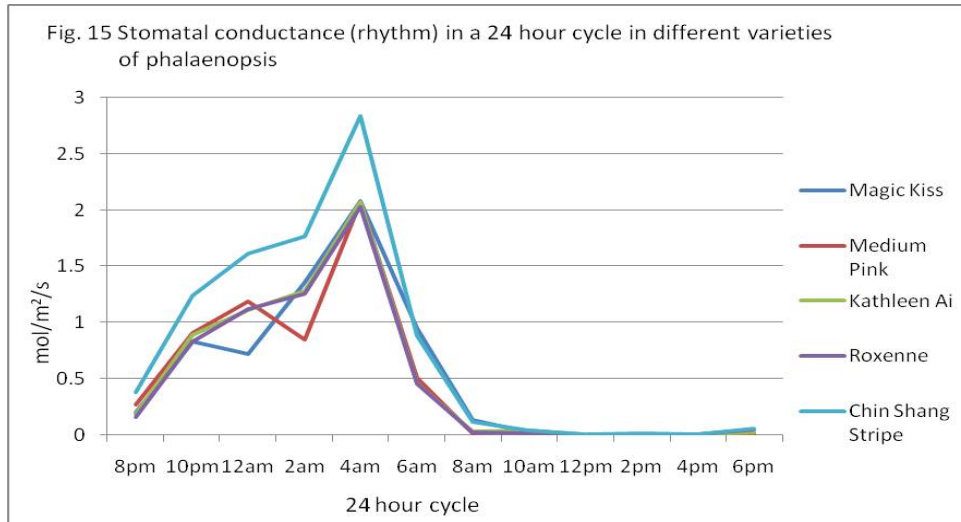
**Fig. 1 Stomatal conductance in a 24 hours cycle in different varieties of *Phalaenopsis* orchids**

**RESEARCH ARTICLE**

# Clinico-Pathological Study of Rabbits Experimentally Infected with *S. enterica.*Serovar *S.enteritidi*s Isolated from Human

Ayat J.Mohammed* and Khalid M Hammadi

Department of Internal and Preventive Veterinary Medicine, College of Veterinary Medicine, University of Diyala, Iraq.

*Address for Correspondence
**Ayat J.Mohammed**
Department of Internal and Preventive Veterinary Medicine,
College of Veterinary Medicine,
University of Diyala, Iraq.

**ABSTRACT**

This study was conducted to investigate the clinical and pathological changes in rabbits experimentally infected with *S. enterica.*serovar *S.enteritidis.* A totalof sixty Iraqi local breed rabbits of both gender were used. In the first experiment twenty rabbit were used to estimate the infective dose of *S.enteritidis*, and the rest 40 rabbits were divided randomly into two groups (n=10), group control one, and (n=30) infected group. In the infected group the bacteria was given via intraperitoneally route, and the control group rabbits was given phosphate buffers saline.The results showed that the infected dose was $4.5 \times 10^8$ cells which was associated with clinical sings without mortality.The body temperatures, heart rate and respiratory rate were increased with dullness and diarrhoea, anorexia, and restlessness.During the gross lesions, investigations in the pathological aspects, which include sever swollen and congested with yellowish spots on internal organ in a comparison to control group.In addition to the previous findings, the histological outcomes were found and recorded during (24, 48, 72, 96,120,144,168 hours) for the second and third weeks. The result in the small intestine showed sever infiltration of inflammatory cells (macrophage and lymphocyte), other organ show infiltration of inflammatory cells.No changes have been found in the control group. Moreover, we found that the bacteria *S.enteritidis* was widely spreads in internal organ of the infected rabbits and we noticed that *S.enteritidis* has the ability to invade the most internal organs (spleen, liver, kidneys, lung, heart, brain, small and large intestine) but in varying degree,whereas no changes have been found in the control group, which gives negative bacterial results.

**Keywords:** *S.enteritidis,*clinical, pathological study, human, rabbits.

16587

**Ayat J.Mohammed and Khalid M Hammadi**

## INTRODUCTION

Salmonellosis is associated with contaminated food of human beings and drinks. It presents major publichealth and economic loss concerns.Bacteremia and sepsis composition consider as primary source of mortality and morbidity in human nations. Non-typhoidal salmonella are important reasons of infections and dissemination infection even in immuno stable host. That infection caused high mortality in human. *S. enterica (*serotype enteritis) is reported to be a major cause of sure illness (Brent AJ,2006). Previous report has found that 172 cases if salmonella bacteremia (70%) of enteritidis serotype. From those people 60% of patients suffer from septic metastasis and 60% died. (Galofre J,.1994).In the mid of 1990s the united states General hospitals a high ratio of mortality was observed in infected patient associated with bacteria induced by  N.T.S (Hohmann, 2001).*Salmonella entritidis*serotype is facultative intracellular pathogens, which is always isolated in human cases salmonellosis. The infection with salmonellosis causelocalized infection mainly in intestine but some tine it also spread systemically in the elder people, children and immuno-compromised people. The infection could be considered as a serious condition for example septicemia and septic shock (Leung DT,2012, Ridings,1994). The main objective of this study was to used rabbit to; study clinically relevant pathogenesis, which like the disease seen in human beside this we focus on development of bacteria caused by salmonella in animal model (rabbit). Moreover, study the histological changes in investigated tissues.

## MATERIALS AND METHODS

### Study design

A total of sixty domestic rabbits of both gender with age range (8-12) months old and weighting between (1500 and 1900) gm, were obtained from local market.During the experimental period, they animals were housed in clean metal cages at a room temperature about (22-+ 3 C$^{\circ}$ at experimental animal house in the college of Veterinary Medicine/ Diyala University.The rabbits were fed commercial pellet, green food (alpha alpha).They had free access to water and to artificial light for (12 hours) per day and animals were adapted for two weeks before started the experiment, then Used in two experiments

### First experiment (I)

Twenty rabbits were used in this experiment to estimating the infective dose (ID) of the *Salmonella entritidis.*

### Second experiment (II)

Forty rabbits were used in this experiment. Ten animals selected randomly as a control group and 30 animalswere infected with estimated infective dose.

### The bacteria

Each five colonies from *Salmonella entritidis* was inoculate in 10 ml  of brain heart infusion agar and incubated at 37$^{\circ}$C for 18 hours then centerifugete in cooling centrifuge at (8000)rpm (round per minutes) for (15)minutes then the sediment(pellet) after washing three times with PBS (PH =7.2),then suspend by using (1ml) of PBS(PH=7.2) and ten fold dilution,$10^{-1}$, $10^{-2}$,$10^{-3}$, $10\text{-}4$,$10^{-5}$   , $10^{-6}$ , $10^{-7}$ ,$10^{-8}$ , $10^{-9}$ ,and $10^{-10}$ were done. The viable plate count of the bacteria in each diluent was made according to (Miles & Misra,1938) and selected the diluents which had these concentrations for injection the rabbits :( $4.5 \times 10^{7}$cells),($4.5 \times 10^{8}$ cells),($4.5 \times 10^{9}$ cells),and ($4.5 \times 10^{10}$ cells).

**Ayat J.Mohammed and Khalid M Hammadi**

### Estimated infective dose

Five groups of rabbits (each group include 4 rabbits) were used.These rabbits had a negative fecal bacteriological culture for *Salmonella*,four groups of rabbits injected intraperitoneal (IP) with one of the calculated diluents ( C.F.U./ml) above dilute with 1ml while the last group served as control and injected with 1ml PBS (PH=7.2).
All groups of rabbits were observed for 3days to calculate the live and dead rabbits.The infective doses (ID) were estimated by choosing the group of rabbits, which showed clinical signs with no mortality.After appearance of clinical signs two rabbits were sacrificed for necropsy finding to isolate *Salmonella enteritidis* from the internal organs.

### Clinical signs

All groups of rabbits were examined daily for clinical signs after induced infection.These signs include temperature, heart rate, and respiratory rate,examination for presence of septicaemia, present or absence of diarrhea and presence or absence of dehydration in infected group. Mortality of the rabbits was recorded throughout the experiment.

### Body weight measuring

All rabbits of each group were weighted weekly until the end of the experiment; this was done to identify the effect of infection on body weight.

### Post-mortem examination

After appearances of clinical signs in the infected group, the post mortem includes:

### A: Gross examination of viscera (macroscopic examination)

The grossexamination of viscera was done for all animals to detect any abnormal gross changes in the internal organs, including colour, location, shape, size, consistency and appearance of cut section.

### B: Histopathological examination

Specimens were taken from internal organs including: intestine, liver, kidney, bladder, spleen, lung and heart at (24hrs,48hrs, 96hrs,120hrs,144,hrs and 168hrs)from infected and control groups , then the tissue were fixed in 10% buffer formaldehyde solution immediately after removal, about (72hrs) of fixation , the specimens were washed with tap water and then processing routinely with a set of upgrading alcoholic concentration from 70% to absolute 100% for( 2 hrs) in each concentration to remove water from the tissue ,after this  clearance was done by xylol, and infiltrate with semi-liquid paraffin wax at 58 °C on two stages,after this, the blocks of specimens were made  with paraffin wax and sectioned by rotary micrometer at 5$\mu$m for all tissues, then stained with  Hematoxylin and Eosin (H& E) and observed the change under the light microscope(Luna and Lee,1968).

## RESULTS

### Clinico- bacteriological findings

The infective dose of *Salmonella entritidis* in rabbit infected intraperitoneally with bacteria $4.5 \times 10^8$  CFU/ml this had been estimated by calculating  the number of alive and dead rabbits in each group during 6 weeks post infection.The

16589
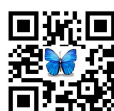
infective dose was recognized when all rabbits were alive and showed clinical signs such as (fever, dullness, loss of appetite, anaroxia and decreased of body weight).

## Clinical signs

The rabbits of group which infected by intraperitoneal route with (4.5x10$^8$ cells) show dullness, loss of appetite , fever, decrease activity, dehydration, and lethargy. Also unresponsive to stimuli. Body temperature were more than 39.5 after one day post infection and disappeared gradually, recovery was complete within (7-9) days, other clinical signs were restlessness and dullness, which appeared after (24) hours post infection followed by diarrhoea,which continued for three days, the colour of feces was dark black to light green and paste in consistency with or without mucus when compared with faeces of the rabbits in the control group

## Re-isolation of bacteria

The results of re-isolation of *S.enteritidis* showed that bacteria were spread in different internal organs in different degree for 7 days from starting the experiment. In the Small intestine the *S. enteritidis* was highly spread in the small intestine after (24, 48, 72, 96, 120, 144,and 168 ) hours and second and third weeks after induce infection from most rabbit which infected intraperitoneally with infective dose only 2 rabbits gave a negative result in 6 and 7 days. While in the liver the*S.enteritidis* was isolated from the liver after (24, 48, 72, 96, 120, 144 and 168) hours after infection only two rabbits gave negative result at 144 and 168 hours from infection. Moreover from the spleen the *S. enteritidis* is moderate isolated from spleen of infected rabbits (only in 3 and 4 day after infection).Though, from the lung the *S. enteritidis* was isolated from lung at (24, 48, 72, 96, 120, and 144 hours).Besides, in the kidney *S. enteritidis* was isolated from kidney at (24, 48, 72 and 120 hours).Also, in the heart the *S. enteritidis* was recorded and isolation from blood heart of infected rabbits at (24, 48, 72, 96,120, and 144 hours). Then, from the large intestine the bacterial isolation from large intestine of infected rabbits showed highly at time (24, 48, 72, 96, 120, 144, and 168 hours).

## Post mortems change in organs of rabbits

### A. Control group

There are no pathological changes in internal organs of control group used in the experiment.

### B. Infected group with infectious dose of *S. enteritidis*

The internal organs of sacrificed rabbits, which injected intraperitoneal with infectious dose (4.5 × 10$^8$ C.F.U/ml),were examined in these time (24, 48, 72, 96, 120, 144, 168) hours, second and third week post infection. Two rabbits sacrified in each time and were found as fallow:

### First week after infection

**Abdominal viscera** show flaccid of small intestine and filled with clear to yellow watery contents and there is sever congestion of large intestine.
**Liver:** enlarge in size (hepatomegaly) and dark- red in color .necrotic foci areas (white –yellow) in color.
**Lung:** enlarge in size, congested, with pale –white in color and focal hemorrhagic.
**Small intestine:** dilated and filled with watery clear to yellow, flaccid, thin wall.
**Large intestine**: congestion and filled with feces.
**Microscopically**: in the intestine of control rabbits the payer patch is normal and no pathological lesions but the infected intestine  there is infiltration  of inflammatory cells (macrophage and lymphocyte) also there is exudate, sluffing of epithelium  and necrosis the liver showed infiltration of inflammatory cells, necrosis, fibrosis and there is

exudate, in severe cases there is granuloma and amyloid degeneration(infiltration of homogenous protein material) .lung, There is sever infiltration of inflammatory cells(macrophage and lymphocyte) ,damaged of the alveoli , and there is exudate and necrosis. In the heart mild infiltration of inflammatory cells in striated muscle (mononuclear cell).

## DISCUSSION

ID of *salmonella enteritidis* in this experiment was similar to the ID of other non typhoid salmonella, that mentioned by AL- Talib,(2010) who found that the infective dose of *S.Newport* in rabbits $2\times10^8$ C.F.U./ml and with study of Blaser and Newman,(1982) which referred that the infective dose range between $10^5 – 10^{10}$ cells, also with AL-Mansory,(2009) who recorded the ID of *S.enteritidis* in rabbits was $2\times10^8$ ( C.F.U./ml). The rout of infection in currentstudy was intra peritoneal, so the result is agreement with AL- Qaisi, (2004) who reported that the inducing infection by intraperitoneal rout was better than oral infection, because of present large number of barrier in gastrointestinal tract such as intestinal acidity, competitive with normal flora and secretory IgA and other barrier, while in intraperitoneal rout were have fewer barrier. The color of feces was dark black to light green and paste in consistency with or without mucus when compared with feces of the rabbits in the control group. These clinical signs were compatible with study of harab (2010) in rabbits which infected experimentally with *S.hadar* which showed the same clinical signs. In our study then these clinical signs disappeared gradually and recovery was complete within (7-9) days.AlsoThe results of the present study was agreement with AL-Mansory, (2009) which recorded the same clinical signs on rabbits infected with *S.enteriditis* .

Rabbits have been chose as a model for diarrheal disease and its sequelae associated with salmonellosis (Brutzki *et al*., 2001). *S.enteritidis* invade the mucosa of small and large intestine and produced toxins, then stimulates the release of pro-inflammatory cytokines and acute inflammatory reaction occurs. *Salmonella* can be disseminated from intestine to other organs and cause systemic infection (Monack and Falkow., 2004).Decreased of body weight after infection of *S.enteritids* due to strong anaroxia that was associated with loss of body weight in infected group, these results were compatible with the results of (Fabienne*et al.,* 2002). While the animals of control group showed increased in body weight due to increase food intake and normal activity of body metabolisim. The results of the gross pathological findings of *S.enteritidis* in rabbits in the infected group after infection resemble those recorded by (Al-Mansory, 2009) in an experimental infection of rabbits by *Salmonella enteritidis* which found the same post mortem findings in (intestine, liver, spleen, kidney, lung, lymph nodes, gall bladder and heart). Also these gross lesions are in agreement with the study of Al-Naqeeb, (2009) on mice that showed various degrees of changes in the internal organs after giving the animals ID of *S. hadar*. The changes were liver and spleen was sever swollen and congested together, with petechial hemorrhages on their surface, the gall bladder was enlarged, the kidneys were swollen and the heart appeared flabby.

Other studies have also shown those pathological findings like Al-Hashimi, (2005) in mice through experimental infection with *S. enteritidis*, Yousif, (2000) in guinea pigs experimental infection with *S. typhimurium* and Yass, (1990) in an experimental infection of calves by *S. typhimurium* they found the same post mortem findings with various degrees of changes in the internal organs after infection. In the infected animals the intestine show proliferation in the payer patch and infiltration mononuclear cell , alsosloughing inepithelial lining of payers patch and infiltration of mononuclear cell these microscopically changes are in agreement with Zhou *et al.* (2003) reported that *S.enteritidis* pathogens induced cellular damage characterized by cellular necrosis, disruption of the epithelium and occasionally bleeding.Inlung, there is emphysema andcongestion of blood vessels and infiltration of mononuclear cell and damaged of the alveoli. The liver in our study there is necrosis and loss ofcellularity details due to karryolyesis of nuclei's of the hepatocytes theseagree withWadolkowski*et. al.,* (1990). Xu and Qi. ( 1988)  as a result from the action of toxin of *S.enteitidis* bacteria,

## CONCLUSIONS

Our results are clearly establish that this bacteria is pathogenic in rabbits and associated with pathological, immunological and histological alteration. More changes (histological and pathological) were seen in the liver, intestine and lung. This bacteria is a highly infect and spread to all organs. The effective dose used here is optimal to do such infection in rabbits.

### Ethical approval

This study was approved by the Ethical and Research Committee of Veterinary Medicine College / University of Diyala/Iraq.

## REFERENCES

1. AI-Hashimi, L.J.M. (2005). Study of some pathological and immunological aspects of *S. enteritidis* in mice. M.Sc.thesis, Vet. Med. College/ Baghdad University - Iraq.
2. AI-Mansory, S.H.H. (2009).Preparation of some *Salmonella enteritidis* antigens isolated from goats and study the immune efficacy of them in Rabbits. M.Sc. thesis, Vet. Med. College / Baghdad University - Iraq.
3. AI-Naqeeb, M.M.N. (2009). Study the pathogenesis of *Salmonella hadar* which isolated from goats in mice. M.Sc. thesis, Vet. Med. College / Baghdad University - Iraq.
4. AL-Qaisi, M.K. (2004). "Pathological and immunological changes for bacillary dysentery bacteria in mice and guinea pigs". Ph. D thesis, Vet. Med. College/Baghdad University- Iraq (in Arabic language).
5. AI-Talib MT (2010). Isolation and Identification of Non- TyphodialSalmonella from Children and Sheep in Baghdad City and Compare The Virulent of The Zoonotic Isolate in Rabbits. M.Sc. thesis, Vet.Med. College / Baghdad University - Iraq.
6. Blaser MJ and Newman LS (1982). A review of human salmonellosis: Infective dose. Reviews of Infectious Diseases. 4: 1096-1106.
7. Brent AJ, Oundo JO, Mwangi I, Ochola L, Lowe B, Berkley JA. *Salmonella* bacteremia in Kenyan children. Pediatrics Infectious Disease Journal. 2006; 25(3):230–6.
8. Brutzki, T.C.; Kulczycky, M.J.; Bardossy, L.; Clarke1, B.J. and Blajchman, M.A. (2001). Rapid in vivo induction of leukocyte tissue factor mRNA and protein synthesis following low dose endotoxin administration to rabbits. The Hematology Journal., 2: 188 – 195.
9. Fabienne, B .; Ruot, B.; Chereau, G .B; Denis, B . and Christiane O .(2002).The response of liver albumin synthesis to infection in rats varies with the phase of the inflammatory process . Clin. Sci, 102:107-114.
10. Glynn MK, Bopp C, Dewitt W, Dabney P, Mokhtar M, Angulo FJ. Emergence of multidrug resistan*Salmonella enterica* serotype Typhimurium DT104 infections in the United States. The New England Journal of Medicine. 1998; 47:151–7.
11. Harab AA (2010). Bacteriological study of salmonella hadar isolated from children: study of serum Biochemical and Hematological changes in rabbits. Veterinary Medicin\ Zoonoses. Infections among fulton county children associated with chitterling preparation. Georgia Epidemiology Report; February,volume 17 number 02.
12. Hohmann EL. Nontyphoidal *Salmonellosis*. Clinical Infectious Diseases. 2001 Jan.32:15
13. Leung DT, Bogetz Itoh M, Ganpathi L, Pietroni MA, Ryan ET, Chisti MJ. Factors associated with encephalopathy in patients with Salomnella enterica serotype Typhi bacteremia presenting to adiarrheal hospital in Dhaka, Bangladesh. The American Journal of Tropical Medicine and Hygiene 2012 Apr;86(4):698-702.(PubMed:22492156).
14. Luna, H. T. and Lee, G. (1968). "Manual of histological staining method of the Armed Forces Institute of Pathology". 3rd Ed.The Blakiston Division. McGraw–Hill Book Co. New York.USA.
15. Miles, A.A. and Misra, S.S. (1938). The estimation of the bactericidal power of blood. J. Hyg., 38: 732-749.

16. Monack, D.M. and Falkow.S. (2004). Development of acquired immunity to *Salmonella*. J. Med. Microbiol., 52: 453-459

17. Ridings, Philip C.; Windsor, Alistair CJ.; Sugerman, Harvey J.; Kennedy, Eugene; Sholley, Milton   M.; Blocher, Charles R.; Fisher, Bernard J.; Fowler, Alpha A.   Beneficial Cardiopulmonary Effects Of Pentoxifylline in Experimental Sepsis Are Lost Once Septic Shock Is Established. Archives of Surgery. 1994; 121:1144–52. [PubMed: 7979946].

18. XWadolkowski, E.; Sung, L.; Burris, J.; Samuel, J. and O'Brien, A.(1990). Acute renal tubular necrosis and death of mice orally infected with Escherichia coli strains that produce Shiga-like toxin type II. Infect. Immun.; 58: 3959-3965.u, J. G., and Qi, G. M. (1988).Microbiological, epidemiologic andclinical features of enterohemorrhagic Escherichia coli infection. Chinese J. Epidem.; 9(4): 174-177.

19. Yass, A.A. (1990). Experimental study on the pathogenesis of *Salmonella typhimurium* infection in calves. PhD thesis, Vet. Med. College/ University of Baghdad- Iraq.

20. Yousif, A.A. (2000). Immunization of pregnant cows and guinea pigs with Aromatic dependent *Salmonellae*. PhD thesis, Vet. Med.College/ Baghdad University- Iraq

21. Zhou, X.; Torres, A. G.; Crawford, J. A.; Negree, E.; Vogel, S. N.; and Kaper, J. B. (2003). Flagellin of enteropathogenic *Escherichia coli* stimulates interleukin-8 production in 84 cells. Infect. Immun .;71:2120-2129
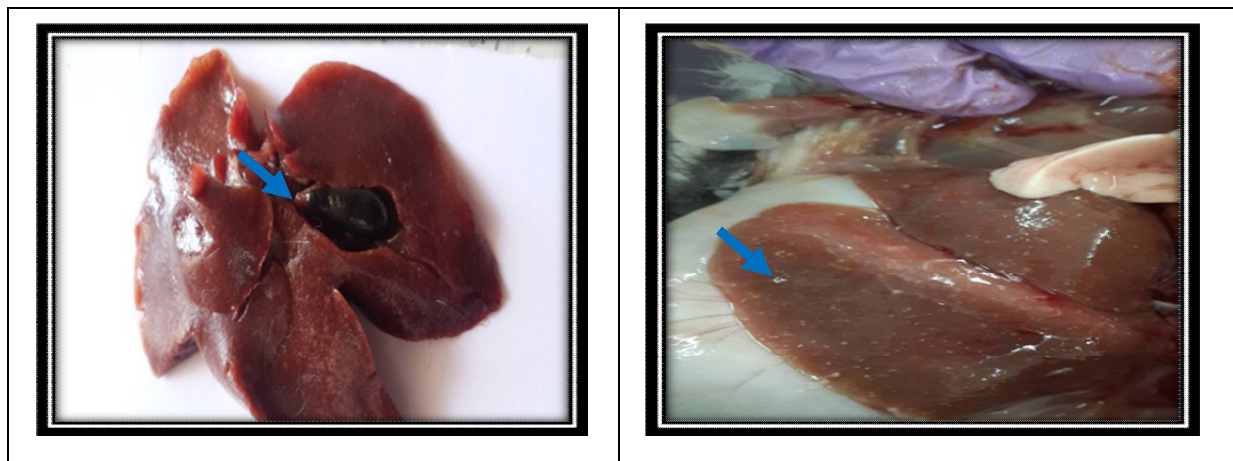
**Figure 1. Liver of infected rabbit showed enlargement, congested and necrotic foci, and fibrosis**
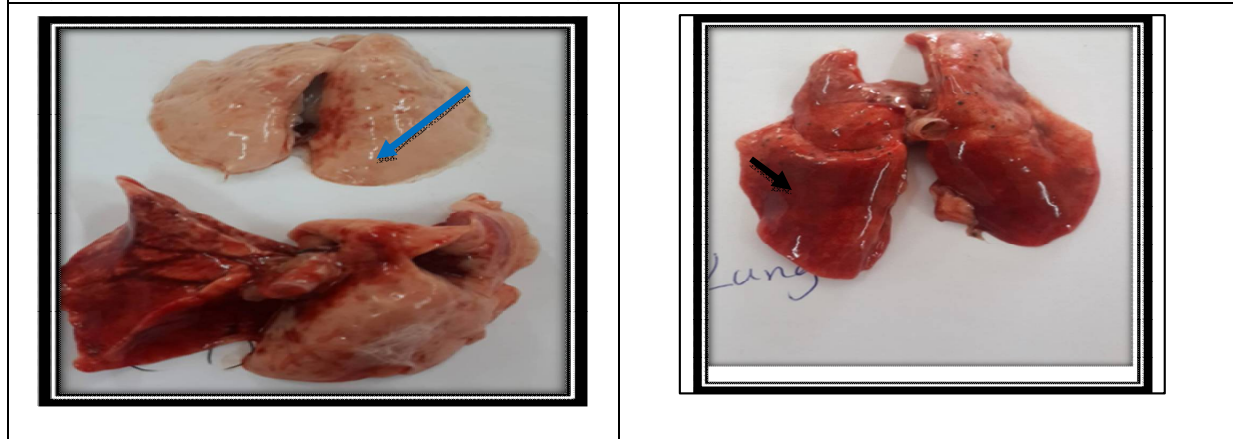


**Figure 2. Lungs showed enlargement in size and there isCongestion and focal haemorrhages, pale –white in colour**

**Ayat J.Mohammed and Khalid M Hammadi**



**Figure 3.Small intestine of infected group showed flaccid and filled by clear to yellow watery content and mucus in large amount**





**Figure 4. Large intestine of infected group showed congested and enlargement**
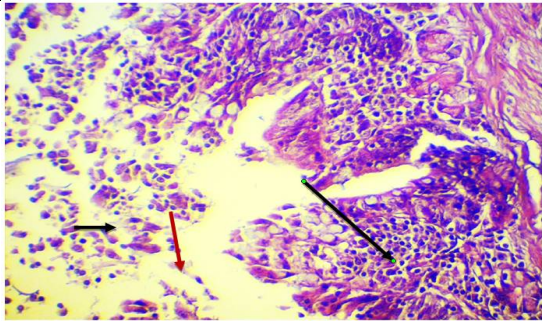
**Figure 5. Infected intestine after 72 hour showed infiltration of inflammatory cells ➡, sluffing of epithelium ➡ (H&E stain 20X).**
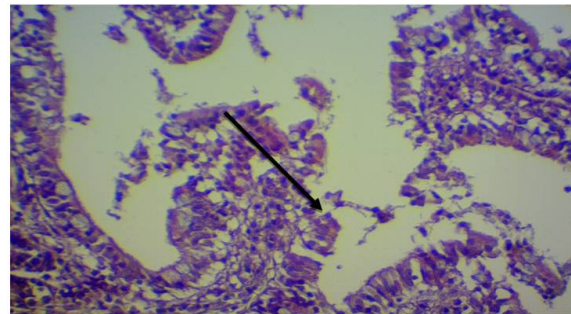


**Figure 6. Infected intestine after 1 week showed sloughing of mucosa (H&E stain 20X).**
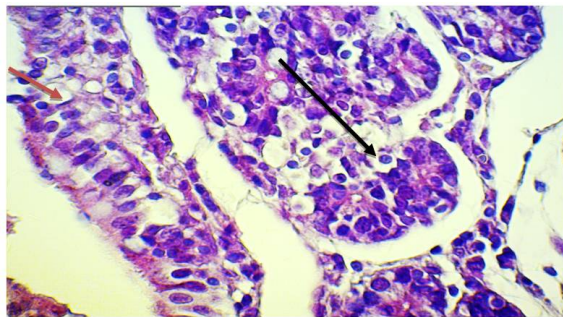


**Figure 7. Infected intestine after 2 weeks, there is present of infiltration of inflammatory cells ➡, exudate and necrosis ➡ (H&E stain 20X).**
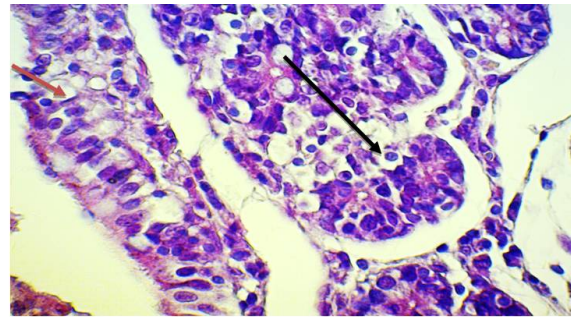


**Figure 8. Infected intestine after 3 weeks of infection showed sloughing of epithelium ➡ and infiltration of inflammatory cells ➡ (H&E stain 10X).**



**Figure .9.Infected liver after 144 hour there is presence of granuloma (macrophage and lymphocyte)➡ amyloid infiltration ➡ and few necrosis (H&E stain 20X)**



**Figure 10. Infected lung after 72 hour after infection, there is few infiltration of inflammatory cell, ➡ exudate and damaged of alveoli ➡ (H&E stain 20X)**

**RESEARCH ARTICLE**

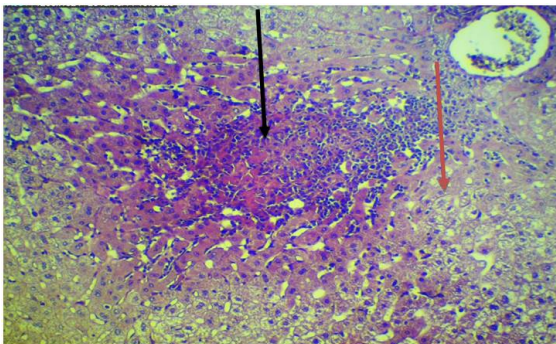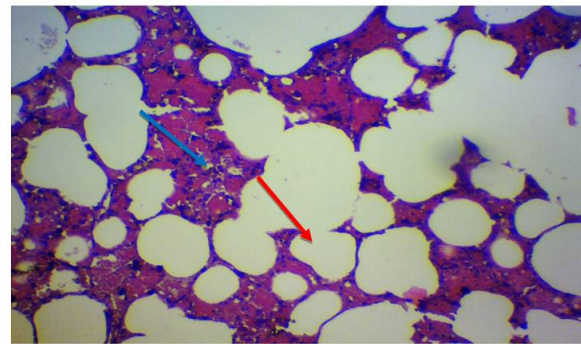# The Derived Air Concentration and Annual Limit of Intake of Airborne Particulate Sampling for Selected Places at Al-Tuwaitha Nuclear Site During Winter-Spring and Summer-Autumn Seasons

Altaf Abdulmajeed Al-Rahmani[1*], Yousif Muhsin Zayir AL-Bakhat[2], Naheel Abbas Mohammed Salih[1], Fadhil H. Mizban[3] and Faeq A. Mohammed[3].

[1]Department of Physics,Collage of Science for Women, University of Baghdad, Iraq.
[2]Ministry of Science and Technology (M0ST) - Radiation and Nuclear Safety Directorate (RNSD), Iraq.
[3]Iraqi Radioactive Sources Regularity Authority (IRSRA), Iraq.

*Address for Correspondence
**Altaf Abdulmajeed Al-Rahmani**
Department of Physics,
Collage of Science for Women,
University of Baghdad, Iraq.
Email: a.alrehmani@yahoo.com

## ABSTRACT

This study presents the results of atmospheric particulates sampling using high volume air sampler then analyzed these sampling for gross alpha /beta radioactivity byLudlum model 3030 instrument in Al-Tuwaitha nuclear site and the surrounding areas for the period from 28/12/2016 to 8 /1/2018.In Winter –spring seasons , the activity concentrations of $\alpha$-particles varied from (0.42-4.18 Bq/m$^3$) and $\beta$-particles varied from (0.93-9.2 Bq/m$^3$), while in Summer- Autumn seasons, the activity concentrations of $\alpha$-particles varied from (0.32-3.14 Bq/m$^3$ )and $\beta$-particles varied from (0.67-6.74 Bq/m$^3$). It is significant to denote that those values have been measured during day. the results show that the metrological parameters (temperature, humidity  and wind speed) have great influence on the measured activities concentration.The activity concentration of nuclides inversely proportional with air temperature and wind speed. The activity concentration of nuclides directly proportional with relative humidity.To determine the type of contaminants, we used Gamma –ray spectroscopy with high purity germanium detector .In Winter- Spring seasons , it had found that the range of activity concentrations of $^{238}$U($^{214}$Bi and $^{214}$Pb vary from <BDL to 2.15±0.037 Bq/m$^3$ and 1.32±0.063 Bq/m$^3$respectively) and $^{232}$Th($^{212}$Bi and$^{212}$Pb vary from <BDL to 0.11±0.027 Bq/m$^3$ and 0.18±0.0079 Bq/m$^3$,respectively ). in addition to $^{40}$K activity concentration was measured and  vary from <BDL to 0.34±0.070 Bq/m$^3$.In Summer- Autumn seasons, it had found that the range of activity concentrations of $^{238}$U($^{214}$Bi and$^{214}$Pb change from <BDL to 1.02±0.025 Bq/m$^3$ and 0.59±0.013 Bq/m$^3$ respectively) and $^{232}$Th($^{212}$Bi within BDL  while $^{212}$pbchangesfrom <BDL to 0.09±0.0061 Bq/m$^3$ ).moreover the range of activity concentrations of $^{40}$K change from <BDL to 0.32±0.057 Bq/m$^3$ . The Inhaled quantities of the radionuclides of concern and airborne activities were considerably lower than the  DAC and ALI recommended by IAEA , indicating the non-hazardous category of airborne radioactivity at Al-Tuwaitha Nuclear Site.

**Altaf Abdulmajeed Al-Rahmani *et al.***

## INTRODUCTION

Atmospheric radioactivity is a matter of concern because the inhalation pathway is a major avenue for the entry of contaminants into the body. We take in a larger mass of air than either food or water; the daily intakes by a reference person are only 1.9 kg of food and2.2 kg of water, but 26 kg of air. Additionally, the area of interface in the lungs—between the body's internal milieu and the outside atmosphere is 50–100 $m^2$. This large interface facilitates the transfer of noxious agents from the inhaled air into the body fluids. Therefore, if the quantity of radioactivity being handled is great enough to pose a significant inhalation hazard, in case of an accidental release of the radioactivity to the air (1). Radiological contamination is the deposition of, or presence of radioactive substances on surfaces or within solids, liquids or gases (including the human body), where their presence is unintended or undesirable Such contamination presents a hazard because of the radioactive decay of the contaminants, which emit harmful ionizing radiation (2).

In 2008, Flury et al.(3) has tested a new high volume air sampler (DIGITEL DHA-80). The filters are analyzed in the laboratory by a high purity coaxial germanium detector. In the test period natural radio nuclides and traces of $^{137}Cs$were measured and monitoring network is to detect rapidly any input of artificial radioactivity, as for example the cosmogenic$^7Be$ and the long-lived radon daughter $^{210}Pb$. The $^{214}Pb$ was in the range 1.03 – 5.59 Bq/$m^3$ and $^{212}Pb$ was in the range 0.0069-0.19 Bq/$m^3$. A detection limit for artificial $^{137}Cs$ of 2 µBq/$m^3$ is obtained (3). In 2010, Todorovis et al.(4) were measured the concentrations of beryllium-7 ($^7Be$), lead-210 ($^{210}Pb$) and cesium-137 ($^{137}Cs$) at two sites in the city of Belgrade (Serbia). One monitoring site was located in the central city area with heavy traffic and the other within the Institute of Nuclear Sciences Vinca, in the suburbs. Presented data cover the period 2004–2009. Aerosol samples were collected on filter papers by constant flow rate sampler. Activity of the radionuclides was determined on an HPGe detector by standard gamma spectrometry. Activities of$^7Be$ and $^{210}Pb$ exhibit a similar seasonal pattern. The mean monthly concentrations of $^7Be$ did not exceed 7 mBq/$m^3$.The activity of $^{210}Pb$ was below 0.9 mBq/$m^3$. Concentrations of $^{137}Cs$ were mainly below the limit of detection(4).

In 2011, Clemenza et al.(5) studied the presence ofairborne $^{131}I$, $^{134}Cs$, and $^{137}Cs$ in air particulate due to accident of Fukushima reactors has been detected and measured in the LowRadioactivity Laboratory operating in the Department of Environmental Sciences of the University of Milano-Bicocca.The sensitivity of the detecting apparatus is of 0.2 µBq/$m^3$ of air. Concentration and time distribution of theseradionuclides were determined and some correlations with the original reactor releases were found. Radioactivecontaminations ranging from a few to 400 µBq/$m^3$ for the $^{131}I$ and of a few tens of µBq/$m^3$ for the $^{137}Cs$ and $^{134}Cs$ havebeen detected(5). In 2017, M.Haque and Ferdous(6)measured the radioactivity levels of naturally occurring radionuclides $^{226}Ra$, $^{228}Ra$ and $^{40}K$ in eighteen water and eight air samples,collectedfrom Savar Atomic Energy Center Bangladesh, were determined using gamma ray spectrometrysystem using a High Purity Germanium (HPGe) detector of 40% relative efficiency. The air samples had activity concentrations of $^{226}Ra$, $^{228}Ra$ and $^{40}K$ varied from 1.49±0.00 to 613.56±0.01, 0.00±0.01 to79.90±0.02 and 19.70±0.05 to 206.82±0.00 mBq/$m^3$respectively. They calculated average activity (6).

In 2017,Karkoush et al.(7) measured the activity of airborne radon in the outdoor air environment near contaminated zones at two scrap yards  at Al-Tuwaitha Nuclear Site was recorded   using RAD7 electronic radon detector. Outdoor air-borne radon activity ranged from 5.9 to 11.84 Bq/$m^3$ for the first zone  and from below detection limit (< 4 Bq/$m^3$) to 17.76 Bq/$m^3$ for second zone, which were less than the International Atomic Energy Agency prescribed action level (1000 Bq/$m^3$) for workplaces(7).In 2018, Abbas et al.(8) determined the activity of atmospheric particulates sampling using high volume air sampler for selected places at Al Tuwaitha nuclear site. The measurement of activity concentrations ranged from (0.42±0.03 to 4.18±0.13) Bq/$m^3$ for alpha particles and from(0.93±0.06 to 9.21±0.26)

16597

Bq/m³for beta particles The collected samples were analyzed for gross alpha /beta radioactivity using Ludlum model 3030 and measurement particles activity in Al Tuwaitha nuclear site and the surrounding areas (8). The aim of this work was to establish activity concentration of alpha and beta particles in the atmosphere  to calculate ALI and  DAC in Al-Tuwaitha site .

# EXPERIMENTAL WORK

### Areas of the Study

The experiment was carried out atAl-Tuwaitha Nuclear Research Center (The majority of Iraq's former nuclear facilities are in the, located about 20 km south of Baghdad(N33.20631,E044.51874) on28/12/2016 to 8 /1/2018(9). In this study, 53 locations were covered, many of them are inside Al Tuwaitha site and the other are located outside are background areas as shown in figure (1)

### Measurement of activity concentration in air

The method is based on the collection of aerosols, by using high volume air sampling (High Volume3000) samplerParticulate from Australia. This devise is used for outdoor sampling, with air flow rate (10-15)m³/hr. The measurement isdone by putting the devise 20 meter far from the building and within established periods of time, usually an hour. The total volume of air can be calculated from the flow –rate multiplied by the sampling time(10). The aspiration is done through an air filter, type No.37030,glass fiber with diameter 5.5 cm,withcollection efficiency 99%(1).Thesamples are collected from many locations at Al-Tuwaitha Nuclear Site and the surrounding areas. The atmosphericparameters are: temperature ; pressure: ; wind speed; and humidity.as shown in fig. (2)

In this study the measurements of airfilters are performed by the measurement of alpha and betaparticles usingLudlum 3030 alpha / beta sample counter from USAwhich have dual-channel counters designed forsimultaneous alpha and beta sample measurement, and scintillation detector type ZnS(Ag) with a shielded chamber and chrome-plated brass sample tray that can accept a maximum samplesize of 5.1 cm (2 inches) in diameter. The instrument was calibrated daily (prior to use) using standard sources supplied by the manufacturer to be used that day,every Twenty-four hours QC must be done, This feature ensures that the instrument is tested dailyand that measurements are valid (11).as shown in fig.(3) The measurement of alpha and beta activity was made by the use of the Alpha-Beta counter Ludlum 3030, having the background counting rates3cpm or less for alpha, and 50cpm or less for beta radiations. The method consists in the followings: after the expiry of the aspiration time (1 hour), the filter is removed from the aspiration motorand putin Ludlum 3030 devise and counted for 1minute then repeat. The measurement was repeated 3 times. The average for the three values was estimated. The following equation was applied for estimating the alpha and beta activity concentration in air (12)

$$A = \frac{activity\ net}{V \times E_f} \ldots\ldots\ldots(1)$$

where *A* is radioactive concentrations (activity densities) expressed in units Bq.m⁻³, *V* is the air total volume (m³), E$_f$ the filter efficiency=99% .The instrument subtracts the background automatically. One Becquerel (Bq) is equal to one disintegration per second. 1 Becquerel (Bq) is equal to 60 DPM (13). Activity (Bq)=(DPM$_{ins}$– DPM$_{B.G}$)/60, where DPM is disintegration per minute, DPM$_{ins}$ is instant disintegration per minute, DPM$_{B.G}$ is background disintegration per minute.Aftermeasured the  activity concentration of depositedradionuclides  byLudlum 3030, the filter was taken togamma–spectrometry laboratory to know the type of radionuclide  and it,s activity concentration. Analysis was performed using a gamma-ray spectrometer with a p-type coaxial HPGe detector (Canberra (USA), relative efficiency

16598

40%; energy resolution (2 keV). The detector was coupled with 8192 Multichannel Analyzer for data acquisition. Genie 2000 software from Canberra was used to analyze the spectra. The detector was covered by a cylindrical lead shield with a fixed bottom and a movable cover to reduce the interference of background radiation from terrestrial and extraterrestrial sources in the measured spectrum. An empty Marinelli beaker was counted periodically in the same way to determine background radiation in the analytical laboratory As shown in figure (4).A proper efficiency calibration was done to convert the total count rate (cps) into corresponding activity per unit volume (Bq/m$^3$) using certified reference material (type filter) of mixed radionuclides$^{241}$Am (607.7 Bq), $^{109}$Cd (2453 Bq), $^{139}$Ce (151.0Bq), $^{57}$Co (137.4 Bq), $^{60}$Co (371.5 Bq), $^{137}$Cs (351.4 Bq), $^{113}$Sn (492.8 Bq), $^{85}$Sr (570.2 Bq) and$^{88}$Y (635.1kBq) The spectrometer was tested for its linearity and calibrated for energy using standard gamma sources ($^{137}$Cs source (activity 0.1 µCi) and $^{60}$Co source (activity 1 µCi)) manufactured by reliable supplier (Oak Ridge Spectrum Techniques (USA)).

### Annual Limit of Intake and Derived Air Concentration

The Annual Limit on Intake (ALI) was defined as an intake (in Bq) of a radionuclide in a year which would lead to a committed effective  dose of 20 mSv. ALIs are calculated separately for each intake pathway. The  annual limit on intake for workers is thus:

**ALI =0.02/E (50)………………..(2)**

(E(50)) was defined as Committed Effective Dose  per unit intake,   is the dose-commitment period E (50) the dose-commitment period in years over which the dose is calculated i.e. 50 y for adults  .And Derived Air Concentration (DAC) was defined as  the activity concentration in air in Bq/m$^3$ of the radionuclide  considered which would lead to an intake of an ALI assuming a breathing rate of the Reference Worker of 1.2 m$^3$.h$^{-1}$ and an annual working time of 2000 h.  Then the relationship between DAC  and ALIis given by(14)

**DAC=ALI/2400……………….(3)**

## RESULTS AND DISCUSSION

### The relationship between alpha-beta activities and meteorological conditions in Winter-Spring seasons

In Winter –spring seasons , the activity concentrations of $\alpha$-particles varied from (0.42- 4.18 Bq/m$^3$) and $\beta$-particles varied from (0.93-9.2 Bq/m$^3$). variations of gross alpha - beta activities as a consequence of meteorological conditions includes temperature, relative humidity, wind speed  during survey period in Winter - Spring seasons. The measured activities in the surface air in the studied area show fluctuations due to fluctuations in metrological conditions. The activity concentration of nuclides inversely proportional with air temperature and wind speed. The increase of temperature or wind speed causes decrease in the amount of activity . The activity concentration of nuclides directly proportional with relative humidity. Positive   relation between activity concentration and humidity.  As shown in table (1) and figure (4),( 5), (6) for alpha emitters  and figure (7), ( 8), ( 9) for beta emitters.To define the relation between  different  metrological parameters related to activity concentration we evaluate the correlation factor (R) by applying the formula below (15)

$$r = \frac{\sum_{i=1}^{n}(x_i - \overline{x})(y_i - \overline{y})}{\sqrt{\sum_{i=1}^{n}(x_i - \overline{x})^2 \times \sum_{i=1}^{n}(y_i - \overline{y})^2}}$$

**Altaf Abdulmajeed Al-Rahmani** *et al.*

### Results of analysis by Gamma spectrometry system

The results obtained for the levels of activity concentrations for radionuclides in air samples from studied area, which were plotted in Figure (10) are of natural origins ($^{238}$U, $^{232}$Th decay series in addition to $^{40}$K). The Bismuth isotope ($^{214}$Bi) has a maximum concentration  at the value of (2.15±0.037) Bq/m$^3$ in 19/2/ 2017  at T26. The Bismuth isotope ($^{212}$Bi ) has a minimum concentration at the value of (0.11±0.027) Bq/m$^3$ in 21/2/ 2017 at T28. The activity of $^{214}$Pb is in the order of magnitude of below detection limit (< 0.015 Bq/m$^3$) to 1.32±0.063 Bq/m$^3$ Moreover, $^{40}$K activity was measured and had its maximum value in 16/2/2017 attaining 0.34±0.070 Bq/m$^3$ at T25. And the activity of $^{212}$Pb is in the order of magnitude of below detection limit to 0.18±0.0079 Bq/m$^3$.

### The relationship between alpha-beta activities and metrological parameters

### Summer - Autumn seasons

In Summer- Autumn seasons , the activity concentrations of $\alpha$-particles varied from (0.32-3.14 Bq/m$^3$ )and β-particles varied from (0.67-6.74 Bq/m$^3$ ) .variations of gross alpha - beta activities as a consequence of meteorological conditions includes temperature, relative humidity, wind speed  during survey period in Summer and Autumn seasons. The activity concentration of nuclides inversely proportional with air temperature and wind speed.  And directly proportionalwithrelativehumidity.As shown in table (2) and figures (11), (12), (13) for alpha emitters and figures (14), (15), (16) for beta emitters.

### Results of analysis by Gamma spectrometry system

The measured isotopes in Summer - Autumnseasons are  drawn in figure (17). The activities of $^{214}$Pb and $^{214}$Bi correlate and tend to a common maximum in 29/8/2017 at T46S. The highest values are 1.02±0.025 Bq/m$^3$ for $^{214}$Bi and 0.59±0.013 Bq/m$^3$ for $^{214}$Pb. In 20 of 43 samples, $^{40}$K was detected and had an average activity of 0.10 Bq/m$^3$. The activity of $^{212}$Pb, is in the order of magnitude of below detection limit to 0.09 ±0.0061Bq/m$^3$.

### Results of Calculated ALI and DAC of airborne activities

The Inhaled quantities of the radionuclides of concern and airborne activities were considerably lower than the  DAC and ALI of recommended by IAEA, indicating the non-hazardous category of airborne radioactivity at Al-Tuwaitha Nuclear Site,table (3) show that.

## CONCLUSIONS

1. All measured radionuclides belong to natural decay series for $^{238}$U and $^{232}$Th series and their progenies in addition to$^{40}$ K and no presence of artificial radionuclides in measured areas in Al-Tuwaitha siteand non-hazardous category of airborne radioactivity at that Site.
2. Explore the relations which govern the behavior of activity concentration with metrological parameters (temperature, relative humidity, wind speed , rain and dust). The activity concentration is inversely proportional withtemperature, wind speed and rain but directly proportional with   relative humidity and dust.

## REFERENCES

1- Cember H, Jonsons D E. Introduction to health physics. McGraw-Hill, Colorado; Fourth edition: 2009.
2- International Atomic Energy Agency. Terminology Used in Nuclear Safety and Radiation Protection. IAEA, 2007.

3- Flury J. Natural and Artificial Radioactivity Monitoring at the High Altitude Research Station Jungfraujoch: Installation and Test of a New High Volume Aerosol Sampler in combination with Laboratory Gamma-Spectroscopy. Master thesis, University of Fribourg, 2008.

4- DraganaT, Dragana P, Jelena N, and Jelenam A. Radioactivity Monitoring in Ground level air in Belgrade urban area. Radiation Protection Dosimetry.2010;142:308–313.

5- Clemenza M O, Fiorini E, Previtali E, Sala E. Measurement of airborne 131I, 134Cs, and 137Cs nuclides due to the Fukushima reactors accident in air particulate in Milan (Italy). J Environ Radioactive. 2012;114:113-118.

6- Haque M, Ferdous J, Natural Radionuclides Present in Air and Water near Nuclear Research Reactor Savar Bangladesh. Int. J. Sci. Eng. Res. 2017;8(5):978–983.

7- Karkoush H, Al-Tameemi N. Measurement of Outdoor RadonLevels and Assessment of Radiological Hazards for Radioactively Contaminate Scrap Yards at Al-Tuwaitha Nuclear Site. Thirteen. Arab Conference Peaceful Uses Atomic Energy.2016;7–8.

8- Abbas N, Al-BakhatY, Al-Rahmani A, Murbat O, Ameen N, Majed N. Assessment of Radiological Air Contamination for Selected Places at Al-Tuwaitha Nuclear Site during Winter and Spring. 2018; 278.

9- Danneels J, Coates R, Cochran J, Chesser R, Phillips C. Proceedings of the 11th International Conference on Environmental Remediation and Radioactive Waste Management.OudSint-Jan Hospital Conference Center, Bruges, Belgium.September 2-6, 2007.

10- Ferntree, G. HiVol-3000PUF/XAD Sampler manual: 2009.

11- Ludlum measurements Inc. measurements. LUDLUM MODEL 3030, 3030-2 &3030E Alpha-Beta Sample Counter manual: 2012.

12- Al Banna, N. Fundamentals of protection from Ionizing radiation in Iraq: Iraqi Technical Institute authority;1990.

13- Reiman, R. Introduction to Radiation Physics, Quantities and Units: Duke University Medical Center Against Radiation; 2002.

14- International Commission on Radiological Protection. Occupational Intakes of Radionuclides 13.ICRP PUBLICATION. Vienna, Austria. Part 1:2012.

15- Tallas M. Basic Principles in Applied Statistics. Syria. 2002.

16- International Atomic Energy Agency. Radiation Protection and Safety of Radiation Sources: International Basic Safety Standards General Safety Requirements. Vienna, Austria.part 3 No. GSR part 3: 2014.

**Table 1. behavior of different parameters in Winter-Spring seasons**

| Parameter 1 | Parameter 2 | proportional | R |
|---|---|---|---|
| Alpha Activity concentration | Temperature | Weak inversely | -0.45 |
| Alpha Activity concentration | Wind speed | Weak inversely | -0.46 |
| Alpha Activity concentration | Humidity | Weak directly | 0.17 |
| Beta Activity concentration | Temperature | Weak inversely | -0.48 |
| Beta Activity concentration | Wind speed | Weak inversely | -0.48 |
| Beta Activity concentration | Humidity | Weak directly | 0.18 |

**Table 2. behavior of different parameters in Summer - Autumn seasons**

| Parameter 1 | Parameter 2 | proportional | R |
|---|---|---|---|
| Alpha Activity concentration | temperature | Weak inversely | -0.14 |
| Alpha Activity concentration | Wind speed | Weak inversely | -0.37 |
| Alpha Activity concentration | humidity | Weak directly | 0.37 |
| Beta Activity concentration | temperature | Weak inversely | -0.17 |
| Beta Activity concentration | Wind speed | Weak inversely | -0.36 |
| Beta Activity concentration | humidity | Weak directly | 0.41 |

**Altaf Abdulmajeed Al-Rahmani** *et al.*

**Table 3. Radionuclide activities and committed effective dose for the inhalation pathway by workersinside Al-Tuwaitha**

| Season | Nuclide | Mean activity concentration (Bq/m³) | Committed Effective Dose(16)(Sv/Bq) | Inhaled quantity (Bq) | ALI (Bq) | DAC (Bq/m³) |
|--------|---------|------|------|------|------|------|
| Winter-Spring | Bi-214 | 1.04 | 2.10E-08 | 2496 | 952381.0 | 396.8 |
| | Pb-214 | 0.63 | 4.80E-09 | 1512 | 4166666.7 | 1736.1 |
| | Bi-212 | 0.02 | 3.90E-08 | 48 | 512820.5 | 213.7 |
| | Pb-212 | 0.08 | 3.30E-08 | 192 | 606060.6 | 252.5 |
| | K-40 | 0.06 | 3.00E-09 | 144 | 6666666.7 | 2777.8 |
| | | | | | | |
| Summer-Autumn | Bi-214 | 0.22 | 2.10E-08 | 528 | 952381.0 | 396.8 |
| | Pb-214 | 0.11 | 4.80E-09 | 264 | 4166666.7 | 1736.1 |
| | Bi-212 | 0.00 | 3.90E-08 | 0 | 512820.5 | 213.7 |
| | Pb-212 | 0.02 | 3.30E-08 | 48 | 606060.6 | 252.5 |
| | K-40 | 0.10 | 3.00E-09 | 240 | 6666666.7 | 2777.8 |
| | | | | | | |



**Figure 1. Aerial photo for Al-Tuwaitha Nuclear Site shows locations of the measurement**

16602

**Altaf Abdulmajeed Al-Rahmani** *et al.*



**Figure 2.High volume air sampler**



**Figure 3. Ludlum 3030 alpha / beta sample counter**



**Figure 4. Variation of gross alpha activities as a consequence of temperature**



**Figure 5.Variation of gross alpha activities as a consequence of wind speed**

16603

**Altaf Abdulmajeed Al-Rahmani** *et al.*



**Figure 6. Variation of gross alpha activities as a consequence of humidity**



**Figure 7. Variation of gross beta activities as a consequence of temperature**



**Figure 8. Variation of gross beta activities as a consequence of wind speed**

**Altaf Abdulmajeed Al-Rahmani** *et al.*



**Figure 9. Variation of gross beta activities as a consequence of humidity**



**Figure 10. Results of radiometric analysis for air filters in winter and spring seasons**
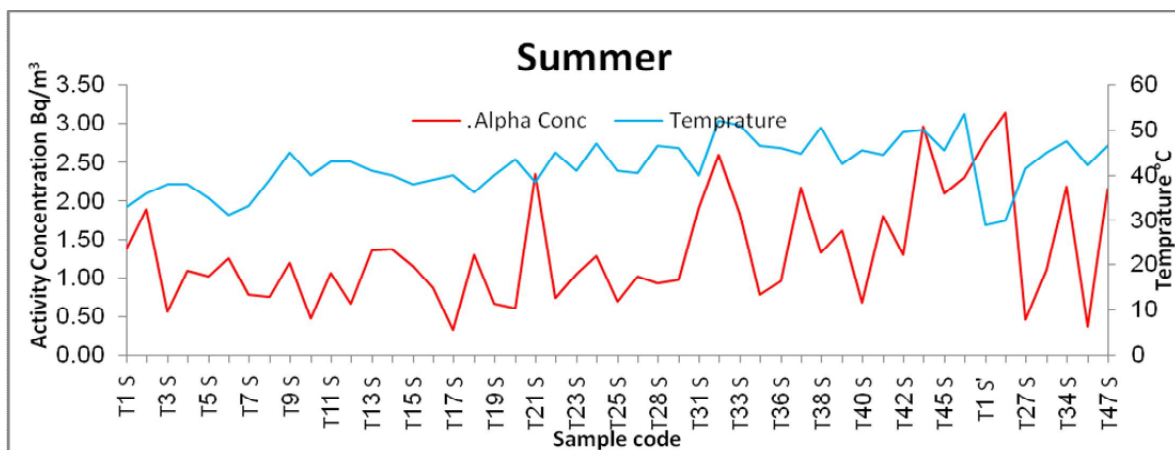


**Figure 11. Variation of gross alpha activities as a consequence of temperature**
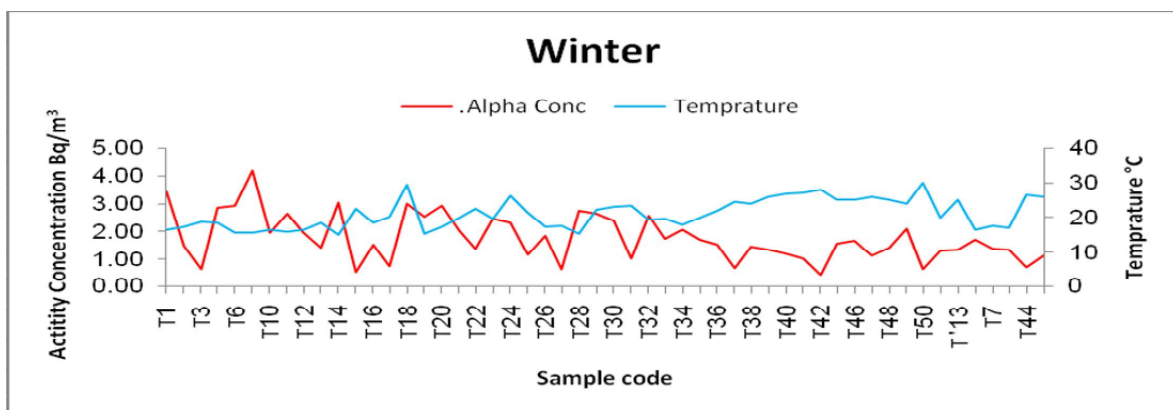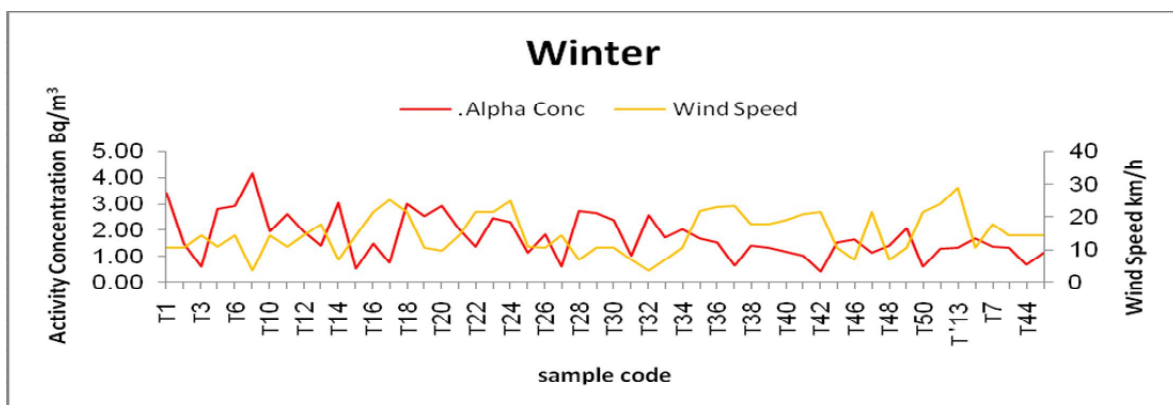
16605

**Altaf Abdulmajeed Al-Rahmani** *et al.*



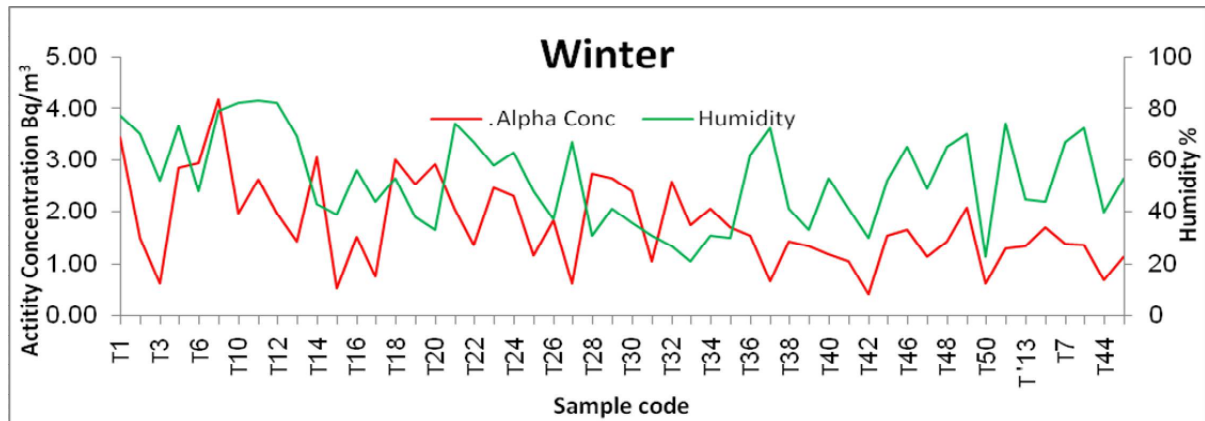**Figure 12. Variation of gross alpha activities as a consequence of wind speed**



**Figure 13.Variation of gross alpha activities as a consequence of humidity**



**Figure 14. Variation of gross beta activities as a consequence of temperature**
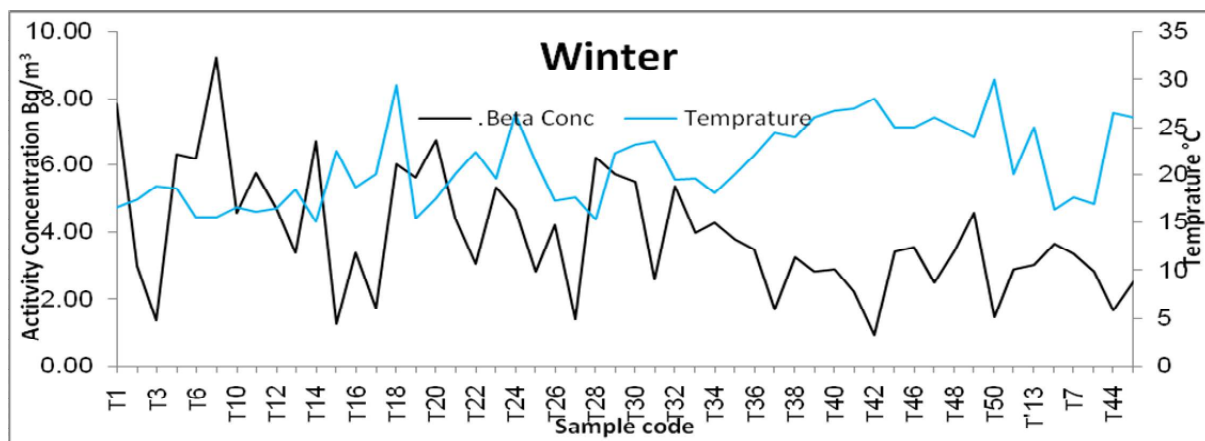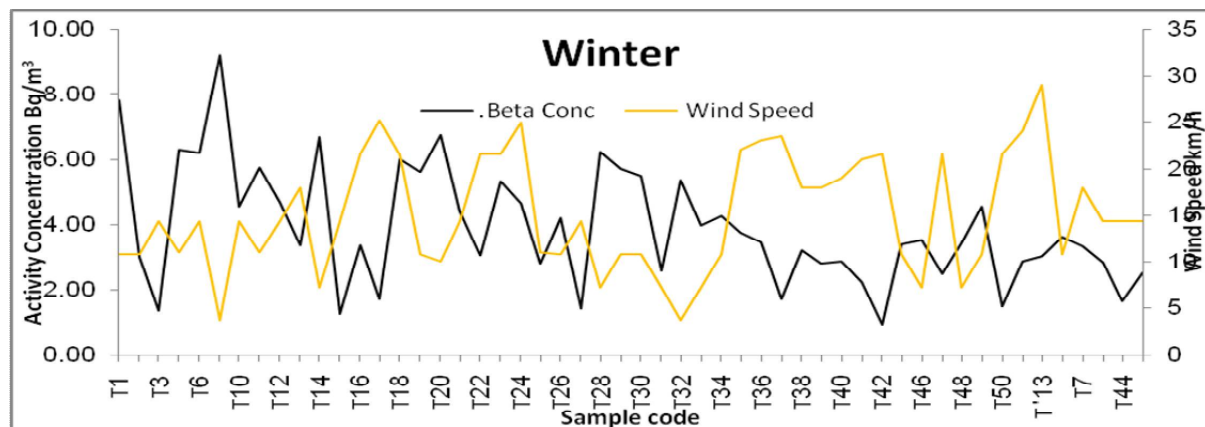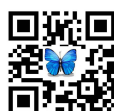
**Altaf Abdulmajeed Al-Rahmani** *et al.*



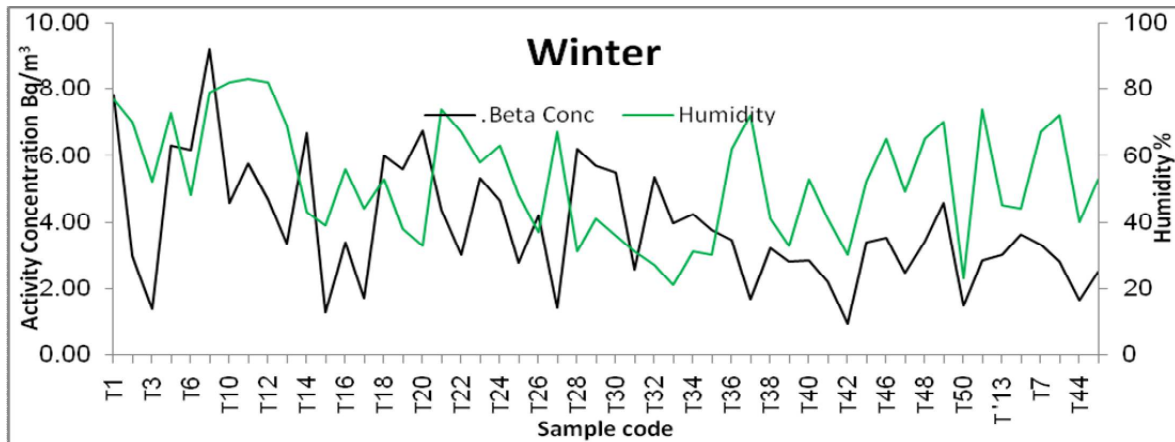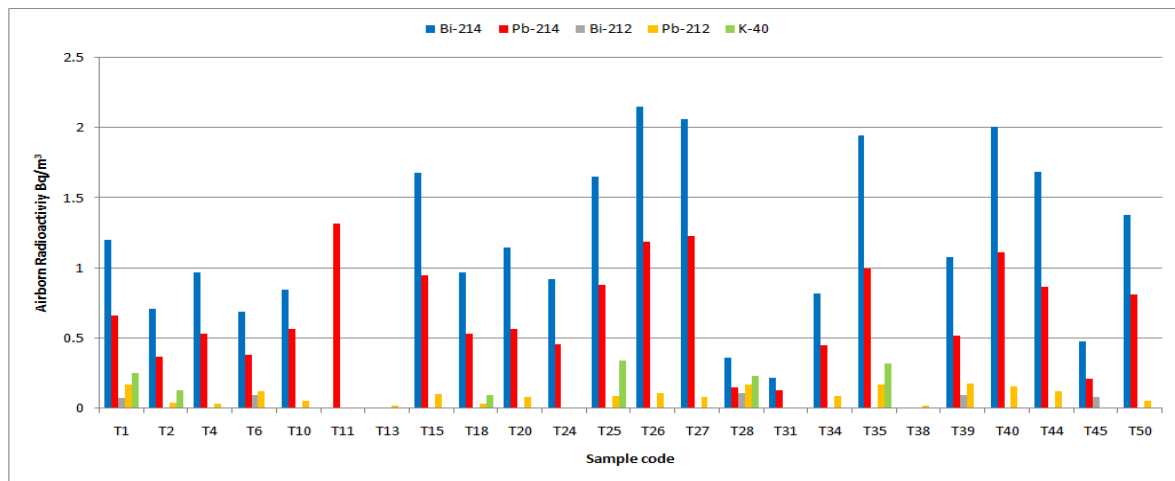**Figure 15. Variation of gross beta activities as a consequence of wind speed**
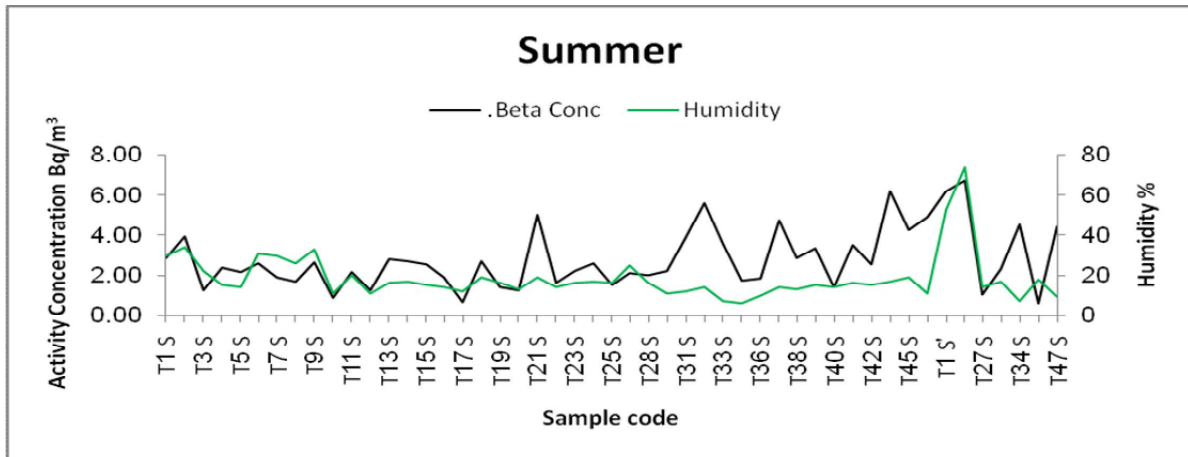


**Figure 16.Variation of gross beta activities as a consequence of humidity**
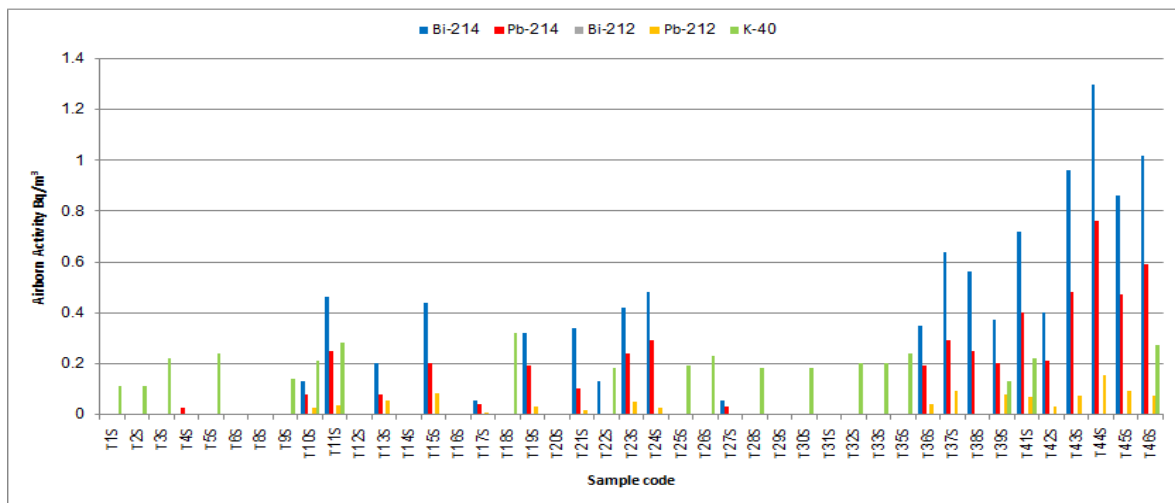


**Figure 17. Results of radiometric analysis for air filters in Summer and Autumn seasons**
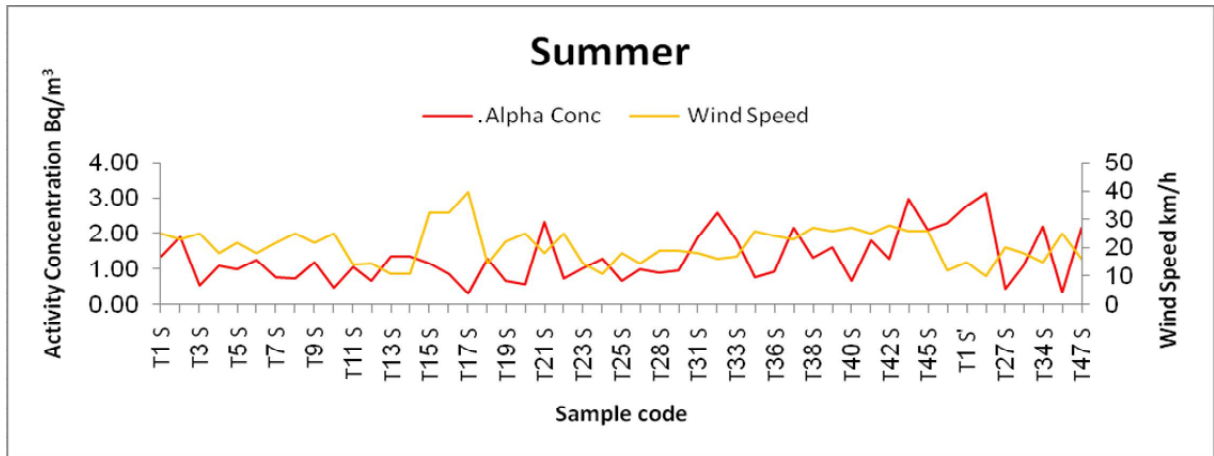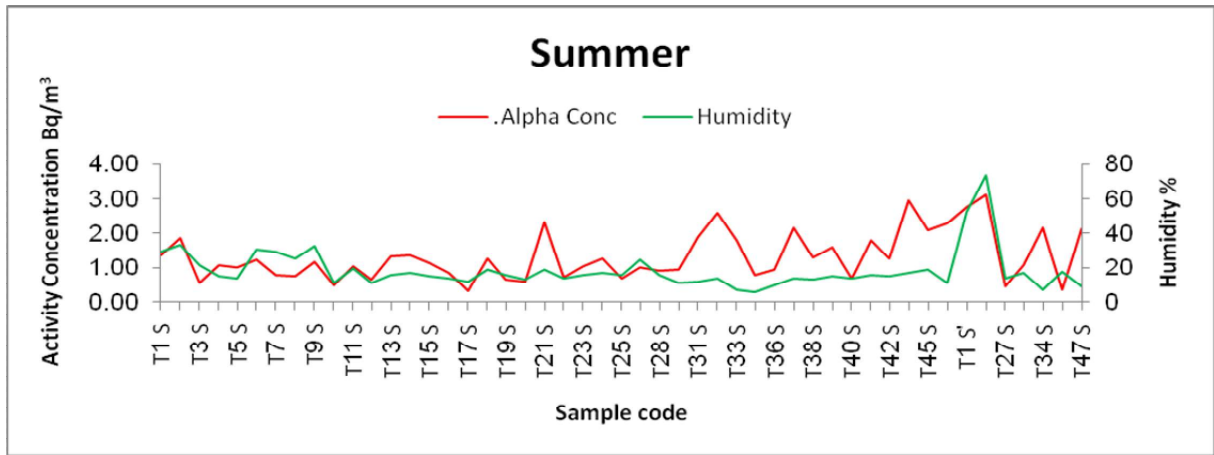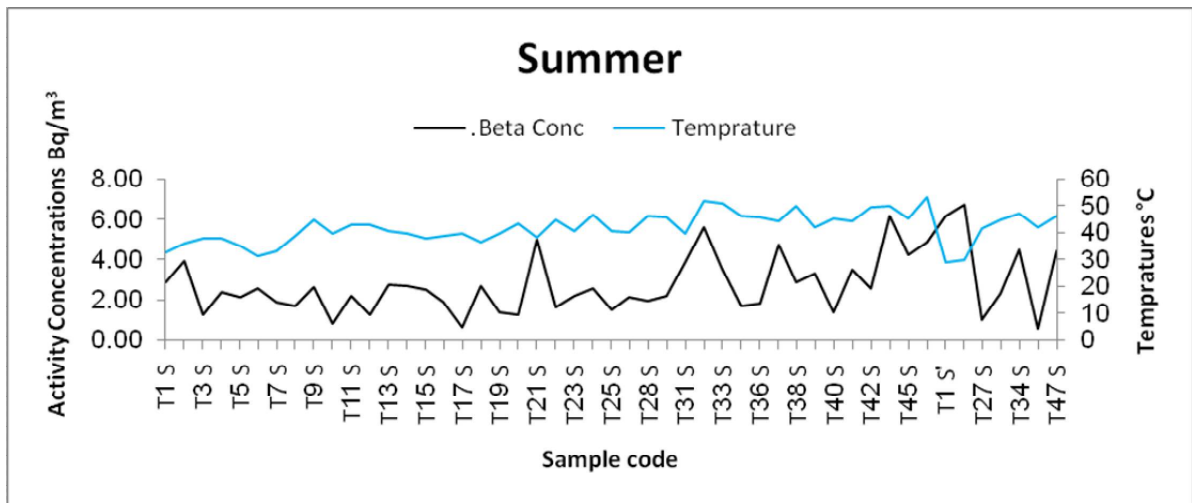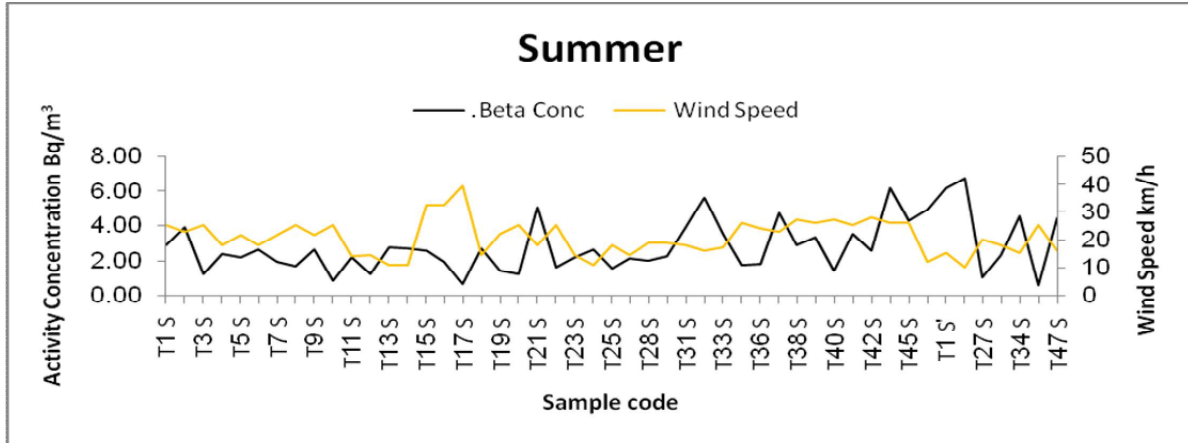
**RESEARCH ARTICLE**

# Effect of Gamma Irradiation on Physical Properties of (NiO) Electrochromic Thin Film

Mayada Kaream Hassan[1], Buthainah Abdulmunem Ibrahim[2*] and Ziad T. Khodair[3]

Department of Physics, College of Science, University of Diyala, Baquba, Iraq

\***Address for Correspondence**
**Buthainah Abdulmunem Ibrahim**
Department of Physics,
College of Science,
University of Diyala,
Baquba, Iraq.
E-Mail: buthmunem@gmail.com.

**ABSTRACT**

Electrochromic (EC) NiO thin film prepared from the solution of Nickel Nitrate Ni $(NO_3)_2$ .6 $H_2O$ and carbamide $(CH_4N_2O)$ deposited on conducted glass FTO by homemade chemical spray pyrolysis at 250°c with thickness 200 nm.NiO thin film is irradiated by gamma ray of energy (0.662 MeV) from Cs-137 for half hour. Optical and electrical properties of the electrochromic NiO thin film was studied by Ultraviolet spectroscopy and Cyclic voltammetry Chronoamperometry traces (CA) before and after irradiation.The results showed, after irradiation absorbance increases for (300- 700 nm) wavelengths, furthermore transmittance decrease for this range. The bleaching voltage of NiO thin film changed after irradiation from -70 mV to +45 mV, as well the bleaching time decreased from 65 s to 50 s and coloring time decreased from 25 s to 20 s.

**Keywords:** Chemical spray pyrolysis; NiO; Electrochromic thin film; Gamma irradiation

## INTRODUCTION

The electrochromism phenomenon, which is a change in color, obtained by a weak electric current, causing chemical oxidation reactions, to change the amount of light, which leads to change the color from transparency to opaque and vice versa [1]. Electrochromic materials are classified into organic and inorganic materials; inorganic materials are easily prepared and more stable. Electrochromic materials are used to control the amount of light and heat in smart windows, which is one of their most important uses. Different types of materials can be used to obtain electrochromic properties, as the transition element oxides are the widest range used in this field, including tungsten oxide (WO3), Nickel oxide (NiO) is widely used in electrodes, other materials are polyaniline, which can be formed from the chemical oxidation of aniline when immersing electrodes in hydrochloric acid containing a small concentration of

16608

**Mayada Kaream Hassan *et al.***

aniline [2]. There are other types of electrochromic materials used in technology applications, including Viologen, Poly oxotungstates and most commonly used in automotive factories. Mirrors are manufactured using halogen with titanium dioxide (TiO2) to form digital displays and blue, it has a high analytical ability to balance the bright white of Titania which has other uses in trains and planes. One of the common types of nickel oxide used in this research is that the thin film has a complex formula for the relationship between the chemistry and optical behavior due to color change with electrical voltage change which can give different color intensity [3].

It is widely used in smart windows and devices that work on this principle because of the rationalization in the consumption of electric power to have the ability to provide the cost of heating, air conditioning and lighting, by keeping the temperatures moderate inside buildings as well as control the levels of internal lighting, Smart phone to 99.4% is not effective for ultraviolet radiation [4]. The scientists' efforts are continuing to use the energy stored in the electrochromic thin film in the smart windows to save energy as they are colored to resist the sun and the possibility of storing the sun's energy & launch it through an external circuit and the possibility of using them to operate equipment inside the building, which is one of the promising uses in the future because it achieves goals which we aspire to, especially in the providing energy [5].

## EXPERIMENTAL

Nickel nitrate (Ni (NO3) 2.6H2O) and carbamide were used to prepare a thin film of nickel oxide. The nickel nitrate is a green powder substance with a molecular weight of 290.81g / mol and purity of 99% Dissolve (1g) of nickel nitrate and (3 g) of carbamide in (80 ml) of distilled water, gradually dissolving at room temperature by using a magnetic stirrer to reach a homogeneous solution of 0.1 M. The weight of the material was calculated using a sensitive balance of (Mettler AE-160). After the solubility process was completed & the solution was obtained, it was left for a suitable period of time to be cooled before spraying. The conducted glass FTO is well cleaned with the acetone and water. (NiO) thin film is deposited on FTO glass (2.5x1.5 cm$^2$) by chemical spray pyrolysis. After performing several procedures to obtain the best thin film with uniformity distributed and high adhesion we found that the best conditions for preparation are: Sedimentation rate and time are (30 ml / min), (5 sec) respectively, height of the humidifier (20cm), stop time (10 sec), air pressure (1.3bar). The thickness of the thin film is measured by using the gravimetric method which is done by weighing the glass substrate before and after deposition NiO film, then the thickness of the film is calculated from the following relationship [6]:

$$t = \frac{\Delta W}{\rho A} \quad \text{..................................................(1)}$$

As

$$\Delta W = (W2 - W1), \text{The weight of NiO film}$$

W1- Weight of the FTO glass before deposition,
W2 - Weight of the FTO glass after deposition NiO film.
A: The thin film area (cm$^2$).
$\rho$: density of NiO film (g / cm$^3$).

The optical measurements, including absorption, transmission and reflectivity measurements were performed using a UV-Visible1800 Spectrophotometer equipped, which is of a two-beam type. The electrical measurements were made using Cyclic Voltametery using three electrodes representing the working electrode NiO/ FTO, the silver electrode is the reference and the platinum electrode is a contrast with sodium hydroxide electrolyte (0.1 M).

**Mayada Kaream Hassan *et al.***

# RESULTS AND DISCUSSION

## Optical properties

### T (Transmittance )

Figure (1) shows the relationship between transmittance as a function wavelength before and after gamma irradiation. It is noticed that the transmittance decreases after irradiation in the range of wave length (300-900 nm) with the same behavior [7].

### A (Absorbance)

Absorption depends on many factors, such as thickness, length of the photon wave and color of the material. Figure (2) shows the absorbance as a function of the wavelength before and after gamma irradiation. It is noticed that, the absorbance decreased in the range of wave length (300-900 nm), but the sharp decrease in the range of (300 – 450 nm) ultra violet - visible rang, nearly constant in the range (451- 900 nm). It is noticed that the absorbance increases after irradiation without changing in its behavior [7].

### Absorption coefficient ($\alpha$)

The absorption coefficient is calculated as a function of photon energy as shown in the following equation:

$$\alpha = 2.303 \, A t \quad\text{.................................................. (2)}$$

Where,
A: Absorption.
t: thickness of NiO thin film (cm). Figure (3) shows the relationship between the absorption coefficient as a function photon energy before and after irradiation, it is clear that the absorption coefficient is greater than ($10^4$ cm$^{-1}$), indicating that direct electronic transitions is predominant [8].The absorption coefficient is increased in the range (300-900 nm) after irradiation.

### E$_g$( Energy gap)

The energy gap for allowed direct electron transition (r=1/2) for nickel oxide (NiO) is calculated by the following equation:

$$\alpha h \nu = \rho ( h \nu - Eg)^{r} \quad\text{.......................................(3)}$$

Figs (4, 5) show the optical energy gap of NiO film before and after irradiation, which are 3.3 eV and 2.9 eV respectively. It is noticed that energy gap decreased after irradiation. The reason is mostly due to the formation of local levels close to the conduction band, which contributed to increase the number of electrons which reach the conduction band [10], means that irradiation has shifted the basic absorption edge to low energies.

### Cyclic Voltammetry (CV)

This technique was carried out to investigate the electrochemical properties of the nickel oxide films before and after gamma irradiation is performed for six cycles at the range of voltages between (-1) to (1).Figures (6, 7) are CV traces; there are two peaks and two bottoms which represent the change of film colors. Table (2) illustrated the values of coloring and bleaching voltages.

16610

From left, the first peak represents change color of the nickel oxide film from transparent to brown. The first bottom represents change color of the film from brown to transparent.The voltages value of bleaching and coloring of NiO thin film are described in table (2). It is shown that the bleaching voltage changed from -70 mV to +45 mV after irradiation, this means change from cathodic peak to anodic peak [10, 8].

### Chronoamperometry traces (CA)

The CA traces determine the change in the current density as function of time for NiO EC film with six cycles. Figures (8, 9) show the coloring and bleaching time before and after irradiation for which table (2), illustrated the results.CA traces of NiO EC films used to confirm the stability of the film during cycling, the value of maxima and minima for different cycles represent number of charges inserted and extracted during coloring and bleaching processes, it is observed that the minima and maxima are the same during cycling of the films that indicate more stability and low degradation in film efficiency.

## CONCLUSIONS

1- Transmittance decrease after irradiation for (300-900 nm) wave length.
2- Strong absorbance after irradiation at a wavelength range of (300 -450) nm made PB films suitable for storage energy.
3- Optical energy gap decreased after irradiation from 3.3 eV to 2.9 eV. This result would make a worthwhile contribution to solar cell applications.
4- Voltage for coloring thin films decrease after irradiation (-70 mV to +45 mV), change from cathodic to anodic, as well the coloring and bleaching time have been decreased after irradiation from 25 s to 20 s and from 65 s to 50 s respectively.

## REFERENCES

1. Monk P, Mortimer R & Rosseinsky D X. Electrochromism and electrochromic devices. Cambridge University Press; 2007.
2. Granqvist C G .Handbook of inorganic electrochromic materials. Elsevier ; 1995.
3. Byker H, MacArthur DA .Electrochromic Materials II, Electrochemical Society. Proceeding Series, Pennington 1994; 94: 3–13.
4. Yang P, Sun P & Mai W. Electrochromic energy storage devices. Materials Today 2016;19(7): 394-402.
5. Korgel BA. Materials science: composite for smarter windows. Nature 2013;500(7462):278.
6. Kadam LD, Patil PS. Studies on electrochromic properties of nickel oxide thin films prepared by spray pyrolysis technique. Solar energy materials and solar cells 2001;69(4):361-9.
7. Vigneshkumar M, Suganya SM, Pandiarajan J, Saranya A, Prithivikumaran N. Structural and optical properties of nanocrystalline nickel oxide thin film by spray pyrolysis technique. International Journal of Technical Research and Applications 2016:52-6.
8. Ibrahim BA, Makki S, Jammal M. *The effect of Irradiation on the Structural, Optical and Electrical Properties of Prussian Blue Electrochromic Thin Film*, Journal of Engineering and Applied Sciences 2018; 13(16):6737-6741.
9. Venter A, Botha JR. Optical and electrical properties of NiO for possible dielectric applications. South African Journal of Science 2011 Feb;107(1-2):1-6.
10. Sialvi MZ, Mortimer RJ, Wilcox GD, Teridi AM, Varley TS, Wijayantha KU, Kirk CA. Electrochromic and colorimetric properties of Nickel (II) oxide Thin films prepared by aerosol-assisted chemical vapor deposition. ACS applied materials & interfaces 2013 Jun 10;5(12):5675-82.

**Mayada Kaream Hassan** *et al.*

**Table 1. Bleaching and coloring voltages of NiO thin film before and after irradiation**

|  | Before irradiation | After irradiation |
|---|---|---|
| Brown → colorless | -70 mV | +45 mV |
| Colorless → brown | +445 mV | +445 mV |
| Brown →green | + 970 mV | +870 mV |
| Green → brown | + 700 mV | + 700 mV |

**Table 2.Coloring and bleaching times for NiO EC films**

|  | before irradiation | After irradiation |
|---|---|---|
| Coloring time White to brown (sec) | 25.05 | 20.2 |
| Bleaching time Brown to white (sec) | 65.05 | 50.00 |



**Figure 1.Transmittance versus wavelength before and after gamma irradiation**



**Figure 2.Absorbance versus wavelength before and after gamma irradiation**



**Figure 3.Absorption coefficient as a function of photon energy before and after irradiation**



**Figure 4.Optical energy gap before irradiation**

16612
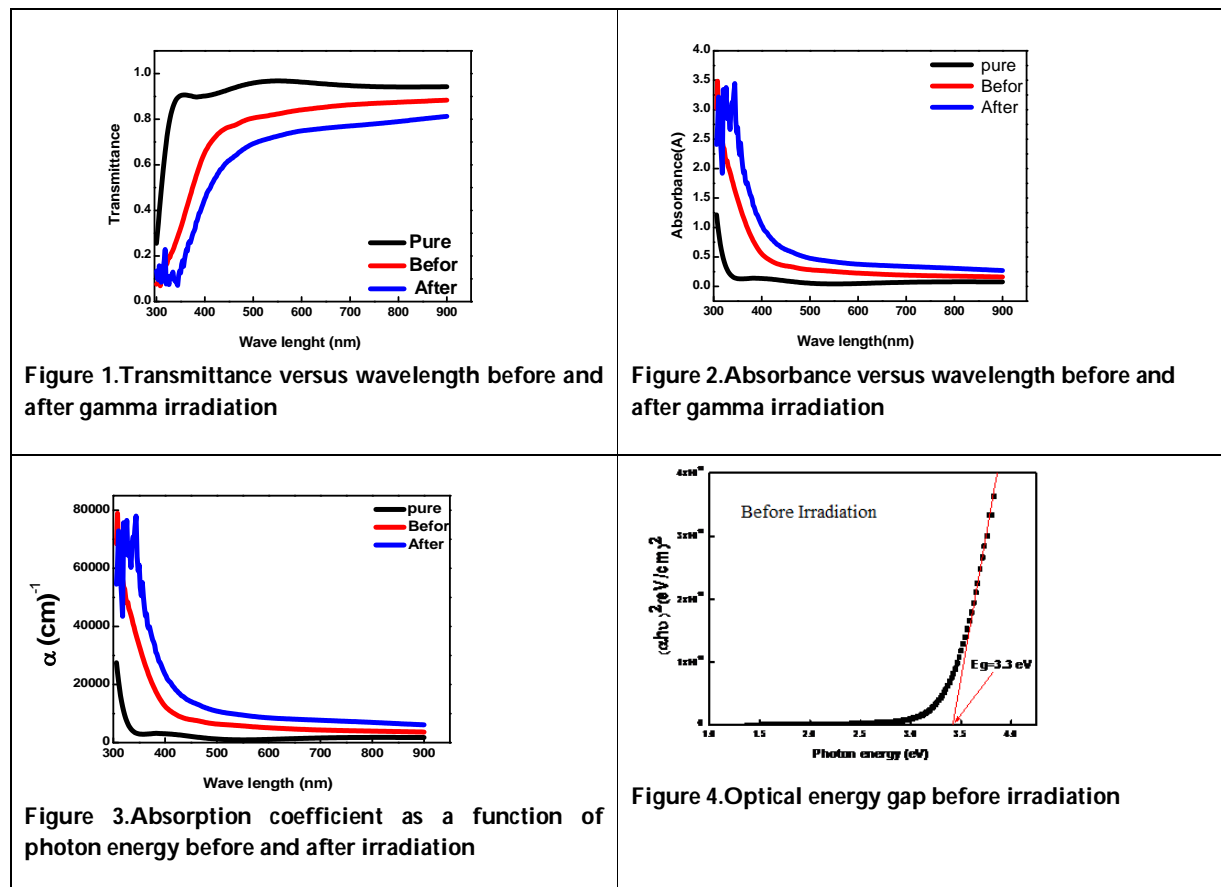
**Mayada Kaream Hassan** *et al.*



**Figure 5.Optical energy gap after irradiation**
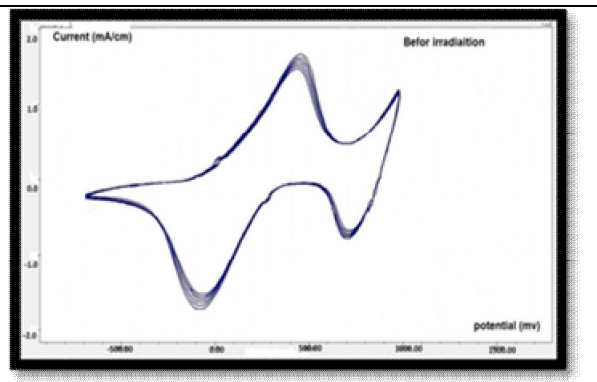


**Figure 6. CV traces before irradiation**
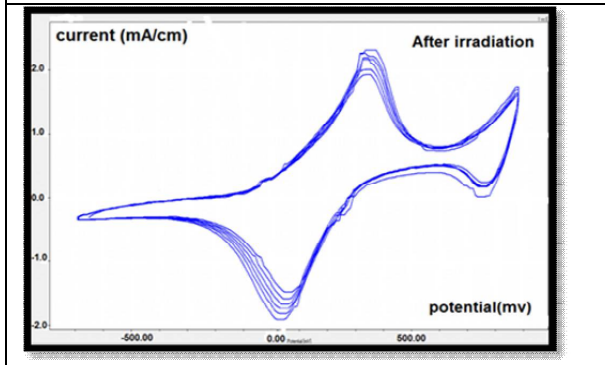


**Figure7. CV traces after irradiation**
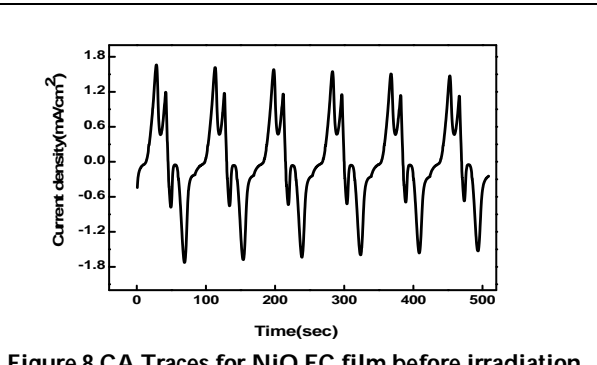


**Figure 8.CA Traces for NiO EC film before irradiation**
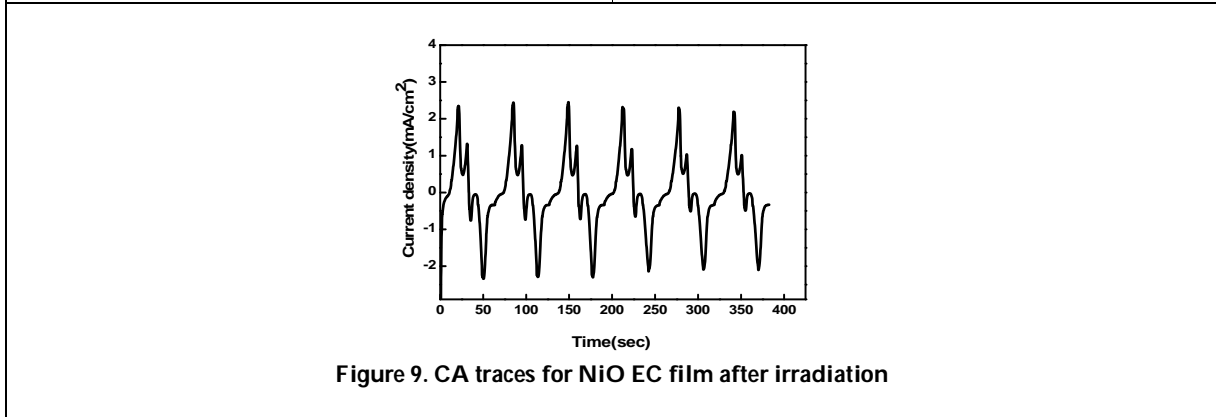


**Figure 9. CA traces for NiO EC film after irradiation**

**RESEARCH ARTICLE**

# A Critical Discourse Analysis of Positive-Self and Negative - Other Representations through English Language Textbooks

Muhammad Kamran Abbas Ismail[1], Muhammad Ahmad[2], Nosheen Akhter[3] and Hafiz Muhammad Adeel[3]

[1]Lecturer in English, University of Okara, Okara, Pakistan.
[2]SSE English, Government High School, Hujra Shah Muqeem, Okara, Pakistan.
[3]Department of Applied Linguistics, Government College University, Faisalabad, Pakistan.

*Address for Correspondence
**Muhammad Kamran Abbas Ismail**
Lecturer in English
University of Okara
Okara, Pakistan.
Email: kamran.ch@ue.edu.pk

**ABSTRACT**

The present research is a critical discourse analysis of the contents related to positive-self representation and negative-other representation projected through Punjab Curriculum & Textbook Board's (PCTB) School English textbooks which are taught in government and non-elite English medium schools at the secondary level (Grades 9 and 10). It aims to find out the ideologies of positive-self representation and negative-other representation in the discourses of PCTB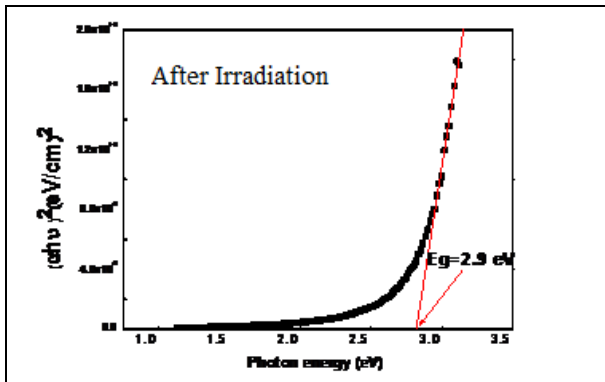 School English textbooks. It employs Van Dijk's (2005) analytical framework of critical discourse analysis to explore the ideologies of positive-self representation and negative-other representation in the discourses of School English textbooks. The findings show that PCTB School English Textbooks are replete with the ideologies of positive-self representation and negative-other representation. The said textbooks are more religious, nationalistic, anti-Israel, anti-Hindus, and anti-Christians. The findings of this study can be useful in a number of ways. They can be useful in developing new curricula and teaching materials including textbooks with less nationalistic, religious and cultural biases.  They can be helpful for policy makers and textbook authors to realize the politics of language textbooks to establish a symmetrical educational system.

**Keywords:** critical discourse analysis; discourse; ideology; negative-other representation; positive-self representation; Punjab Textbook Board.

## INTRODUCTION

This research study is a Critical Discourse Analysis (CDA) of the contents related to national self-glorification and also related to positive-self representation and negative-other representation in English textbooks. Ironically enough, school English textbooks have become agents of ideologies of Positive-Self Representation and Negative-Other Representation in the hands of concerned authorities. The ideological school English textbooks shape the world views of teenagers. According to Galbraith (1984: 131-4) "Social conditioning through schooling is the most important way of changing worldview whether taken by business organization or by the state". Furthermore, the particular world view and mindset, created by these school English textbooks, are parts of problem rather than parts of solution where our children learn to internalize a discriminatory framework. For example, these textbooks are the representatives of their own cultures. The contents in PTB English textbooks mostly represent Pakistani culture positively and the western culture negatively and is likely to make the learners religious, nationalistic, patriotic and militaristic. Unfortunately, the majority of people in educational institutions are unaware of the power of ideological discourses. But it is not difficult to manipulate the discourses for sustaining the relations of power, for creating ideologies of 'us' and 'them'. After the fall of Dhaka, in order to unite the distorted nation and Islamization in Pakistan in the eras of Zulfiqar Ali Bhutto (1971-1977) and General Muhammad Zia-ul-Haq (1978-1988), the ideologies of positive-self representation and negative-other representation were ideologically included in the textbooks.

This Curricula and textbooks help create a particular mindset. Our schools and universities should be a defense against the dissension within, and not locations where our children learn to internalize a discriminatory framework. Textbooks are unimaginatively written and the contents are presented in ways that they promote different ideologies among the students. Among these ideologies, a prominent one is the 'national self-glorification'. National self-glorification is actually a way for positive self-presentation or praise of one's own country, glorification of its history as well as traditions. It is a part of the problem rather than a part of the solution. Critical discourse analysis is a technique to locate these ideologies that have been disseminated in these PCTB English textbooks. The present study implies Van Dijk's (2005) analytical framework to find out implicit as well as explicit discursive moves to represent 'us' with positive attributes and 'them' with negative attributes. As it has been proved by many research studies that CDA is a very useful tool for analysis of language, or discourse (Fairclough, 1995), the major aim of CDA in these research studies is to deconstruct those implicit and explicit ideologies of discourses which help produce and reproduce unequal power relations in society (Van Dijk, 1998; Wodak & Meyer, 1997). Since, PCTB English textbooks are discourses, this research study carries out a semantic and lexical analysis of these PCTB English textbooks. The present study also determines to highlight the gap lying between the ideologies of positive-self representation and negative-other representation in discourses of PCTB English textbooks and tries to fill the gap through research in the domain of ELT curricula.

### Role and Development of Textbooks

The word 'Textbook' is metaphorically used to define and convey a sequence of actions which do not deviate from an agreed procedure towards the completion of a task. It is obvious that school textbooks are important things to create a mindset and worldview of the learners. A single textbook carries a variety of discourses and each discourse is embedded with certain ideologies. Therefore, school textbooks are the crucial organs in the process of constructing legitimated ideologies of the 'self' and 'others' by powerful groups in a society. It has been claimed that the function of a textbook is to "...tell children what their elders want them to know" (Fitzgerald, 1979: 47). But a question attracts the attention how ideologies become the part of a textbook. One way to answer the question is to look at the way these textbooks are developed. Textbooks are "…conceived, designed and authored by real people with real interests" (Apple, 1993: 46). The Curriculum Wing of the Ministry of Education is the respective authority for the

**Muhammad Kamran Abbas Ismail** *et al.*

development of PCTB English Textbooks according to the educational policy of Pakistan. Therefore, the Curriculum Wing is responsible for disseminating such type of ideologies in School English textbooks of PCTB.

## Theoretical and Methodological Perspectives

Before going to deal with the analysis of national self-glorification, positive-self representation and negative-other representation, it is necessary to discuss some theoretical and methodological perspectives which are used to explore ideologies. For example, according to Rahman (2002b, p. 61-2) "ideology represents politico-religious dogmas and beliefs, and they are embodied by the term 'worldview' as a whole". He asserts that owing to the influence of social institutions like media and education this term cannot be applied easily to the people of educated societies because their ideas and beliefs keep fluctuating. Therefore, no monolithic worldview can be found in any society. The term 'world view' can easily be utilized to the ideas and beliefs of subgroups of a society such as learners, farmers, and merchants etc. Hence, in a language and discourse, the ideologies exist (Gruber, 1990). In fact, ideologies are produced through languages and propagated through texts (Blommaert, 2005). According Fairclough (2003), "ideologies are embedded in features of discourse which are taken for granted as matters of common sense", and according to Van Dijk (2005) notion of 'ideology' has also become the central element in the common sense and the systems of self-serving ideas of dominant groups ( Dijk, 2005). In a nutshell, ideologies and discourses can be said to be the corresponding features of one another. Rizwan adds that the ideologies are produced, propagated and circulated through discourses (Rizwan, 2006).

Deciphering the underlying ideologies is the most significant area of (CDA) of discourse that "helps produce and reproduce unequal power relations in the society" (Fairclough & Wodak, 1997, p. 258). On the other side, the symbolic as well as indistinct constructions get clear by unveiling their efficient role in maintaining uneven power distribution in a society. The dormant ideologies under the cover of apparently harmless and neutral discourse undergo a dissection or post-mortem procedure called CDA to expose the toxic, debilitating agents (Rahimi & Sahragard, 2006). Ideology, actually, is known to be a group of overt and inherent themes deep-seated in textbook discourses in order to foster certain changes in the learners' worldviews to advantage the state and the dominant strata; these ideological themes are created through different strategies in discourse. These underlying ideologies of the material are interpreted as reality by the young learners and streamline their knowledge and work accordingly. Even the ELT practitioners and academics are not exploring these ideological themes in Pakistani educational contexts through CDA. The discussion of CDA in this research is aimed to identify effectively the inherent ideological themes rooted in the Pakistani English textbook discourses. Despite having the same agenda different approaches of CDA have been proposed that vary from one another according to the discipline. Moreover, CDA requires no monolithic approach. Moreover, different analytical frameworks are needed for effective analysis of various types of texts. For example, the present study which is focused on long stretched messages of texts, Van Dijk's framework (2005) seems more practical than the others.

Van Dijk (2005) takes the texts as ideological representations of the 'self' and 'others' or polarization between 'us' and 'them', 'us' as in-group and 'them' as out-groups. Therefore, that polarization is social. On the Other hand, through the term 'discourse', he refers to spoken or written language declaring discourse as a social phenomenon influenced by ideologies. Hence, his theoretical framework is multidisciplinary related to discourse and society. Ideologies, thus, form the basis of social representation and practices of group members, including their discourse, which at the same time serves as the means of ideological production, reproduction and challenge (Dijk, 1998). Therefore, according to van Dijk (2005), ideologies may serve to establish or maintain social dominance, as well as to organize dissidence and opposition. Social representation is the direct input into the semantic module of discourse. Van Dijk's approach to CDA is based on the hypothesis that social representation of groups is ideologically biased (2005).Van Dijk's (2005) analytical framework focuses on semantic analysis. To unveil power and disparity existing in a society, Van Dijk (2005) suggests two levels of analysis: (1) macro level and (2) micro level. Macro level operates on a broader scale and comprises of power relations between groups and institutions, power as a tool to control, control of text as well as

16616

discourse, access and dominance. On other hand, micro level of CDA deals with power relations between the social actors of a group. It consists of language, discourse, verbal interaction and social practices. Analytical framework employs two macro strategies i.e. positive-self representation and negative-other representation. This means, different social groups confront with an ideological conflict and this leads to different ideological positions in the world. 'Us' and 'them' are presented through ideologies. Where there is no conflict and no struggle, there is no ideology. Ideologies normally organize social groups in a polarized way as 'us' and 'them'. In ideologies of positive-self representation, they disseminate and emphasize positive things about 'us' or de-emphasize negative things about 'us', but in ideologies of negative-other representation, they disseminate and emphasize negative things about 'them' or de-emphasize positive things about 'them'. The discursive moves that mediate these ideologies are: topics, level of description, implications and presupposition, local coherence, synonymy, paraphrase, contrast, examples and illustrations, disclaimers, actor description, modality, evidentiality, hedging and vagueness, number game, national self-glorification, lexicalization and victimization ( Dijk, 2005).

A brief description of discursive moves by Dijk (2005) is as follows: (1) Topic; Topics represent such gist or main and important information about discourses as can be best recalled. Mostly, this type of information is topicalized a way that presents 'us' positively and 'others' negatively, (2) Level of Description; Level of description means the degree of details about good things of 'us' and about bad things of 'others'. Level of description means 'to give many or few details about an event, or to describe it at a rather abstract, general level, or at the level of specifics', (3) Implication; It means inferring or deducing implicit information or implied meaning from the texts. Implicitness is one of the pervasive properties of discourses or texts, (4) Paraphrase/Synonymy; Paraphrases are typical expressions which have more or less the same meaning' (Van Dijk, 2005). 'The word 'synonym' means near in sense while, paraphrase is an amplification or explanation of the meaning of a segment of the text (Newmark, 1988), (5) Contrast; Contrast can also be marked by negative-positive sequence, whereas the negative is likely to introduce an opposite or heightened the meanings of the positive (Newmark, 1988).

It is a form of polarization to emphasize our good things and others' bad things (Van Dijk, 2005), (6) Actor Description; Actors may be described as the members of a group or as an individual, or as by their first name, or by their family name, or by their positions, or relations to the other people' (Van Dijk, 2005). Actually, actor description is controlled by ideologies of 'us' and 'them'. (7) Authority; Authority means quoting authorities' statements to support a claim. According to Van Dijk (2005), speakers are accountable for what they say. Therefore, they quote an authority's statement as an evidence of a belief for those who deny it, (8) Categorization, The construction of the in-groups and out-groups and associating the people with different ideological groups is called categorization. This discursive construction starts with labeling of social actors, proceeds to the generalization of in-group 'us' with positive attributions and out-group 'them' with negative attributions. Social actors are polarized on the basis of inclusion and exclusion, (9) Evidentiality; Using facts to support a claim, (10) Hyperbole; A device for deliberate exaggeration of meaning, (11) Lexicalization; Selection of words for negative representation of the 'other'. (12) Polarization; Categorization 'our' members of groups with good attributes and 'their' members with bad attributes, (13) Vagueness; Creating ambiguity and uncertainty in meaning, (14) Number Game; Using numbers/statistics to make a claim appear credible, (15) National Self-Glorification; Representing someone positively by glorifying one's own country.

## MATERIALS AND METHODS

For CDA, the content has been taken from Punjab Curriculum Textbook Board's (PCTB) Textbooks for English Language. These PCTB English textbooks are further divided into two subcategories: i.e. (a) English 9 and (b) English 10. The Curriculum Wing of the Ministry of Education is the respective authority for the publication of PCTB textbooks which are taught in all government as well as in non-elite English medium schools at secondary level (Grades 9 and 10). For CDA, these textbooks are mentioned as, PCTB 9 and PCTB 10 respectively. PCTB 9 consists of

12 lessons and PCTB 10 consists of 13 lessons i.e. 25 lessons in total. The division of the lessons of these two English textbooks is as: poems, narratives, letters, essays, autobiographies, articles etc. All of these lessons relate to the themes of gender, religion, morality, nationalism, patriotism, war, racism, society, science, technology, education, nature, health and general knowledge. But, the focus of this study is only those lessons in which ideologies of positive-self representation and negative-other representation have been embedded. These ideological lessons are, therefore, critically analyzed by using the selected framework. The analysis has been carried out at sentence level. The sentences are randomly selected from ideological lessons for the critical analysis and it is quite impossible to discuss all the lines/sentences carrying the ideologies of positive-self representation and negative-other representation. In short, ideologies of positive-self representation and negative-other representation are being embedded in discourse like PCTB school English textbooks. Therefore, critical discourse analysis is very useful tool with its discursive moves to explore these ideologies.

## RESULTS AND DISCUSSION

The researchers performed critical discourse analysis of Punjab Curriculum & Textbook Board's (PCTB) English Textbooks at secondary level to find out the ideologies of positive-self representation and negative-other representation in the contents related with culture, religion, nationalism, 'us' and 'them' and society. In order to find out these ideologies, they used the analytical devices of Van Dijk's analytical framework (2005) which have been mentioned earlier.

### Topic

Topics of various units of PCTB's textbook 9 and textbook 10 are ideological because they provide a gist of religious, national and cultural events and practices for the Pakistani society. The units 1, 2, 4, 6, 7 in PCTB's textbook 9 and units 1, 13 in PCTB's textbook 10 are the best examples for these things. They become 7 out of 25 (28 percent). Topics of these units not only provide a gist of lessons but also topicalize positive information about 'us' which is an ideological function of the topics (Van Dijk, 2005). Topics of unit 1 of PCTB's textbook 9, 'The Saviour of Mankind', and title of unit 1 of PCTB's textbook 10, 'Hazrat Muhammad (Peace be upon Him) an Embodiment of Justice' refer to the attachment of Pakistani society with Prophet Muhammad (peace be upon Him) as both textbooks start with direct reference to Prophet Muhammad (peace be upon Him), the most reverend figure of Islamic world. Though explicitly, there is no negative-other representation but implicitly, they refer that these textbooks are for the Muslim readership as well as for the Muslim society.

Ideologically, Pakistan is an Islamic Republic that came into being on the basis of the religion of Islam. Topic of unit 4 of PCTB textbook 9, 'Hazrat Asma', also regards ideological function, implicitly.It also refers that it is for the Muslim community. The Muslims have great respect for the companions of the Holy Prophet (peace be upon Him). Similarly, The topic of unit 6 of PCTB's textbook 9, 'The Quaid's Vision and Pakistan' also topicalizes an ideological function because it conveys social and national fervor of the Pakistani community as Quaid-e-Azam is a national hero and founder of Pakistan. Topic of unit 7 of PCTB textbook 9, 'Sultan Ahmad Mosque' ideologically says positive information about historical/cultural heritage and Muslim architecture of the world in seventeenth century. The topic of unit 13 of PCTB's textbook 10, 'Faithfulness' is ideological through and through, though explicitly, there is no negative-other representation, yet the authors in expression of ideology follow two of four principles: 'Emphasize positive things about 'Us' and De-emphasize negative things about 'Us' (Van Dijk, 2005).

### Level of Description

In unit 1 of PCTB's textbook 9, after the selection of topic, 'The Saviour of Mankind' the details about topic cover four pages. In these details, the author tells about the condition of Arabia especially the city of Makkah before the birth of

**Muhammad Kamran Abbas Ismail *et al.***

the Holy prophet (peace be upon Him), how pagan Arabs put a lot of pressure on the Holy prophet (peace be upon Him) and his companions to restrain from the preaching of Islam, what answer the Holy Prophet (peace be upon Him) gave to his caring Uncle, Abu Talib, what Hazrat Aysha (R.A) said about the life of the Holy Prophet (peace be upon Him). Similarly, in unit 1 of the PCTB's textbook 10, the level of description about topic, 'Hazrat Muhammad an Embodiment of Justice' covers four pages, the writer tells that no one could be more just and equitable than the Holy Prophet (peace be upon Him), due to good reputation and equitable plan, he settled the tribal conflict on the issue of Black Stone during construction of Ka'bah, what he said to Hazrat Usama bin Zaid (R.A) about the punishment of a Quraishi woman who was caught red handed, the Jews in spite of being his bitter enemies came to him for justice. In the same way, in unit 2 of the PCTB's textbook 9, the details of specific information about the topic, 'Patriotism' cover the range of what origin of word patriotism means, what patriotism gives to the people. Sovereignty, integrity and honour of the country are supreme values for a patriot and Quaid-e-Azam (The Great Leader) Muhammad Ali Jinnah said about patriotism, 'We must develop a sense of patriotism which galvanizes us all into one united and strong nation'. Nishsn-e-Haider, the highest military award was given to great patriots who laid down their lives for the motherland. Similarly, in unit 6 of the PCTB's textbook 9, in level of description about topic, 'The Quaid's Vision and Pakistan', the author tells why the Quaid (The Leader) took a countrywide tour, what he said in his speeches about the nation and country, what the Quaid's motto was, on which fundamental principle, ideology of Pakistan was based and why Pakistan was facing numerous challenges. All of these detailed descriptions are actually the depictions of 'our good things and about bad things of others' (Van Dijk, 2005). These details support to ideologically topicalized information and information that is already present in mental as well as social models of the readers.

## Presupposition and Implication

The PCTB's textbooks include various examples of presupposition and implication. The way, they are practiced, help the people know about their ideologies. Notable examples for presupposition and implication include;

1   "It is no wonder that Allah Almighty chose the Arabic Language for His final dispensation and preservation of His Word" (PCTB 9, p. 2, l.12-14).
2   "They told him to restrain the Holy Prophet (peace be upon Him) from preaching Allah Almighty's message, or face their enmity" (PCTB 9, p.3, l.16-17).
3   "He had a pressing urge to eradicate wrong beliefs, social evils, cruelty and injustice. The moment had arrived when he was to be bestowed with Prophethood" (PCTB 9, p. 2, l.25-27).
4   "We are a nation", he affirmed three years before birth of Pakistan (PCTB 9, p. 63, l.16).
5   "The spirit of patriotism makes us stay alert in the wake of foreign invasion" (PCTB 9, p. 13, l.17).

Lines (1, 2, and 3) reflect the Muslims' ideology. The words 'Chose the Arabic language' imply that this language is superior to other languages as it is the language of the Holy Book of Muslims. The words 'His Final Word' imply that according to the Muslim ideology, the Holy Quran is the last book of Allah Almighty, which was revealed on the Last Prophet, Muhammad (peace be upon Him). The words 'preaching' and 'Allah Almighty's message' imply that these are used for Islam, the religion of peace. All of these words are used in positive connotation and ideologically support 'positive-self representation'. But the words 'restrain' and 'enmity' presuppose that non-believers are against the preaching of Islam and they are the enemies of the Muslims. Plus, they were more powerful and used their power against Islam and Muslims. The word 'wrong beliefs', 'cruelty' and 'injustice' presuppose that there was chaos in Arabia, the people were idol worshipers, they were cruel, even buried their innocent daughters as well as there was lawlessness all over the world especially in Arabia. All of these words have been used for negative representation of the 'others'. Similarly, the words in line (4) 'we', 'nation' and 'Pakistan' imply and presuppose for Pakistani nation and particularly for the Muslims because according to two nations' theory, the Muslims are a one nation and the Hindus and the Christians are not included in it. Ideologically, these words have been used for 'positive-self representation'. Here 'we' means those who belong to 'us'. Likewise, in line (5), the phrase 'foreign invasion' implies

**Muhammad Kamran Abbas Ismail *et al.***

that India attacked Pakistan on many occasions because the Hindus were our enemies. This line is also ideological because it makes distinction between 'us' and 'them'.

### Synonymy and Paraphrase

There are many instances of synonymy and paraphrase in English Textbooks of PTB which are ideological as follows:

1   "Hazrat Muhammad (peace be upon Him) practically proved that no one could be more just and equitable than the Messenger of Allah Almighty" (PTB 10, p.2, l.8-9).
2   "Oh Messenger of Allah! Their ancestors killed a member of our family" (PTB 10, p.3, l.6).
3   "The pagan Arabs started to mount pressure on the Holy prophet (peace be upon Him) and his followers" (PTB 09, p.3, l.12-13).
4   "They told him to restrain the Holy Prophet (peace be upon Him) from preaching Allah Almighty's message, or face their enmity" (PTB 09, p.3, l.16-17).
5   "On the night of the migration, a tribal chief of disbelievers, Abu Jehl, in a fit of fury headed towards Hazrat Abu Bakr Siddique's home" (PTB 09, p.33, l.16-17).
6   The villager replied, "Commander of the Faithful, I plead to the charge" (PTB 10, p.150, l.08).
7   "Patriotism means love for the motherland or devotion to one's country" (PTB 09, p.13, l.1).
8   "He gave the Muslims a sense of identity by securing a separate homeland for them" (PTB 09, p.13, l. 12-14).
9   "The spirit of patriotism makes us stay alert in the wake of foreign invasion" (PTB 09, p.13, l. 17).
10  "This is my own, my native land" (PTB 09, p.14, l.6).

In these lines, there are different words which have been used as ideological agents for shaping the teenager's worldviews about religious perspective of the world. The words like 'The messenger of Allah Almighty' and 'messenger of Allah' are paraphrase of the word 'prophet' and are used in positive connotation for the Muslims. The words 'pagan' and 'disbelievers' are the synonyms of the word 'non-believer'. Though, no two words in a language are ever exact synonyms. But here these words are ideological agents for 'negative-other representation'. It indicates the ideologies of 'us' and 'them'. In line (6) the words 'Commander of the Faithful' are paraphrase of the word 'Caliph'. Faithful is used as a metaphor for the Muslims. Metaphorical expression of 'Commander' is indirectly reference towards 'Jihad'. The very word 'Commander' is used for the second Caliph of Islam and it romanticizes this aspect of religion.

Ideology not only covers the religious aspect of life, but it also involves all other aspects cultural and nationalist ideologies. Words in lines (7, 8, 9 and 10) like 'motherland', 'homeland' and 'native land' are synonymous with 'country'. But these are more ideological in the sense than the word 'country' and give the sense of identity to the inhabitants. The words 'foreign invasion' is synonymous with 'attack of enemy' and here these words indirectly refer to India that has attacked Pakistan many times as in 1965, 1971, and 1999. The use of this technique also disseminates positive information about 'us' and negative information about 'them'.

### Contrast

Here are some examples of this ideological move regarding contrast in the PCTB's English textbooks;

1   "As head of the state of Madina, He decided all cases on merit with justice and equity, irrespective of colour, creed, or race" (PCTB 10, p. 2).

These lines semantically stand in contrast to the non-Muslim Arabs, who decided their cases on the basis of ethnicity, creed, and colour, (because before Islam, law and justice were just for the elite class). On the other hand, Hazrat

**Muhammad Kamran Abbas Ismail** *et al.*

Muhammad (Peace be upon Him) decided all cases on merit without any discrimination of race, colour or creed. Semantically, here is a polarization of 'us' and 'them'.

2    "The Holy Prophet (Peace be upon Him) very furiously said, "Bani Israil was ruined because of this. They applied law to the poor and forgave the rich" (PCTB 10, p. 3,).

Here in contrast to Bani Israil, where law was applicable to the poor only. The Bani Israil was destroyed due to injustice. The Holy Prophet (Peace be upon Him) was an embodiment of justice. He did not accept the request of Hazrat Usama (R.A) because it was a form of nepotism. He punished the Quraishi woman who was found guilty of stealing. Ideologically, negative things of Bani Israil are explained to heighten the positive things of Islam. Hence, the ideologies of positive representation of the 'self' and negative representation of the 'others' have been depicted through these lines.

## Actor Description

Here are some examples of actor description ideology taken from English Textbooks of PCTB;

1    "The Holy Prophet (Peace be upon Him) did go the way Allah Almighty had chosen for mankind" (PCTB 09, p. 3).
2    "Hazrat Muhammad (Peace be upon Him) practically proved that no one could be more just and equitable and the Messenger of Allah Almighty" (PCTB 10, p. 2).
3    "This response shows the wisdom and courage of Hazrat Asma" (PCTB 9, p. 34).
4    "Quaid-e-Azam Muhammad Ali Jinnah was a nation builder and a great patriot (PCTB 9, p.13).

In lines (1 and 2), the ideological move for the strategy of Positive-self representation depicts the actor description. In the first four sentences, there is a reference to the most reverend figure of Islam. The description is in positive sense. The Holy Prophet (Peace be upon Him) is described by words like 'go the way chosen for mankind', 'practically proved', 'just', 'equitable', and 'Messenger of Allah Almighty'. Semantically, all of these words are used for 'positive-self representation'. Hazrat Muhammad (Peace be upon Him) proved practically what he said, he did not believe only in theory. His life was a practical model of The Holy Quran. Islam is a right path chosen by Allah for humanity. Because of his Justice and fairness, he was popular among all others. In Line (3), Hazrat Asma (R. A) is described through the words like 'wisdom' and 'courage'. This description is in positive sense because commonly in different cultures such types of attributions are not given to female gender but Islam gives high status to females. In the next line (4), there is a description of Quaid-e-Azam with positive attribution by using words like 'nation builder' and 'patriot'. The title 'Quaid-e-Azam' means 'the great leader' is used instead of his real name Muhammad Ali Jinnah. It is considered blasphemy to call by real name.

5    "On the night of the migration, a tribal chief of disbelievers, Abu Jehl, in a fit of fury headed towards Hazrat Abu Bakr Siddique's home" (PCTB 09, p. 33).

In the given lines, the actor description is with negative attribution of 'chief of disbelievers' and 'in a fit of fury'. These words are used in negative connotation. Moreover, title given to him is 'Abu Jehl' which means 'the father of ignorance' instead of his real name. Thus, here is a strategy of 'Actor Description' to negatively represent the 'other'.

## Authority

In any ideological discourse, the statements of different personalities are quoted for supporting a claim which carries the 'ideologies positive-self representation' and 'negative-other representation'. According to Van Dijk (2005), speakers are accountable for what they say. So, they quote an authority's statement as an evidence of belief for those

who deny it. This move is also ideologically biased in any discourse because at first the authors make claim then they quote the personalities to support their claim. There are many examples of this ideological move in English Textbooks of the Punjab Curriculum & Textbook Board for Secondary level students. Such as;

1   "In the words of Michael Hart, a great historian: "Muhammad ((Peace be upon Him)), however, was responsible for both the theology of Islam and its main ethical and moral principles" (PCTB 9, p. 4).
2   "Hazrat Aysha said: His morals and character are an embodiment of the Holy Quran" (PCTB 9, p. 4)

In these given lines, the authors have employed the ideological move of authority and given the references not only from religious figures but also from a famous historian who was a Christian to support their details  about the most reverend and influential figure of Islam, Hazrat Muhammad ((Peace be upon Him)) and to make discourse more credible to the readers. Michael Hart says that the Holy Prophet (Peace be upon Him) is the only man in history, who stands supremely successful on both secular and religious grounds, a man who prefers words to swords. Hazrat Aysha (R.A), one of the wives of the Holy Prophet Hazrat Muhammad ((Peace be upon Him)) says that The Holy Prophet ((Peace be upon Him)) was a practical model of verses of the Holy Quran.

3   "In the words of S.W. Scott, a man devoid of patriotic spirit, is like the one who: Breathes there the man with soul so dead" (PCTB 9, p. 14).

In these lines, the ideological move of authority is used. The authors have cited from the poem of Sir Walter Scott about patriotism. In the lesson, the authors gave details or arguments about patriotism and patriotic spirit of Quaid-e-Azam Muhammad Ali Jinnah as a great patriot as well as the patriotism of many brave soldiers of Pakistan who laid their lives for the protection of their country. At the end, the writers quote the authority to devoid the charge of accountability of this act. The authority, S.W. Scott said that it was a universal spirit among human beings and without this sense of patriotism, one is dead.

## Categorization

According to Van Dijk (2005), the construction of in-group and out-group and associating the people with different ideological groups is called categorization. The ideological description of the people as 'us' and 'them' is the foundation of ideological discourse. This discursive construction starts with labeling of social actors, proceeds to the generalization of in-group, 'us' with positive attributions and out-group, 'them' with negative attributions. Social actors are polarized on the basis of inclusion and exclusion. They are referred to in terms of major categories by means of which a given society or institution differentiates between classes of the people. '*Us*' and '*Them*' are classified by provenance, ethnicity and religion (Leeuwen, 2008). But this identification or classification becomes ideological when in-group 'us' is polarized with positive attributions for 'positive-self presentation' and out-group 'them' is polarized with negative attributions for 'negative-other presentation'. Particular sorts of categorization, establish both a relatively negative sense of 'others' and positive sense of 'self' (Mckinlay & Mcvittie, 2008). Following lines have been taken from some lessons of the PCTB's English Textbooks for secondary classes;

1   "Once a Quraishi woman was found guilty of stealing" (PCTB 10, p. 2).
2   "Since this belief was threatening their dominance in society, the pagan Arabs started to mount pressure on the Holy Prophet ((Peace be upon Him)) and his followers. They wanted them to renounce their cause and take to idol-worshipping" (PCTB 09, p. 34).
3   "She simply posed a counter question that infuriated Abu Jehl. He slapped Hazrat Asma's face so hard that her ear-ring fell off" (PCTB 9, p. 34).

In these lines, the Muslims and the pagan Arabs have been categorized as two different ideological groups. It is important to look here that the members of the latter group have been described negatively as the out-group

**Muhammad Kamran Abbas Ismail** *et al.*

semantically with negative connotation or derogatory terms like 'guilty of stealing', 'pagan' and 'idol-worshiping'. Moreover, the members of the other group are categorized as a pressure group. In last sentence, Abu Jehl is categorized as a member of the other group. Thus, this description of 'others' is done for 'negative-other representation' and 'positive-self representation'.

4   Bani Israil was ruined because of this. They applied law to the poor and forgave the rich" (PCTB 10, p. 3).
5   "The Holy Prophet (Peace be upon Him) was so well known for his justice that even the Jews, who were his bitter enemies, brought their suits to him and he decided cases in accordance with the Jewish law' (PCTB 10, p. 3).

In these lines, the Bani Israil and the Jews are categorized the members of out-group. They are described with negative connotation as 'ruined', 'injustice' and 'bitter enemies'. Thus, the description is done for 'negative- other representation'.

6   "We are a nation," he affirmed three years before the birth of Pakistan, with our own distinctive culture and civilization" (PCTB 9, p. 63-64).
7   "The ideology of Pakistan was based on the fundamental principle that the Muslims are an independent nation" (PCTB 9, p. 63).
8   "We should face it bravely to save the honour of Pakistan and Islam" (PCTB 9, p. 63).

In these given lines, the Muslims and citizens of Pakistan are categorized as the members of in-group with their own culture and civilization. They are a separate nation. Pakistan came into being in the name of Islam. Therefore, we are a nation and we are different from the 'others' particularly from Hindus as it shows the context of this lesson. All the description of in-group members in this lesson is with positive connotation for positive-self representation.

**Game Number**

Game number means using number or statistics to support the credibility of the ideologies of positive-self representation and negative-other representation (Van Dijk, 2005). This analytical device is very helpful in showing the objectivity in the ideologies of positive-self representation and negative-other representation. There are many examples of this analytical move in the school English textbooks of PCTB at secondary level. For example,

1   "In the fifth and sixth centuries, mankind stood on the verge of chaos. It seemed that the civilization which had taken four thousand years to grow had started crumbling. At this point in time, Allah Almighty raised a prophet from among themselves who was to lift humanity from their ignorance into the light of faith" (PCTB 09, p. 2).

In these lines, for negative-other representation, the ideological move of game number has been used. For making it clear to the readers about the importance and need of The Prophet (Peace be upon Him) for humanity, the authors have used the figures 'four thousand' years. But, now after crumbling the civilization, before the advent of Islam, the people were living in ignorance. Therefore, Allah sent the Prophet (Peace be upon Him) who showed the right path to the ignorant people. Hence, here, it is the ideologies of positive-self representation and negative-other representation.

2   "The flow of the Divine message which continued for the next twenty-three years had begun, and the Holy Prophet (Peace be upon Him) had arisen to proclaim Oneness of God and the unity of mankind" (PCTB 9, p. 3).

In these lines, through the ideological device of game number, the ideology of 'positive-self representation' has been disseminated. The figure 'twenty three' years has been used to enhance the credibility of the claim. It has also been used to show that Islam did not spread within a day; rather it took a long time to get established. The phrases 'Oneness of God' and 'unity of mankind' have been used for 'positive-self representation'.

16623

3    "The interior of the mosque at lower level is lined with more than 20,000 hand-made ceramic tiles in more than 50 different tulip designs. More than 200 stained glass windows with intricate designs allow natural light to brighten up its intricate and the chandeliers further illuminate it with their glow. The decorations include verses from the Holy Quran" (PCTB 9).

In these lines, the ideology of positive-self representation has been emphasized through the ideological and analytical device, game number. In these lines, the figures '20,000', '50' and '200' have been used to enhance the credibility of the ideological information about the magnificence of the Blue Mosque that is a wonderful monument of the Muslim architecture with hand-made ceramic tiles with tulip designs and with stained glass windows. The decorations have been done with carved verses from the Holy Quran. Here, positive things of 'us' have been emphasized through statistical figures. Thus, it is the ideology of 'positive-self representation'.

## CONCLUSION

In the light of above critical discourse analysis of school English textbooks at secondary level, it can be concluded that the PCTB's textbooks are replete with the examples of ideologies of 'positive-self representation' and 'negative-other representation'. Therefore, the textbooks of English language for grades 9 & 10 are highly ideological. In this era of terrorism and chaos, Pakistan needs moderate youth as well as nation. Therefore, the government should have a strong check and balance on the publication of such textbooks.

## REFERENCES

1.  Althusser, L. (1971). *Ideology and ideological state apparatuses. In Lenin and Philosophy and Other Essays*:121-173. London: Verso.
2.  Apple, M. W. (2004). *Ideology and curriculum.* New York and London: Routledge Falmer.
3.  Apple, M. (1993). *Official knowledge: Democratic education in a conservative age.* London: Routledge.
4.  Aziz, K. K. (1993). *Murder of history in Pakistan.* Lahore: Vanguard Books.
5.  Blommaert, J. (2005). *Discourse: A critical introduction.* Cambridge: Cambridge University Press.
6.  Brown, G. & Yule, G. (1983). *Discourse analysis.* Cambridge: Cambridge University Press.
7.  Creswell, J. W. (2003). *Research design: Qualitative, quantitative, and mixed methods approaches.* (2nd ed.). Thousand Oaks: Sage Publications.
8.  Fairclough, N., & Wodak, R. (1997). CDA. In T. van Dijk. (Ed.), *Discourse studies: A multidisciplinary introduction,* Vol. 2, (pp. 258-84). London: Sage.
9.  Fairclough, N. (2001). *Language and power.* (2nd ed.). London: Longman.
10. Fairclough, N. (2003). *Analyzing discourse: Textual analysis for social research.*
11. Galbraith, J. K. (1984). *The anatomy of power.* London: Hamish Hamilton.Gee, J. P. (1999). *An introduction to discourse analysis: Theory and method.* London: Routledge.
12. Gray, J. (2000). The ELT coursebook as cultural artefact: How teachers censor and adapt. *ELT Journal 54*(3), 274-283.
13. Hanks, W. (1996). *Language and communicative practice.* Boulder: West view.
14. Hartley, J. (2004). *Key concepts in communication, cultural and media studies* (3rd ed.).London and New York: Routledge.
15. Hawkes, D. (1996). *Ideology.* London and New York: Rutledge.
16. Larrain, J. (1979). *The Concept of ideology.* London: Hutchinson.
17. Mills, S. (2002). *Discourse.* London: Routledge.
18. Nayyar, A. H. & Salim, A. (2003). Glorification of war and the military. In *SDPI's DraftReport, April 2003.* pp. 79-90).

19. Pinsent, P. (May, 1997). Race and Ideology in Textbooks. *Colloquium's Journal Paradigm, No. 22.* London. Retrieved December, 23, 2014 from http://faculty.ed.uiuc.edu/westbury/Paradigm/

20. Rahman, T. (1996). *Language and politics in Pakistan.* Karachi: Oxford University Press.

21. Rahman, T. (1999). *Language, education, and culture.* Karachi: Oxford University Press.

22. Rahman, T. (2002a, April 16-20). Language-teaching and power in Pakistan. Paper presented at World Congress on Language Policies, Barcelona.

23. Rahman, T. (2002b). *Language, ideology and power.* Karachi: Oxford University Press.

24. Rahman, T. (2004). *Denizens of alien worlds.* Karachi: Oxford University Press.

25. Rahman, T. (2007). *Images of the 'Other' in Pakistani textbooks.* Retrieved June 6, 2008, from http://www.tariqrahman.net /language/images, last accessed 11/01/2015

26. Rizwan, S. (2006). *English and Urdu newspapers of Pakistan: Ideology in discourses.*Unpublished M. Phil thesis, Department of English, BahauddinZakariya University,Multan.

27. Saigol, R. (2004), October-December). Curriculum in India and Pakistan. *Online South Asian Journal,* 6. Retrieved March 13, 2015 from http://www.southasianmedia.net/magazine/Journal/6_curriculum_india.htm

28. Saigol, R. (1995). *Knowledge and identity.* Lahore: ASR Publications.

29. Schaffner, C. (1995). Editorial. *Current Issues in Language & Society. 2*(2), 109-114.

30. Singh, I. (1999). Language, thought and representation. In Ishtla Singh and Jean Stilwell Peccei. (Ed.), *Language, society and power* (pp. 17-34). London: Routledge.

31. Tahir, M. (2013). A Critical Discourse Analysis of Religious Othering of Muslims in the Washington Post. *Middle-East Journal of Scientific Research 1* (6), 744-753

32. Van Dijk, T. A. (2004), September). *Ideology and discourse analysis.* Paper presented at Ideology Symposium, Oxford.

33. Williams, R. (1961). *The long revolution.* London: Chatto & Windus.

34. Yaqoob, M. T. (2008). Ideology and Worldview in Textbooks: A Study of Cultural Aspects in ELT in Pakistan. PhD dissertation, Pakistan Research Repository.

35. Zia, R. (2003). Religion and education in Pakistan: An overview. *Perspectives, 33*(2), 165-178.

36. Zubair, S. & Yaqoob, T. (2008). Language ideology and the state: CDA of Religious Contents in Punjab English Language Textbooks. *The Journal of Humanities and Social Sciences16*(1), 160-177.